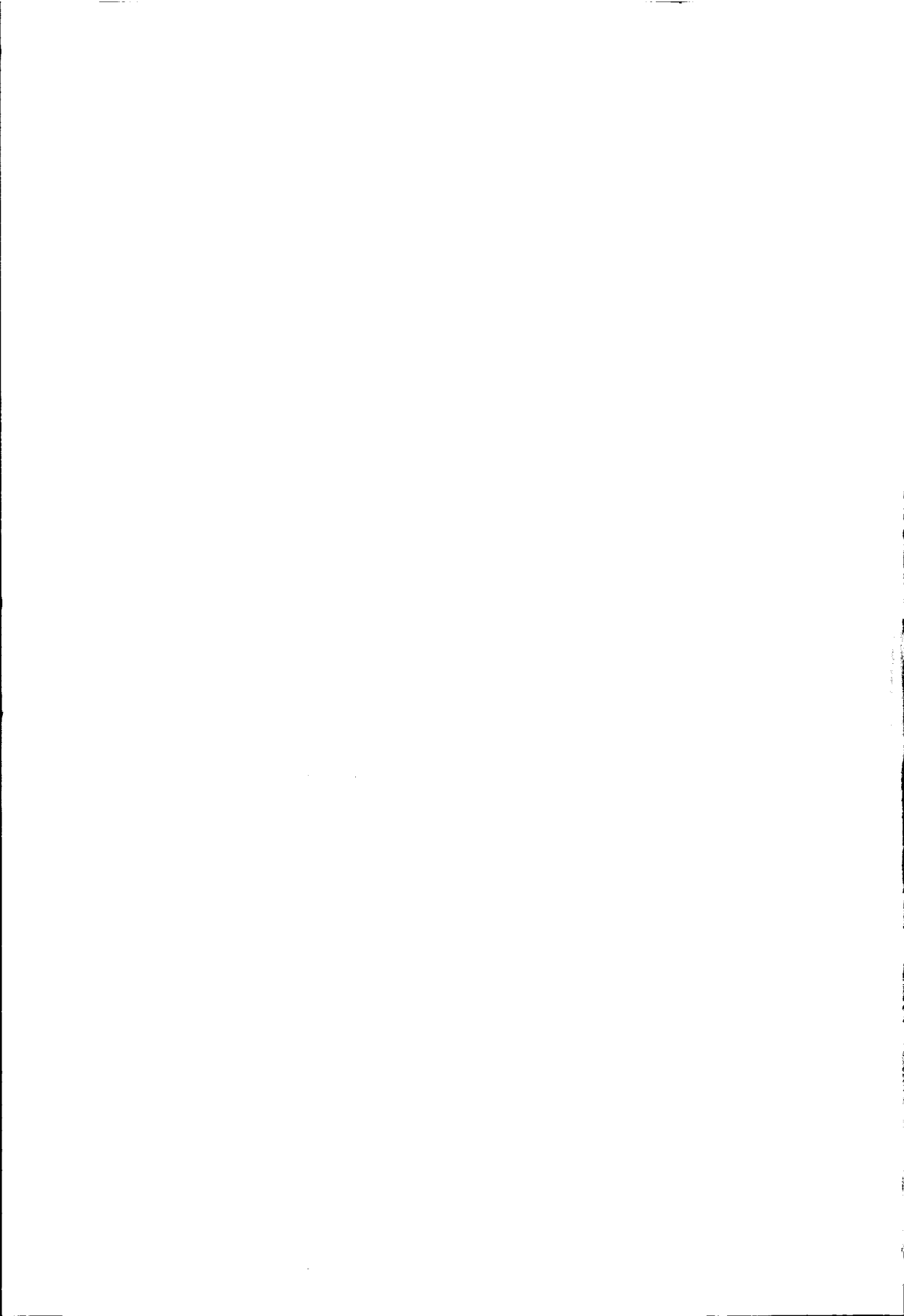


**Development of
Design Rules for
Structural Adhesive Bonded Joints**



A Systematic Approach

isbrand Jan van Straalen



Development of Design Rules for Structural Adhesive Bonded Joints

A Systematic Approach

by IJsbrand Jan van Straalen

1. The classification of the mechanical behaviour of adhesives might be the first step in developing simple design rules for adhesive bonded joints.
2. The number of publications about new solutions for the stress distribution within the bondline of a single overlap joint almost looks like the medieval quest for the Holy Grail.
3. The formulation and validation of mechanistic models describing the ageing behaviour is essential to develop design rules for adhesive bonded joints.
4. The most essential step within the procedure for calibration of partial and conversion factors with use of probabilistic techniques is the definition of the test programme.
5. It is a widespread misunderstanding to connect fatigue with dynamics.
6. A test is also a model.
7. The value of a consistent methodology in planning a research programme is ignored by many engineers.
8. Accepted design rules are too often used as a motive to prevent product developments.
9. A good photograph starts with the position of the frame.
10. Amateur astrophotography only promotes uselessness.

Development of Design Rules for Structural Adhesive Bonded Joints

A Systematic Approach

door Ijsbrand Jan van Straalen

1. De klassificatie van het mechanische gedrag van lijmen kan een eerste stap zijn in het opstellen van eenvoudige rekenregels voor gelijmde verbindingen.
2. De reeks van publicaties over nieuwe oplossingen voor de spanningsverdeling in de lijmlaag van een enkele overlapverbinding begint verdacht veel te lijken op de middeleeuwse speurtocht naar de heilige graal.
3. Het opstellen en valideren van modellen die het mechanisme van het verouderingsgedrag beschrijven, is essentieel voor de ontwikkeling van rekenregels van gelijmde verbindingen.
4. De meest essentiële stap in de procedure om de partiële factor en de conversiefactor met behulp van probabilistische technieken te kalibreren is het vaststellen van het proevenprogramma.
5. Het is een wijdverbreide misvatting om vermoeiing in verband te brengen met dynamica.
6. Ook een proef is een model.
7. Het nut van een consistente methodologie bij het opzetten van een onderzoeksprogramma wordt door veel ingenieurs genegeerd.
8. Geaccepteerde ontwerpregels worden al te vaak als excuus aangevoerd om productontwikkelingen tegen te houden.
9. Een goede foto begint bij het vastleggen van het kader.
10. Amateurastrafotografie heeft uitsluitend tot doel het nutteloze te bevorderen

TR 3640



3648
750582
301 4410

Development of Design Rules for Structural Adhesive Bonded Joints

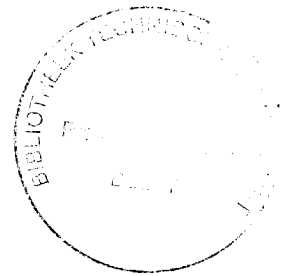
A Systematic Approach

Ijsbrand Jan van Straalen



Development of Design Rules for Structural Adhesive Bonded Joints

A Systematic Approach



Proefschrift

ter verkrijging van de graad van doctor
aan de Technische Universiteit Delft,
op gezag van de Rector Magnificus prof.ir. K.F. Wakker,
voorzitter van het College voor Promoties,
in het openbaar te verdedigen op dinsdag 23 januari 2001 om 13.30 uur,

door Ijsbrand Jan VAN STRAALLEN

civiel ingenieur
geboren te 's-Gravenzande

Dit proefschrift is goedgekeurd door de promotoren:

Prof.dr.ir. J. Wardenier

Prof.ir. F. Soetens

Prof.ir. L.B. Vogelesang

Samenstelling promotiecommissie:

Rector Magnificus,

Prof.dr.ir. J. Wardenier

Prof.ir. F. Soetens

Prof.ir. L.B. Vogelesang

Prof.ir. A.C.W.M. Vrouwenfelder

Prof. A. Beevers

Ir. A. Kwakernaak

Dr. O.T. Thomsen

Voorzitter

Technische Universiteit Delft

Technische Universiteit Eindhoven

Technische Universiteit Delft

Technische Universiteit Delft

Oxford Brookes University

Hechtingsinstituut

Aalborg University

ISBN 90-9014507-9

Copyright 2001 by IJ.J. van Straalen

All rights reserved. No part of this material protected by this copyright notice may be reproduced or utilized in any form or by any means, electronic or mechanical, including photocopying, recording or by any information storage or retrieval system, without written permission of the author.

Printed in The Netherlands

Preface

This thesis focuses on the design of adhesive bonded joints for structural applications and provides techniques to develop reliable design rules. The proposed systematic approach is based on knowledge of the adhesive bonding technology and structural reliability methods. As such, it is of interest for researchers who work in the field of adhesives, writers of standards and designers who want to apply adhesive bonded joints in practice.

Many people contributed to this thesis. I would like to thank my supervisors Prof. Jaap Wardenier (Delft University of Technology, Faculty of Civil Engineering and Geosciences), Prof. Frans Soetens (Eindhoven University of Technology, Faculty of Building and Architecture) and Prof. Boud Vogelesang (Delft University of Technology, Faculty of Aerospace Engineering) for their stimulating and fruitful comments. Furthermore, I would like to acknowledge the members of IOP Metals and the members of industry (Casco Products, Corus, Fabriek van Plaatwerken H. van Dam, Henkel Industrial Adhesives, Rockwool Lapinus, SAB Profiel, Scholten Lijmen and XX-Architecten) who financially supported the project related to this PhD study. They were involved within the whole project and they inspired me to look after practical applications of adhesive bonded joints and sandwich structures. I would also like to thank the members of TNO Industry and the Adhesion Institute of the Delft University of Technology for their contribution to the project.

Then, I would like to thank Prof. Ton Vrouwenvelder (Delft University of Technology, Faculty of Civil Engineering and Geosciences), Prof. Alec Beevers (Oxford Brookes University), Adrie Kwakernaak (Adhesion Institute) and Dr. Ole Thomsen (Aalborg University) for their valuable comments and sharpening of ideas. Furthermore, I am grateful to my colleagues of TNO Building and Construction Research. In many ways they contributed to the results of the thesis.

Finally, I am grateful to my partner Henny Reemer for her unconditional support and patience throughout the whole task.

Rijswijk
September 2000

Ijsbrand Jan van Straalen



Summary

There is a need for design rules in various sectors of industry to validate the reliability of adhesive bonded joints for structural applications. Such design rules have to be based on a structural reliability method. For practical applications it is proposed to formulate design rules within the format of the partial factor approach. This approach compares the design value of the resistance with the design value of the action effect. As long as the value of the resistance is higher than the action effect, the required reliability target is met. For adhesive bonded joints the design value of the action effect can be taken from existing standards, while for the design value of the resistance guidelines have to be formulated. To develop reliable design rules to calculate the design value of the resistance of adhesive bonded joints, a systematic approach is presented in this thesis.

The design value of the resistance is defined as the characteristic value divided by the partial factor. The characteristic value of the resistance has to be calculated by a proper prediction model that is based on the knowledge of the adhesive bonding technology. To predict the mechanical behaviour a failure criterion has to be defined, material properties have to be determined with use of standard tests and a theory has to be selected to calculate the mechanical action effects. The partial factor reduces this calculated value in such a way that the required reliability level is reached. Additionally a conversion factor is introduced to take into account the degradation behaviour due to environmental ageing. To calibrate the partial factor and conversion factor probabilistic techniques are defined.

For adhesive bonded overlap joints under static load conditions a design rule to calculate the strength is developed. The used prediction model is based on a pressure dependent yield criterion with failure at a maximum strain. Adhesive properties are determined with small-scale tensile and compression tests. A non-linear theory is used to calculate the stress and strain states within the bondline. A general applicable simple spring model approach is proposed, but also a finite element calculation can be used, as long as physical non-linear behaviour of the adhesive and geometrical non-linear behaviour of the joint are included. For the studied cold-cured two-component epoxy and cold-cured two-component polyurethane adhesives the predicted strengths are in line with results of tests on single overlap joints and double strap joints. Partial factors for both adhesives are calibrated by comparing a large number of test results and matching predicted values with statistical means. If the characteristic values of the strength are calculated on the basis of the mean stress-strain curves of the considered adhesives, the partial factor is in the range of 1.2 to 1.9.

To take into account the effects of the degradation of the strength during time, a method is presented to determine the conversion factor. The CIB/RILEM procedure is used to structure the research process. The degradation of the strength is described by an empirical relation and the actual reduction of the strength is determined by tests on specimens that are aged under accelerated conditions. The statistical interpretation of the test results using a time transformation function indicates that these results are affected by post-curing of the adhesive and that it is important to have enough data available in the region where the degradation stabilises. The calibrated values of the conversion factors for overlap joints made of polyester coated steel sheeting and bonded with cold-cured two-component polyurethane adhesives from two suppliers, are both approximately 0.75 if the characteristic values are based on fully cured adhesives.

To show the general applicability of the proposed systematic approach also design rules for

sandwich panels are developed. These deal with the shear strength of the core material and delamination of the adhesively bonded interface between the core material and the face of the sandwich. It is found that the ultimate shear stress can be used as the criterion to predict shear failure of the core, while the ultimate tensile stress of the core can be used to predict delamination of the interface. Core material properties are determined with standardized tests. A linear elastic theory is used to calculate the stress state. It is advised to take a higher-order theory or a detailed finite element calculation to calculate effects caused by local details. It is also shown that the proposed prediction model can be extended to a sandwich panel with a loaded plate adhesively bonded on one of the faces. The predictions are in line with results of tests on sandwich panels with thin steel faces and mineral wool or polystyrene core material. Partial factors are calibrated by comparing selected test results and matching predicted values with statistical means. If the characteristic values of respectively the ultimate shear stress and tensile stress are calculated on a target probability of 0.05, the partial factor for shear failure of the considered mineral wool core material is 1.8, while for delamination of both core materials the partial factor is 1.4.

It is concluded that with use of the proposed systematic approach, design rules for structural adhesive bonded joints can be developed for daily design practice. These design rules meet the target reliability. Examples of design rules for adhesive bonded overlap joints and sandwich panels under short-term static load conditions support this conclusion. Further development of design rules has to be supported by research on various aspects of the adhesive bonding technology and probabilistic methods.

Samenvatting

In verschillende sectoren van de industrie is er een behoefte om te kunnen beschikken over ontwerpregels, die de betrouwbaarheid van gelijmde verbindingen voor constructieve toepassingen toetsen. Dergelijke ontwerpregels dienen te zijn gebaseerd op een methode, die de constructieve betrouwbaarheid vaststelt. Het voorstel is om voor praktische toepassingen ontwerpregels te formuleren op basis van partiële factoren. Deze benadering vergelijkt de ontwerpwaarde van de sterktefunctie met de ontwerpwaarde van de belastingsfunctie. Zolang de waarde van de sterktefunctie groter is dan die van de belastingsfunctie, wordt aan de gestelde eis voor de betrouwbaarheid voldaan. Voor gelijmde verbindingen kan de rekenwaarde van de belastingsfunctie volgens de bestaande normen worden bepaald, terwijl voor de rekenwaarde van de sterktefunctie rekenregels dienen te worden geformuleerd. Voor gelijmde verbindingen is in deze dissertatie een systematische methodiek gepresenteerd, waarmee ontwerpregels zijn te ontwikkelen voor de berekening van de ontwerpwaarde van de sterktefunctie.

De ontwerpwaarde van de sterktefunctie is gedefinieerd als de karakteristieke waarde gedeeld door de partiële factor. De karakteristieke waarde van de sterktefunctie dient te worden berekend met een geschikt voorspellingsmodel, dat is gebaseerd op de lijmtechnologie. Het mechanische gedrag wordt voorspeld door een bezwijkcriterium te definiëren, door de materiaaleigenschappen te bepalen met behulp van standaardproeven en door een theorie te selecteren waarmee de effecten van mechanische belastingen zijn te berekenen. De partiële factor reduceert deze berekende waarde zodanig dat het vereiste niveau van de betrouwbaarheid wordt gehaald. In aanvulling hierop is in deze dissertatie een conversiefactor geïntroduceerd, die het degradatiegedrag ten gevolge van veroudering door invloeden van de omgeving in rekening brengt. Om de partiële factor en de conversiefactor te kalibreren zijn probabilistische methoden uitgewerkt.

Voor de berekening van de sterkte van statisch belaste gelijmde overlapverbindingen is een ontwerpregel ontwikkeld. Het gebruikte voorspellingsmodel is gebaseerd op een drukafhankelijk vloeicriterium, waarbij bezwijken optreedt bij een maximum rek. De lijmeigenschappen zijn bepaald met trek- en drukproeven op kleine proefstukken. Om de spannings- en rekverdeling in de lijmlaag te berekenen is een niet-lineaire theorie toegepast. Hiervoor is een algemeen toepasbare benadering voorgesteld, die uitgaat van een eenvoudig verenmodel. Een eindige-elementenberekening kan ook worden gebruikt, zolang het fysische niet-lineaire gedrag van de lijm en het geometrische niet-lineaire gedrag van de verbinding maar zijn beschreven. Voor de bestudeerde kouduithardende twee-component epoxylijm en kouduithardende twee-component polyurethaanlijm komen de voorspelde sterkten goed overeen met de proefresultaten uitgevoerd op enkele en dubbele overlapverbindingen. De partiële factoren voor beide lijmen zijn gekalibreerd door met behulp van statistische technieken een groot aantal proefresultaten te vergelijken met de overeenkomende voorspelde waarden voor de sterkte. Indien de karakteristieke waarden van de sterkte zijn gebaseerd op de gemiddelde spannings-rekrelaties van de betreffende lijmen, dan ligt de waarde van de partiële factor in de range van 1.2 tot 1.9.

Om de gevolgen van de degradatie van de sterkte gedurende de tijd in rekening te brengen, is een methode gepresenteerd waarmee de conversiefactor wordt bepaald. De door CIB/RILEM voorgestelde procedure is gebruikt om het onderzoeksproces te structureren. De degradatie van de sterkte is beschreven met een empirische relatie en de feitelijke reductie van de sterkte

is bepaald met proeven op proefstukken die versneld verouderd zijn onder geïntensiverde condities. De statistische interpretatie van de proefresultaten met behulp van een tijdverschuivingsfunctie geeft aan dat de resultaten zijn beïnvloed door een na-uitdienen van de lijm. Tevens geven deze interpretaties aan dat het belangrijk is te beschikken over voldoende data in het gebied waar het verloop van de degradatie stabiliseert. De gekalibreerde waarden van de conversiefactoren voor een overlapverbinding gemaakt van polyester gecoat plaatmateriaal en gelijmd met twee-component polyurethaanlijmen van een tweetal leveranciers, zijn beide ongeveer gelijk aan 0.75 indien de karakteristieke waarden gelden voor een volledig uitgeharde lijm.

Om de algemene toepasbaarheid van de voorgestelde systematische methodiek te illustreren, zijn er ook ontwerpregels voor sandwichpanelen ontwikkeld. Deze hebben betrekking op de afschuifsterkte van het kernmateriaal en op de delaminatie van de gelijmde laag tussen het kernmateriaal en de huid van de sandwich. Er is vastgesteld dat de uiterste afschuifsterkte een bruikbaar criterium is om bezwijken van het kernmateriaal op afschuiving te voorspellen, terwijl de uiterste treksterkte van het kernmateriaal kan worden gebruikt om bezwijken van de grenslaag te voorspellen. De eigenschappen van het kernmateriaal zijn bepaald met standaard proeven en een lineair elastische theorie is gebruikt om de spanningen te berekenen. Geadviseerd wordt om voor het berekenen van de effecten van lokale geometrische details een hogere-orde theorie of een gedetailleerde eindige-elementen-berekening te gebruiken. Tevens is aangetoond dat het voorgestelde voorspellingsmodel kan worden uitgebreid voor een sandwichpaneel met een opgelijmde plaat die wordt belast. De voorspellingen komen overeen met resultaten van proeven op sandwichpanelen gemaakt van dunne stalen huiden en een kernmateriaal van minerale wol of polystyreen. Partiële factoren zijn gekalibreerd door met statistische technieken geselecteerde proefresultaten te vergelijken met de bijbehorende voorspelde waarden. Indien de karakteristieke waarden voor de uiterste afschuifspanning en trekspanning zijn gebaseerd op een kans gelijk aan 0,05, dan is de partiële factor voor de beschouwde minerale wol gelijk aan 1,8, terwijl voor delaminatie van beide beschouwde kernmaterialen de partiële factor gelijk is aan 1,4.

Geconcludeerd is dat met de voorgestelde systematische methodiek voor gelijmde verbindingen in constructies ontwerpregels voor de dagelijkse ontwerp praktijk kunnen worden ontwikkeld. De ontwerpregels voldoen dan aan de gestelde betrouwbaarheid. Deze conclusie wordt ondersteund door voorbeelden van rekenregels voor gelijmde overlapverbindingen en sandwichpanelen, die kortdurend statisch worden belast. De verdere ontwikkeling van ontwerpregels dient te worden ondersteund door onderzoek naar de vele aspecten van de lijmtechnologie en probabilistische methoden.

Contents

Preface	i
Summary	iii
Samenvatting	v
Contents	vii
List of Symbols	xi
1. Introduction	1
2. Structural Adhesive Bonding Technology	3
2.1 Applications in engineering	3
2.2 Structural behaviour of adhesive bonded joints	4
2.2.1 Failure modes	4
2.2.2 Cohesion	7
2.2.3 Adhesion	9
2.2.4 Ageing and degradation	10
2.2.5 Stochastic nature of the strength	12
2.3 Design of structural adhesive bonded joints	13
2.3.1 Selection of an adhesive bonding system	13
2.3.2 Structural design of a joint	14
2.3.3 Manufacturing process	15
3. Development of Design Rules	17
3.1 Historical developments	17
3.2 Structural reliability methods	18
3.2.1 Use of the limit state concept	18
3.2.2 Partial factor approach	20
3.2.3 Time dependent effects	23
3.3 Developing design rules for structural adhesive bonded joints	26
4. Calibration Techniques for Design Rules	29
4.1 Engineering judgement and probabilistic techniques	29
4.2 Statistical description of the resistance	30
4.2.1 Stochastic distribution functions	30
4.2.2 Design and characteristic values based on test data	32
4.2.3 Selection of a distribution function on basis of tests	34
4.2.4 Selection of a distribution function on basis of theoretical considerations	36
4.3 Probabilistic calibration techniques	37
4.3.1 Generation of a set of data	37
4.3.2 Calibration of the partial factor	38
4.3.3 Calibration of the conversion factor for time dependent effects	42
5. Modelling of Mechanical Behaviour	45
5.1 Methods of modelling	45
5.2 Adhesive bonded joints	46

5.2.1	Mechanical behaviour	46
5.2.2	Choice of failure criteria	47
5.2.3	Determination of material properties	48
5.2.4	Theories to calculate mechanical action effects	49
5.2.5	Proposal for a prediction model	50
5.3	Sandwich structures	53
5.3.1	Mechanical behaviour	53
5.3.2	Choice of failure criteria	54
5.3.3	Determination of material properties	55
5.3.4	Theories to calculate mechanical action effects	56
5.3.5	Proposal for a prediction model	56
6.	Modelling of Durability	57
6.1	Methods of modelling	57
6.2	Adhesive bonded joints	58
6.2.1	Ageing and degradation behaviour	58
6.2.2	CIB/RILEM procedure	58
6.2.3	Degradation mechanisms	60
6.2.4	Accelerated ageing tests	60
6.2.5	Statistical evaluation techniques	60
6.3	Sandwich structures	61
7.	Design Rules for Overlap Joints	63
7.1	Mechanical behaviour	63
7.1.1	Studied overlap joints	63
7.1.2	Background of the hydrostatic dependent failure criterion	64
7.1.3	Background of tensile and compression tests	68
7.1.4	Background of stress and strain analyses	74
7.1.5	Unified spring model approach	75
7.1.6	Comparison between tests and predictions	80
7.1.7	Calibration of the partial factor	86
7.2	Ageing behaviour	95
7.2.1	Studied overlap joints	95
7.2.2	Preliminary study	96
7.2.3	Prediction of the degradation	98
7.2.4	Calibration of the conversion factor for time dependent effects	103
8.	Design Rules for Sandwich Panels	107
8.1	Mechanical behaviour of the support region	107
8.1.1	Description of the case study	107
8.1.2	Background of considered failure criteria	108
8.1.3	Background of tensile, compression and shear tests on the core material	109
8.1.4	Background of stress analyses	112
8.1.5	Higher-order theory	114
8.1.6	Comparison between tests and predictions	117
8.1.7	Calibration of the partial factor	119

8.2	Mechanical behaviour of a sandwich panel with an adhesively bonded plate	122
9.	Conclusions	129
10.	Future Research Activities	131
	References	135
	Appendix A - Unified Spring Model Approach	143
	Appendix B - Higher-Order Theory for Sandwich Beams and Panels Loaded in Bending	153
	Appendix C - Combination of Higher-Order Theory and Spring Model Approach for a Sandwich Panel with an Adhesively Bonded Plate	159
	Curriculum Vitae	167



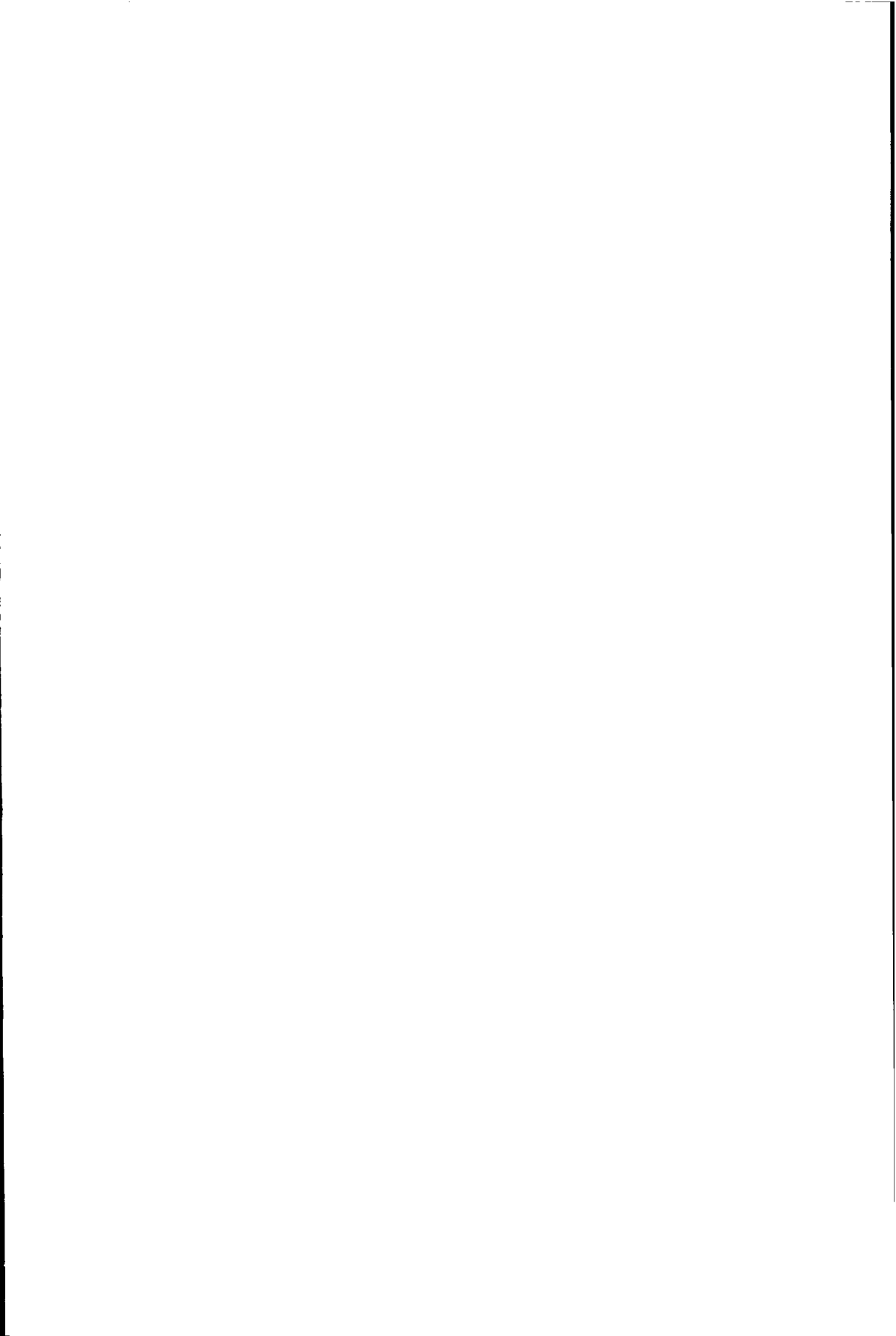
List of Symbols

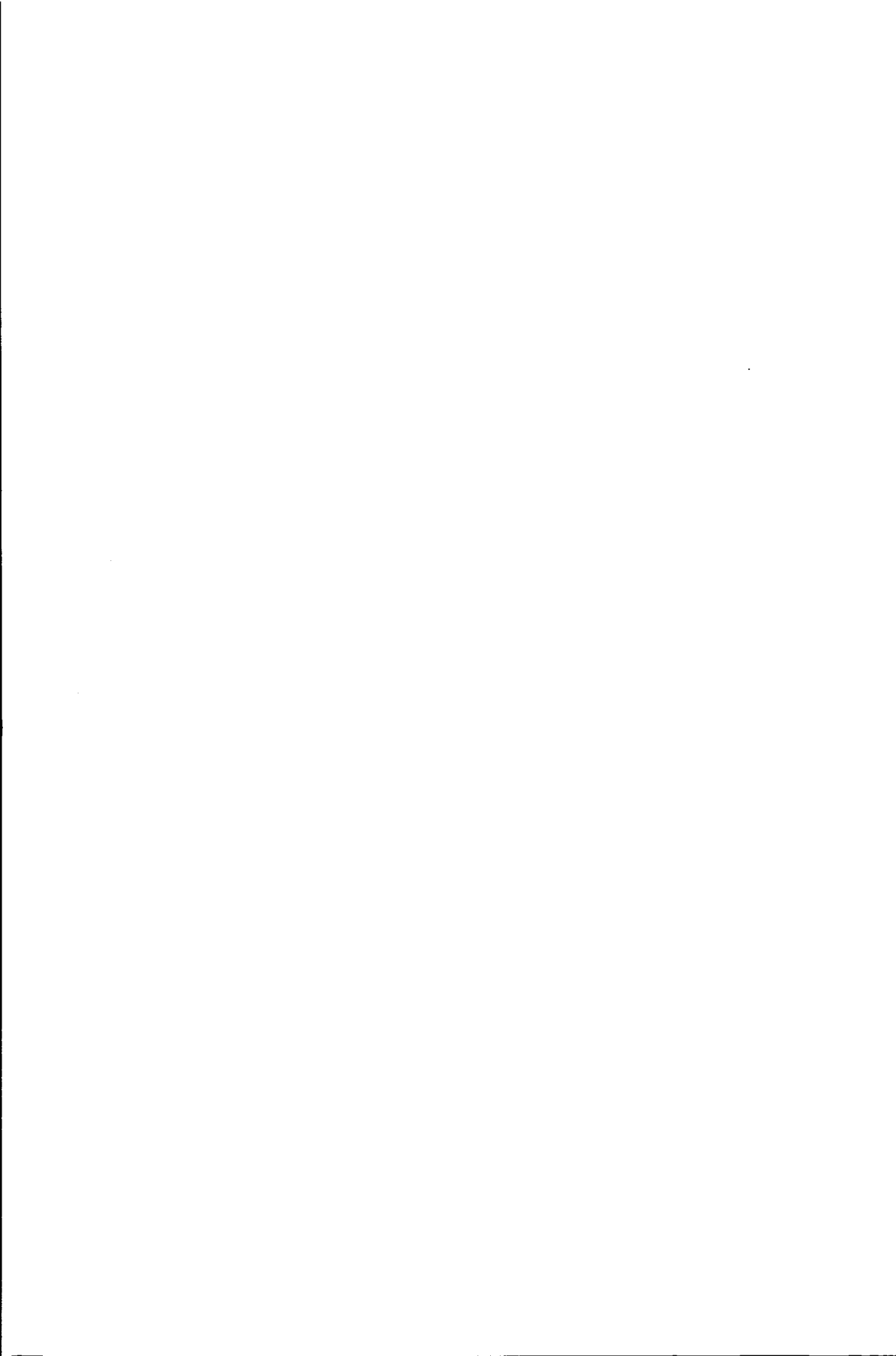
A	axial rigidity of adherend or face	$N \cdot mm^{-1}$
B	shear coefficient of adherend or face	$N \cdot mm^{-1}$
C	constant of prediction model	-
C_1	constant of relation time dependent resistance	s^{-1}
C_2	constant of Arrhenius relation	-
C_3	constant of Arrhenius relation	K
C_s	parameter of hydrostatic yield criterion	-
C_v	parameter of hydrostatic yield criterion	-
$CTOD$	crack tip opening displacement	mm
D	flexural rigidity of adherend or face	$N \cdot mm$
E	Young's modulus of adherend or face	$N \cdot mm^{-2}$
E_a	Young's modulus of adhesive	$N \cdot mm^{-2}$
$E_{a;c}$	Young's modulus of adhesive under compression	$N \cdot mm^{-2}$
$E_{a;t}$	Young's modulus of adhesive under tension	$N \cdot mm^{-2}$
E_c	Young's modulus of core material	$N \cdot mm^{-2}$
$E_{c;c}$	Young's modulus of core material under compression	$N \cdot mm^{-2}$
$E_{c;t}$	Young's modulus of core material under tension	$N \cdot mm^{-2}$
F_a	modulus of empirical stress-strain relation of an adhesive	$N \cdot mm^{-2}$
$F_R(\cdot)$	cumulative distribution function	
$F_X(\cdot)$	cumulative distribution function	
F_x	axial force applied on adherend or face	$N \cdot mm^{-1}$
F_z	shear force applied on adherend or face	$N \cdot mm^{-1}$
G	shear modulus of adherend or face	$N \cdot mm^{-2}$
G	strain energy release rate	$N \cdot mm^{-1}$
G_a	shear modulus of adhesive	$N \cdot mm^{-2}$
G_c	shear modulus of core material	$N \cdot mm^{-2}$
I_1	first invariant of general strain tensor	-
I_{2D}	deviatoric strain tensor	-
J_1	first invariant of general stress tensor	$N \cdot mm^{-2}$
J_{2D}	deviatoric stress tensor	$N^2 \cdot mm^{-4}$
J	J-integral	$N \cdot mm^{-1}$
K	stress intensity factor	$N \cdot mm^{-3/2}$
K_a	adding factor of prediction model	
$K_{a;d}$	design value of adding factor of prediction model	
K_m	multiplying factor of prediction model	
$K_{m;d}$	design value of multiplying factor of prediction model	
N_{xx}	axial force in adherend or face	$N \cdot mm^{-1}$
M_{xx}	bending moment in adherend or face	$N \cdot mm \cdot mm^{-1}$
P	probability	
Q	stress intensity factor near a point of singularity	$N \cdot mm^{-3/2}$
Q_{xx}	shear force in adherend or face	$N \cdot mm^{-1}$
R	resistance	
R_0	resistance at time $t = 0$	
R_d	design value for resistance	

R_{inf}	resistance stabilized after a long period of time	
R_k	characteristic value of resistance	
R_m	mean value of resistance	
R_{pm}	resistance according to predicting model	
$R_{ref;d}$	design value of resistance valid for whole reference period	
R_{test}	resistance according to test result	
S	action effect	
S_d	design value of action effect	
S_k	characteristic value of action effect	
S_t	extreme load	N
T	bending moment applied on adherend or face	N·mm·mm ⁻¹
T	temperature	°C, K
W	deterministic variable	
\underline{W}	vector consisting variables with a deterministic nature	
X	continuous random variable	
\underline{X}	vector consisting variables with a stochastic nature	
X'	continuous random variable	
X_{nom}	vector consisting variables assumed to be deterministic	
Y	continuous random variable	
Z	limit state function	
c_1, c_2	dimensionless constants empirical stress-strain relation for an adhesive	-
e	effective strain	-
$f_R(\cdot)$	probability density function of resistance	
$f_S(\cdot)$	probability density function of action	
$f_X(\cdot)$	continuous distribution function	
k	constant of normal probability distribution	-
$k(\cdot)$	parameter	-
l	overlap length	mm
l_0	length outer adherend	mm
m	estimated mean value	
m	distributed bending moment	N·mm·mm ⁻²
m_{ln}	estimated mean value based on natural logarithm	
n	number of tests or situations	-
n	distributed normal load	N·mm ⁻²
p	number of time periods	
p	constant of prediction model	
p_1, p_2	dimensionless constants empirical stress-strain relation for an adhesive	-
q	constant of prediction model	
q	distributed longitudinal load	N·mm ⁻²
r	resistance	
r_c	mean value of resistance of one reference volume	
s	action effect	
s	effective stress	N·mm ⁻²

s	estimated standard deviation	
s	alternative estimator of standard deviation	
s_{com}	combined alternative estimator of standard deviation	
s_{ln}	estimated standard deviation based on natural logarithm	
t	time or point in time	s, days
t	thickness of adherend or face	mm
$t(\cdot)$	value of the Student distribution	-
t_a	thickness of adhesive bondline	mm
t_c	thickness of core	mm
t_p	time of a period	s, days
t_{ref}	time of reference period	s, days
u	longitudinal displacement of adherend or face	mm
u_0	longitudinal displacement of centre line of adherend or face	mm
u_a	longitudinal displacement of adhesive bondline	mm
u_c	longitudinal displacement of core	mm
w	transverse displacement of adherend or face	mm
w	width of adherend or face	mm
w_a	transverse displacement of adhesive bondline	mm
w_c	transverse displacement of core	mm
x	x-coordinate	mm
x	continuous random variable	
z	z-coordinate	mm
α	weight factor related to partial factor approach	-
α	scale parameter of Weibull distribution	
α'	estimated scale parameter of Weibull distribution	
α_R	weight factor for resistance related to partial factor approach	-
α_S	weight factor for action effect related to partial factor approach	-
β	reliability index	-
β	shape parameter of Weibull distribution	-
β'	estimated shape parameter of Weibull distribution	-
$\Gamma(\cdot)$	gamma function	
γ_a	shear angle of adhesive	-
γ_c	shear angle of core	-
γ_R	partial factor for resistance	-
γ_S	partial factor for action effect	-
Δ	distance	mm
$\epsilon_1, \epsilon_2, \epsilon_3$	principle strains	-
ϵ_a	strain of adhesive	-
$\epsilon_{a;c}$	compression strain of adhesive	-
$\epsilon_{a;c;ult}$	ultimate compression strain of adhesive	-
$\epsilon_{a;t}$	tensile strain of adhesive	-
$\epsilon_{a;t;ult}$	ultimate tensile strain of adhesive	-
$\epsilon_{c;c;ult}$	ultimate compression strain of core material	-

$\epsilon_{c;t;ult}$	ultimate tensile strain of core material	-
ϵ_e	engineering strain	-
$\epsilon_{f;ult}$	ultimate strain of face	-
ϵ_{xx}	longitudinal normal strain in adherend or face	-
$\epsilon_{xx;a}$	longitudinal normal strain in bondline	-
$\epsilon_{xz;a}, \epsilon_{zx;a}$	shear strain in bondline	-
$\epsilon_{yy;a}$	perpendicular normal strain in bondline	-
$\epsilon_{zz;a}$	transverse normal strain in bondline	-
$\epsilon_{zz;c}$	transverse normal strain in core	-
η_m	conversion factor for manufacturing effects	-
η_t	conversion factor for time-dependent effects	-
κ	correction factor of shear coefficient of adherend or face	-
λ_a	ratio compressive and tensile stresses of adhesive	-
μ	mean value	-
μ_R	mean value of resistance	-
ν	degrees of freedom of the Student distribution	-
ν	Poisson's ratio of adherend or face	-
ν_a	Poisson's ratio of adhesive	-
ν_c	Poisson's ratio of core	-
$\rho(\cdot, \cdot)$	time transformation function	-
σ	standard deviation	-
σ_0	stress of empirical stress-strain relation	N·mm ⁻²
$\sigma_1, \sigma_2, \sigma_3$	principal stresses	N·mm ⁻²
σ_a	stress of adhesive	N·mm ⁻²
$\sigma_{a;c;ult}$	ultimate compression stress of adhesive	N·mm ⁻²
$\sigma_{a;t;ult}$	ultimate tensile stress of adhesive	N·mm ⁻²
σ_c	stress in core material	N·mm ⁻²
$\sigma_{c;c;ult}$	ultimate compression stress of core material	N·mm ⁻²
$\sigma_{c;t;ult}$	ultimate tensile stress of core material	N·mm ⁻²
σ_e	engineering stress	N·mm ⁻²
$\sigma_{f;ult}$	ultimate tensile stress of face	N·mm ⁻²
$\sigma_{f;y}$	yield stress of face	N·mm ⁻²
σ_R	standard deviation of resistance	-
σ_t	true stress	N·mm ⁻²
$\sigma_{xx;a}$	longitudinal normal stress in bondline	N·mm ⁻²
$\sigma_{xz;a}, \sigma_{zx;a}$	shear stress in bondline	N·mm ⁻²
$\sigma_{yy;a}$	perpendicular normal stress in bondline	N·mm ⁻²
$\sigma_{zz;a}$	transverse normal stress in bondline	N·mm ⁻²
$\sigma_{zz;c}$	transverse normal stress in core	N·mm ⁻²
τ_a	shear stress in bondline	N·mm ⁻²
$\tau_{a;ult}$	ultimate shear stress of adhesive	N·mm ⁻²
τ_c	shear stress in core	N·mm ⁻²
$\tau_{c;ult}$	ultimate shear stress of core material	N·mm ⁻²
$\Phi(\cdot)$	standard normal distribution function	-
ψ	rotation of adherend or face about its midplane	-





Introduction

Today, there is a growing interest in industry to use adhesive bonded joints for structural applications. This method of joining offers advantages over more conventional methods. Substantial economic profits can be made by the development of new design solutions. By using adhesive bonded joints, new materials can be applied and there is the ability to work out novel structural configurations. A good example of this development is the sandwich panel. Different types of materials for the faces and core are combined to form the layered structure and the faces can be reinforced locally by bonding stiffeners at critical locations. The developments of such new design solutions require new design concepts.

For structural applications of adhesive bonded joints, present practice is confronted with the absence of reliable design rules. Only experiments are appropriate to validate if the required reliability level is reached. Various reasons can be put forward. A large variety of potential prediction models are discussed by researchers over the years, but without conformations. There is still a lack of knowledge about failure mechanisms, ageing and the stochastic nature of the strength. Also the experience with the selection of adhesive bonding systems, the structural design of a joint and the development of manufacturing processes is limited. The key reason is that the adhesive bonding technology is faced with difficulties to predict the structural behaviour and durability of adhesive bonded joints within coherent approaches.

Another reason for the absence of design rules has a historical background. The first designs of structural adhesive bonded joints were made in aerospace industry. From the period after the Second World War up till now the aerospace airworthiness authorities have only accepted design solutions validated with use of extensive test programmes. It will normally take several years to develop a solution that meets the high level of requirements. There is no urge to optimise an accepted design solution, because the costs will be higher than the profits. This situation hinders the development of design rules for validation. In the automotive industry adhesive bonded joints were introduced during the 1980's. Compared to aerospace applications, the manufacturing process had to be cheaper. This initiated the development of other adhesive bonding systems, but still the design method based on tests has been used to validate design solutions. The high costs of tests can be afforded easily, because of the large scale of production. In both automotive as well as the aerospace industry a driving force is missing to develop design rules for validation.

In other sectors of industry like marine, transport, building and civil engineering new design solutions have to be developed with a limited budget and within a short period of time. This is because these unique design solutions are custom-made and are mostly produced in small series. The use of extensive test programmes will be too expensive and time consuming. The only alternative to validate design solutions of adhesive bonded joints is to make use of reliable design rules.

Reliable design rules are based on two essential issues: a prediction model and a structural reliability method. The prediction model has to give a proper description of the structural behaviour under given mechanical and environmental actions. The structural reliability method has to guarantee the reliability level of the structure. Reliability is defined as the ability to fulfil prescribed requirements during a specified lifetime. It is equal to the probability that the structure will not fail and will perform its intended function. This means that the stochastic nature of the strength should be taken into account. To develop reliable

Introduction

design rules these two subjects have to be combined systematically.

The objective of the study presented in this thesis is to present a systematic approach to develop reliable design rules for structural adhesive bonded joints. To illustrate the potential of this approach, the study focuses on the joining of metals under short-term static load conditions and under high humidity conditions. Both the structural behaviour as well as the degradation behaviour of adhesive bonded joints are considered. The systematic approach is formulated in such a way that it can be used for all kinds of adhesive bonded joints under various actions.

The presented systematic approach is based on current knowledge about the behaviour of adhesive bonded joints and on structural reliability methods widely accepted nowadays. To introduce both subjects various fields covered by the structural adhesive bonding technology are discussed in chapter 2 and the development of modern design rules is presented in chapter 3. To meet the required reliability level, design rules have to be calibrated. In chapter 4 different calibration techniques are discussed and specific modifications are proposed for the application of adhesive bonded joints. The starting point of developing design rules is the composition of prediction models. In chapters 5 and 6 coherent approaches are proposed for the modelling of structural behaviour and durability. Their possibilities are illustrated for two kinds of applications. In chapter 7 design rules for metallic overlap joints are developed and in chapter 8 design rules for adhesive bonded joints used in sandwich panel structures are developed. Finally the conclusions are summarized in chapter 9, followed by recommendations for future research activities given in chapter 10.

Structural Adhesive Bonding Technology

An essential issue engineers are confronted with is the joining of structural parts. A wide variety of joining methods has been developed over the years, which are generally categorised into the following groups: mechanical, physical and chemical joining methods (Brandon and Kaplan, 1997). The interest in using adhesive bonded joints for structural applications is still increasing, due to the use of new materials, other fields of application and the necessity to reduce costs. This tendency confronts a larger group of engineers with the need of a better understanding of the adhesive bonding technology and its multi-disciplinary aspects. In this chapter those aspects are highlighted.

2.1 Applications in engineering

One of the first known examples of the use of bonding technology is the Greek legend of Daedalus who constructed for his son Ikaros a pair of wings made of bird's feathers bonded by wax. The flight became a disaster, because Ikaros ignored his father's warning not to fly close to the sun. The use of adhesives based on plant and animal substances goes back to 3000 BC and was applied by the Egyptians, the Romans and the Chinese to bond paper, stone and wood (Schindel-Bidinelli and Guthertz, 1988). During the industrialisation in the 19th century the performances of these vegetable and animal adhesives were modified synthetically and the first steps were made to develop new types of adhesives. The real break through became around the Second World War, when the first fully synthetic versions were invented. The improved properties of these synthetic adhesives gave engineers the opportunity to use them for structural applications.

The structural adhesive bonding technology has been applied successfully within many sectors of industry. See for example Schliekelmann (1970), Mays and Hutchinson (1992) and The Institute of Structural Engineers (1999). The aerospace industry has the longest tradition; almost every modern aeroplane contains adhesive bonded joints. The automotive industry makes frequently use of its advantages. By bonding the front and back windows the stiffness of the car frame can be improved significantly. Also other sectors of industry, like marine, transport, building and civil engineering, are recognizing the advantages of adhesive bonded joints for structural use.

An adhesive bonded joint is fabricated by putting a liquid or paste, mostly organic, between the components that have to be joined. The liquid and paste are known by the term adhesive and the component is indicated by the term adherend or the term substrate. A rigid connection is formed after curing of the adhesive. The material of the adherends is mostly unaffected by this process. The term "structural adhesive bonded joint" is used if the connection has to transfer a load from one adherend to another.

The use of structural adhesive bonded joints has several advantages and disadvantages in comparison with other joining methods like mechanical fastening, welding or soldering. Significant advantages are:

- the ability to bond dissimilar adherends;
- the ability to bond thin adherends;
- the better control of the tolerances;
- the ability to make almost invisible connections;
- the ability to produce complex joint configurations;

Structural Adhesive Bonding Technology

- the fact that the properties of the adherend as cross section area, straightness and material behaviour are not affected;
- the good sealing properties of the adhesive layer against gases, moisture or chemicals;
- the good insulating properties of the adhesive layer against electricity, heat or sound;
- the ability to avoid galvanic corrosion between dissimilar adherends.

With a proper design and manufacturing process the following advantages can be added to this list:

- the increase of the stiffness;
- the increase of the dynamic damping;
- the reduction of the sensitivity to fatigue;
- the reduction of the capital and labour costs.

There are also disadvantages that should be taken into account:

- the complexity of the manufacturing process with skills like surface preparation, preparation of the adhesive, control of the processing temperature, pressure and humidity conditions, and use of equipment;
- the curing time during which the bonded adherends have to be fixed;
- the significant influence of environmental actions on the durability;
- the fact that the properties of the adhesive are affected by temperature;
- the fact that the properties of the adhesive are time dependent;
- the possible toxicity and its effects on the environment and labour conditions;
- the difficulty to apply non-destructive test methods to control the bondline;
- the difficulty to dismantle the joint for repair or re-use of the materials.

To realise an optimum design it is necessary to utilize the advantages and to minimize the effects of the disadvantages.

The design process of a structural component contains in general an initial, a conceptual, an optimisation and a validation phase. In the initial phase the problem statement and so-called objective functions are formulated. The aim of these objective functions is to quantify the required performances under given operating circumstances. The conceptual phase ends up with a number of potential outline solutions. The formulation of these is based on experience, insight and creativity of the engineer. The optimisation phase results in a final design and the validation phase shows formally that this final design meets the requirements. For the application of structural adhesive bonded joints the following issues have to be covered within each phase of the design process:

- the selection of an adhesive bonding system;
- the structural design of the joint;
- the manufacturing process and use of a quality assurance system.

For a successful design of a structural adhesive bonded joint it is necessary to understand the background of its structural behaviour, durability and the wide variety of multidisciplinary aspects related to the above mentioned three issues.

2.2 Structural behaviour of adhesive bonded joints

2.2.1 Failure modes

By choosing an adhesive bonded joint to connect two adherends, a variety of alternative solutions can be applied. In structural terms a distinction can be made between adhesive

bonded joints globally loaded in shear, tension or peel, as indicated in figure 2.1. A design solution loaded in shear is preferred, while solutions loaded in tension or peel should be avoided as much as possible. This is, because for tension and peel the stress state in the vicinity of the bondline is dominated by high tensile stresses, which are difficult to sustain. The magnitude of these stresses is much lower for a joint primarily loaded in shear. To optimise a potential solution the configuration and dimensions of the joint can be changed.

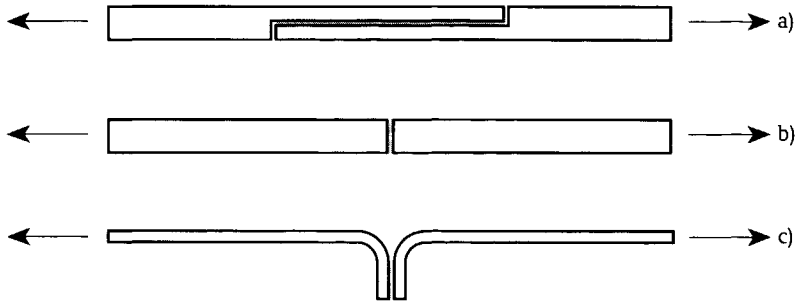


Figure 2.1 Adhesive bonded joints globally loaded in: a) shear, b) tension and c) peel

During all stages of the design process the nature of the load acting on the adhesive bonded joint has to be considered. The following distinction can be made between the various mechanical actions, as also indicated in figure 2.2:

- Short-term static load. During its lifetime the joint is incidentally loaded by a non-varying load for relatively short periods of time. An example of a short-term static load is the maximum wind load, which only occurs during a storm.
- Impact load. This is a special case of the short-term static load, in which the total load is applied within a fraction of a second. The response of the material differs significantly for what is normally found for static loads. An example of an impact load is a gas explosion.
- Long term static load. The joint is loaded by a non-varying load for a longer period time. This type of load might have a significant effect on the behaviour of the joint due to creep. Beside the fact that irreversible deformations occur, the joint might fail after a period of time. An example of a long-term static load is the dead weight of a structure.
- Low cycle fatigue load. In fatigue the value of the load acting on the joint varies during time. The fatigue load is characterised by minimum and maximum load levels reached and the number of cycles during lifetime. For low cycle fatigue cracks can be formed in the bondline, causing a degradation of the performance of for example the static strength of the joint.
- High cycle fatigue load. For high cycle fatigue load a continuing process of crack growth is active, until the joint fails. An example of a fatigue load is the cyclic traffic load of passing cars.

To validate the joint performances the significance of the above mentioned mechanical actions and their values have to be known.

Besides the above mentioned mechanical actions an engineer also has to take into account the effects of environmental actions on the performances of the adhesive bonded joint. A

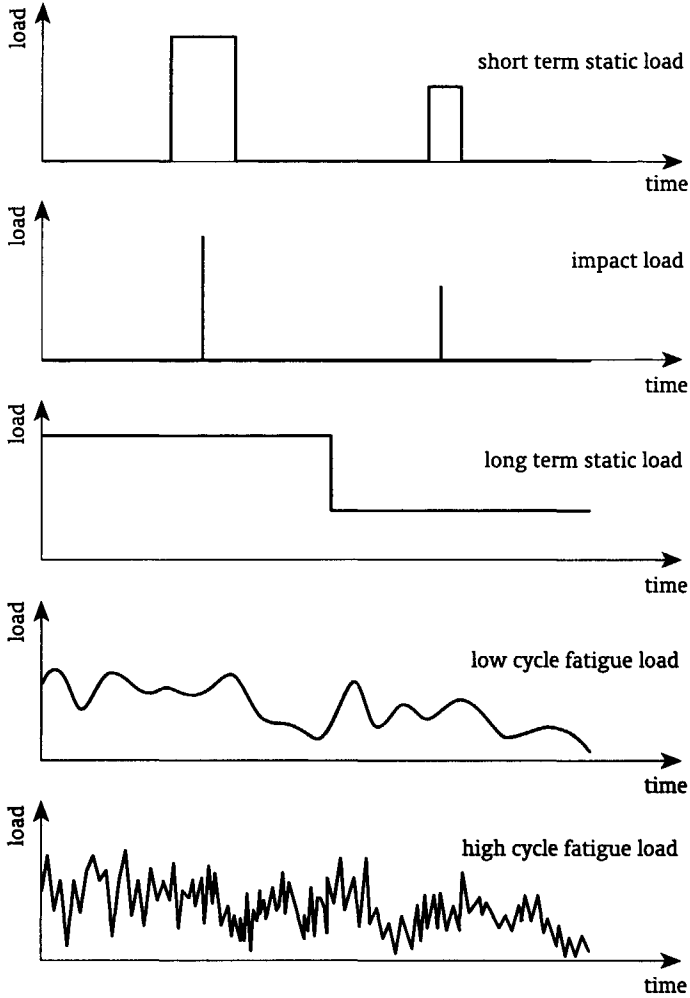


Figure 2.2 Overview of various mechanical actions

higher temperature normally reduces the stiffness and strength of the adhesive, while for the accidental action of fire most adhesives disintegrate rapidly. Other environmental actions like water, high humidity and ultraviolet radiation normally have a long-term effect on the joint by reducing the strength. Cyclic behaviour of these actions might cause additional effects. The reduction of the strength caused by ageing is known by the term degradation.

Due to mechanical and environmental actions an adhesive bonded joint might fail. The actual failure occurs in one of the following locations, see figure 2.3:

- In the bondline. It might be expected that failure initiates at a location with the highest stress state. This is also known by the term cohesive failure.
- At the interface between the bondline and the adherend. It is possible that failure of an interlayer between the adherend and the adhesive occurs, for example a coating. This is also known by the term adhesive failure.

- In one of the adherends.

From observations of fracture surfaces it is known that in many cases a mixture of cohesive and adhesive failure near the interface occurs. The failure mode is not only affected by the used adhesive bonding system, but also by the manufacturing process and the quality assurance system implemented. These findings are confirmed in detail by an extensive research project by Crocombe et.al. (1995) performed during the 1990's.

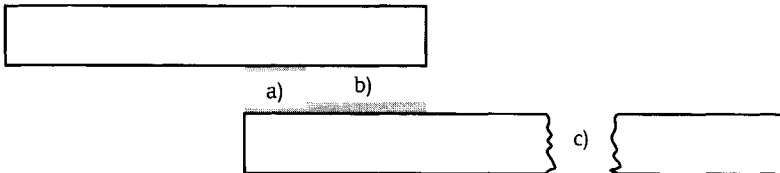


Figure 2.3 Failure of an adhesive bonded joint: a) in the bondline, b) at the interface between the bondline and the adherend, and c) in the adherend

2.2.2 Cohesion

If an adhesive bonded joint fails cohesively, the location of failure initiates within the bondline at a position with the highest stress state. From detailed observations, see for example Crocombe et.al. (1995), it is known that cracks occur locally and that due to crack growth and branching of cracks final failure occurs. Since adhesives are mostly synthetic and organic, its cohesive behaviour can be explained with what is known from the polymer technology.

Polymers are macromolecules synthesized by a reaction of smaller molecules, known by the term monomers. The polymer technology distinguishes four different molecular structures of polymers: linear, branched, crosslinked and network (Young and Lovell 1991). For a linear polymer long, flexible chains of molecules are weakly bonded by physical bonds. For a branched polymer side chains are connected to these long chains, but these are still bonded by physical bonds. For a cross-linked polymer on the other hand the side chains are connected by stronger chemical bonds. Finally the strongest structure of polymer is the network with more chemical bonds between the molecules forming a connected net of molecules. Of all these four types of molecular structures adhesives are members, but most of the structural adhesives are crosslinked and network polymers.

Another classification system used by the polymer technology is based on the behaviour of the polymer (Young and Lovell, 1991). Three types of polymers are classified: elastomer, thermoset and thermoplastic. An elastomer is based on a polymer with a low degree of crosslinking, is capable to stretch to a high extension and recovers without permanent deformations. A thermoset is based on a polymer with a high degree of crosslinking, forming a complete network polymer. Its behaviour is more rigid than for an elastomer, but both types degrade rather than melt above a certain temperature. A thermoplastic on the other hand can be melted easily. It is based on linear or branched polymers. A distinction between adhesives based on a thermoplastic on one hand and adhesives based on an elastomer or a thermoset on the other hand can be made relatively easily, but there are several adhesives that can be classified as an elastomer as well as a thermoset.

To influence the behaviour of an adhesive not only the molecular structure is controlled, but also additives are used. The polymer technology distinguishes the following types of

additives: filler, plasticiser and stabiliser. A filler does not interact with the polymer and is added to improve properties like processability, strength, toughness, dimensional stability and thermal stability. A plasticizer influences the flexibility, ductility and toughness by increasing the distances between the polymer chains. A stabilizer avoids the deterioration of the polymer due to environmental actions as ultraviolet radiation and oxidation. More types of additives are known, but for the structural behaviour of adhesives the filler, plasticizer and stabilizer are most important.

Before discussing the mechanical behaviour of polymers, attention is given towards the physical behaviour relevant for structural applications of adhesives. Polymers normally show a temperature range where the polymer melts. Below the so-called glass transition temperature the material is considered to be an amorphous solid; above this temperature it is a rubbery solid with completely different properties and at higher temperatures it becomes a viscous liquid or desintegrates. For various adhesives the glass transition temperature can be in the temperature range of practical applications, which means that the adhesive properties change significantly.

Another important phenomenon of polymers related to ageing effects is their permeability. Two mechanisms of liquid or gas uptake are distinguished (Elias, 1997). One mechanism describes that molecules diffuse into the polymer. The other mechanism describes that molecules enter with a front characterized by a sharp boundary between the unaffected polymer and the swollen polymer. For adhesives mostly the diffusion mechanism described by a Fick's diffusion law is used.

The stress-strain behaviour of polymers is fairly complex (Hertzberg, 1976). For low stresses the polymer's bonds are stretched and energy is stored in a quite reversible manner. This means that the stress-strain behaviour shows a linear relation, which can be described by the modulus of elasticity. An additional phenomenon is the lateral strain, which can be described by the Poisson's ratio. For higher stresses the stress-strain behaviour is no longer linear. A part of the energy is dissipated in a viscous manner and the stress-strain behaviour is not reversible. In literature this onset of yielding is described by various theories. A straightforward group of theories considers a pressure dependent yield criterion, which takes into account that for polymers the compressive yield stress is usually higher than the tensile one (Young and Lovell, 1991). For high strains the polymer's bonds fail and fracture occurs. These theories can also be used to describe the mechanical behaviour of adhesives.

Under long-term loads polymers normally show a kind of visco-elastic behaviour. It is a mixture of the mechanical behaviour of viscous liquids for which the stress is proportional to the strain rate and the mechanical behaviour of an elastic solid. The response depends upon the rate or time period of loading and temperature. Various theories are developed to describe the visco-elastic behaviour under different conditions, see for example Young and Lovell (1991). These theories might also be useful to describe the visco-elastic behaviour of adhesives.

Instead of using the above given description of the mechanical behaviour based in continuum mechanics, it is also possible to make use of fracture mechanics (Ewalts and Wanhill, 1984) to describe the mechanical behaviour of polymers (Young and Lovell, 1991). This approach assumes that there exists a crack in the solid. Due to the applied load stress and strain concentrations occur near the vicinity of the crack tip. For polymers this concentration is mostly described by a single parameter known as the strain energy release rate. It represents the amount of energy necessary per unit crack extension. If it exceeds a critical

value, fracture will occur. An advantage of the parameter strain energy release rate is that it can also be used to predict crack growth in polymers (Hertzberg and Manson, 1980). Using an empirical relationship between the crack growth rate and the strain energy release rate range the number of cycles from an initial defect until final failure can be calculated. The strain energy release rate range is defined as the difference between the maximum and minimum strain energy release rates calculated for a load cycle. Theories based on the fracture mechanics approach might also be used to describe the failure behaviour of adhesives.

Another aspect related to the mechanical behaviour of polymers is the degradation of their properties due to ageing. It is a process in which the degree of polymerization decreases during time due to environmental actions like water, ultraviolet radiation and chemicals. There is also the possibility that degradation occurs by swelling or dissolution of parts of polymer. In Eurin's contribution to Masters (1985) attention is given to the degradation mechanisms of polymers within the context of the so-called chemico-physical theory. The distinguished processes are found to be extremely complex and they are the resultant of a series of sometimes unknown elementary mechanisms. These mechanisms depend upon numerous factors, like the nature of the basic polymer, used additives, impurities, defects and environmental conditions. These factors are considered to be the principle agents of polymer degradations. Eurin also mentions that once mechanisms have been identified, other difficulties remain. Particular the analysis of relations of causality between basic mechanisms and variation of properties is difficult. A proper description of the degradation mechanisms of adhesives seems to be far too complex, in particular because it is directly related to the adhesion of the interface between the bondline and the adherend.

2.2.3 Adhesion

If an adhesive bonded joint fails adhesively, the location of failure is within the interface between the bond layer and the adherend. In design the occurrence of this failure type is mostly avoided by engineers, but after ageing of the joint adhesive failure might become dominant. To explain adhesion the interaction within the interface has to be known.

A variety of theories of adhesion are presented in the existing literature. These theories are principally based on the existence of bonds responsible for the interaction between atoms or molecules. A distinction is made between physical and chemical bonds, see for example Habenicht (1990) or Kinloch (1990). Weaker physical bonds based on Van der Waals forces, dipole forces and hydrogen bonds, are formed by an electrostatic attraction between chemical neutral molecules. The stronger chemical bonds, based on ionic, covalent and metallic bonds, require reactive chemical groups that tightly bond on the adherend surface and in the adhesive. Some theories try to give a more advanced description of the adhesion phenomena. For example the diffusion theory proposes that the polymers of the adhesive diffuse into the adherend and apply to compatible molecules of the adherend. An additional theory also mentioned in literature is the theory of mechanical interlocking. It proposes that the adhesive mechanically keys into the roughness or pores of the adherend surface. The number of developed theories indicates that there is still controversy regarding a useful one.

Since most of the research on the selection of adhesive bonding systems has focussed on techniques to avoid adhesive failure, less is known about the actual physical and mechanical behaviour of the interlayer. Textbooks give qualitative indications about some physical and mechanical properties, but theoretical considerations upon this topic are very rare. It is believed that a better understanding of the physical and mechanical behaviour of the

interface is very useful.

Another aspect related to the mechanical behaviour of interlayers is the degradation of their properties due to ageing. It is a process in which the performance of the bonding degrades during time due to environmental actions like water, ultraviolet radiation and chemicals. A proper description of the degradation mechanisms of interlayers is still not available. The degradation of an adhesive bonded joint is for this reason mostly studied by testing.

2.2.4 Ageing and degradation

Environmental actions, which depend upon the application and the geographical site, can have a significant influence on the performances of adhesive bonded joints. Due to ageing the mechanical properties of a joint can degrade during time. To illustrate this phenomenon an example of the degradation of the strength of a single lap joint is given in figure 2.4. The performed ageing tests were accelerated by a higher temperature. It is generally concluded by research that water in a liquid or vapour state, temperature, time of exposure, long-term loads and cyclic behaviour of temperature have a major effect on the durability (Kinloch, 1983). Water seems to be the most important one in practice. A full understanding of degradation mechanisms in relation to these actions is still missing.

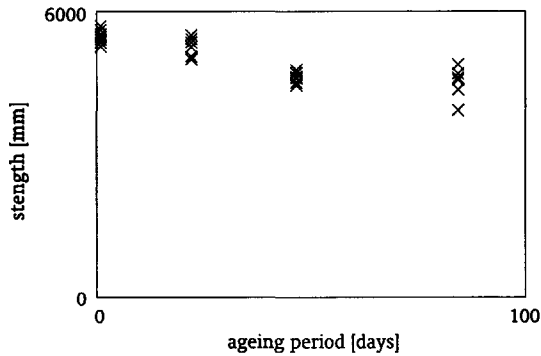


Figure 2.4 Example of the degradation of the strength of a single lap joint aged at 60 °C and 95 % RH, as will be discussed in section 7.3

Over the years many degradation mechanisms and their effects have been considered. All these mechanisms are based on empirical formulations. Most of these are discussed by Comyn in his contribution to Kinloch (1983). The performances of the adhesive layer might be affected by:

- Plasticisation. When the polymer absorbs water, the strength and the modulus of elasticity of the adhesive is lower. It is suggested that the decrease of the glass transition temperature is related to this mechanism. The mechanism is reversible.
- Swelling. During the process of water uptake the volume of the polymer increases, causing residual stresses. These might relax after some time due to creep. The mechanism is reversible.
- Hydrolysis. If water reacts with the polymer, the strength lowers and the modulus changes.

The mechanism is irreversible.

- **Crazing and cracking.** Due to varying environmental actions crazing and cracking of the polymer may occur, resulting in a weakening of the bondline strength. An additional effect is that the water uptake increases. The mechanism is irreversible.

The performance of the interface might be affected by the following interface attacks:

- **Displacing of the adhesive.** The presence of water might have an effect on the thermodynamic work of adhesion, causing a displacement of the adhesive from the interface. If this is the case, complete failure occurs. The mechanism is irreversible.
- **Deactivating of chemical bonds.** The water acts with the tight bonds on the adherend surface and in the adhesive, resulting in a decrease of the strength. The mechanism is reversible.
- **Corrosion of the adherend surface.** Due to water a corrosion product might be formed on the adherend surface. This process results into a decrease of the strength or even a complete failure. The mechanism is irreversible.

This variety of possible mechanisms shows how difficult it is to predict the degradation effects of ageing.

On basis of test results Comyn assumes in his contribution to Kinloch (1983) a linear relationship between the amount of water uptake and the magnitude of degradation. A higher temperature accelerates the process, while long-term loads and cyclic actions intensify degradation effects. But Comyn also concludes that for several mechanisms a threshold is present below which no degradation appears. These findings are confirmed by others, see for example Schmitz (1989).

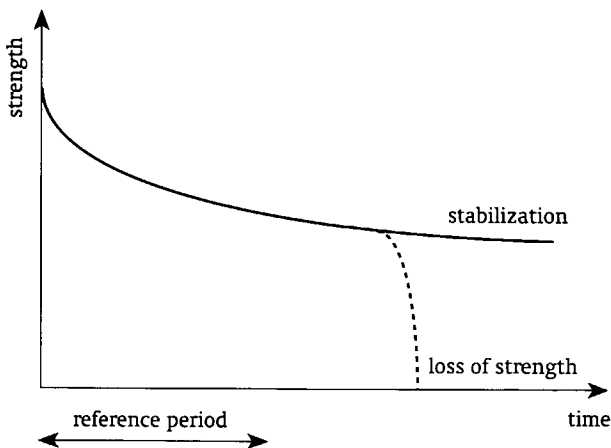


Figure 2.5 Schematic presentation of the development of the degradation of the strength during lifetime

An issue not mentioned in literature is how the magnitude of degradation develops during time. It is possible that due to ageing the mechanical properties of an adhesive bonded joint degrade and after a period of time stabilise. But is also possible that the joint suddenly loses its strength completely. In figure 2.5 a schematic illustration is presented.

2.2.5 Stochastic nature of the strength

From test series it is generally known that the values of the strength of adhesive bonded joints lie within a scatterband. To illustrate this phenomenon an example of a series of 15 tests on single lap joints is considered here. The failure loads are tabulated in figure 2.6 together with a histogram of the frequency distribution. The difference between the lowest and highest value is less than 15%. Up till now most researchers do not take this stochastic nature of the strength into account, in spite of the fact that it influences the structural performances significantly.

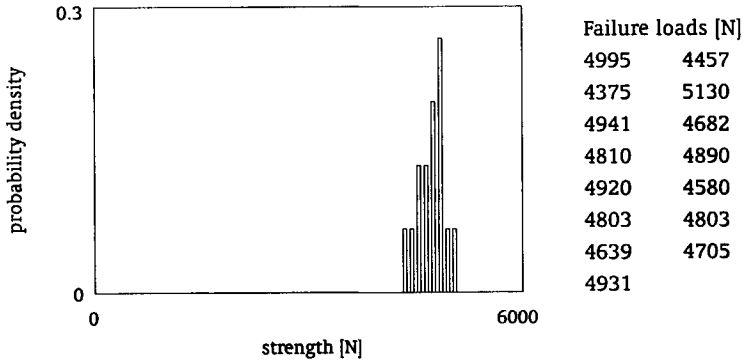


Figure 2.6 Example of the frequency distribution of a test series on single overlap joints with an overlap of 12 mm, a width of 25 mm, 1 mm thick polyester coated steel adherends and the cold cured two-component polyurethane UK 8202 of Henkel

The stochastic nature of the strength of adhesive bonded joints is affected by several factors. The variations in joint geometry, cohesion properties, adhesion properties and the distribution of defects, can be seen as one group of factors related to the impossibility to produce identical joints. Another group of factors is related to the circumstances, which vary during the process of bonding and curing. The temperature and the humidity change from day to day and the procedures followed by different workshops are not identical. It is known that the variations of these circumstances can have a significant contribution to the found differences. A last group of factors affecting the stochastic nature are related to ageing. The intensity of environmental actions and the history of both environmental and mechanical actions vary from one joint to another. This means that the degradation of the resistance also varies. To understand the stochastic nature more profoundly, it is necessary to study the influence of all these factors.

The main factors that influence the stochastic nature are identified, but almost nothing is known about the actual distributions. The width of the scatterband, the type of distribution and the influence of various factors are not studied in detail up till now. It is essential to have a better understanding, because then it is possible to relate the stochastic nature with the structural performances of adhesive bonded joints.

2.3 Design of structural adhesive bonded joints

2.3.1 Selection of an adhesive bonding system

The selection of adhesives and surface preparations is an essential aspect within the design process of adhesive bonded joints. Several types of adhesives with their own specific properties can be used for structural applications. The performances of the joint are influenced by the surface preparation of the adherends. Special attention has to be given to possible ageing effects. For a proper design the engineer must have knowledge about the available adhesive bonding systems, their advantages and their limitations.

The most widely used groups of adhesives for structural applications are epoxies, polyurethanes and acrylics. They do not only have favourable strength properties, but they also have toughness and degradation properties that meet the requirements. Epoxies are available in many formulations and can be used to bond a wide variety of materials. Their strength properties are good, but they can be rather brittle; the toughened versions are more favourable for structural applications. The one-component epoxies cure at higher processing temperatures, while the two-component versions cure at room temperature by the additional hardener. An intensive surface preparation might be necessary to guarantee the durability. Polyurethanes are available in a wide variety of formulations. The one- and two-component versions are mostly used for structural applications with different materials. The one-component version cures by a reaction with moisture and its strength properties are rather low. The two-component version cures by the additional hardener and its strength properties are medium. But the toughness properties of both polyurethane versions are mostly excellent and the durability properties are mostly good, even with a simple surface preparation. Acrylics, or more precisely modified acrylics, are available in different formulations. They are mostly available in a two-component version for which no mixing is required; one component is applied to one surface, the other to the second and both are joined. The strength and toughness properties of modified acrylics are in general good. A moderate surface preparation is necessary to guarantee the durability. More detailed information regarding available formulations, the advantages and limitations of these adhesives is discussed in many handbooks, see for example Brinson (1990), Habenicht (1990), Hussey and Wilson (1996), Lankreijer and Logtenberg (1991), Shields (1985) and Skeist (1990).

To influence the behaviour of the layer between the bondline and adherend, different techniques have been developed to control and optimise the surface properties. The purpose of surface pretreatments is to remove contaminations and weak surfaces, to improve the adsorption of the adhesive onto the solid surface (good wettability) resulting in a good bonding, to make a conversion by modifying the texture of the surface or to add an additional layer. The available techniques are based on the principles of degreasing, chemical cleaning, mechanical cleaning and chemical conversion. Additional layers such as primers are used to change the adherend surface geometry or to introduce new chemical groups to provide a better bonding. The selection of the proper surface preparation is directly related to the used adherends and the selected adhesive. Overviews of available surface preparations and their performances are given in many handbooks, see for example Brinson (1990), Habenicht (1990), Hussey and Wilson (1996), Lankreijer and Logtenberg (1991), Shields (1985) and Skeist (1990).

Essential within the selection process of an adhesive bonding system is the estimation of the degradation of the properties due to ageing. These are not only influenced by the adhesive used, but also by the adherend and the selected surface preparation. It is impossible to

quantify the degradation effects in general due to the large number of parameters influencing the degradation process, of which some are even unknown. The degradation properties can only be determined by tests for a given adhesive bonding system.

The selection of a proper adhesive bonding system for a given application should be based on the adhesive bonding technology, available data, tests and experience. Valuable information can be taken from already mentioned handbooks, from expert systems available on the market and from information provided by adhesive suppliers.

2.3.2 Structural design of a joint

The prediction of the structural behaviour is an essential aspect within the design process of adhesive bonded joints. The structural behaviour is influenced by the layered composition of the joint with relatively stiff adherends and a flexible adhesive layer, and by degradation effects. For a proper design knowledge about joint configurations and available methods to evaluate mechanical performances is necessary.

The screening of possible joint configurations for the application under consideration is an important step in the design process. Examples of practical solutions are given in figure 2.7. The basic assumption of the screening process is to avoid tensile stresses within the bondline as much as possible. Recommendations for preferable joint configurations in relation to the applied load are summarized by Adams and Wake (1984), Kaasschieter and Van der Sluis (1991) and Shields (1985).

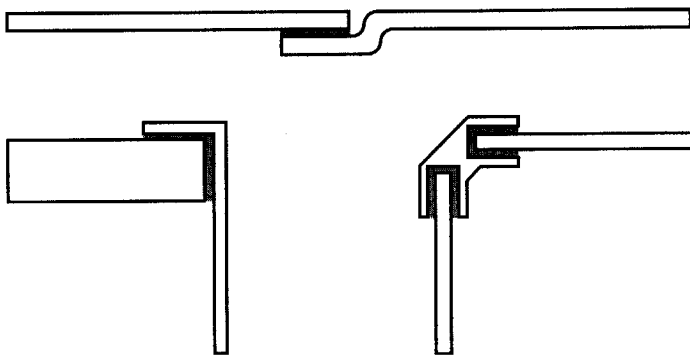


Figure 2.7 Examples of various joint configurations used in practice

Methods to evaluate the mechanical performances of adhesive bonded joints can be based on either theoretical basis or tests (Adams and Wake, 1984). Various analytical solutions have been proposed over the years and with finite element methods it is possible to make detailed calculations including physical and geometrical non-linear behaviour. Issues directly related to these theoretical analyses are the determination of material properties and the selection of a proper failure criterion. A test programme on the other hand focuses on particular applications. Theoretical analyses are mostly used for optimization purposes, while tests are mostly used to validate a final design.

Methods to evaluate degradation effects after ageing of adhesive bonded joints are based on

tests (Kinloch, 1983). The ageing process is accelerated by intensifying the environmental actions in a climate chambers. Issues related to these tests are the definition of the environmental actions, how to accelerate the tests and the translation of the results for in-use conditions. These tests are mostly used to select an appropriate adhesive bonding system.

2.3.3 Manufacturing process

The development of a manufacturing process is an essential aspect within the design process of adhesive bonded joints. Performances are sensitive to variations in the production and might have a significant influence on the scatterband of the resistance. For a proper design the engineer must have knowledge about available quality assurance systems to control the manufacturing process.

The manufacturing process can be seen as a sequence of activities. The preparation of the adherends is the first step within this process. Normally a surface pretreatment is done and sometimes an additional layer is formed. The next step is related to the actual bonding of the components. Aspects related to this step are the mixing of the adhesive, the pot life representing the effective time for an adhesive after preparation that can be used to perform the actual bonding, the use of equipment, and the influence of temperature and humidity. The curing of the adhesive is the following step. In many cases the joint is fixed. Sometimes the curing process has to be activated by a higher processing temperature, higher processing humidity or ultraviolet radiation. After curing the joint is strong enough to be loaded.

The development of the manufacturing process and quality assurance system is not only related to the adhesive bonding system, but is also influenced by the potential of the workshop involved and legislations related to safety and environmental requirements. A quality assurance system might be very useful to be sure that all requirements are met during and after manufacturing. Aspects that are related to this, are the use of checklists, the control by non-destructive testing, the education and training of personnel, and the definition of safe handling precautions. Several tools and techniques to evaluate those aspects are reviewed within the European research project Eureka EU716 (1995) during the 1990's.



Development of Design Rules

The design of structures is concerned with the generation of solutions and the verification of the reliability. Potential design solutions are a result of a process of problem formulation, definition of objective functions, conceptual design and optimization. To control this process, many strategies have been developed over the years. An example of a practical approach is the mix of creative and systematic methods proposed by Cross (1994). The reliability of the selected design solution is mostly verified with use of design rules. For engineering practice it is essential that these rules are generally accepted. Codes and standards can be seen as such state-of-the-art guidelines. In this chapter philosophies of reliable design are discussed and a proposal is made for the development of design rules for structural adhesive bonded joints (Van Straalen, et.al., 1999A).

3.1 Historical developments

In the old days the experience of ancient builders guaranteed the reliability of structures. The Gothic cathedral of Amiens in France build during the period 1220-1280 is generally seen as one of the best examples of the ultimate knowledge of medieval builders. They made use of the principles described by the Roman master builder Vitruvius approximately 30 BC (Vitruvius, Morgan and Warren, 1960). A well-known handbook is the 'Vitruvius-Teutsch' (Gualtherum and Rivium, 1548), which can be regarded as a medieval design guideline. These design methods had been used for many centuries. A turning point in the guarantee of the reliability of structures was the industrial revolution in the early 19th century. The use of new materials and other applications forced modern builders to change their design philosophy.

Since the introduction of materials such as cast iron used in for example bridges and industrial buildings, new techniques have been developed to design by calculation. One of the pioneers in developing the theory of mechanics was Navier (1833). As a professor at the École des Ponts et Chaussées in Paris he formulated the basic principles of the theory of elasticity. But probably of greater importance is that he tried to implement these principles in practical engineering, as for example in making new designs for suspension bridges. Further developments in design were initiated by the use of mild steel, reinforced concrete, aluminium and fibre reinforced materials in the 20th century. Related to these new calculation methods was the introduction of the safety factor.

The safety factor used in design takes into account the uncertainties about loads and strengths. In a comprehensive overview Beeby (1994) shows the major developments in the application of safety factors over the years. The early development of ideas on reliability shows that these are strongly related to the method of design, as is properly documented in a paper by Pugsley (1951). In the early 19th century the ultimate load design was introduced for cast iron structures. In this approach the load is increased by a safety factor of 4 to 6, and this value is compared with experimental determined resistance of cast iron beams and columns. During the second half of that century, however, the theory of elasticity was well understood and a direct link was made with allowable stresses. In this approach the stress in the material is limited to some fraction of its failure stress and this value is compared with the calculated stress under a specified loading. The allowable stress design approach was widely accepted by the end of the 19th century and has been extensively used in the 20th century. The specified loads and allowable stresses were mainly based on engineering practice and depended

Development of Design Rules

strongly on the field of application. The resulting inconsistencies and uncertainty of reached reliability level were the reasons for a growing dissatisfaction about these approaches amongst leading structural engineers in several fields around the Second World War. During this period more consistent reliability concepts based on statistical means were discussed.

The possibilities of designing a structure directly for a specified reliability were first investigated in the aeronautical industry during the Second World War. Serious attempts to apply probabilistic techniques to design were made a decade later. From that time on these techniques have been developed and implemented in design practice. A disadvantage of probabilistic methods is that the calculations can only be performed by experts and that these calculations are too extensive for daily design practice.

Another more consistent reliability concept developed simultaneously, known as the partial factor approach, combines the ultimate load design and allowable stress design approaches. This approach has its roots in composite materials such as reinforced concrete and most of the modern structural design codes make use of it. The general principles were adopted by the Comité Européen du Béton (1964). The aim of the approach is to achieve a more uniform reliability of a structure than that given by the allowable stress approach. This could be reached by using specific partial factors for each type of loading and material dependent partial factors. This flexible system has the advantage that it can deal with different levels of uncertainties for both loads as well as materials. The use of statistical means led the Comité Européen du Béton (1964) to describe the partial factor approach as semi-probabilistic. The relation between the partial factor approach and probabilistic methods is well established nowadays.

3.2 Structural reliability methods

3.2.1 Use of the limit state concept

Discussions about the use of new theories to quantify the reliability of a structure are going back to the years before the Second World War. For example Van den Broek (1940) developed during this period attempts to modify the allowable stress approach, by taking the post-elastic behaviour of structural components into account. Freudenthal (1945) on the other hand discussed the possibilities of using statistical techniques to quantify the safety factor within the scope of the generally used allowable stress approach. The common issue within all these papers, see also the discussion of Pugsley (1951) about future trends, is the application of the term "probability of reaching a limit state". These developments and discussions can be seen as the first steps in developing a new concept of design, which also incorporates the so-called limit state concept.

The limit state is defined as the condition in which the structure is no longer capable to fulfil its function under given actions. In practice this means that the structure collapses or that the structure can not be used normally. A mathematical presentation is given by the limit state function defined as the difference between the resistance R and the action effect S :

$$Z = R - S \quad (3.1)$$

As long as $Z > 0$ the structure fulfils its function, while for $Z < 0$ it does not; the limit state is reached if $Z = 0$.

Both the resistance R and the action effect S can be regarded as stochastic variables. They are represented by their probability density functions $f_R(r)$ and $f_S(s)$ respectively. If the resistance and the action effect are statistically independent, their combined probability density function is defined as $f_R(r)f_S(s)$. This function can be graphically presented by contours in its R - S plane, as indicated in figure 3.1. The probability of reaching the limit state is equal to the integral of the combined probability function for which $Z < 0$. Mathematically this probability is given by:

$$P(Z < 0) = \iint_{R < S} f_R(r) f_S(s) dr ds \quad (3.2)$$

This integral can also be applied to time-dependent limit state functions. To solve equation 3.2 several methods have been developed, see for example Benjamin and Cornell (1969). Exact probabilistic methods like those based on a direct numerical solution of the above given integral and the Monte Carlo simulation, take the full probability density functions of all variables into account and the exact non-linear limit state function if present. Methods like the first-order reliability method (FORM) and second order reliability method (SORM) that are approximations for non-linear limit state functions, simplify the problem. These exact and approximate methods are also known as level III and level II methods respectively. The essence of the level II methods is that they linearise the limit state function Z around a point of the limit state $Z = 0$ with the highest probability density. This point is known as the design point. The advantages of the level II methods over the level III methods are that they are easier to use for practical applications and that they give additional information about the contribution of each variable to the probability of reaching the limit state. Using these probabilistic methods it is now possible to quantify the structural reliability and, perhaps more importantly, the results can be used to calibrate design rules for daily engineering practice.

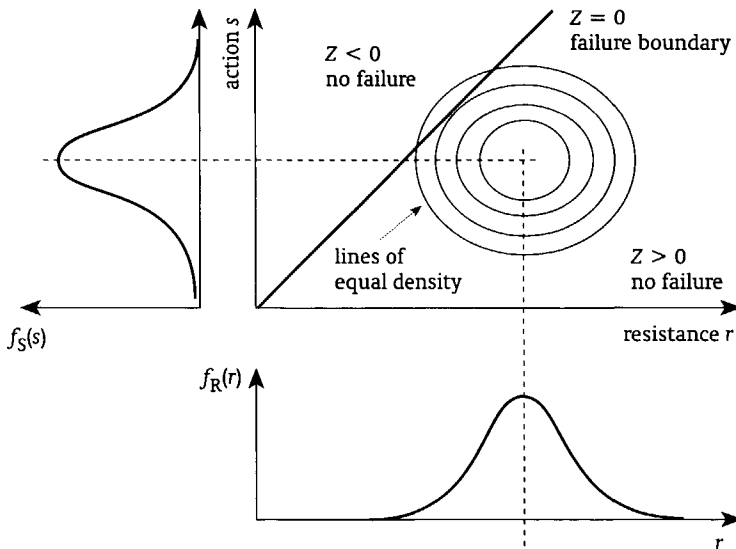


Figure 3.1 Statistical presentation of the limit state concept

Development of Design Rules

Instead of presenting the results of probabilistic methods in terms of the probability of reaching the limit state, the reliability index β as proposed by Hasofer and Lind (1974), is commonly used in level II analyses. The relation between the probability of reaching the limit state $P(Z < 0)$ and the reliability index β is given by:

$$P(Z < 0) = \Phi(-\beta) \quad (3.3)$$

where $\Phi(\cdot)$ is the standard normal distribution function. In EN 1991 (1995/1997/1998) indicative values for the target reliability index β are given for three limit states. Values given as a requirement per year are presented in table 3.1 together with matching probabilities of reaching the limit state. For the ultimate limit state failures as yielding of a cross section, brittle fracture, buckling of a shell element or collapse of a joint are checked. For the fatigue limit state, for which potential crack growth due to cyclic loads is checked, the value of the reliability index depends on the degree of inspectability, repairability and damage tolerance. Finally the serviceability limit state considers issues as deformations, vibrations and cracks. The reliability index β can be related to the partial factor approach, which is also known as the level I method.

Table 3.1 Indicative values for the target reliability index β given as a requirement valid for 50 years, together with matching probabilities (EN 1991, 1995/1997/1998)

limit state	target reliability index β	matching probability
ultimate	3.8	0.000072
fatigue	1.5 to 3.8	0.067 to 0.000072
serviceability	1.5	0.067

3.2.2 Partial factor approach

The most convenient structural reliability method for daily design practice is the partial factor approach. After the introduction of this approach by the Comité Européen du Béton (1964) the term partial safety factor was used, but nowadays the term partial factor is preferred. This approach is derived from the limit state concept and takes the stochastic nature of both the resistance and action effects into account by using partial factors.

Within the partial factor approach the structural reliability is validated by comparing the so-called characteristic values for the action S_k and the resistance R_k :

$$\gamma_S S_k \leq \frac{R_k}{\gamma_R} \quad (3.4)$$

where γ_S and γ_R are the partial factors for the action effects and the resistances respectively. The use of characteristic values was already introduced by the Comité Européen du Béton (1964). Mostly the characteristic values are based on statistical means. For the action wind load the characteristic value might be equal to the load that occurs once in a 50 years period, while for the action floor load the probability of overload during lifetime has to be lower than a defined target. Comparable definitions are given for the characteristic value of the resistance. If the resistance can be described by a normal probability distribution with a mean

value μ_R and a standard deviation σ_R , the characteristic value is equal to:

$$R_k = \mu_R - k \sigma_R \quad (3.5)$$

where k is the constant of the standard normal probability distribution. If the probability is less than 0.05 the value of k is equal to 1.64. The values of the partial factors on the other hand have to be determined by calibration. In the second recommendations of the Comité Européen du Béton (1970) it is stated that these values are only intended to take account of those aspects not yet amenable to statistical treatment. This means that the reliability is based on engineering judgement. But developments in probabilistic techniques since 1970 has opened new ways to calibrate partial factors.

To relate the partial factor approach with probabilistic techniques, a relation between level I and II methods has been developed. The key to this relation is the level II design point, defined as the point of the limit state $Z = 0$ with the highest probability. In figure 3.2 the definition of the design point (R_d , S_d) according to a level II method, is illustrated for normal probability distributions of the action effect and the resistance. Due to the fact that in this graph for both axes S and R are divided by their standard deviations, the meaning of the reliability index β becomes clear. The reliability index β is equal to the number of standard deviations between the mean value of the limit state function Z and the design point. The so-called weighting factors α_S and α_R indicate which part of the reliability index counts for the action effect and for the resistance respectively. Their absolute values range between 0 and 1. A higher value indicates a more significant influence to the reliability. According to this presentation the design values for the resistance and action effect are defined such that the probability of having a more unfavourable value equals:

$$P(S > S_d) = \Phi(-\alpha_S \beta) \quad (3.6)$$

$$P(R < R_d) = \Phi(\alpha_R \beta) \quad (3.7)$$

The essence of the method is the setting α_S and α_R to fixed values. According to EN 1991 (1995/1997/1998) both equal to -0.7 and $+0.8$ respectively. These values are given for dominating variables and seem to be valid for a wide field of applications. If an action or resistance model contains more basic variables, the fixed values of α_S or α_R for additional non-dominating variables are chosen equal to -0.3 and $+0.3$ respectively. The above given definition might indicate that design values for the resistance and the action effect are fully independent, but this is not the case. From figure 3.2 it can be seen that the values of the weighting factors α_S and α_R are related to each other by the relative values of the standard deviations of the resistance and the action effect. They are influenced by the scatterbands of both the action effect and the resistance. Using equations 3.6 and 3.7 it is possible to calculate the design values S_d and R_d for all kinds of distributions. If normal probability distributions for the action effect and resistance are assumed, the design values for the ultimate limit state are:

$$S_d = \mu_S - \alpha_S \beta \sigma_S = \mu_S + 0.7 \cdot 3.8 \sigma_S = \mu_S + 2.66 \sigma_S \quad (3.8)$$

$$R_d = \mu_R - \alpha_R \beta \sigma_R = \mu_R - 0.8 \cdot 3.8 \sigma_R = \mu_R - 3.04 \sigma_R \quad (3.9)$$

Development of Design Rules

The relation between the level I and II methods can now be determined with use of equation 3.4:

$$\gamma_s = \frac{S_d}{S_k} \tag{3.10}$$

$$\gamma_s = \frac{R_k}{R_d} \tag{3.11}$$

The above given simplified presentation of the procedure to determine partial factors is the fundamental method of the calibration of design rules with use of probabilistic techniques.

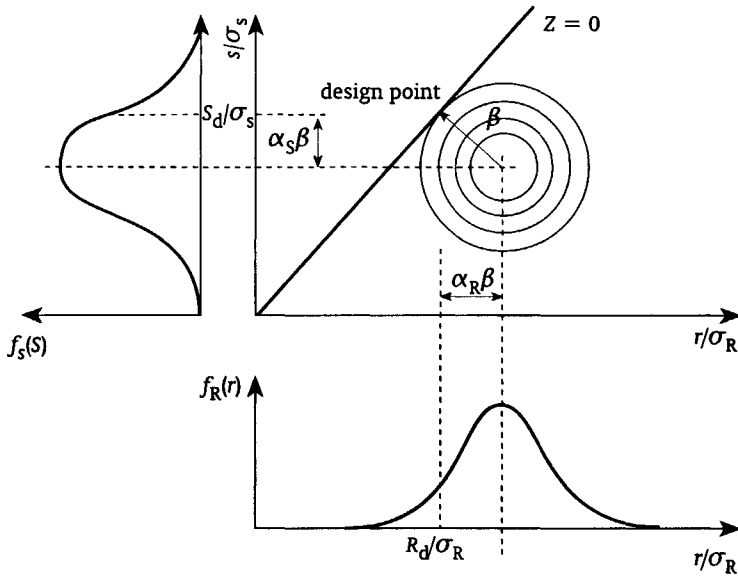


Figure 3.2 Location of the design point on the limit state boundary $Z = 0$

From a practical point of view the partial factors take the stochastic nature of the action effect and the resistance into account. The partial factor of the action γ_s covers:

- the possibility of unfavourable deviations of the action effect from the characteristic value;
- the uncertainty in the action model;
- the uncertainty in the assessment of the action effect.

The partial factor of the resistance γ_R on the other hand covers:

- the possibility of unfavourable deviations of the resistance from the characteristic value;
- the uncertainty in the resistance model, including for example geometrical and material properties.

The above mentioned aspects have to be considered while calibrating partial factors.

In principle the partial factor approach according to equation 3.4 defines the action effect S and the resistance R in general terms. For practical purpose their values can represent respectively the applied load and the strength of the component. But in some cases it is more convenient to determine the action effect and to compare this value with a failure criterion.

For example for an adhesive bonded joint the stress state within the bondline due to the applied load can be calculated and compared with a proper failure criterion. Design rules mostly represent the action effect S and the resistance R in a formulation, which is the most convenient one for the considered situation.

The partial factor approach opens the possibility to develop a coherent set of design rules. Instead of determining the partial factors for each possible application according to the procedure described in the preceding section, researchers and code-writers have harmonised design rules for wider fields of applications. It is found that for comparable applications the use of characteristic values results into consistent values for partial factors. This is based on extended probabilistic studies, see for example Vrouwenvelder and Siemes (1987). The advantage for daily design practice is that a consistent set of design rules with only a limited number of partial factors can be used.

Nowadays the partial factor approach has been applied in many design codes. The Eurocodes primarily used for building applications, EN 1991 (1995/1997/1998), EN 1992 (1994/1996/1997), EN 1993 (1995/1996/1997/1998), EN 1994 (1994/1995/1997), EN 1995 (1994/1995/1997), EN 1996 (1995/1998/1999), EN 1997 (1995), EN 1998 (1995/1996/1997/1998) and EN 1999 (1998), give characteristic values of both actions and resistances together with matching partial factors. Following the discussions of the Delft IABSE Colloquium (Vrouwenvelder, 1996) it becomes clear that each of these codes has its own format due to a different elaboration of the partial factor approach. To avoid the possibility of developing inconsistent design rules that do not meet the required target reliability, it is necessary to define a coherent system of characteristic values and matching partial factors.

The reliability of most of current design codes is guaranteed by many decades of engineering practice. Up till now probabilistic techniques have mainly been used for differentiating partial factors. For example in case of the Dutch building codes extensive calibration studies were performed during the 1980's (Vrouwenvelder and Siemes, 1987) and different parts of Eurocode 3 (EN 1993, 1995/1996/1997/1998) and Eurocode 4 (EN 1994, 1994/1995/1997) were considered in this way. But probabilistic methods have also the possibility of calibrating design rules for new applications like adhesive bonded joints (Van Straalen, et.al., 1997A, 1998A and 1998C).

3.2.3 Time dependent effects

To develop design rules for structural adhesive bonded joints it is necessary to take time dependent effects into account. As explained in section 2.2 the structural behaviour of adhesive bonded joints can be significantly influenced by both mechanical and environmental actions during its lifetime. These time dependent effects as degradation have an influence on the structural reliability and for this reason they have to be considered within probabilistic methods. But up till now no comprehensive overview on this issue is available in literature; only a broad variety of publications on specific topics and applications can be found.

To take time dependent effects on both the resistance $R(t)$ and the action effect $S(t)$ into account, the limit state function given by equation 3.1 has to be reformulated as follows:

$$Z(t) = R(t) - S(t) \quad (3.12)$$

As long as $Z(t) > 0$ is fulfilled during the time period $(0, t)$ no failure will occur, while the structure fails at time t if $Z(t) < 0$. To calculate the probability of reaching the limit state

Development of Design Rules

during the period $(0, t)$ it is possible to divide the action history in a sequential series of actions, which are no longer time dependent within one period. See figure 3.3. The probability of reaching the limit state within one time period can be calculated with equation 3.2. But to calculate the probability of reaching the limit state for the sequential series of actions an extended procedure has to be followed. Before discussing such a procedure, the principles are illustrated for the case that only the action effect is time dependent. The total time is divided into two periods $(0, t_1)$ and (t_1, t_2) . The probability of reaching the limit state is given by:

$$P(Z(t) < 0 \text{ for } 0 \leq t \leq t_2) = \iiint_{s_1 > r \text{ or } s_2 > r} f_R(r) f_{S_1, S_2}(s_1, s_2) dr ds_1 ds_2 \quad (3.13)$$

where $f_R(r)$ is the probability density function of the resistance and $f_{S_1, S_2}(s_1, s_2)$ the probability density function of the action effect. If the resistance R is a constant value, the probability of reaching the limit state is equal to:

$$P(Z(t) < 0 \text{ for } 0 \leq t \leq t_2) = P(S_1 > R) + P(S_2 > R \text{ and } S_1 < R) \quad (3.14)$$

The probability of reaching the limit state for a complete sequential series of actions can be presented by extended versions of equations 3.13 or 3.14. The suitability of these formal descriptions is limited for practical cases. For this reason researchers have looked after simplified methods.

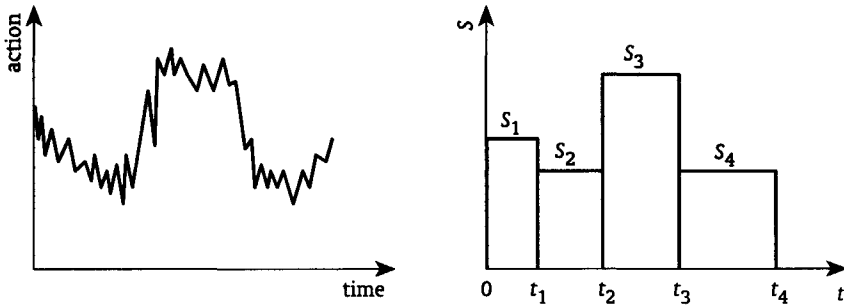


Figure 3.3 Transformation of a history of action in a sequential series of actions

An example of a time dependent action is the wind load. One of the simplest methods to model this action is to determine the extreme load S_t during the reference period t_{ref} . This implies that the value of the load is no longer time dependent. The probability of reaching the limit state can now be determined easily by:

$$P(Z(t) < 0 \text{ for } 0 \leq t \leq t_{ref}) = P(S_t > R) \quad (3.15)$$

In this model the problem of the time dependent effect is changed into the determination of the probability density function of the extreme load S_t . But there are other methods used to model the wind load and to place this action within the context of probabilistic design.

Besides the effects of the time dependency of actions, also the change of the resistance during the lifetime has an influence on the probability of reaching the limit state of a structure.

The following time dependent effects relevant for the resistance of adhesive bonded joints, can be distinguished:

- Fatigue. If a joint is sensitive for crack initiation and growth, its resistance depends on the history of the applied cyclic loads.
- Creep. If the deformation of the joint increases during time due to creep, its resistance depends on the history of the applied long-term load.
- Degradation of material properties. If the properties of the adhesive or the interface are effected by the environment, the resistance of the joint degrades during its lifetime.

In principle it is possible to consider all these time dependent natures of the resistance within the context of probabilistic methods. To illustrate the potential of statistics the time is assumed to be the only significant parameter.

If the degradation of the resistance only depends on the parameter time, it can be represented by the generalized function $R(t)$. For the simplest situation of a constant action effect during the time period $(0, t_p)$, the probability of reaching the limit state is equal to:

$$\begin{aligned} P(Z(t) < 0 \text{ for any } t \text{ in } 0 \leq t \leq t_p) = \\ P(S > R(t) \text{ for any } t \text{ in } 0 \leq t \leq t_p) = P(S > R(t_p)) \end{aligned} \quad (3.16)$$

This means that the probability of reaching the limit state during the total time period is equal to the probability of reaching the limit state at the end of the time period, assuming that $R(t)$ is a monotone decreasing function. Instead of a constant action, in practice the action has a fluctuating nature. To calculate the probability of reaching the limit state for this case, it is necessary to divide the action history in a sequential series of actions as already indicated in figure 3.3. For two periods $(0, t_1)$ and (t_1, t_2) , the probability of reaching the limit state can be calculated according to a slightly modified version of equation 3.13:

$$\begin{aligned} P(Z(t) < 0 \text{ for any } t \text{ in } 0 \leq t \leq t_2) = \\ \iiint_{s_1 > r(t_1) \text{ or } s_2 > r(t_2)} f_R(r, t) f_{s_1, s_2}(s_1, s_2) dr ds_1 ds_2 \end{aligned} \quad (3.17)$$

where $f_R(r, t)$ is the time dependent version of the probability density function of the resistance. R_1 and R_2 are the values of the resistances for the points in time t_1 and t_2 respectively. For practical means it is probably better to use a modified version of equation 3.14, which can be easily extended for p periods:

$$\begin{aligned} P(Z(t) < 0 \text{ for any } t \text{ in } 0 \leq t \leq t_p) = \\ P(S_1 > R_1) + \sum_{i=2}^p P(S_i > R_i \text{ and } S_j > R_j \text{ for all } j = 1 \text{ to } i - 1) \end{aligned} \quad (3.18)$$

The value of this probability can be estimated by the following conservative approximation:

$$P(Z(t) < 0 \text{ for } 0 \leq t \leq t_p) = \sum_{i=1}^p P(S_i > R_i) \quad (3.19)$$

To solve equation 3.18 or 3.19 for practical applications probabilistic techniques based on level III or level II methods have to be used. The calculated probability can be compared with the target reliability index β .

The above given procedure is far too complicated for practical design purposes. The partial

Development of Design Rules

factor approach seems to be the most appropriately alternative. To take time-dependent effects into account, a so-called conversion factor η_t is introduced by ISO/DIS 2394 (1996) in addition to the original partial factor approach:

$$\gamma_s S_k \leq \frac{\eta_t R_k}{\gamma_R} \quad (3.20)$$

The calibration of the value of the conversion factor has to be based on the principles discussed in this section.

3.3 Developing design rules for structural adhesive bonded joints

As explained in chapter 2 the structural application of adhesive bonded joints is based on a technology with multi-disciplinary aspects. The main issues of the design process are the selection of an adhesive bonding system, the structural design and the development of a manufacturing process. Identified aspects related to these issues are the choice of the joint configuration, the type of mechanical action, types of environmental actions, the mode of failure, degradation effects and the stochastic nature. These issues and related aspects have to be taken into account while developing a design rule.

For adhesive bonded joints the same weighted target reliabilities as for other structural components (EN 1991, 1995/1997/1998) might be used, because the stochastic nature does not differ such that structural reliability changes significantly. This means that current design rules can be used for the determination of the design values of the actions. Various standards and codes dealing with mechanical actions like static, impact and fatigue loads are available for all kind of applications. Modern versions, see for example EN 1991 (1995/1997/1998), give characteristic values as well as matching partial factors for mechanical actions.

To develop widely accepted design rules to determine the design value of the resistance, it is necessary to have agreement about the conditions. This is because the resistance of adhesive bonded joint depends strongly on time and temperature. The following conditions related to equation 3.20, are defined here:

- The prediction model to calculate the characteristic value of the resistance R_k has to take into account the mode of failure.
- The characteristic value of the resistance R_k and the matching partial factor γ_R represent the strength after curing of the adhesive, without any degradation effects. Mostly a room temperature condition is used, but it is possible to take the temperature dependency of the adhesive into account.
- The degradation effect caused by an environmental action, is represented by the conversion factor η_t . This means that this environmental action is directly related to the right term of equation 3.20 and not to the left term. An important aspect related to degradation effects is the development of the strength during lifetime, see also figure 2.5. In principle it has to be confirmed that this development stabilizes during the lifetime.
- Manufacturing effects are directly related to the determination of the characteristic value of the resistance R_k and the calibration of the partial factor γ_R . If these values do not take all manufacturing effects into account, an additional conversion factor η_m has to be defined. Such a factor can also be used within the scope of a quality assurance system.

These conditions are together with the checking formula given by equation 3.20 the basis of a

systematic approach to develop design rules for structural adhesive bonded joints (Van Straalen, et.al., 1998D and Van Straalen, 2000A).



Calibration Techniques for Design Rules

Design rules for structural adhesive bonded joints have to fulfil a prescribed target reliability level. To reach this target design rules based on the partial factor approach have to be calibrated. In the past this was done by engineering judgement, but probabilistic analyses open new possibilities. In addition to what is said in chapter 3 about the development of design rules, in this chapter detailed background information is provided how to calibrate partial and conversion factors.

4.1 Engineering judgement and probabilistic analyses

As mentioned in section 3.2, the calibration of partial and conversion factors can be done by either engineering judgement or probabilistic analyses. The judgement of engineers in design gathered during many decades gives qualitative indications which values of the partial and conversion factors are realistic. Objective probabilistic analyses on the other hand provide quantitative information about the reached reliability levels and the values of partial and conversion factors. For design rules with a long tradition, probabilistic analyses are only used to make some refinements. For structural components for which the design experience is limited, probabilistic analyses are essential in gathering valuable data. Since design rules for adhesive bonded joints are not crystallized into guidelines, probabilistic analyses are a straightforward tool in the calibration process.

Engineering judgement has always been important in the calibration of design rules. Pugsley (1951) explained that with the introduction of cast iron in the early nineteenth century, engineers developed the first rudimentary system for measuring a margin of safety by a single factor. Material development, experience in design and refined calculation methods gave engineers the opportunity to lower the value of this factor without reducing the level of reliability. Pugsley also showed that engineering judgement is based on the experience of designers and on compromises. He mentioned for example that after the First World War British designers with different backgrounds had to develop large airships. The engineers with a naval background were used to the allowable stress design, while those with an aerospace background trusted the ultimate load design. With their combined experiences they decided to define a series of load cases representing various modes of operation of an airship and multiplied these loads by a load factor equal to 3. The structures had to be strong enough to withstand these factored loads. Also nowadays engineering judgement is still an important tool. For example in the recently published Eurocomp Design Code and Handbook (Clarke, 1996) for polymer composite structures, the partial factor approach is introduced for this application. The extended system of partial factors prescribes values between 1.5 and 10, which depend on used materials and given circumstances. The background information explains that the proposed values are based on those given in the Eurocodes and those used in the daily practice of designing fibre reinforced composites. In general it can be concluded that experience in design and confronting opinions from different points of views initiate the development of design rules.

Additional to engineering judgement probabilistic analyses can be used successfully. Since this study focuses on the strength of structural adhesive bonded joints, only the process of the calibration of design rules related to the prediction of the resistance are considered.

A prediction model is in principle deterministic. The stochastic nature of the resistance is taken into account by the partial factor and if relevant by an additional conversion factor. To calibrate these factors, the deterministic prediction model has to be compared with a data set incorporating all relevant stochastic variances. These data can be based on either test series or numerical simulations. The complete field of applications of the design rule and the stochastic nature of all essential parameters, like dimensions, material properties, temperature dependency and degradation effects, should be covered. Using the test series or numerical simulations the design value has to be determined for the prescribed reliability index β and weight factor α . Additionally the characteristic values according to the prediction model have to be determined. Based on these values, the values of the partial and conversion factors can be established. Advantages of probabilistic analyses are that quantitative information becomes available and that all kind of effects can be studied in detail.

4.2 Statistical description of the resistance

4.2.1 Stochastic distribution functions

In section 3.2.1 it is explained that the stochastic nature of the resistance of a structural component can be represented by a probability density function. Mostly normal, lognormal and Weibull distributions as indicated in figure 4.1, are used.

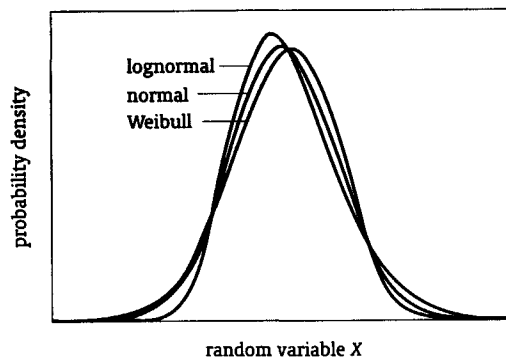


Figure 4.1 Probability density functions of the normal, lognormal and Weibull distributions

To be able to work with the normal, lognormal and Weibull distributions within the calibration process, it is necessary to understand their statistics (Mood et.al., 1974):

- Normal distribution. This is the best-known distribution used in many technical applications. A random variable X is defined to be normally distributed if its density is given by:

$$f_X(x) = \frac{1}{\sqrt{2\pi}\sigma} e^{-\frac{(x-\mu)^2}{2\sigma^2}} \quad (4.1)$$

where the parameters μ and σ are the mean and standard deviation respectively. The cumulative probability function can only be determined by integrating the probability density distribution function:

$$F_X(x) = \int_{-\infty}^x f_X(u) du \quad (4.2)$$

For practical purpose handbooks contain tables to solve this integral. This is done by giving the probability for the standard normal distribution $\Phi(X')$ with the mean and standard deviation of the random variable X' equal to 0 and 1 respectively. The probability $P(x \leq X)$ is now equal to $\Phi\left(\frac{X-\mu}{\sigma}\right)$.

- Lognormal distribution. This distribution is related to the normal distribution. If X is a positive random variable and the new variable Y is defined as the natural logarithm of X ($Y = \ln X$), X is said to have a lognormal distribution if Y has a normal distribution. This means that for practical calculations the statistics for the normal distribution can be used.
- Weibull distribution. This distribution is less known by engineers. A random variable X is defined to be Weibull distributed if its density is given by:

$$f_X(x) = \frac{\beta}{\alpha^\beta} x^{\beta-1} e^{-(x/\alpha)^\beta} \quad (4.3)$$

where β is the shape parameter and α is the scale parameter. The cumulative probability function is equal to:

$$F_X(x) = 1 - e^{-(x/\alpha)^\beta} \quad (4.4)$$

If a distribution function has to be fitted on a series of data, its parameters should be estimated. Let X_1, X_2, \dots, X_n be the sample of data, then the estimate of the mean is equal to:

$$m = \frac{1}{n} \sum_{i=1}^n X_i \quad (4.5)$$

and the estimate of the standard deviation is equal to:

$$s = \sqrt{\frac{1}{n-1} \sum_{i=1}^n (X_i - m)^2} \quad (4.6)$$

To estimate the shape and scale parameters for the Weibull distribution, several methods are proposed. One method makes use of the known relations between these parameters and the mean and standard deviation (Mood, et.al., 1974):

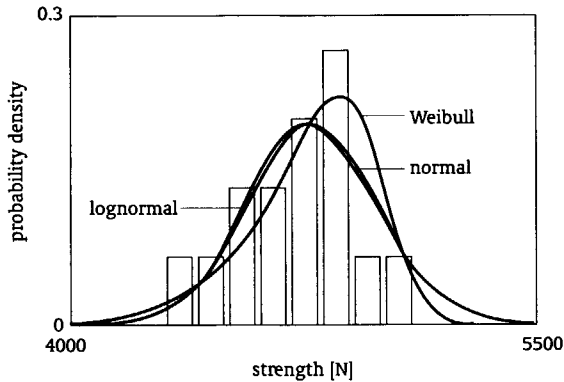
$$\mu = \alpha \Gamma\left(1 + \frac{1}{\beta}\right) \quad (4.7)$$

$$\sigma^2 = \alpha^2 \left[\Gamma\left(1 + \frac{2}{\beta}\right) - \Gamma^2\left(1 + \frac{1}{\beta}\right) \right] \quad (4.8)$$

where $\Gamma(\cdot)$ is the gamma function. The values of the estimated shape parameter β' and scale parameter α' can be calculated by substituting the estimated mean and standard deviation according to equations 4.5 and 4.6 and solving β and α from the coupled equations 4.7 and 4.8. To illustrate the estimation of the parameters of the normal, lognormal and Weibull distribution, the example presented in figure 2.6 is evaluated in figure 4.2.

To develop design rules for structural adhesive bonded joints, it is important to know by which distribution function the resistance is represented best. This is, because design values of the resistance are located within the tail region, where the probabilities differ significantly

for the three considered distributions. The selection of the best distribution can be done on either evaluation of large series of tests or on basis of theoretical considerations.



distribution	parameter	value
normal	mean:	$m_n = 4777 \text{ N}$
	standard deviation	$s_n = 206 \text{ N}$
lognormal	mean (units in N):	$m_n = 8.471$
	standard deviation (units in N):	$s_n = 0.044$
Weibull	shape parameter	$\beta' = 29.033$
	scale parameter	$\alpha' = 4869 \text{ N}$

Figure 4.2 Estimation of parameters of the normal, lognormal and Weibull distributions for an example of a single overlap joint

4.2.2 Design and characteristic values based on test data

To explain the calibration process of a prediction model with use of a data set, the theory of statistics essential for a limited number of observations is presented here. This is done by introducing a procedure to determine the design and characteristic values of the resistance of a structural component by direct evaluation of data. This procedure is based on the Bayesian approach, see for example Raiffa and Schlaifer (1961) and Box and Tiao (1992). The advantage of the Bayesian approach over standard statistics is that it provides a formal mechanism for taking account of prior knowledge instead of interpreting a statistical analyses afterwards.

ISO/DIS 2394 (1996) proposes to use the Bayesian approach to evaluate test data in view of the partial factor approach. If the n test results are assumed to be normal distributed, the design value of the resistance R_d is equal to:

$$R_d = m - t_{\alpha_R \beta}(\nu) s \sqrt{1 + \frac{1}{n}} \quad (4.9)$$

The values of the estimated mean m and standard deviation s have to be calculated according to equations 4.5 and 4.6 respectively. The parameter $t_{\alpha_R \beta}(\nu)$ is the value of the Student distribution. Its value depends upon the parameter ν and the target probability that matches

with the product $\alpha_R \beta$ of the weight factor and the reliability index. The degrees of freedom ν is a function of n , which is equal to $\nu = n - 1$ if no prior knowledge is used. For practical purpose handbooks contain tables to determine the value of the parameter t , a compressed version is presented in table 4.1. Instead of determining the design value of the resistance, this procedure can also be used to calculate the characteristic value R_k . For a target probability of 0.05, the following value has to be determined:

$$R_k = m - t_{0.05}(\nu) s \sqrt{1 + \frac{1}{n}} \quad (4.10)$$

Due to its relation to the normal distribution, the above given procedure can also be used for the lognormal distribution by evaluating data defined as the natural logarithm of the results.

Table 4.1 Value of the Student distribution

target	ν									
	2	3	4	5	6	7	8	9	14	∞
$t_{0.05}(\nu)$	2.92	2.35	2.13	2.02	1.94	1.89	1.86	1.83	1.76	1.64
$t_{\alpha_R \beta}(\nu)^*)$	20.5	9.65	6.86	5.67	5.04	4.64	4.37	4.14	3.70	3.11

$$*) \alpha_R \beta = 0.8 \cdot 3.8$$

For a Weibull distribution the design and characteristic values of the resistance should be determined with a different procedure. If the n test results are assumed to be Weibull distributed, the design value of the resistance R_d is equal to (Van Straalen and Vrouwenvelder, 2000I):

$$R_d = \alpha' \left[-\ln(1 - \Phi(\alpha_R \beta)) \right]^{1/(k \alpha_R \beta^{(n)} \beta')} \quad (4.11)$$

The values of the estimated shape parameter β' and scale parameter α' have to be calculation with use of the coupled equations 4.7 and 4.8. The function $\Phi(\alpha_R \beta)$ gives the target probability that match with the product $\alpha_R \beta$ of the weight factor and reliability index. To determine the value of the parameter $k(n)$ a Monte Carlo simulation can be used (Van Straalen and Vrouwenvelder, 2000I). For practical purpose a compressed table is presented in table 4.2.

Table 4.2 Value of the parameter $k(n)$

target	n									
	3	4	5	6	7	8	9	10	15	∞
$t_{0.05}(\nu)$	0.51	0.63	0.69	0.73	0.76	0.78	0.80	0.81	0.86	1.00
$t_{\alpha_R \beta}(\nu)^*)$	0.15	0.34	0.47	0.55	0.61	0.65	0.68	0.71	0.79	1.00

$$*) \alpha_R \beta = 0.8 \cdot 3.8$$

It is noted here that the choice is made to correct only the shape factor, because this affects the width of the scatterband without introducing a shift of it as a whole. Instead of determining the design value of the resistance, this procedure can also be used to calculate

Calibration Techniques for Design Rules

the characteristic value R_k . For a target probability of 0.05, the following value has to be determined:

$$R_k = \alpha' [-\ln(1 - 0.05)]^{1/(k_{0.05}(n)\beta^1)} \quad (4.12)$$

To illustrate the discussed procedures to calculate the design and characteristic values of the resistance, the example of figure 4.2 is worked out in table 4.3 for the normal, lognormal and Weibull distributions. Comparing the results of these evaluations indicates that the design and characteristic values for the normal and lognormal distribution are in this example close together, while the values for the Weibull distribution are significantly lower. These findings can also be observed from figure 4.2. The presented procedures to evaluate test data are essential within probabilistic analyses to calibrate design rules.

Table 4.3 Calculation of the design and characteristic values of the resistance for the example presented in figure 4.2

distribution	design value R_d [N]	characteristic value R_k [N]
normal	3989	4402
lognormal	4035	4407
Weibull	3616	4270

4.2.3 Selection of a distribution function on basis of tests

To evaluate large series of tests for the selection of the best distribution statistical techniques are available, which give both qualitative as well as quantitative information (Van Straalen, 1998F). It is necessary to understand the limitations of these techniques and to use proper data, otherwise it is not possible to draw up any conclusion. If the analyses are done properly, valuable information about the distribution function becomes available.

To analyse the data of a series of tests several statistical techniques have been developed. Graphical means give a qualitative indication about how well the reference distribution fits with the data. To get the proper dimensions of this function, it is necessary to estimate its parameters on basis of the data. This distribution function and matching data can be graphically evaluated by comparing the probability density distribution, by comparing the cumulative probability distribution, or by using so-called probability paper (Box and Tiao, 1992). These three graphical means are illustrated in figure 4.3. Of these methods the use of probability paper gives the most valuable information, because it is easy to see if the data fits the straight line by which the distribution function is represented, especially near the tail regions.

Additional to those graphical means quantitative methods have been developed. The Chi-square and the Kolmogorov-Smirnov tests (Mood, et.al., 1974) are two well-known goodness-of-fit tests. The Anderson-Darling test (Lawless, 1982) is an alternative. The result of these tests is that they reject a reference distribution for a bad fit with a certain probability of being wrong. This is also a restriction of these tests; they do not verify if a reference distribution is correct. The Chi-square test is not recommended to analyse the resistance of structural components, because this test is not preferred for continuous distributions (Trividi, 1982). In

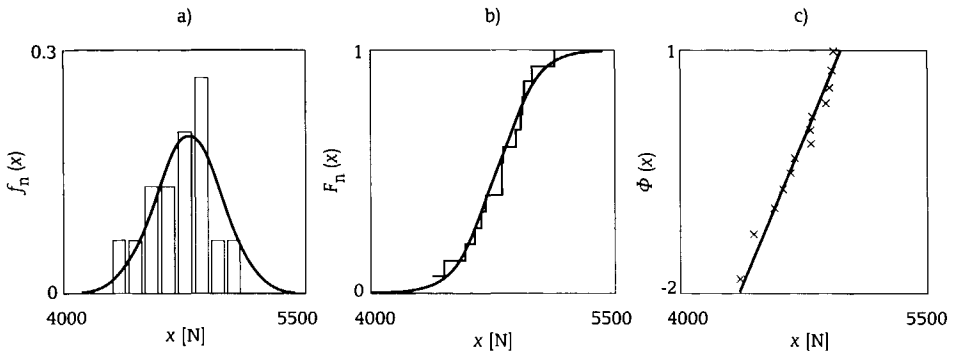


Figure 4.3 Graphical comparison of a normal distribution with 15 data points X of the example presented in figure 4.2: a) probability density $f_n(x)$, b) cumulative probability distribution $F_n(x)$, c) by using so-called probability paper $\Phi(x)$

comparison with Kolmogorov-Smirnov, the Anderson-Darling test is more sensitive to discrepancies in the tail region as argued by Lawless (1982). Additional to this Van Straalen (1998F) concludes that a goodness-of-fit test should only be used to indicate which reference distribution is preferable.

To select a distribution function for the failure load of adhesive bonded joints three series of test data are analysed by Van Straalen (1998F). As a part of the British DTI MTS Adhesive programme from 1994 to 1996 a round robin was undertaken by five laboratories (Beevers, 1997). For two adhesives, the two-component acrylate F241 of Permabond and the two-component epoxy Araldite 2001 of Ciba, single overlap joints with an overlap of 10 mm, a width of 25 mm and 1.2 mm thick steel adherends, were tested. Each laboratory fabricated 30 specimens for each adhesive. These were equally distributed over the laboratories and tested. Most of the results of these two series of tests are used in this analysis. The third test series considered is from Fokker (De Regt, 1998). During the production of the Fokker 100 single overlap joints with an overlap of 12.5 mm, a width of 25 mm and 1.6 mm thick aluminium adherends were prepared and tested as a part of the quality assurance procedures. In this analysis eight batches of 7 specimens each for the two-component epoxy EC2216 of 3M are used. Additional series and sub-sets were analysed in the original study by Van Straalen (1998F), but these results indicate that for 30 or less data points no consistent conclusions can be drawn up.

Using probability paper and the Anderson-Darling goodness-for-fit test the three series of test data are compared with the normal, lognormal and Weibull distributions. The results of these analyses are presented in figure 4.4. The graphs indicate how well the straight line of the reference distribution follows the data, while the Anderson-Darling test calculates the so-called observed significance level. Its theoretical meaning is that if the value is less than 0.05, the hypothesis that the reference distribution does not fit is rejected with at most a five percent probability of being wrong. Its practical meaning is that the reference distribution with the highest value fits best. The results presented in figure 4.4 indicate that a Weibull distribution gives the best fit with the three considered series of test data and that a normal distribution gives an acceptable fit.

Calibration Techniques for Design Rules

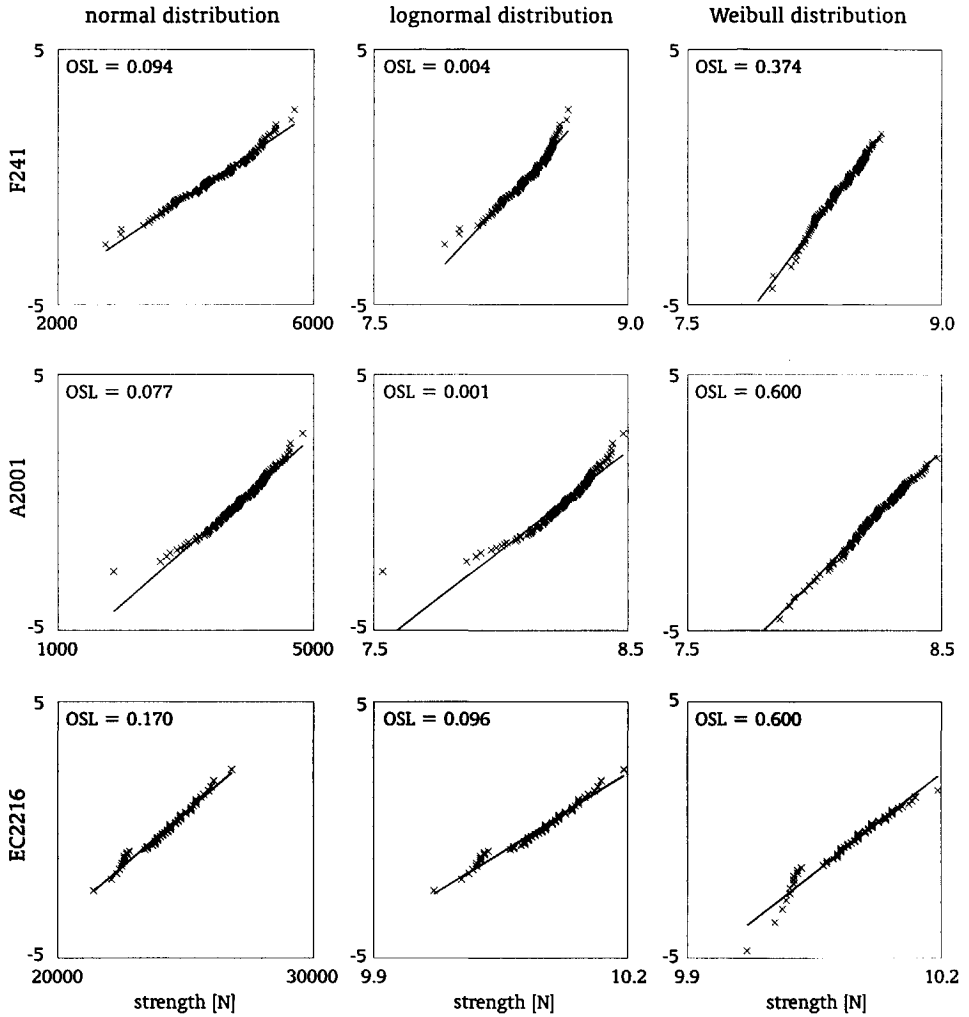


Figure 4.4 Comparison of three considered test series with the normal, lognormal and Weibull distributions; the horizontal axis represents the failure load, the vertical axis represents the standard distribution $\Phi(X)$ of the considered distribution and OSL is the calculated observed significance level according to the Anderson-Darling goodness-for-fit test (Van Straalen, 1998F)

4.2.4 Selection of a distribution function on basis of theoretical considerations

The failure behaviour of adhesive bonded joints can be described by the weakest link theory as discussed by many researchers, see for example Tippett (1925) and Weibull (1949). It is developed for materials like timber and composite fibres with brittle failure behaviour. It assumes that the material can be modelled by a series of reference volumes, which resistance is as strong as its weakest link.

The statistics of the weakest link theory is described by Weibull (1949). The probability of

failure of one reference volume i is equal to the probability that the resistance R_i is smaller or equal to level r :

$$P_i = P(R_i \leq r) = F_{R_i}(r) \quad (4.13)$$

The weakest link theory assumes that the lower tail of the cumulative distribution function $F_{R_i}(r)$ can be described by the following function:

$$F_{R_i}(r) = \left(\frac{r}{r_c}\right)^\beta \quad (4.14)$$

where r_c is the mean value of the resistance of one reference volume. A system of n reference volumes survives if each of the members survives. The probability of survival of the whole system is now equal to:

$$P(R > r) = P(R_1 > r \text{ and } R_2 > r \text{ and } R_n > r) \quad (4.15)$$

If all reference volumes are independent and identical with a probability of failure described by equations 4.13 and 4.14, this expression can be worked out as follows:

$$\begin{aligned} P(R > r) &= P(R_1 > r) \cdot P(R_2 > r) \cdot \text{.....} \cdot P(R_n > r) \\ &= \{P(R_i > r)\}^n \\ &= \{1 - F_{R_i}(r)\}^n \\ &= e^{-n F_{R_i}(r)} \\ &= e^{-n (r/r_c)^\beta} \end{aligned} \quad (4.16)$$

Using this result the cumulative distribution function of the resistance can be determined:

$$\begin{aligned} F_R(r) &= P(R \leq r) \\ &= 1 - P(R > r) \\ &= 1 - e^{-n (r/r_c)^\beta} \end{aligned} \quad (4.17)$$

This relation is similar to the Weibull distribution given by equation 4.4. On basis of these theoretical considerations it is concluded that for brittle failure behaviour the Weibull distribution fits well.

Together with the results of the evaluation of the test series, it is concluded that the stochastic nature of the resistance of adhesive bonded joints can be described properly by a Weibull distribution. The normal distribution might be used as an alternative, if difficult statistical calculations have to be avoided.

4.3 Probabilistic calibration techniques

4.3.1 Generation of a set of data

The probabilistic analyses to calibrate design rules make use of sets of data that incorporate the stochastic nature of the resistance. As explained in section 4.1, these data can be based on either tests or numerical simulations and have to cover the field of application of the

Calibration Techniques for Design Rules

considered design rule. Since the experience and confidence in numerical simulations for adhesive bonded joints is limited, in this study only the use of tests is considered. To end up with valid results it is necessary to pay attention to the planning, execution and evaluation of test series.

The planning of a test series starts with the formulation of the objective, followed by a qualitative analysis. With this analysis various aspects have to be investigated. Aspects to be mentioned are failure mechanisms, boundary conditions, loading conditions, environmental conditions, time effects and differences between testing and reality. On basis of these results a relevant test arrangement has to be defined. This includes the specification of the type of specimen, definition of the execution of tests, choice of environmental conditions, methods of observation and recording, method of evaluation, number of tests, selection procedure of specimens and design of the test rig. The whole process is not an easy task and requires appropriate theoretical knowledge, experience in testing and engineering judgement.

After the planning of the test series has been worked out, specimens have to be produced and selected, the test rig has to be built and the test programme has to be carried out. To ensure that the results are valid, the chosen measurement techniques have to be in accordance with the required tolerances. It is important that the execution of tests is in accordance with the planning. If there is a discrepancy between the testing and the original planning, for example if an unexpected failure mechanism occurs, the planning of the test series must be reconsidered. After the tests are finished, the results have to be evaluated. Attention should be paid to the behaviour during execution and the failure mechanism of the tests. Now the screened test results can be used as input of probabilistic calibration techniques.

4.3.2 Calibration of the partial factor

Design rules developed within the scope of the partial factor approach, make use of prediction models that are assumed to be deterministic. These models can be represented by the general formula:

$$R_{pm,det} = f(\underline{W}, \underline{X}_{nom}) \quad (4.18)$$

The vector \underline{W} consists of variables with a deterministic nature. The the vector \underline{X}_{nom} on the other hand consists of variables which are in principle stochastic, but are assumed to be deterministic. To calibrate the partial factor the set of data has to incorporate all essential scatters. For this type of prediction models the proposed procedure of calibrating design rules can deal with either rather simple models or more complicated one's like finite element calculations.

A reduced set of data might be used if the stochastic nature of some of the variables is known and taken into account:

$$R_{pm,sto} = f(\underline{W}, \underline{X}) \quad (4.19)$$

The vector \underline{X} consists variables that are stochastic. To calibrate the partial factor the probability distributions of the stochastic variables have to be known. For this type of prediction models the proposed calibration procedure is better but far more complicated.

The essence of the calibration procedure is the comparison of the set of data with the matching resistances predicted by the considered model. The set of data comprises the results

$R_{test,i}$ for all data points i . The corresponding resistances $R_{pm,i}$ have to be calculated with the prediction model, by using the following values for the variables of the model:

- If a deterministic variable W is used as a known value in the design rule, a measured value has to be taken.
- If a deterministic variable X_{nom} is assumed in the design rule, while it is known that it is a stochastic nature in principle, the mean of the measured values or a nominal value as will be used in the final design rule, has to be taken.
- For a stochastic variable X , the mean value of the stochastic distribution is taken. This choice is based on the assumption that the stochastic distribution of the variable used in the set of data is representative for the whole population. As an alternative the measured value might be taken.

A graph with the set of data on the vertical axis and the corresponding calculated values on the horizontal axis, gives a qualitative indication how well the prediction model fits with the available data. The differences between both provide quantitative information that can be used to perform a statistical analysis.

To quantify the differences between the set of data and matching calculated values predicted by the model, correction factors for all data points i have to be determined. Mostly this is done by adding a factor $K_{a,i}$ to the prediction model:

$$R_{test,i} = R_{pm,i} + K_{a,i} \quad (4.20)$$

or by multiplying the prediction model with a factor $K_{m,i}$:

$$R_{test,i} = K_{m,i} R_{pm,i} \quad (4.21)$$

The followed procedures for both proposed correction factors are illustrated in figure 4.5 by plotting a $R_{pm} - R_{test}$ diagram for one data point i . When all the correction factors are calculated for the complete set of data, their distribution function has to be determined.

To calibrate a design rule based on a prediction model as represented by equation 4.18, a straightforward method can be used. The choice in which way the prediction model is

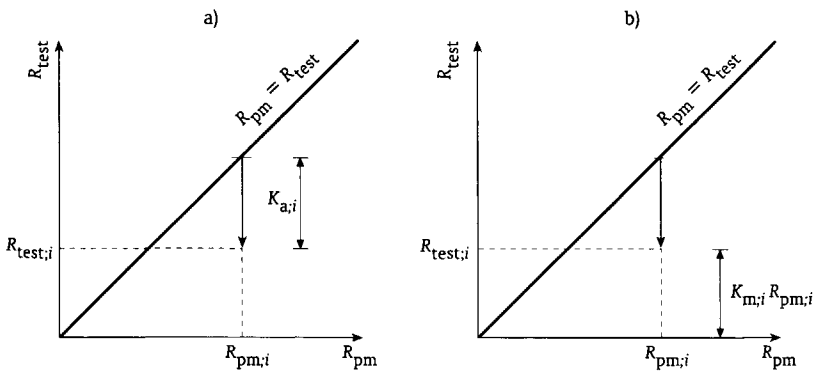


Figure 4.5 Procedure to calculate the correction factors K_a and K_m :
a) adding correction factor $K_{a,i}$; b) multiplying with correction factor $K_{m,i}$

Calibration Techniques for Design Rules

corrected depends on the stochastic nature of the resistance. For the correction factors according to equations 4.20 or 4.21 the stochastic distribution has to be of the same kind as the one by which the resistance of the considered structural component is represented. The parameters of the selected distribution function for the correction factor have to be estimated according to the methods presented in section 4.2.1. For the design rule based on the correction of the prediction model according to equation 4.20, the design values referring to all data points i are equal to:

$$R_{d,i} = R_{pm,i} + K_{a,d} \quad (4.22)$$

and for the design rule based on the correction of the prediction model according to equation 4.21, the design values referring to all data points i are equal to:

$$R_{d,i} = K_{m,d} R_{pm,i} \quad (4.23)$$

where the design values of the correction factors $K_{a,d}$ and $K_{m,d}$ have to be based on a statistical analysis presented in section 4.2.2. The followed procedures for both proposed correction factors are illustrated in figure 4.6 by plotting a $R_{pm} - R_{test}$ diagram for all data points.

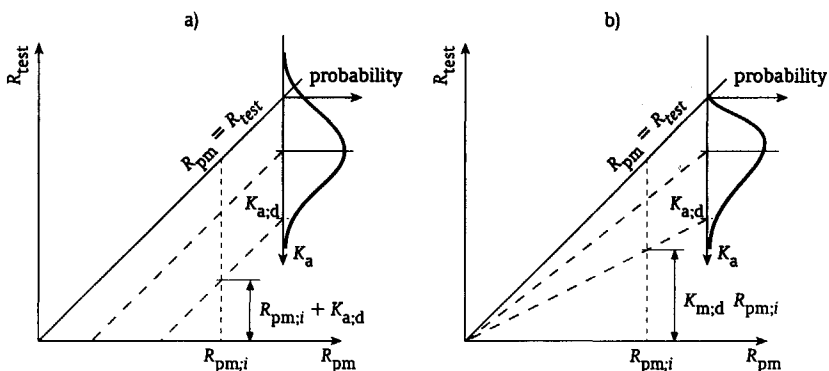


Figure 4.6 Procedure to calculate the design value of the resistance for a deterministic prediction model: a) adding correction factor $K_{a,i}$; b) multiplying with correction factor $K_{m,i}$

For each considered data point i the partial factor $\gamma_{R,i}$ can now be calculated:

$$\gamma_{R,i} = \frac{R_{d,i}}{R_{k,i}} \quad (4.24)$$

The calculation of the characteristic values $R_{k,i}$ with the prediction model have to be based on a well-prescribed procedure defined as a part of the design rule. To propose a general applicable partial factor, the results of these probabilistic analyses have to be interpreted and generalized with use of engineering judgement.

To calibrate a design rule based on a prediction model with one or more stochastic variables, as represented by equation 4.19, far more complicated methods have to be used. Also for these methods the prediction model has to be corrected according to equation 4.20 or

4.21 and the matching distribution function for the correction factor has to be determined. The corrected stochastic prediction model can be represented by the following general formulation:

$$R_{\text{pm;sto};K} = f(\underline{W}, \underline{X}, K) \quad (4.25)$$

where K is the correction factor K_a or K_m , which is stochastic. Now the design values $R_{d,i}$ referring to all data points i according to this corrected model have to be determined. This can be done by using available probabilistic level III or level II methods. These methods can take into account the types of distribution function of the variables and the correction factor, and are capable to handle dependencies between variables.

As an alternative a less complicated method can be derived on basis of principles of the simplest level II methods. A complete independency between all stochastic variables is assumed and the type of distribution function of each stochastic variable is ignored. Only the mean μ and the standard deviation σ of the stochastic variables \underline{X} and the correction factor K have to be known. To calculate the mean and standard deviation of the corrected prediction model, equation 4.25 has to be linearized around point (\underline{X}_0, K_0) :

$$f(\underline{W}, \underline{X}, K) = f(\underline{W}, \underline{X}_0, K_0) + \sum_j (X_j - X_{0,j}) \frac{\partial}{\partial X_j} f(\underline{W}, \underline{X}_0, K_0) + (K - K_0) \frac{\partial}{\partial K} f(\underline{W}, \underline{X}_0, K_0) \quad (4.26)$$

If the coefficients of variation of the stochastic variables are small, the mean and standard deviation of the corrected prediction model can be approximated by:

$$\mu(f(\underline{W}, \underline{X}, K)) \approx f(\underline{W}, \underline{X}_0, K_0) + \sum_j (\mu(X_j) - X_{0,j}) \frac{\partial}{\partial X_j} f(\underline{W}, \underline{X}_0, K_0) + (\mu(K) - K_0) \frac{\partial}{\partial K} f(\underline{W}, \underline{X}_0, K_0) \quad (4.27)$$

and:

$$\sigma^2(f(\underline{W}, \underline{X}, K)) \approx \sum_j \left[\frac{\partial}{\partial X_j} f(\underline{W}, \underline{X}_0, K_0) \sigma(X_j) \right]^2 + \left[\frac{\partial}{\partial K} f(\underline{W}, \underline{X}_0, K_0) \sigma(K) \right]^2 \quad (4.28)$$

Mostly the corrected prediction model is linearized around the mean value of the point (\underline{X}_0, K_0) , because this simplifies the calculation procedure. By assuming a distribution function representative for the corrected prediction model, design values referring to all data points i can be calculated with use of the procedures given in section 4.2.2. The value of the partial factors $\gamma_{R,i}$ can now be determined with use of equation 4.24.

The above presented method is worked out in Annex Z of Eurocode 3 (CEN, 1994) for the following corrected prediction model:

$$R_{\text{pm};K} = K_m C W_1^{p_1} \dots W_n^{p_n} X_1^{q_1} \dots X_m^{q_m} \quad (4.29)$$

where C , p and q are constants. All the stochastic variables, as well as the correction factors

Calibration Techniques for Design Rules

are assumed to be lognormal distributed. Additional to this a comparable calculation procedure is derived by Van Straalen (1997D) for the following corrected prediction model:

$$R_{pm;k} = C + p_1 W_1 + \dots + p_n W_n + q_1 X_1 + \dots + q_m X_m + K_a \quad (4.30)$$

All the stochastic variables, as well as the correction factors are assumed to be normally distributed.

4.3.3 Calibration of the conversion factor for time dependent effects

If the action is constant and the resistance decreases monotonously during time, the value of the conversion factor η_t introduced in equation 3.20, can be determined easily.

A straightforward procedure is presented to calibrate the value of the conversion factor for the short-term static load condition.

The complete reference period is divided into a sequential series of p time periods as indicated in figure 4.7. The length of each time period is chosen in such a way that the degradation effects are small within one period. It is a conservative approximation to take for the resistance of a period the value at the end of this period. The distribution function of the resistance has to be formulated as a function of time. In chapter 6 a consistent method will be presented based on accelerated ageing tests. As indicated in figure 4.8, mostly a time dependent relation of the mean value of the resistance is determined together with a constant value of the standard deviation on basis of n test results.

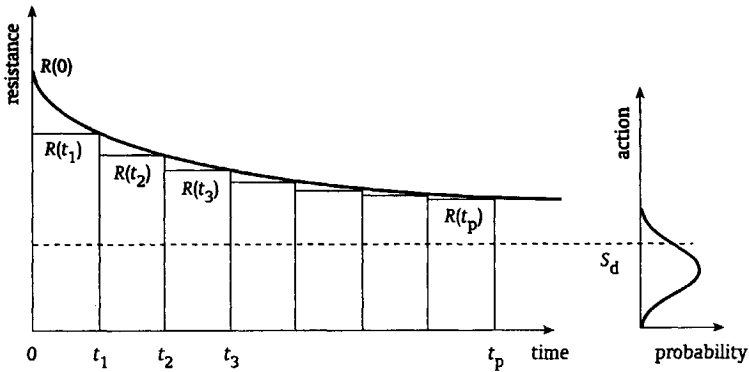


Figure 4.7 Division of the reference period into p periods of time and definition of the resistance for each time period for a stationary action

The value of the conversion factor η_t to be determined, is defined by:

$$\eta_t = \frac{R_{ref;d}}{R_d(t_0)} \quad (4.31)$$

where $R_d(t_0)$ is the design value of the resistance for time $t = 0$ and $R_{ref;d}$ is the unknown design value of the resistance. This value is also valid for each time period i . If the relation that describes the degradation, is based on test results, for each period i a relation between the unknown design value $R_{ref;d}$ and the probability of failure $P(S_i > R_i)$ can be formulated

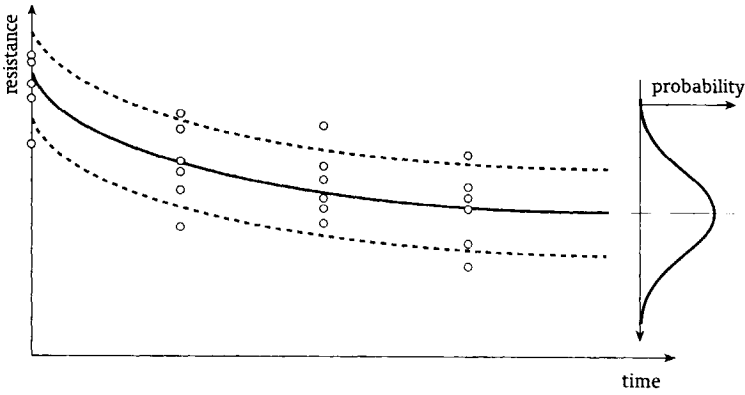


Figure 4.8 Degradation of the distribution function of the resistance as a function of time

with use of the methods described in section 4.2.2. Assuming a normal distribution and a constant standard deviation a set of p relations for $i = 1$ to p is found:

$$R_{\text{ref};d} = m(t_i) - t_{P(S_i > R_i)}(v) s \sqrt{1 + \frac{1}{n}} \quad (4.32)$$

while for a Weibull distribution the following set of p relations for $i = 1$ to p is found:

$$R_{\text{ref};d;i} = \alpha'_i [-\ln(1 - P(S_i > R_i))]^{1/(k_{P(S_i > R_i)}(n) \beta'_i)} \quad (4.33)$$

It is noted here that the values of β'_i , α'_i and $k_{P(S_i > R_i)}$ depend upon the considered period i . This set of relations contains the $p + 1$ unknowns $R_{\text{ref};d}$ and $P(S_i > R_i)$ for $i = 1$ to p . The additional relation necessary to find a solution is based on equation 3.19, which has to meet the target probability $\Phi(\alpha_R \beta)$ valid for the whole reference period:

$$\sum_{i=1}^p P(S_i > R_i) \frac{t_i - t_{i-1}}{t_{\text{ref}}} = \Phi(\alpha_R \beta) \quad (4.34)$$

The resistance $R_{\text{ref};d}$ can now be determined by solving the complete set of relations given above. Finally the value of the conversion factor has to be calculated with use of equation 4.31.

A conservative approximation can be made by assuming only one period in time for the whole reference period. This means that the conversion factor is calibrated on basis of the degraded resistance at the end of the reference period. If the distribution function of the resistance is known as a function of time, the design value of the resistance at the end of the reference period $R_d(t_p)$ can be determined with use of the methods described in section 4.2.2. The value of the conversion factor is now equal to:

$$\eta_\tau = \frac{R_d(t_p)}{R_d(t_0)} \quad (4.35)$$

If the degradation process stabilizes within a short period of time the differences between the results of both proposed procedures will be small.



Modelling of Mechanical Behaviour

To calculate the strength of adhesive bonded joints design rules have to be based on prediction models. Various models describing the mechanical behaviour for different kinds of mechanical actions, are available or under development. A general distinction can be made between those based on continuum mechanics and those based on fracture mechanics. In this chapter their backgrounds are highlighted. For the application of adhesive bonded joints and sandwich panel structures under short-term load conditions, consistent mechanical prediction models are proposed.

5.1 Methods of modelling

Within the partial factor approach the calculation of the characteristic value of the resistance is normally based on a mechanical prediction model. To guarantee the target of the required reliability level and to avoid high values for the partial factors as a result of the calibration of the design rule, it is necessary to make use of consistent prediction models. The predictions have to be representative for the real behaviour within the defined field of application. Researchers active in the field of adhesive bonded joints have rarely presented coherent proposals. Most of their studies focus on specific issues. A lot of information is available about failure modes, testing and calculations. But up till now only occasionally prediction models are proposed that deal with these three issues.

The prediction model has to be based on a failure criterion, on test methods and a theory to calculate the mechanical action effects (Van Straalen, et.al., 1998B). It is important to look after a failure criterion that is representative for the dominant failure mode observed in tests. Its value has to be determined by testing. But test methods are also necessary to determine material properties that are used as input for the theory that calculates the effects of the applied mechanical actions. The prediction model has to give a relation between these mechanical actions and the used failure criterion.

Prediction models to describe the mechanical behaviour are mostly based on either continuum mechanics or fracture mechanics. Continuum mechanics model the structure as a solid and give a description between applied loads, the stress state, the strain state and deformations. Various models are available that can take physical linear material, non-linear material or creep behaviour into account. It is also possible to model geometrical non-linear behaviour. Fracture mechanics on the other hand model a cracked structure and give a description of the stress or strain field around the crack tip. For linear elastic fracture mechanics this field is represented by the stress intensity factor K or the strain energy release rate G , while for elastic-plastic fracture mechanics this field is described by the crack tip opening displacement $CTOD$, or the J-integral J . Continuum mechanics and fracture mechanics have provided a wide variety of mechanical prediction models and many of them can be used.

Another issue that influences the development of a prediction model, is the active mechanical action as categorised in section 2.2.1. The behaviour of an adhesive bonded joint strongly depends on it. For the short-term static load condition and the impact load condition comparable models based on continuum mechanics or fracture mechanics might be used. For the long-term static load condition an adhesive bonded joint creeps, which might cause a reduction of the strength in time, followed by final failure. To describe this type of failure special models for the adhesive material are used. Under a low cycle fatigue load cracks might

appear within the bondline, which causes reduction of the ultimate strength of the joint in time. This behaviour can be described with a degradation model. For the high cycle fatigue load condition a crack might initiate at a location within the bondline with high stresses. After initiation stable crack growth occurs. Available fatigue models are the experimentally based SN-approach and crack growth models based on fracture mechanics. On basis of this general overview it is concluded that the choice of a prediction model is directly related to the active load condition.

5.2 Adhesive bonded joints

5.2.1 Mechanical behaviour

One of the most intensively studied adhesive bonded joint configurations is the single overlap joint given in figure 5.1. The two metal adherends are bonded together over a certain length. The configuration of an overlap joint is preferred for practical applications, because the strength of an adhesive bondline loaded in shear is higher than that of a bondline loaded in tension.

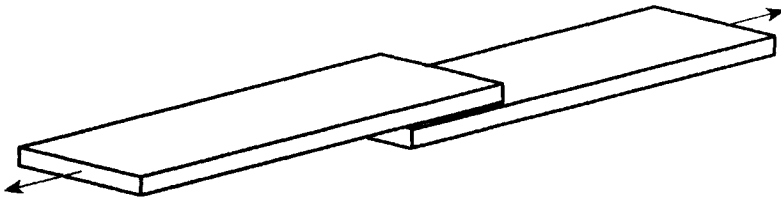


Figure 5.1 Single overlap joint

The mechanical behaviour of the single overlap joint is strongly influenced by the difference in stiffness and strength of the adhesive compared to the metal adherends. The axial stresses due to the applied load have to be transferred between the lower and upper adherends by the

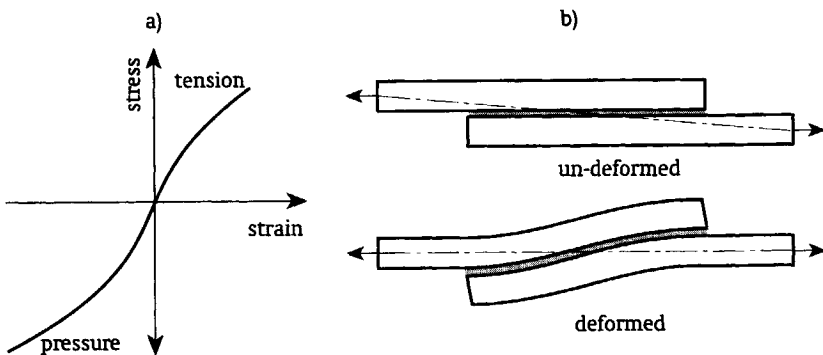


Figure 5.2 Non-linear behaviour of a) an axial loaded adhesive material, and b) the geometry

adhesive bondline. These give complex stress and strain states within the bondline. The physical non-linear behaviour of the adhesive and the non-symmetric geometry causing a significant geometrical non-linearity, see figure 5.2, complicate the development of a proper prediction model.

To describe the mechanical behaviour of adhesive bonded joints various assumptions have to be made. These deal with issues about the description of the material behaviour, the modelling of the bondline, the adherends, the fillet shape, the dimensioning of the crack size and the choice between a two-dimensional or three-dimensional representation of the geometry. The assumptions are directly related to the coherent proposal of a failure criterion, test methods to determine material properties and a theory to calculate mechanical action effects.

5.2.2 Choice of failure criteria

In general a distinction is made between cohesive failure of the adhesive bondline and adhesive failure of the interface between the adhesive and adherend. Most of the proposed failure criteria used in prediction models deal with the cohesive failure mode. For the adhesive failure mode on the other hand only a few criteria are described in literature. As a part of the British MTS Adhesive Project several failure criteria were investigated, see Crocombe and Kinloch (1994) and McCarthy (1996).

In view of continuum mechanics ultimate stress or strain criteria are most straightforward. These criteria assume that the joint fails when a critical value of the transverse normal, shear or principal stress or strain is reached at any point within the adhesive bondline. Alternatively criteria are proposed, which consider the stress or strain at a distance from the most critical point. Also more advanced yield criteria are available, of which the Von Mises yield criterion is probably the best known. The general conclusion of the British MTS Adhesive Project (McCarthy, 1996) is that none of the current failure criteria works for all types of adhesive bonded joints. A selected criterion only gives satisfying results for one type of joint. This conclusion is supported by the following reasons:

- The failure criteria are not based on parameters having physical relevance.
- The failure process is progressive and not a simple fail or no-fail scenario.
- The failure process tends to be interfacial and might differ to the failure process that occurs within the bulk of the adhesive.
- The failure parameters and adhesive properties are subjected to scatter.

The first three reasons deal with the accuracy of the used criterion. As long as the results are satisfying, even physical incorrect failure criteria might be acceptable within a prediction model. Also the scatterband discussed in the fourth reason is not harmful, as long as the design rule is calibrated with use of the probabilistic techniques discussed in section 4.3.

In view of fracture mechanics the critical stress intensity factor, the critical energy release rate, the critical crack tip opening displacement and the critical value of the J-integral are proposed as candidate failure criteria. For adhesive bonded joints there are advantages of using the energy release rate instead of the others. It is directly related to the energy absorbing process of cracking and it can deal with cracks at the interface between the adhesive and the adherend. But there are still some drawbacks (Crocombe and Kinloch, 1994). Fracture mechanics principles can only be applied for macro-sized cracks, which are for polymers in the order of millimetres. This is much larger than the actual flaw sizes. The critical energy release rate seems to depend on the three modes of loading defined in fracture

mechanics (opening mode I, sliding mode II and tearing mode III), which have different effects. Also the thickness of the adhesive layer, the joint width and the load rate seem to influence its value. Despite these drawbacks the critical energy release rate might be useful within a prediction model.

To deal with the disadvantages of the above described failure criteria, researchers looked after alternatives. One of these alternatives discussed by Crocombe and Kinloch (1994) is the critical stress intensity factor. The stress intensity factor Q describes the stress field near a point of singularity around bi-materials and sharp corners. It is still not clear if this failure criterion can be applied in general. Of probably greater interest are failure criteria formulated within the theory of damage modelling (Crocombe and Kinloch, 1994). The essence of this theory is that for a given load level at locations with critical conditions the adhesive bondline is assumed to be damaged. After the properties of the adhesive are adapted, the calculation process is proceeded for higher load levels until this process becomes unstable. Damage modelling can be based on either continuum mechanics or fracture mechanics.

Failure criteria for the adhesive failure mode are rarely discussed in literature. One of the proposed failure criteria is based on the combination of normal and shear stresses acting on the interface, as discussed by Van den Berg (2000). Further developments are foreseen in the near future.

5.2.3 Determination of material properties

Both the value of the selected failure criterion as well as values of relevant input parameters for theories to calculate mechanical action effects, have to be determined by testing. Various test methods have been developed over the years. To apply these for a consistent mechanical prediction model it is essential that test results are representative for the actual situation.

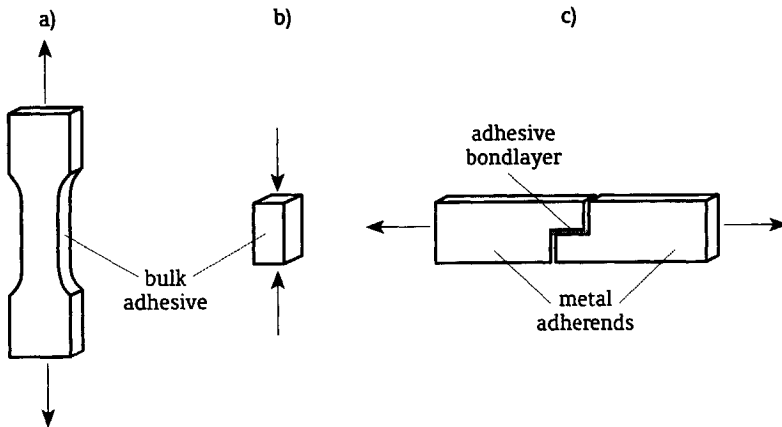


Figure 5.3 Overview of continuum mechanics based specimens: a) unidirectional tensile test, b) unidirectional compression test, and c) thick adherend lap shear test

The values of adhesive bulk properties to be used for continuum mechanics, are based on small-scale tests. An overview of various useful specimens is given in figure 5.3. The unidirectional tensile test provides information about the Young's modulus $E_{a,t}$, the Poisson's ratio ν_a , the ultimate tensile stress $\sigma_{a,t;ult}$ and the ultimate tensile strain $\epsilon_{a,t;ult}$. The

unidirectional compression test provides information about the Young's modulus $E_{a;c}$, the ultimate compression stress $\sigma_{a;c;ult}$, and the ultimate compression strain $\epsilon_{a;c;ult}$. On basis of both tests the stress-strain curve of the bulk adhesive can be determined. The thick adherend lap shear test gives information about the shear properties of the bulk adhesive. These are the shear modulus G_a and the ultimate shear stress $\tau_{a;ult}$. Beside these straightforward test methods also more complicated methods as for example the tensile butt-joint test, the torsion-pendulum test and the Arcan test are proposed by researchers.

For fracture mechanics various adhesive properties like the Young's modulus, the Poisson's ratio and the stress-strain curve have to be determined with test methods described above. Only the value of a failure criterion as the critical energy release rate has to be based on specific small-scale tests. An overview of some useful specimens is given in figure 5.4. The advantage of the tapered double cantilever beam specimen over the thick double cantilever beam specimen is that the calculated strain energy release rate does not depend on the crack length. Using a scarfed joint specimen it is possible to determine the influence of mixed modes of loading. Beside these test methods also others as for example the wedge cleavage test and the blister test are proposed by researchers.

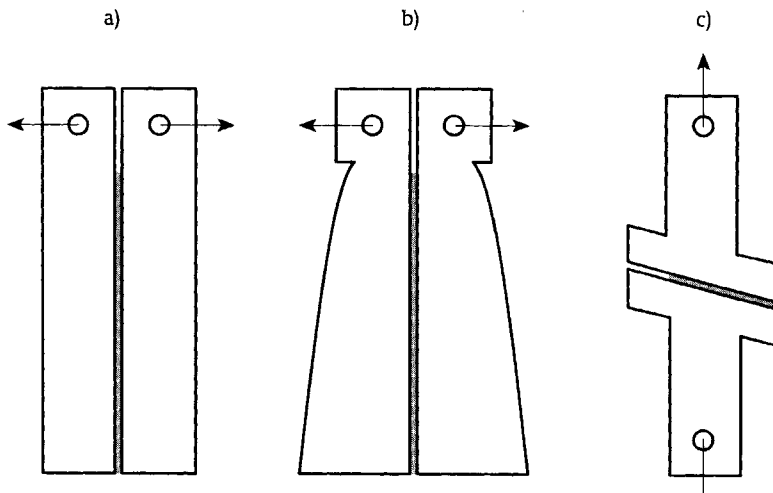


Figure 5.4 Overview of fracture mechanics based specimens: a) thick double cantilever beam test, b) tapered double cantilever beam test, and c) scarfed joint test

Many of the above presented test specimens and matching test procedures are described in various standards. But still research is going on and it might be expected that the harmonisation of test methods and procedures will take a long period of time.

5.2.4 Theories to calculate mechanical action effects

Theories to calculate mechanical action effects for adhesive bonded joints are either based on continuum mechanics or fracture mechanics. To develop these theories it is necessary to make assumptions.

For continuum mechanics it is necessary to model the adherends and the adhesive bondline.

Modelling of Mechanical Behaviour

The adherend can be modelled as a beam, a plate or a rigid body. Beam and plate theories are mostly used for analytical solutions. Rigid body theories are used for finite element methods; for the two-dimensional case the adherend is modelled with plain strain or plain stress elements, while for the three-dimensional case it is modelled with solid elements. For analytical solutions the adhesive bondline can be modelled as a series of springs. The most simple spring model only deals with the shear behaviour of the adhesive, while other spring models also take the normal behaviour in transverse direction into account. These simple models assume that there is no deviation of stresses and strains in thickness direction of the bondline. They do not take into account a zero-shear stress condition at bondline endings. Higher-order theories on the other hand are more sophisticated. Transverse normal stresses and strains deviate over the bondline thickness and shear stresses equal zero at bondline endings. Using finite element methods the bondline is modelled as a rigid body. Due to the flexibility of the application of finite element methods it is also possible to model the actual shape of the spew fillet. The material properties of the adherends are mostly assumed to be linear elastic. For the adhesive both linear elastic as well as elastic-plastic material properties are assumed. It is noted here that the physical non-linear behaviour of the adhesive under tension and under compression might differ significantly. Finally it is mentioned here that for non-symmetric joints geometrical non-linear effects have to be considered.

For fracture mechanics the adherends and the adhesive bondline have to be modelled in a similar way as described above. Additional assumptions have to be made to take the effects of the cracked geometry into account. The singularity of the stress and strain fields around the crack tip can be described in various ways. The stress intensity factor determines the magnitude of the elastic stresses in the crack tip field. The energy release rate determines the amount of energy that remains available for crack extension. This parameter assumes linear elastic material behaviour, while its counterpart for elastic-plastic material behaviour is the J-integral. The crack tip opening displacement determines the opening of the crack tip by taking non-linear material behaviour into account. Linear elastic fracture mechanics are also used to predict crack growth. An essential material property is the relation between the stress intensity factor or the energy release rate and the crack growth rate. Detailed information how to apply fracture mechanics for calculation is described in handbooks (Ewalds and Wanhill, 1984).

For theories dealing with damage modelling the damage can be modelled at various levels of sophistication. At locations where a critical condition is exceeded the material can be simply removed, softened gradually to a state with no-load carrying capacity, or combined with a proper yield criterion. During the calculation process the load is increased gradually. After each load step the properties of the affected material are adapted and the calculation process is proceeded. As soon as the calculation process becomes unstable, it is assumed that the failure strength is reached.

All the above mentioned calculation models have been studied extensively over the years. For adhesive bonded joints most experience is gathered with continuum mechanics. This is probably due to the fact that researchers and engineers are more familiar with these theories. But also the difficulties in gathering fracture mechanics based material properties might be a reason.

5.2.5 Proposal for a prediction model

To illustrate the process of developing design rules for adhesive bonded joint in view of the

partial factor approach, overlap joints under short-term static load conditions are studied for the cohesive failure mode in chapter 7. Since most experience is gathered with continuum mechanics, the selected mechanical prediction model is based on these.

A failure criterion based on global yielding of the adhesive seems to be promising. Criteria assuming failure when a critical value of a stress or a strain is reached, can be seen as an intuitive starting point for joint strength prediction. In various studies such criteria were used reasonably successful, but none of them is general applicable (Crocombe and Kinloch, 1994). For this reason it was proposed to look after a stress or strain at a distance. There are several drawbacks to mention, but the main disadvantage is that these failure criteria do not have a physical background. Better confidence is found for global yield criteria, see for example Jeandrau (1987), Crocombe (1989) and McCarthy (1996). Pressure dependent yield criteria used for polymers, as proposed by Bauwens (1970) and Raghava and Caddell (1973), seem to be fairly straightforward. The essence of these criteria is that a polymer yields or fails at a higher level if the hydrostatic pressure increases. In figure 5.5 these pressure dependent yield criteria are schematically represented by yield contours within the principal stress field for a two-dimensional situation. On the perimeter of this contour the adhesive yields. If strain hardening occurs an extending yield contour is found with increasing stresses. Final failure occurs as soon as an ultimate strain is reached. An additional advantage of these yield criteria is that they can be used to model physical non-linear behaviour of the adhesive. Raghava and Cadell (1973) conclude that the differences between their proposal and the yield criterion suggested by Bauwens (1970) are not significant as long as the ratio of the compressive and tensile stresses is smaller than 1.5. An extended study by Gali et.al. (1981) gives all relevant backgrounds and experimental evidence for adhesives of the hydrostatic pressure dependent yield and failure criterion proposed by Bauwens (1970). This criterion is used in the study described in section 7.1.

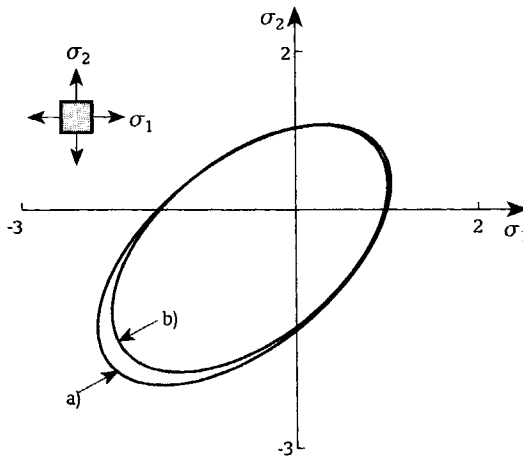


Figure 5.5 Hydrostatic pressure dependent yield contours within a two-dimensional principal stress field ($\sigma_3 = 0$) for a ratio of the compressive and tensile stresses equal to 1.5: a) yield criterion proposed by Bauwens (1970), and b) yield criterion proposed by Raghava and Caddell (1973)

Development of Design Rules

The input of this criterion and of the model to calculate the mechanical action effects, has to be determined by testing. Useful and well established procedures to determine these properties were standardised by the American Society for Testing and Materials. ASTM D 638-96 (1996) describes the test method to determine tensile properties and ASTM D 695-96 (1996) describes the test method to determine compression properties.

The simplest approach to calculate the stress and strain state is to model the adherends as beams or plates and the bondline as continuously distributed springs. These springs have to connect the adherends in longitudinal and transverse direction to be able to determine the shear and transverse normal stresses. The values of these stresses are constant over the

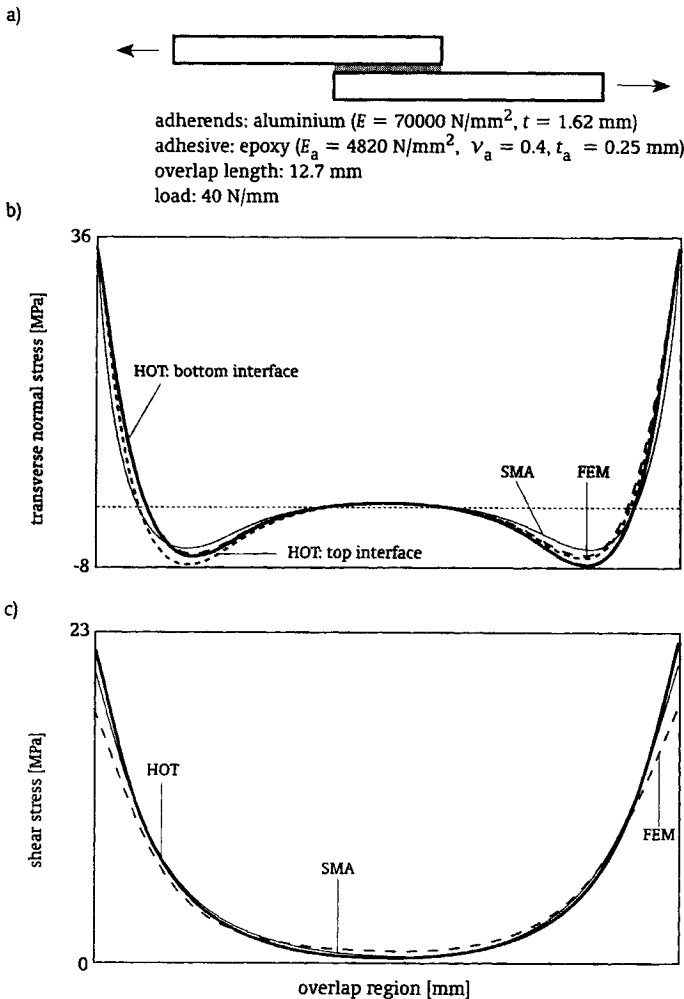


Figure 5.6 Comparison stress state in single overlap joints with spew fillet according to a spring model approach (SMA), a higher-order theory (HOTA) and a finite element method (FEM): a) considered joint, b) transverse normal stresses, and c) shear stresses, (Mortensen, 1998)

bondline thickness. More complicated approaches as higher-order theories and finite element methods can take into account a zero-shear stress condition at the bondline endings and varying normal stresses over the bondline thickness. Nevertheless Frostig et.al. (1999) and Mortensen (1998) conclude that if the spew fillet is modelled with higher-order theories or finite element methods, the spring model approach gives comparable results as for example shown in figure 5.6.

5.3 Sandwich structures

5.3.1 Mechanical behaviour

A sandwich panel is a composition of a thick, light and weak core material with thin, strong and stiff faces bonded on the upper and lower sides. An example of a sandwich panel under a four-point bending load is illustrated in figure 5.7. A large variety of materials is used for practical applications. Well known core materials are honeycomb material, corrugated material, wood, expanded plastic foam and mineral wool. Widely used face materials are thin metal sheet, wooden plate and fibre reinforced composite. Phenomena as bending, buckling and vibration have to be taken into account during design. In this study sandwich panels primarily loaded in bending are considered.

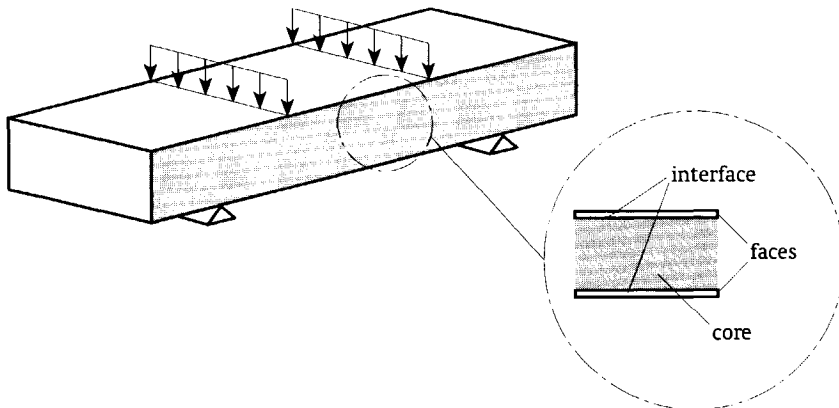


Figure 5.7 Sandwich panel under four-point bending

The mechanical behaviour of a sandwich panel is based on the principle that the faces act together to carry the applied bending moment, while the core resists the applied shear load and stabilises the faces against buckling and wrinkling. Local details as near load points and support regions, have a negative effect on the advantages of this principle. Complex stress and strain states in faces, the core and the interface are a result. The most important failure modes for short-term static load condition are yielding of the face, wrinkling or dimpling of the face, shear failure of the core and delamination of the interface, see figure 5.8. The effects of local details and the large variety of possible failure modes complicate the development of a proper prediction model.

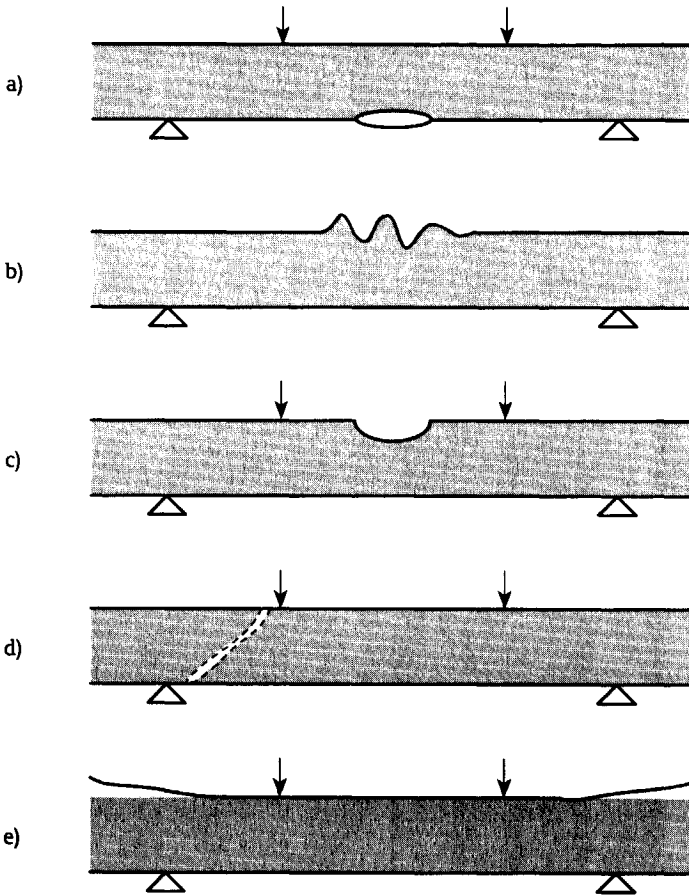


Figure 5.8 Failure modes: a) yielding of the face, b) wrinkling of the face, c) dimpling of the face, d) shear failure of the core and e) delamination of the interface

To develop a proper prediction model for the mechanical behaviour of sandwich panels various assumptions have to be made. These deal with issues about the description of the material behaviour, the modelling of the core and the faces, the detailing of local geometry and the choice between a two-dimensional and a three-dimensional modelling of the geometry. The assumptions are directly related to the coherent proposal of a failure criterion, test methods to determine material properties and a theory to calculate mechanical action effects.

5.3.2 Choice of failure criteria

For each of the failure modes discussed in the preceding section, failure criteria have to be chosen, however possible failure criteria for sandwich panels are rarely reviewed in literature. Mostly well-known criteria used for mono-materials or fairly simple failure criteria are applied.

For yielding of the face mostly a common ultimate yield stress criterion is used. For

wrinkling and dimpling of the face the situation is more complicated, because the failure criterion is directly related to the used calculation model. The ultimate buckling stress is calculated, which is related to the ultimate yield stress. Shear failure of the core is mostly based on an ultimate shear stress. Delamination of the interface can be based on an ultimate tensile strength of the core material, but if the adhesive bonded joint between the core and face fails more complicated criteria as discussed in section 5.2.2, have to be used.

5.3.3 Determination of material properties

Both the selected failure criterion as well as the relevant input parameters for theories to calculate the mechanical action effects, have to be determined by testing. Researchers have developed various test methods over the years. To apply these for a consistent mechanical prediction model it is essential that the test results are representative for the actual situation.

The values of the core properties are based on small-scale tests. An overview of various useful specimens is given in figure 5.9. The tensile test provides information about the Young's modulus $E_{c,t}$, the ultimate tensile stress $\sigma_{c,t,ult}$, and the ultimate tensile strain $\epsilon_{c,t,ult}$. The compression test provides information about the Young's modulus $E_{c,c}$, the ultimate compression stress $\sigma_{c,c,ult}$, and the ultimate compression strain $\epsilon_{c,c,ult}$. On basis of both tests the stress-strain curve of the core material can be determined. The four-point bending load test gives information about the shear properties of the core material. These are the shear modulus G_c and the ultimate shear stress $\tau_{c,ult}$. Also other test methods are proposed by researchers to determine the shear properties, but it is assumed that the four-point bending load test gives proper values that are representative for practical situations.

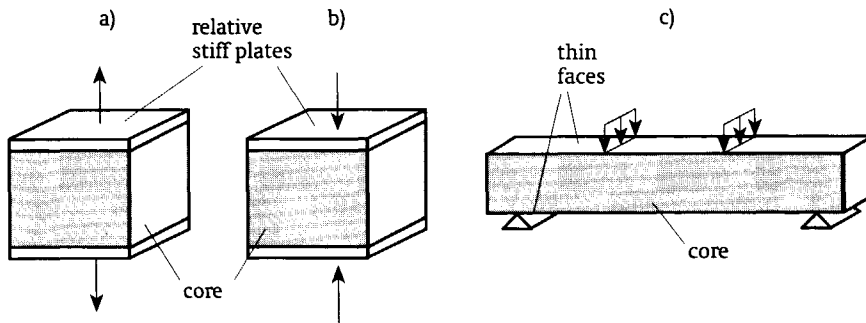


Figure 5.9 Overview of specimens to determine core properties: a) tensile test, b) compression test and c) four-point bending test

The values of the face properties are mostly based on a small scale unidirectional tensile test. This test provides information about the Young's modulus E_f , the Poisson's ratio ν_f , the yield tensile stress $\sigma_{f,y}$, the ultimate tensile stress $\sigma_{f,ult}$ and the ultimate tensile strain $\epsilon_{f,ult}$. On basis of this test also the stress-strain curve can be determined.

The above presented test specimens and matching test procedures are described in various standards. Unidirectional tensile tests to determine the face properties are generally accepted, but for tests to determine the core properties still research is going on. It might be expected that the harmonisation of these test methods and procedures will take a long period of time.

5.3.4 Theories to calculate mechanical action effects

Most of the prediction models proposed in literature for sandwich panel structures are based on continuum mechanics. To develop calculation models it is necessary to make a number of assumptions.

For continuum mechanics it is necessary to model the faces and the core. The face can be modelled as a beam, a plate or a rigid body. The beam and plate theories are mostly used for analytical solutions. Rigid body theories are used for the finite element methods; for the two-dimensional case the face is modelled with plain strain or plain stress elements, while for the three-dimensional case it is modelled with solid elements. For analytical solutions the core can be modelled as a series of springs. Classical theories, as summarised by Zenkert (1995), only deal with the shear behaviour of the core. These theories assume that there is no variation of shear stresses over the core thickness. They also assume that no transverse stresses occur and they do not take into account a zero-shear stress condition at sandwich endings. The superposition approach, as for example described by Thomsen (1992A), is an extension of classical theories. Effects of local circumstances as a load point, are formulated separately and superposed upon a solution of a classical theory. Higher-order theories on the other hand, as for example proposed by Frostig et.al. (1992A), are more sophisticated. Normal stresses deviate over the core thickness and shear stresses equal zero at the sandwich endings. Finite element analyses, as reviewed by Noor et.al. (1996), can be based on either classical theories, higher-order theories or rigid body modelling. Due to its flexibility it is also possible to model the actual shape of local geometry. The material properties of the face and the core are mostly assumed to be linear elastic. In some cases also elastic-plastic material properties and geometrical non-linear effects are considered.

The above mentioned calculation models have been studied extensively over the years. Most experience was gathered with classical theories. This is due to the fact that current design rules for sandwich panels use closed-form solutions based on classical theories. Finite element methods are also used more frequently nowadays. The application of higher-order theories on the other hand is still very rare, but seem to be promising. An overview of these models is given by Van Straalen (1998E).

5.3.5 Proposal for a prediction model

To illustrate the process of developing design rules for sandwich panel in view of the partial factor approach two cases are studied in chapter 8. For the failure modes shear failure of the core and delamination of the interface between the sandwich face and the core the criteria recommended by ECCS and CIB (1995) are taken. The input of the proposed failure criteria and of the theory to calculate the mechanical action effects, has to be determined by testing. Useful and well-established procedures to determine these properties are standardised by ECCS and CIB (1995). To calculate the stress state near a local detail, a sophisticated calculation model is necessary. Analytical models or finite element methods based on classical theories are not capable to provide detailed results. Only analytical models based on higher-order theories and finite element methods using rigid modelling, can give satisfying results (Van Straalen, 1998E).

Modelling of Durability

To calculate the degradation of the strength of adhesive bonded joints during lifetime design rules have to be based on prediction models, which take durability effects into account. Various methods to analyse durability for different kinds of mechanical and environmental actions, are available or under development. A general distinction can be made between methods based on current practice and on the reliability theory. In this chapter their backgrounds are highlighted. For the application of adhesive bonded joints and sandwich panel structures under short-term load conditions, a consistent approach is proposed.

6.1 Methods of modelling

Within the partial factor approach as adopted in section 3.3 for the verification of adhesive bonded joints, the calculation of the characteristic value of the resistance is based on a condition without ageing. To guarantee the required reliability level during the whole lifetime, it is necessary to reduce the characteristic value of the resistance. This can be done by using the conversion factor for time dependent effects discussed in section 3.2.3. The calibration of the conversion factor has to be based on a description of the degradation of the resistance as a function of time. The description has to be representative for the real behaviour within the defined field of application. Within the field of adhesive bonded joints coherent approaches have rarely been presented. Most of the performed studies focused on the comparison of potential design solutions. Up till now approaches that provide quantitative information about the degradation of the resistance have been proposed only occasionally.

Current methods to analyse the durability of adhesive bonded joints mainly focus on the experimental comparison of combinations of adherends, adhesives and pretreatments. Specimens are aged under short-term laboratory based environments and their strength is compared with the strength of specimens not aged. Alternative methods more frequently used for predicting the service life of all kind of products, compare the ageing effects of specimens exposed under laboratory based environments with those exposed under in-use environments. Special techniques are developed to correlate both environments and to estimate service life. But none of the laboratory-based test procedures developed from the early 1900's on has consistently produced a significant correlation with long-term in-use exposures (Martin, et.al., 1994). This is caused by several inadequacies:

- The comparison of the laboratory-based environments with in-use environments is strongly dependent on the actual weathering conditions. For practical time scales it is not possible to reproduce the results. This implies that it is not possible to find a direct relation between laboratory based accelerated ageing conditions and in-use environments.
- No attention is given to the fundamental degradation mechanisms. An advantage of the use of this knowledge is that information is provided about the influence of various environments on the degradation process.
- The stochastic nature of the test results is not taken into account. Using statistical techniques it is possible to distinguish various effects.

In general it is concluded that methods used in current practice are not suitable for a quantitative prediction of the durability.

Alternative methods not affected by the inadequacies of current methods are based on the

reliability theory. Since the 1960's reliability methods have been successfully applied to many materials, components and systems (Nelson, 1990). Most of these methods deal with the prediction of the service life, but the used theory can also be applied for the prediction of the degradation of the resistance.

Reliability methods try to quantify the relationship between in-use environments and degradation mechanisms. Environmental actions are identified and quantified. For each of these distinguished actions degradation mechanisms are formulated. These mechanisms can be analysed with use of data from tests under long-term in-use exposures, with use of data from tests under short-term laboratory-based exposures, on basis of fundamental mechanistic studies and with statistical evaluation techniques. Data from tests under long-term in-use exposures provide valuable insight in dominant degradation mechanisms during lifetime. Data from tests under short-term laboratory based exposure and mechanistic studies provide information about the cause of degradation and the rate of degradation. Combining these three sources with statistical techniques and relating the environmental actions with the weathering circumstances, result into a quantitative description of the degradation of the resistance during lifetime.

To reduce the number of ageing tests reliability methods might also be based on simulated data. Simulations can make use of modified versions of the prediction models described in chapter 5 by taking time dependent material behaviour of the adhesive bondline and interface into account. Up till now such models are only proposed occasionally.

6.2 Adhesive bonded joints

6.2.1 Ageing and degradation behaviour

The ageing and degradation behaviour of adhesive bonded joints is described in section 2.2.4. The main conclusions are that water has a major effect on the durability and that a full understanding of degradation mechanisms is still missing. It is also mentioned that two types of degradations can be distinguished: the mechanical properties of the joint degrade and stabilise after a period of time or the joint loses its strength completely after a certain time.

6.2.2 CIB/RILEM procedure

To support and structure reliability methods for practical research activities, a procedure was developed by CIB and RILEM (Masters and Brandt, 1987). This generic procedure deals with service life prediction of building materials and components. It is mainly based on the procedure outlined in ASTM E632-81 (1981). In origin the CIB/RILEM procedure is used for service-life predictions, but it can also support and structure a method to predict the degradation of the resistance during lifetime.

The CIB/RILEM procedure is a systematic guideline. It is applicable to a broad range of building materials and components, it leads to identification of data needed, it is based upon proper test methods or feedback data, it provides guidance on interpretation of data and it leads to documentation of assumptions made. The procedure itself is divided into five primary phases, which can be summarised as follows:

- 1) Definition. The users' needs have to be specified, the building context, performance requirements and criteria have to be identified, and finally the material or the component has to be characterised.

- 2) Preparation. Possible degradation mechanisms and expected environmental actions have to be identified. Based on this most significant effects of degradation have to be identified to serve as indicators. Finally a proposal has to be postulated how ageing tests can induce degradation characteristics of in-use performance.
- 3) Pre-testing. Accelerated ageing tests have to be performed to demonstrate failure and to indicate degradation mechanisms.
- 4) Testing. Short-term ageing tests using relevant environmental actions and long-term ageing tests under in-use conditions have to be performed. Type and rate of degradation have to be determined and compared with each other. If short-term tests are not representative, the procedure has to be continued from phase 1 on.
- 5) Discussion and interpretation. The relationship between short-term and long-term ageing tests has to be identified and a mathematical model to predict the service lifetime or the degradation of the resistance has to be developed. Finally the data has to be reported and results have to be discussed.

A significant feature of this procedure is that it can be used by iteration. This is important, because it provides data and testing procedures that are based on the best knowledge available in the course of conducting research. Another important feature of this procedure is that it shows that scientific judgement is essential for the prediction of the degradation.

To analyse the degradation of the resistance of adhesive bonded joints, the CIB/RILEM procedure seems to be promising. For this specific application the following additional and more detailed remarks regarding the five primary phases summarised above, can be made (Van Straalen, et.al., 1997B, and Van Straalen, 1997C):

- 1) Definition. For the considered case the actual mechanical actions and the environment actions have to be identified. It is important to make a distinction between short-term static load, impact load, long-term static load, low cycle fatigue load and high cycle fatigue load. This is, because the actual load influences the performance of the joint significantly. Environmental circumstances depend on the actual conditions as weathering and the location of the joint in the structure. For structural applications the performance requirement is represented by the target reliability index β described in section 3.2.1.
- 2) Preparation. Degradation mechanisms are related to a change of the properties of the adhesive and the properties of the interface between the adhesive and the adherend. It is difficult to give a description on a physico-chemical basis and for this reason mostly empirical relationships are used. Relevant environmental actions are water, temperature, time of exposure and cyclic behaviour of the temperature. If the degradation of the resistance is studied, the strength of the specimen can serve as the indicator for the ageing tests.
- 3) Pre-testing. To limit the ageing period as much as possible, it is necessary to age under extreme conditions. But one should be aware of the fact that the degradation mechanism might change significantly under extreme circumstances. This is for example the case for temperatures above the glass transition temperature of the adhesive.
- 4) Testing. Short term tests have to be performed in such a way that valuable data becomes available. This means that a proper selection of accelerated ageing conditions, ageing periods and number of tests have to be made.
- 5) Discussion and interpretation. No remarks are made.

Essential issues within this procedure are the identification of degradation mechanisms, the application of accelerated tests and the use of statistical techniques. A drawback of Masters and Brandt (1987) is that only general indications are given how to handle these issues.

6.2.3 Degradation mechanisms

An essential step within the CIB/RILEM procedure is the identification of degradation mechanisms as mentioned in section 2.2.4. This can be done within the context of chemico-physical theories, which are rather complex. An additional complicating factor for adhesive bonded joints is the fact that not only the polymer degrades, but that also the interface between the adhesive and the adherend ages. It is concluded that the identification of degradation mechanisms within the context of chemico-physical theories is difficult.

Useful alternatives for chemico-physical theories are descriptions based on empirical models. One of these is based on the assumption that water is the main environmental action causing ageing. As already mentioned in section 2.2.4 a linear relationship between the amount of water uptake and magnitude of degradation is found (Kinloch, 1983). Diffusion through the adhesive, transport along the interface, capillary action through crazes and cracks, and diffusion through the adherend are distinguished as the principle mechanisms of water uptake. Only for diffusion through the adhesives empirical models are formulated to predict the water uptake as a function of time. Most of these derived relations, see for example Schmitz (1989), are based on exponential relations. It is assumed that such an exponential relation as a function of time gives an useful description of the degradation of the strength of adhesive bonded joints.

6.2.4 Accelerated ageing tests

Accelerated tests are preferred to in-use exposure tests for several reasons. Short-term ageing tests performed in laboratories are less time consuming and less expensive. In combination with a proper description of the acceleration mechanism it is possible to apply the test results to any given weathering condition. Short-term tests are also valuable in the optimisation of design concepts. This is, because the environment to which the specimens are exposed, is quantified. For in-use tests this is not the case, because the weathering conditions can not be reproduced.

The degradation process can be accelerated by a severe increase of one or more environmental actions. To translate the results of accelerated tests for in-use conditions, it is necessary to identify for each essential environmental action the relation between the degradation mechanism and the reaction rate. It is assumed that the acceleration of the ageing process can be described by an change of the time response of the studied properties. This means that the reaction rate is time dependent, while the magnitude of degradation is not affected. For this purpose various time transformation functions are presented in literature (Martin, 1982).

6.2.5 Statistical evaluation techniques

Using statistical evaluation techniques a mathematical relation that represents a selected degradation model and a time transformation function, can be fitted to data from accelerated ageing tests. Various techniques are available (Nelson, 1990). For the evaluation least squares analyses are useful. These provide estimates for the model parameters, mean and confidence limits.

Important aspects related to the statistical evaluation of accelerated ageing tests are the development of the actual failure mode and the statistical uncertainty during lifetime. Least squares analyses are best suited for products with a single failure mode. This means that if the

failure mode of the adhesive bonded joint changes during ageing, the results for both failure modes have to be interpreted separately. Statistical uncertainties are caused by the fact that the degradation of the strength might develop differently for each specimen and by the fact that there is a random variation around a degradation relationship. But accelerated ageing tests do not provide information about the development of the degradation of the strength of a specimen, because only the strength after a given period of ageing is determined. This means that all test results can be considered statistical independent and might be used to determine the mean curve. If it is assumed that the statistical uncertainty does not change during lifetime, the standard deviation of the strength predicted by the mean curve can be determined with available techniques.

Statistics also provide information that can be used to optimise test plans. Issues that have to be considered are the accelerated environmental conditions, the ageing periods and the number of tests. To plan test series, researchers have to make use of experiences gathered in previous test series and of pre-tests under extreme conditions as mentioned in phase 3 of the CIB/RILEM procedure. Based on the considerations given by Nelson (1990), the following recommendations to reduce the statistical uncertainty are made:

- Test specimens aged for a short period will mostly yield better estimates for the model parameters related to the degradation process. Be aware of the fact that adhesive bonded joint might post-cure due to the accelerated environmental conditions.
- Test more specimens aged for the shortest and longest periods, and fewer at intermediate periods. This yields more accurate estimates, since a wider range of ageing periods is used. The only drawback is that less information becomes available about the development of the statistical uncertainty during lifetime.
- Test more specimens at the less severe accelerated environmental condition than at the most severe. This condition is closest to the design environmental condition and can be extrapolated more accurately.
- Intensify the most severe accelerated environmental condition as much as possible. This yields a more accurate estimate for model parameters related to the acceleration process. Be aware of the fact that under such an extreme condition the failure mode might change and that the degradation mechanism is no longer representative for normal conditions.

These recommendations do not include guidance to determine the actual sample size. As a rule of thumb it is recommended to test at least five specimens for each considered situation.

6.3 Sandwich structures

Sandwich structures made of metal faces adhesive bonded on a core material are also effected by ageing. It is well known that the properties of a core material as mineral wool or polystyrene, degrade due to the environment (Tiainen and Hiekkanen, 1995). But also the strength of the adhesive bonded interface between the face and the core material degrades. Since the degradation behaviour of sandwich structures is similar to the behaviour of adhesive bonded joints, the same method as proposed in the previous section might be used to quantify the degradation behaviour.



Design Rules for Overlap Joints

Overlap joints are the simplest types of adhesive bonded joints for structural applications. These overlap joints are mainly used by designers, because of their performances. They are globally loaded in shear, which is preferable over joints loaded in tension or peel, and they can be produced with a high level of quality at relatively low costs. To guarantee the required reliability level proper design rules are needed. These have to deal with the prediction of the mechanical behaviour and the degradation of the performances of the joint. In this chapter design rules based on the partial factor approach are developed for overlap joints. Attention is given towards useful prediction models and the calibration of partial and conversion factors.

7.1 Mechanical behaviour

7.1.1 Studied overlap joints

There is a large variety of overlap joints available that can be used for practical applications. An overview of most common overlap joints made of plate material is given in figure 7.1. The present study focuses on the single overlap joint and the double strap joint. The mechanical behaviour of these overlap joints is influenced by the dimensions and properties of the adherends and the adhesive. To investigate these influences a detailed research programme is

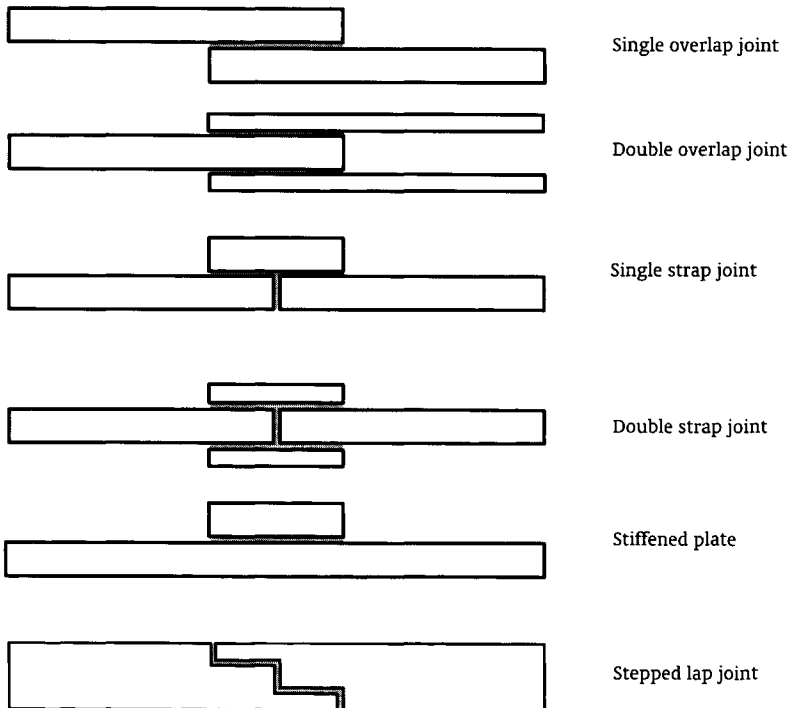


Figure 7.1 Overview of most common overlap joints made of plate material

worked out. The adhesives studied in detail are the cold cured two-component epoxy adhesive DP 490 of 3M and the cold cured two-component polyurethane adhesive UK 8202 of Henkel.

The research programme contains a theoretical and an experimental part. Within the theoretical part a prediction model for single overlap and double strap joints with metal adherends is developed. Cohesive failure of the bondline is assumed. The prediction model as proposed in section 5.2.5, is based on a pressure dependent yield criterion. The adhesive properties were determined with use of standard tensile and compression tests. The stress and strain states within the adhesive bondline are calculated with a spring model approach. Besides tests on bulk adhesives, the experimental part of the research programme contained tests on 25 mm wide steel and aluminium single overlap and double strap joints. Overlap lengths of 10, 20 and 40 mm and plate thickness of 2, 4 and 6 mm were considered. The adhesives DP 490 as well as UK 8202 with a bondline thickness of approximately 0.2 mm were used. The main objectives of these tests are to verify the proposed prediction model and to calibrate the partial factor.

7.1.2 Background of the hydrostatic dependent failure criterion

Since most adhesives exhibit an elastic-plastic behaviour, plastic strains will occur in the bondline of loaded overlap joints even at low load levels. The hydrostatic dependent yield criterion described by Gali, et.al. (1981) gives a proper description of this behaviour on basis of effective stresses and strains. This concept applies a plastic yield hypothesis, which takes into account that for adhesives the compressive yield stress is usually higher than the tensile one. It relates the multidirectional stress state within the bondline to a unidirectional tensile stress state. Final failure is defined by a ultimate yield strain.

To describe the elastic-plastic non-linear behaviour of adhesives an adequate relation between stresses and strains has to be used. Various relationships are possible. In this study the following empirical relation between the stress σ_a and the strain ϵ_a for bulk adhesives under unidirectional tension or compression is proposed:

$$\sigma_a = E_a \epsilon_a \left[\frac{1}{1 + (c_1 \epsilon_a)^{p_1}} \right] + (\sigma_0 + F_a \epsilon_a) \left[1 - \frac{1}{1 + (c_2 \epsilon_a)^{p_2}} \right] \quad (7.1)$$

A schematic presentation is given in figure 7.2. This relation is a combination of two parts, which are added together. The first part represents the linear elastic behaviour of the adhesive at lower strain levels. The term between square brackets reduces its influence if the strains increase. Within the first part the parameter E_a is the Young's modulus and the parameters c_1 and p_1 are dimensionless constants. The second part of equation 7.1 represents a linear behaviour of the adhesive at relative high strain levels. The term between square brackets reduces its influence as long as the strains are low. Within the second part of equation 7.1 the parameter σ_0 is stress valid for the second branch for the a strain equal to zero, F_a is the modulus representing the slope of the curve and the parameters c_2 and p_2 are dimensionless constants. In section 7.1.3 it is shown that this empirical relation fits quite well with the studied adhesives.

Generally the yield behaviour of adhesives under unidirectional tension and compression differs significantly. Under tension the adhesive will mostly fail rapidly after plasticizing, while under compression the resistance of the adhesive might still increase without any failure. To model this behaviour the plastic yield hypothesis has to include besides deviatoric stress components hydrostatic stress components (Chakrabarty, 1987). The deviatoric stress is

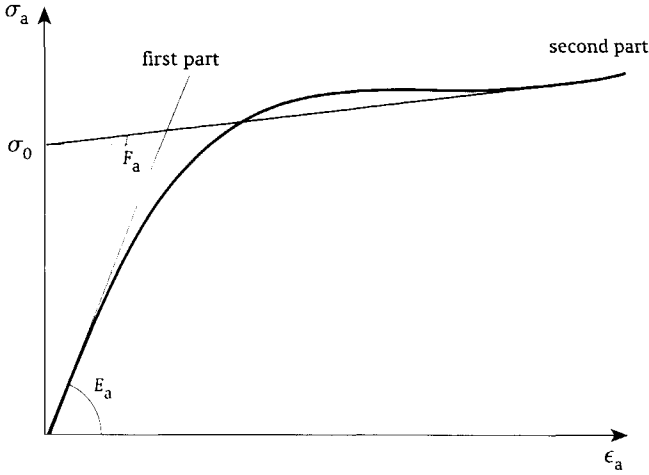


Figure 7.2 Schematic overview of the proposed stress-strain relation

the normal stress reduced by the value of the hydrostatic stress component, while the hydrostatic stress component is the mean of the three normal stresses. According to the concept of Gali, et.al. (1981) the effective stress s is equal to:

$$s = C_2 \sqrt{J_{2D}} + C_v J_1 \quad (7.2)$$

The second invariant of the deviatoric stress tensor J_{2D} is defined as:

$$J_{2D} = \frac{1}{6} [(\sigma_1 - \sigma_2)^2 + (\sigma_2 - \sigma_3)^2 + (\sigma_3 - \sigma_1)^2] \quad (7.3)$$

and the first invariant of the general stress tensor J_1 is defined as:

$$J_1 = \sigma_1 + \sigma_2 + \sigma_3 \quad (7.4)$$

The parameters C_s and C_v are defined as follows:

$$C_s = \frac{\sqrt{3}(\lambda_a + 1)}{2\lambda_a} \quad (7.5)$$

$$C_v = \frac{\lambda_a - 1}{2\lambda_a} \quad (7.6)$$

where λ_a is the ratio between compressive and tensile stresses in the adhesive. According to the proposed concept of Gali, et.al. (1981) the ratio between the compressive and tensile stresses λ_a is defined as the ratio valid for equal tangent moduli ($E_{a;c} = E_{a;t}$), as indicated in figure 7.3. This means that this ratio is a function of the effective strain level, but as an assumption a constant value is used here.

Design Rules for Overlap Joints

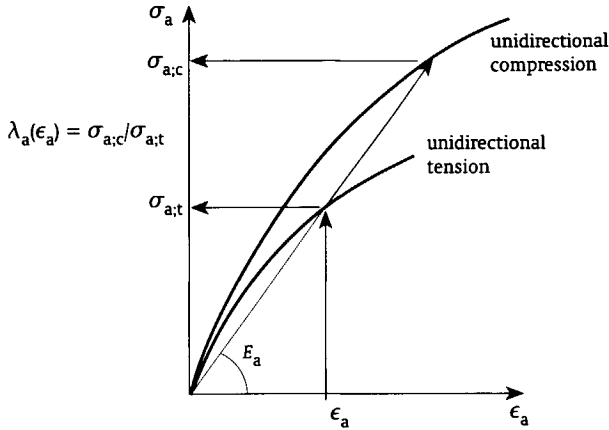


Figure 7.3 Definition of the ratio λ_a between compressive and tensile stresses of the adhesive

The effective strain is equal to:

$$e = C_s \frac{1}{1 + \nu_a} \sqrt{I_{2D}} + C_v \frac{1}{1 - 2\nu_a} I_1 \quad (7.7)$$

The Poisson's ratio of the adhesive ν_a is a function of the effective strain level. The second invariant of the deviatoric strain tensor I_{2D} is defined as:

$$I_{2D} = \frac{1}{6} [(\epsilon_1 - \epsilon_2)^2 + (\epsilon_2 - \epsilon_3)^2 + (\epsilon_3 - \epsilon_1)^2] \quad (7.8)$$

and the first invariant of the general strain tensor I_1 is defined as:

$$I_1 = \epsilon_1 + \epsilon_2 + \epsilon_3 \quad (7.9)$$

According to the proposed concept of Gali, et.al. (1981) the Poisson's ratio is a function of the effective strain level, but results of unidirectional tensile tests as for example discussed in section 7.1.3, indicate that a constant value might be assumed.

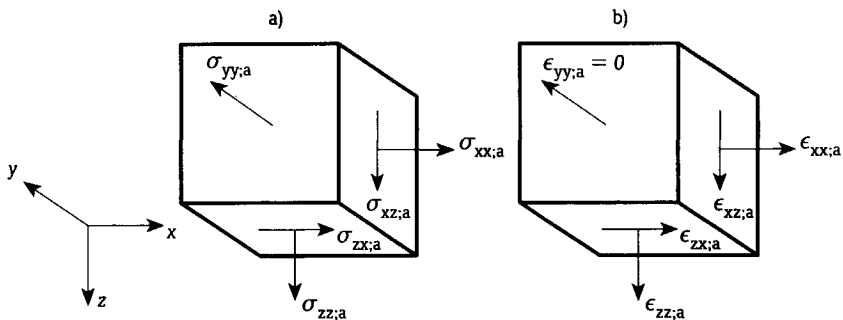


Figure 7.4 Elementary volume of the adhesive bondline under plane strain conditions, with: a) the stress state, and b) the strain state

The principal stresses σ_1 , σ_2 and σ_3 , and the principal strains ϵ_1 , ϵ_2 and ϵ_3 active in the adhesive bondline are calculated on basis of the stress and strain states respectively. The stress and strain states on one elementary volume within the bondline is indicated in figure 7.4. Since the width of the overlap joints is relatively large compared to the bondline thickness, a plane strain condition is assumed. The principal stresses are equal to:

$$\sigma_1 = \frac{\sigma_{zz;a} + \sigma_{xx;a}}{2} + \sqrt{\left(\frac{\sigma_{zz;a} - \sigma_{xx;a}}{2}\right)^2 + \sigma_{zx;a}^2} \quad (7.10)$$

$$\sigma_2 = \frac{\sigma_{zz;a} + \sigma_{xx;a}}{2} - \sqrt{\left(\frac{\sigma_{zz;a} - \sigma_{xx;a}}{2}\right)^2 + \sigma_{zx;a}^2} \quad (7.11)$$

$$\sigma_3 = \sigma_{yy;a} = \nu_a (\sigma_{zz;a} + \sigma_{xx;a}) \quad (7.12)$$

The principal strains are equal to:

$$\epsilon_1 = \frac{\epsilon_{zz;a} + \epsilon_{xx;a}}{2} + \sqrt{\left(\frac{\epsilon_{zz;a} - \epsilon_{xx;a}}{2}\right)^2 + \epsilon_{zx;a}^2} \quad (7.13)$$

$$\epsilon_2 = \frac{\epsilon_{zz;a} + \epsilon_{xx;a}}{2} - \sqrt{\left(\frac{\epsilon_{zz;a} - \epsilon_{xx;a}}{2}\right)^2 + \epsilon_{zx;a}^2} \quad (7.14)$$

$$\epsilon_3 = \epsilon_{yy;a} = 0 \quad (7.15)$$

To calculate the stress and strain states within the bondline of an overlap joint by taking into account the elastic-plastic behaviour of the adhesive as for example represented by equation 7.1, the theory of plasticity (Chakrabarty, 1987) has to be applied. When a point of the bondline is loaded along a certain strain-path, yielding will occur as soon as the stress reaches the yield surface of the criterion represented by equation 7.2. If strain hardening occurs, which means that the stress-strain relation is an increasing function, the load can be increased until the failure criterion of a maximum effective strain is reached. The value of the effective strain can be calculated with use of equation 7.7. The theory of plasticity gives a description how the stresses and strains will develop if the load is changed. This is done by making use of the so-called associated flow rule and the hardening hypothesis. The flow rule gives a description of the plastic strain rate after the yield criterion is reached. The hardening hypothesis on the other hand specifies the evolution of the internal stress and strain states in relation to the plastic strain rate. Instead of using this well-defined but rather complex theory of plasticity, Bigwood and Crocombe (1990), Thomsen (1992B) and Mortensen (1998) developed simplified calculation procedures for adhesive bonded overlap joints. It is assumed that the elastic-plastic behaviour can be described by one variable, the modulus. No proper flow rule is postulated to ensure that during plastic yielding the stresses remain on the yield surface. In spite of this, it is found that the obtained results compare well with test results and finite element calculations that make use of a proper flow rule. Based on these findings it is concluded that a simplified calculation procedure can be used.

Design Rules for Overlap Joints

7.1.3 Background of tensile and compression tests

To determine the properties of the adhesives used for the research programme, tensile and compression tests according to respectively ASTM D 638-96 (1996) and ASTM D 695-96 (1996) were performed. The results and interpretation of these tests are reported for the cold cured two-component epoxy adhesive DP 490 of 3M by Van Straalen (1999I) and for the cold cured two-component polyurethane adhesive UK 8202 of Henkel by Van Straalen (1999H). An overview of the test results is given and empirical relations for the stress-strain curves of both adhesives are proposed in this section.

For the two adhesives tensile test specimens according to figure 7.5 were prepared and axially loaded. The specimens were made of bulk adhesives, which were prepared according to the specifications of the adhesive suppliers. Just after mixing of the two components the uncured bulk adhesive was placed in a vacuum chamber for 5 minutes to avoid air inclusions as much as possible. The bulk adhesive was added in a casting mould and was cured under ambient laboratory conditions for at least 1 week. After the rough specimens were removed from the casting moulds, the specimens were milled to the desired dimensions. The specimens were stored under ambient laboratory conditions for at least 4 weeks. The specimens were loaded in a tensile testing machine with wedge grips, which were fixed. Tests were done under ambient laboratory conditions within the temperature range 21-25 °C. The load was applied at a testing rate of the clamping devices of 15 mm/minute until the specimen failed. This value was calibrated in such a way that a rate of approximately 5 mm/minute was reached between the displacement transducers over the joint height with a span of 50 mm. The load cell, the average displacement over the joint's height and the average contraction of the joint thickness were registered. On basis of these measurements the axial stresses are calculated by dividing the force by the cross-section area, the axial strains are calculated by dividing the lengthening by the initial span of 50 mm and the transverse strains are calculated by dividing the contraction by the initial thickness. The stress-strain curves for both adhesives are given in figure 7.6. It is observed that there were some air inclusions within the bulk adhesive, which might have influenced the measured failure load. But it is still assumed that for those cases the determined stress-strain curves are representative for the bulk adhesive. On basis of these stress-strain curves the values of the Young's modulus are

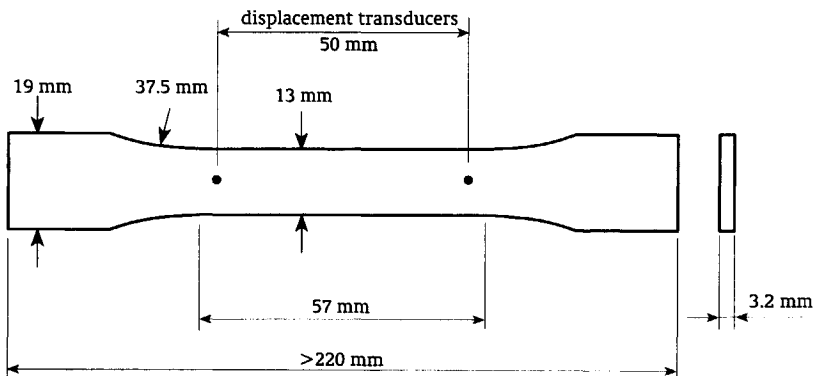


Figure 7.5 Dimensions of the tensile test specimens according to ASTM D 638-96 (1996)

calculated by taking the secant modulus at an axial strain of 0.2%. The Poisson's ratio is calculated by dividing the change in transverse strain by the change in axial strain (ASTM D 638-96: 1996) at an axial strain of 0.2%. An overview of the results is given after the discussion of the compression tests.

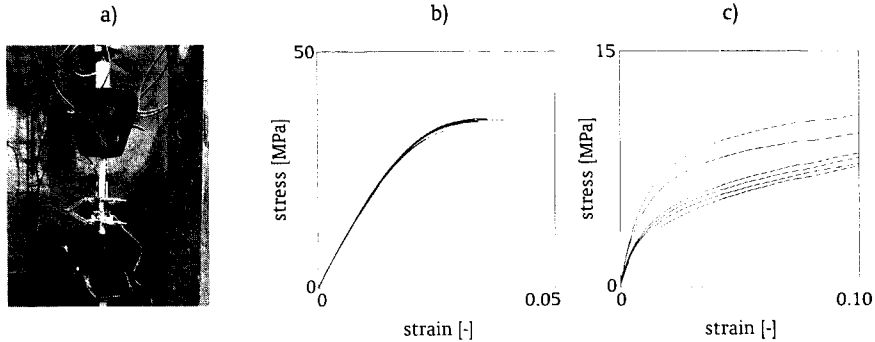


Figure 7.6 Tensile tests: a) test rig, b) stress-strain curve for DP 490, c) stress-strain curve for UK 8202

For the two adhesives compression test specimens according to figure 7.7 were prepared and axially loaded. The specimens were made in the same way as described for the tensile specimens. The specimens were loaded in a compression testing machine with a special tool. The supporting faces were fixed. Tests were done under ambient laboratory conditions within the temperature range 21-25 °C. The load was applied at a testing rate of the supporting faces of 1.3 mm/minute until large displacements were reached. The load cell and the average displacement over the joint's height were registered. On basis of these measurements the axial stresses are calculated by dividing the force by the cross-section area and the axial strains are calculated by dividing the lengthening by the initial height. The stress-strain curves for both adhesives are given in figure 7.8. It is observed that there were some air inclusions within the bulk adhesive, which might have influenced the measured loads. But it

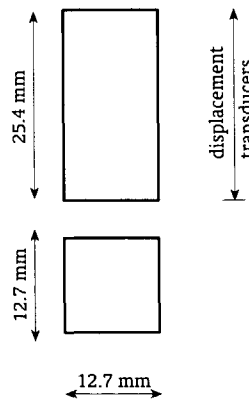


Figure 7.7 Dimensions of the compression test specimens according to ASTM D 695-96 (1996)

Design Rules for Overlap Joints

is still assumed that for those cases the determined stress-strain curves are representative for the bulk adhesive. On basis of these stress-strain curves the values of the Young's modulus are calculated by taking the secant modulus. For DP 490 this is done at an axial strain of 1%, because the development of the initial part of the stress-strain curve is strongly influenced by the fact that the specimens were not directly in full contact. For the UK 8202 adhesive on the other hand an axial strain of 0.2% as used for the tensile tests is taken.

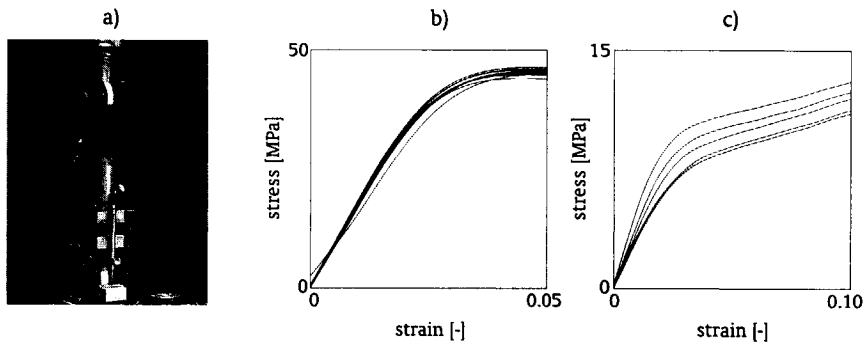


Figure 7.8 Compression tests: a) test rig, b) stress-strain curve for DP 490, c) stress-strain curve for UK 8202

Overviews of the properties of the DP 490 and UK 8202 adhesives based on the test results are given in table 7.1 and 7.2 respectively. The given values for the ultimate tensile stress $\sigma_{a;t;ult}$ and ultimate tensile strain $\epsilon_{a;t;ult}$ are the highest measured values. These tables include the mean values and standard deviations of the considered test samples. An observation is that the Young's modulus based on the tensile tests is higher than the value

Table 7.1 Overview of test results for the DP 490 adhesive properties

	tensile properties			compression properties	
	$\sigma_{a;t;ult}$ [MPa]	$\epsilon_{a;t;ult}$ [-]	$E_{a;t}$ [MPa]	ν_a [-]	$E_{a;c}$ [MPa]
test results	35.2	0.035	2014	0.40	1550
	33.3	0.028	1900	0.37	1817
	31.5	0.023	1905	0.35	1799
	35.3	0.032	1866	0.41	1863
	35.6	0.034	1886	0.46	1803
	35.9	0.036	1925	0.41	1771
	35.6	0.040	1938	0.41	1816
	33.7	0.020	1926	0.43	1721
<i>m</i>	34.5	0.031	1920	0.41	1768
<i>s</i>	1.5	0.007	45	0.03	97

Table 7.2 Overview of test results for the UK 8202 adhesive properties

	tensile properties			compression properties	
	$\sigma_{a;t,ult}$ [MPa]	$\epsilon_{a;t,ult}$ [-]	$E_{a;t}$ [MPa]	ν_a [-]	$E_{a;c}$ [MPa]
test results	12.6	0.179	897	0.46	585
	11.4	0.182	642	0.50	449
	12.1	0.178	523	0.47	370
	12.4	0.180	688	0.54	367
	14.1	0.183	915	0.51	313
	12.7	0.183	674	0.66	
<i>m</i>	12.6	0.181	723	0.52	417
<i>s</i>	0.9	0.002	153	0.07	106

based on the compression tests. Another observation is that the Young's modulus of the UK 8202 adhesives shows a rather large scatterband.

The determined stress-strain curves of the DP 490 and UK 8202 adhesives can be represented by the proposed empirical relation given by equation 7.1. Instead of using the engineering stress-strain curves as presented in figure 7.6 and 7.8, the engineering stress σ_e and strain ϵ_e are corrected to the true stress-strain curves. The stress-strain curves according to the test results presented above are based on the undeformed geometry, while it might be expected that for larger deformations the measurement length and cross-section differ significantly from the initial ones. In ASTM D 638-96 (1996) it is explained that if it is assumed that the volume of the specimen does not change, the true stress is equal to:

$$\sigma_t = \sigma_e \frac{L}{L_0} = \sigma_e (1 + \epsilon_e) \quad (7.16)$$

and the true strain is equal to:

$$\epsilon_t = \int_{L_0}^L \frac{1}{L} dL = \ln\left(\frac{L}{L_0}\right) = \ln(1 + \epsilon_e) \quad (7.17)$$

where L_0 is the original measurement length, L is the measurement length at any time and dL is the increment of the elongation when the measurement length is equal to L . The true stress-strain curves are used for further analyses.

To determine the values of the unknown constants of equation 7.1 on basis of a true stress-strain curve represented by the data set (σ_t, ϵ_t) , a least squares method is mostly used (Mood et.al., 1974). In principle the stress σ_t and strain ϵ_t are both stochastic variables, but within the least squares method one has to be deterministic. It is assumed that the strain is deterministic, while the stress is stochastic. There are two reasons for this assumption; firstly a constant strain rate was applied during the tests and secondly it is expected that this will give the most consistent results if large plastic deformations occur. The values of E_a , c_1 , p_1 , σ_0 , F_a , c_2 and p_2 that minimize the following sum of squares of the total number of data points n_{tot} :

Design Rules for Overlap Joints

$$\sum_{i=1}^{n_{\text{tot}}} ((\sigma_{t,i}, \epsilon_{t,i}) - \sigma_a(\epsilon_{t,i}))^2 \quad (7.18)$$

are defined to be the least-square estimators. It is noted here that the term $\sigma_a(\epsilon_t)$ represents equation 7.1. This least squares method does not give an estimation for the standard deviation. An alternative estimator s is proposed, which is based on equation 7.1 and the least-squares estimators determined with equation 7.18:

$$s = \sqrt{\frac{1}{n_{\text{tot}} - 7} \sum_{i=1}^{n_{\text{tot}}} ((\sigma_{t,i}, \epsilon_{t,i}) - \sigma_a(\epsilon_{t,i}))^2} \quad (7.19)$$

For each of the stress-strain curves given in figures 7.6 and 7.8 the least square estimators and the estimator s are determined. For both adhesives the value of the Young's modulus E_a is fixed to a value equal to the matching one given in tables 7.1 or 7.2 and corrected for the true stress-strain curve. Additionally it is assumed for the DP 490 adhesive that the value of σ_0 is fixed to the highest stress level of the curve and that the value of F_a is assumed to be a low value (1 MPa). Instead of presenting the results for the individual stress-strain curves, here the average stress-strain relations are presented for the tensile and compression situation of both considered adhesives. A similar analysis is performed. It is decided not to use the actual data points of a series of stress-strain curves, because the number of data points of the individual stress-strain curves are not equal to each other. Instead, a set of data points is generated on basis of the determined individual relations with equally distributed strain levels and matching stress values calculated with equation 7.1. Using the above given procedure the values of E_a , c_1 , p_1 , σ_0 , F_a , c_2 , p_2 and s for the average stress-strain curves are determined. It is noted here that the calculated estimator s only represents the stochastic nature of the differences between the individual relations. This value, here represented by the symbol s_r , has to be combined with the values s_{ind} of the individual curves. A conservative approximation for the combined estimator s_{comb} of n_c curves is:

$$s_{\text{comb}} = \sqrt{\sum_{j=1}^{n_c} s_{\text{ind},j}^2 + s_r^2} \quad (7.20)$$

As an alternative it is also possible to calculate the combined estimator for each considered strain level, which results into a more realistic presentation of the linear elastic part of the stress-strain relation. The results for the average stress-strain relations of the DP 490 and UK 8202

Table 7.3 Overview of the determined values of the coefficients of equation 7.1, the value for the combined estimator s_{com} of the standard deviation and the ratio λ_a between the compression and tensile stresses

adhesive	average curve	E_a [MPa]	c_1 [-]	p_1 [-]	σ_0 [MPa]	F_a [MPa]	c_2 [-]	p_2 [-]	s_{com} [MPa]	λ_a [-]
DP 490	tensile	1926	87.28	2.15	35.48	1.00	58.88	2.79	0.53	1.2
	compr.	1773	32.76	3.54	38.00	1.00	28.22	3.94	0.70	
UK 8202	tensile	726	791.0	1.64	7.03	36.10	102.0	1.12	1.25	1.2
	compr.	418	79.79	2.29	7.23	30.86	56.80	2.82	0.67	

adhesives are presented in table 7.3 and figure 7.9. On basis of these results the ratio λ_a between the compressive and tensile stresses as defined in figure 7.3, are calculated. In figure 7.9 the ratio λ_a is presented as a function of the strain for both adhesives. Within the proposed model a constant value is assumed equal to the value that match with a strain of 0.05. For the DP 490 adhesive the ratio is assumed to be $\lambda_a = 1.2$ and for the UK 8202 adhesive the ratio is assumed to be $\lambda_a = 1.2$. The determined average stress-strain curves will be used for the validation of the proposed prediction model and the calibration of a design rule.

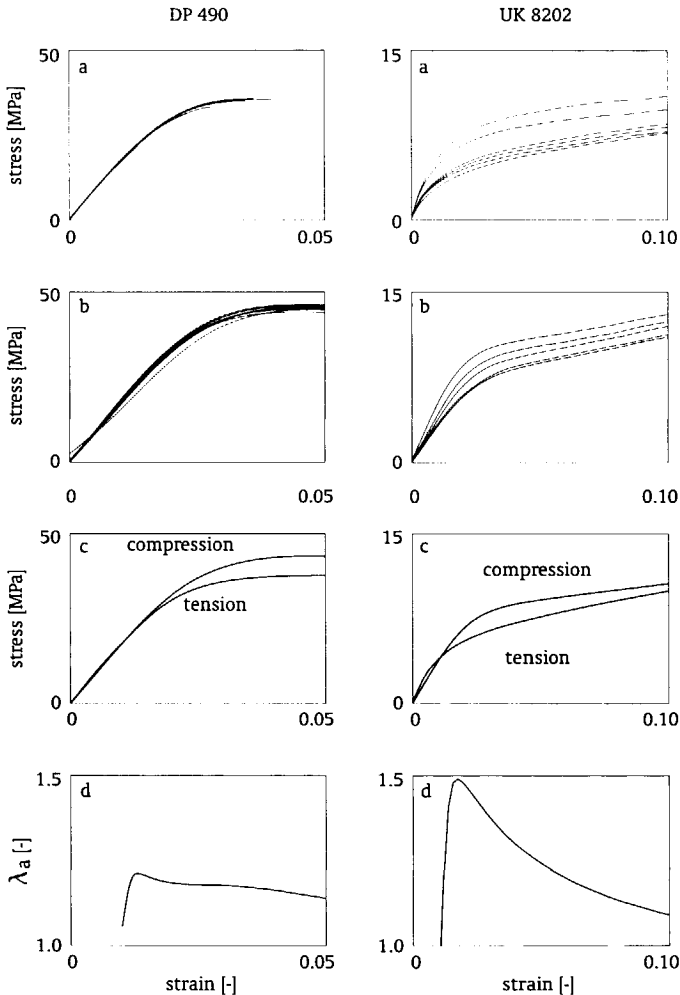


Figure 7.9 Stress-strain relations of the DP 490 and UK 8202 adhesives: a) results tensile tests, b) results compression tests, c) average stress-strain relations, and d) ratio λ_a as a function of the strain for tension

7.1.4 Background of stress and strain analyses

Since the publication of the first solution of a stress analysis for overlap joints by Volkersen (1938), a large variety of analytical solutions has been proposed. To get an overview and a better insight into the advantages and disadvantages of various solutions, researchers have made reviews. Three kinds of reviews can be distinguished: a survey of published solutions, a study of assumptions and a discussion of the assessment of various theories.

Van Ingen and Vlot (1993) survey various analytical solutions, which are based on an approach that model the adhesive bondline with series of shear and transverse tensile/compression springs. The first discussed group of solutions is based on rather simple assumptions. The two best known solutions are the Goland and Reissner (1944) and the Hart-Smith (1973) solutions. The second group of solutions, of which the Delale et.al. (1981) and the Yuceoglu and Updike (1981) solutions are discussed, accounts for transverse shear effects in the adherends. The third group of solutions, of which those of Allman (1977), Renton and Vinson (1977) and Chen and Cheng (1983) are discussed, satisfies the zero shear stress condition at the adhesive layer endings. The solutions of Allman (1977) and Chen and Cheng (1983) also model a variation of normal stresses over the bondline thickness. Most of these solutions assume linear elastic material behaviour and predict average stresses over the thickness of the bondline. None of them takes the effect of a spew fillet into account. Van Ingen and Vlot (1993) recommended the solution of Delale et.al. (1981), because it allows for general joint configurations with two bonded plates and because it can be used for joints with dissimilar isotropic or orthotropic adherends. Van Ingen and Vlot (1993) also discussed analytical solutions to take the effects of the geometrical non-linear behaviour of the single overlap joint loaded in tension into account. Tsai and Morton (1994) considered this aspect more completely. The solutions of Goland and Reissner (1944), Hart-Smith (1973) and Oplinger (1994) are discussed. Tsai and Morton (1994) compared these solutions with finite element calculations and concluded that the solution of Hart-Smith (1973) is more feasible and reasonable for single overlap joints with short overlaps, while the solution of Goland and Reissner (1944) and the more complex solution of Oplinger (1994) are better approximations for long overlaps. The surveys of Van Ingen and Vlot (1993) and Tsai and Morton (1994) give a good overview of available solutions and their prospects.

Carpenter (1991) investigates comprehensively various assumptions made in analytical solutions, by using a special finite element technique and examining several load cases, Carpenter (1991) was capable to quantify the effects on the predicted stress state within the bondline. Considered assumptions are:

- a) plane stress and plane strain;
 - b) zero and finite adhesive thickness;
 - c) incomplete and complete shear-strain relation for the adhesive;
 - d) constant and linear distributed strains over the adhesive thickness;
 - e) no shear deformation and shear deformation of the adherends;
 - f) different stress-strain relations for the adhesive;
 - g) use of inconsistent and consistent plane strain assumption for the adherends.
- Carpenter's main conclusions are that the maximum adhesive shear stress is unaffected by the used assumptions, that the maximum transverse normal stress is relatively unaffected and that if the shear deformation of the adherends is neglected, the transverse normal stress is affected by 15 to 30%.

Adams (1989) focusses on the assessment of analytical solutions and the application of

finite element methods. Adams' criticism about analytical solutions is that they cannot describe the stress and strain states within the adhesive bondline adequately. Finite element methods on the other hand are more flexible. These can accommodate with geometrical non-linear effects, physical non-linear material behaviour, spew fillets and corner roundings. From Adams' point of view only finite element methods can be used successfully.

The application of available analytical models is not only restricted by the limitations mentioned by Adams (1989), but also by the fact that most solutions are only valid for a specific joint geometry. In spite of these conclusions it is still believed here that an analytical solution formulated within a unified approach can deal with these limitations. Useful derivations given in literature are those presented by Delale et.al. (1981) and Yuçeoğlu and Updike (1981) and (1980). The derivation of Delale et.al. (1981) gives a closed-form solution for the three-layer overlap region of figure 7.10 a), while the solution of Yuçeoğlu and Updike (1980) gives sets of differential equations for the three- and five layer overlap regions of figure 7.10. These sets of differential equations have to be solved numerically. The derivations are based on a spring model for the adhesive bondline. There are a number of drawbacks to be mentioned. The modelling of the stiffness of the adhesive seems to be incorrect (Van Straalen, 1999C), resulting in higher normal stresses. Geometrical non-linear behaviour has to be taken into account with use of approximated analytical solutions, which are in fact only available for single overlap joints (Tsai and Morton, 1994). Finally Delale et.al. (1981) give a proposal to model the physical non-linear material behaviour of the adhesive, but this model is not worked out in a closed-form solution. A more generic unified approach also based on a spring model for the adhesive bondline is proposed by Thomsen (1992B) and Mortensen (1998). They use a general applicable method of derivation. The mechanical behaviour of overlap joints is represented by a set of first order differential equations and matching boundary conditions. To solve such a boundary value problem a numerical method is used. The main advantage of this unified spring model approach is that it can be applied for all kinds of overlap joints.

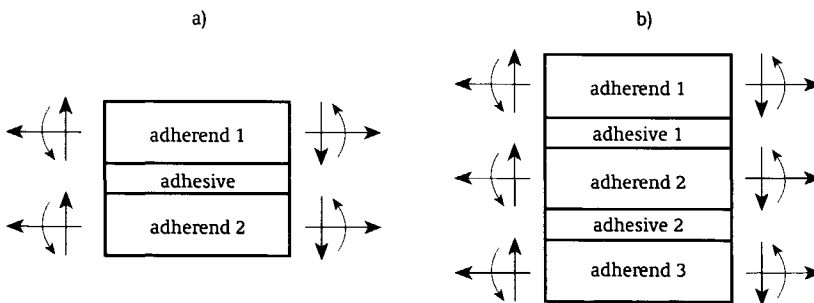


Figure 7.10 Overlap region: a) three-layer, and b) five-layer

7.1.5 Unified spring model approach

The unified spring model approach models the adherends as plates and the adhesive layer as series of continuously distributed shear and transverse tensile/compression springs. This modelling is illustrated in figure 7.11 for a single overlap joint. To consider the complete geometry it is necessary to model the overlap region and outer adherends separately. Using proper boundary and continuity conditions the complete geometry can be evaluated.

Design Rules for Overlap Joints

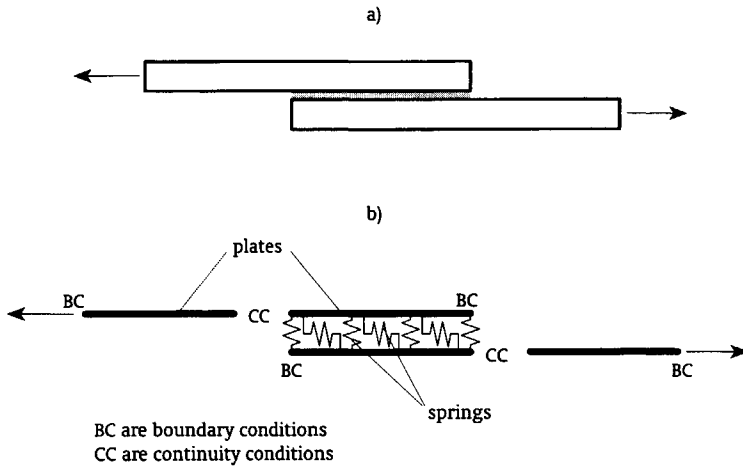


Figure 7.11 Spring model for a single overlap joint: a) geometry, and b) modelling

To model the mechanical behaviour of the overlap region and outer adherends the following general procedure of derivation is followed:

- 1) Describe the kinematic relations. For the adherends the longitudinal strain of the plate ϵ_{xx} is expressed in terms of the longitudinal displacement u and the rotation ψ . For the adhesive the shear angle γ_a is expressed in terms of the longitudinal displacement u_a and the transverse strain $\epsilon_{zz;a}$ is related to the transverse displacement w_a .
- 2) Describe the compatibility conditions of the interface layer. The displacements of the adherends u and w are related to the displacement of the adhesive u_a and w_a .
- 3) Describe the equilibrium equations of the interface layer. The axial force N_{xx} , bending moment M_{xx} and shear force Q_{xx} in the adherends are related to the shear stress τ_a and the transverse normal stress $\sigma_{zz;a}$ in the adhesive.
- 4) Describe the constitutive relations. For the adherends the axial force N_{xx} is related to the longitudinal displacement u and the bending moment M_{xx} and shear force Q_{xx} are related to the vertical displacement w and rotation ψ . For the adhesive the shear stress τ_a is related to the shear angle γ_a and the transverse normal stress $\sigma_{zz;a}$ is related to the transverse normal strain $\epsilon_{zz;a}$.

A summary of this procedure is given in figure 7.12. Using these derived relations the governing differential equations of the complete overlap region and the outer adherends are described. To combine these differential equations it is necessary to give a full description of the boundary and continuity conditions. This so-called boundary value problem has to be solved analytically or numerically.

For the three- and five-layer overlap regions, as indicated in figure 7.10 and the outer adherends the unified spring model approach is worked out in this study. The derivations are based on the method of derivation used by Thomsen (1992B) and Mortensen (1998). The following assumptions are made:

- No spew fillets.
- Cylindrical bending of adherends. Instead of using a beam theory as proposed by Thomsen and Mortensen, the thin plate theory is adapted.
- Plane strain conditions.

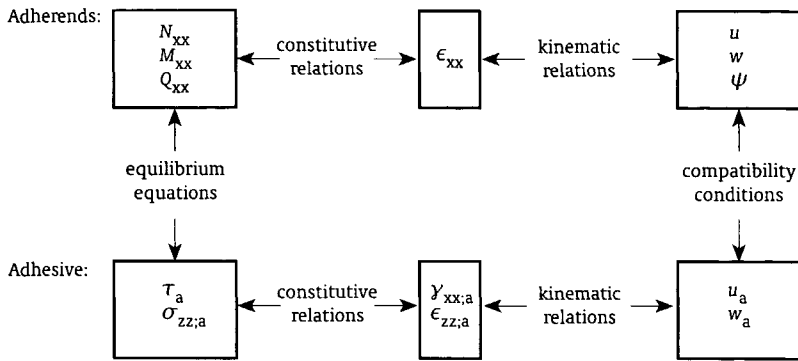


Figure 7.12 General procedure of derivation

- Elastic material behaviour of adhesive and adherends. Thomsen and Mortensen derived their model for composite laminates, while in this study isotropic materials like steel and aluminium are considered. It is noted here that by using an additional calculation procedure, the non-linear adhesive material behaviour is taken into account.
- Shear deformation of the adherends. Thomsen and Mortensen did not consider this effect. In this study it is decided to take this effect into account, because Carpenter (1991) concluded that this assumption has a significant influence on the results. It is noted here that Oplinger (1994) proposed an alternative method, which corrects the value of the shear modulus of the adherends.
- Constant shear stress over the adhesive layer thickness by using continuously distributed shear springs.
- No zero shear stress condition at the adhesive layer's ends.
- Constant transverse normal stress over the adhesive layer thickness by using continuously distributed tension/compression springs.
- No longitudinal normal stress in the adhesive layer. It is noted that this assumption follows from the two preceding assumptions.
- Unequal adherends (thickness and material properties) and unequal adhesives if a five-layer overlap region is considered.

The derivations of the differential equations, continuity and boundary conditions are presented by Van Straalen (1999C).

The result of these derivations is a set of first order differential equations and matching continuity and boundary conditions. An overview for the three- and five-layer overlap regions and the outer adherends is given in Appendix A. The derived boundary value problem for the three-layer overlap region is of the 12th order, for the five-layer overlap region of the 18th order and for the outer adherend of the 6th order. The derived sets of differential equations contain the unknown functions of the displacements of the adherends (longitudinal displacement in the centre line u_0 , transverse displacement w and rotation ψ) and the cross-section forces of the adherends (normal force N_{xx} , bending moment M_{xx} , and shear force Q_{xx}). The matching continuity and boundary conditions are also formulated within these displacements and cross-section forces. The stress and strain states within the bondline (shear stress τ_a , transverse normal stress $\sigma_{zz;a}$, shear strain γ_a and transverse normal strain $\epsilon_{zz;a}$) are formulated in terms of the unknown functions.

Boundary value problems can be solved with a numerical algorithm. Well known are shooting and finite difference methods. As proposed by Thomsen (1992B) and Mortensen (1998) the multi-segment method of integration developed by Kalnins (1964) is used in this study (Van Straalen, 1999B). It is based on a transformation of the boundary value problem into a series of initial value problems. To avoid loss of accuracy the geometry has to be divided into a number of segments. For each segment a solution in terms of the unknown functions at both segment endings, is accomplished by a standard numerical method like the Runge-Kutta formula. The values of the unknown functions at all segment endings are determined by solving a set of equations, which represents the requiring continuity between all segments together with the already given continuity and boundary conditions. To use this method for the overlap joints considered in this study, the original version is extended by Van Straalen (1999B). With this extended version of the multi-segment method of integration it is possible to divide the overlap joint in a number of elements. The advantages of this extension are that the mixture of continuity and boundary conditions between the overlap region and the outer adherends can be modelled properly and that each segment can have its own properties. This last mentioned advantage is important if physical non-linear material behaviour of the adhesive and geometrical non-linear behaviour are considered. It is generally concluded that the multi-segment method of integration is generally applicable and that its results are accurate.

To model geometrical non-linear behaviour most solutions presented in literature simplify the problem by determining second order effects separately from the stress and strain states within the bondline. For example the well-known solution of Goland and Reissner (1944) assumes for a single overlap joint with identical adherends that the adherends are lumped together in the overlap region neglecting the adhesive layer. It derives a solution for the second order normal force, bending moment and shear force acting on the overlap region. The calculated cross-sectional forces are applied on the overlap region. A separate closed-form solution is derived to calculate the shear and transverse normal stresses within the bondline. Drawbacks of the solutions presented in literature are that these only consider the single overlap joint and that various simplifications are made. The deformations over the adherends in the overlap region are ignored and long outer adherends are assumed. The unified approach on the other hand can be formulated in such a way that the geometrical non-linear behaviour is predicted more accurately without restriction on the joint geometry.

The geometrical non-linear behaviour of overlap joints is modelled by extending the derived set of differential equations. Firstly the effects of the transverse deflection of the adherends on the equilibrium equations are taken into account. Secondly the effects of stretching of the middle surface of the adherends due to large deflections are modelled. An overview of results of these additional derivations according to Van Straalen (1999C) is given in Appendix A for the three- and five-layer overlap regions and for the outer adherends. This adapted boundary value problem can not be solved directly with use of a numerical procedure. The reason for this is that the value of one parameter, the derivative of the transverse deflection of the adherends dw/dx , is unknown. The problem can only be solved with use of an iterative calculation procedure. The following procedure is used:

- 1) Perform a geometrical linear calculation by taking start values of dw/dx at each point of the adherends equal to 0.
- 2) Add for each point of the adherends the results for dw/dx of the preceding calculation and perform a new calculation.

3) Repeat steps 2 and 3 until the results converge and stabilize.

To obtain the best calculation results the load has to be applied gradually.

To evaluate a loaded overlap joint under the assumption of the defined stress-strain relationship and the hydrostatic dependent yield criterion, the simplified calculation procedure based on the principles proposed by Thomsen (1992B) and Mortensen (1998), is followed:

- 1) Determine the stress-strain relation for bulk adhesive under tension according to equation 7.1 and determine the ratio between compressive and tensile stresses λ_a . Both are based on unidirectional tensile and compression tests.
- 2) Calculate the stress and strain states within each point of the adhesive bondline. A uniform Young's modulus based on a unidirectional tensile test is assumed.
- 3) Calculate the principal stress and strain states with use of equations 7.10 to 7.15.
- 4) Calculate the effective stress and strain states with use of respectively equations 7.2 and 7.7.
- 5) Calculate for each point of the bondline the reduction of the modulus according to equation 7.1 that matches with the effective strain state calculated in step 4. It is proposed to use the secant modulus (Thomsen, 1992B) as illustrated in figure 7.13. The tangent modulus can be adapted as an alternative, but the calculation procedure will be complicated by the appearance of an initial stress for a strain equal to zero.
- 6) Calculate the stress and strain states of each point of the adhesive bondline with use of a linear elastic prediction model in combination with the reduced secant's moduli for each point of the bondline.
- 7) Repeat steps 3 to 7 until the results converge and stabilize.

The load acting on the overlap joint might be increased until the calculated effective strain within a point of the bondline reaches the maximum strain of the unidirectional tensile test. This calculation procedure can be combined with the procedure of the geometrical non-linear calculation.

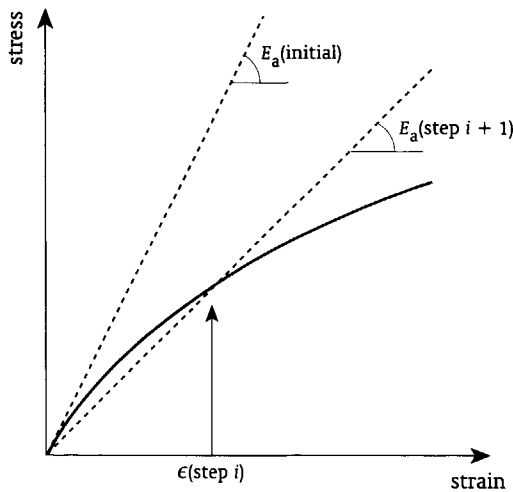


Figure 7.13 Determination of the reduction of the secant's modulus

Design Rules for Overlap Joints

7.1.6 Comparison between tests and predictions

To validate the proposed prediction model and to study various effects, calculations are compared with test results on double strap joints and single overlap joints. The geometry of the studied overlap joints are given in figure 7.14 and the nominal dimensions are given in table 7.4. The endings of the adherends were clamped and loaded in tension. The loading of the specimens was displacement controlled. The applied load and the displacement over the joint with a span of 100 mm were continuously recorded. For each situation 6 or 7 specimens were tested. A complete description of the test and the results is given by Van Straalen (1999E) and (1999F). The ultimate loads and the load-displacement curves are compared, and the effects of the bondline thickness, the selected stress-strain curves and geometrical non-linearities are studied.

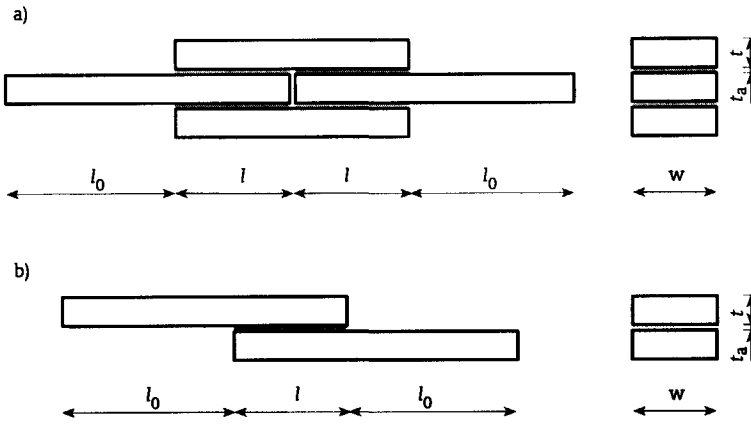


Figure 7.14 Geometry of the studied joints: a) double strap joint, b) single overlap joint

The used prediction model is based on the unified spring model approach discussed in the preceding section. For the stress-strain relations of the adhesives DP 490 and UK 8202 the average tensile curves given in table 7.3 are used. For the properties of the steel adherends a Young's modulus of $E = 210000$ MPa and a Poisson's ratio of $\nu = 0.3$ are used, while for the properties of the aluminium adherends a Young's modulus of $E = 70000$ MPa and a Poisson's ratio of $\nu = 0.3$ are used. Since the geometry of the double strap joint is symmetrical, only the left hand side is modelled. The geometry of the single lap joint on the other hand is completely modelled. Figure 7.15 gives an overview of the division of these two types of overlap joints into elements. The mechanical behaviour of each element is described by a set of differential equations. These elements are connected with proper boundary and continuity conditions. Boundary conditions are formulated for the line of symmetry of the double strap joint, and for the free endings of the overlap region and the clamped endings of both types of overlap joints. Continuity conditions are formulated between the outer adherends and the overlap region. An essential aspect of the modelling is the division of each element in a number of segments. It is possible to give each segment its own properties, which means that the iterative procedure proposed in the preceding section can be performed to take the geometrical and physical non-linear behaviour into account. The length of each segment has

to be selected in such a way that the difference between the derivative of the transverse deflection dw/dx and the reduction of the Young's modulus of the adhesive vary only slightly between connecting segments. Detailed information about the used differential equations, boundary conditions, continuity conditions and geometrical non-linear effects is given in appendix A.

Table 7.4 Nominal dimensions of the studied joints

joint type	adherend material	bondline thickness t_a [mm]	adherend thickness t [mm]	overlap length l [mm]	width w [mm]	length outer adherend l_0 [mm]		
double strap	steel	0.2	2	10	25	175		
				20	25	175		
				40	25	175		
			4	10	25	175		
				20	25	175		
				40	25	175		
	6	10	25	175				
		20	25	175				
		40	25	175				
		single overlap	steel	0.2	2	10	25	170
						20	25	165
						40	25	155
4	10				25	170		
	20				25	165		
	40				25	155		
6	10	25	170					
	20	25	165					
	40	25	155					
	aluminium	0.2	2	20	25	170		
				4	25	165		
				6	25	155		

To illustrate the ability of the prediction model to take geometrical and physical non-linearities into account, a single overlap joint with 4.03 mm thick steel adherends, a 19.75 mm overlap length, a 25.05 mm width and a 0.18 mm thick adhesive bondline is studied for the adhesive DP 490. The calculations are based on nominal values for the adherend properties and mean values for the adhesive properties. Linear-elastic, geometrical non-linear, physical non-linear, and combined geometrical and physical non-linear calculations are compared. To perform the non-linear calculations, it is necessary to apply the action (displacement of one of the endings) stepwise. If the action is increase by one step, the calculation has to be repeated until the results converge. After the results are stabilized, the following step can be made. To avoid problems with the accuracy and stability of the iteration process without long computer runs, it is important to divide the three elements of the specimens in a limited number of

Design Rules for Overlap Joints

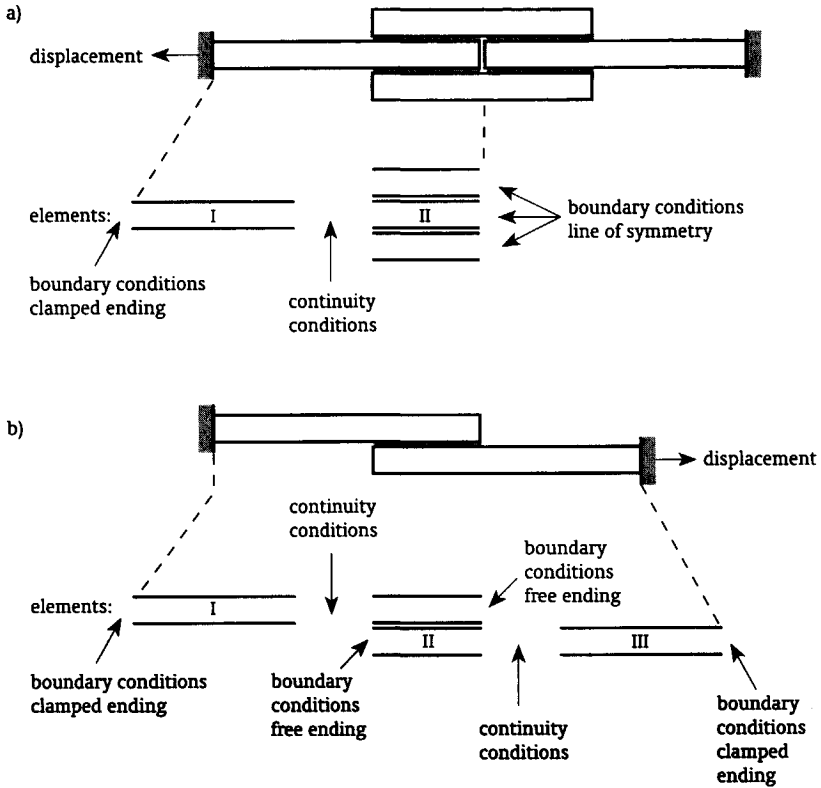


Figure 7.15 Modelling of the geometry: a) double strap joint, b) single overlap joint

segments properly distributed over the elements. In this study it is found that the overlap region has to be divided into 10 to 20 segments. The length of these segments varies from 0.2 mm near the overlap ends to more than 12 mm near the middle of the overlap. More care has to be taken with the division of the segments for the outer adherends. For the thicker adherends it is found that a division into 20 segments with lengths between 0.2 and 20 mm is adequate, while for the 2 mm thick adherend these lengths have to be smaller. In figure 7.16 the load-displacement curves are given for the four considered calculations. The main observations are that the displacement decreases due to geometrical non-linear effects and that the strength stabilizes due to the non-linear stress-strain curve of the adhesive.

As explained in section 7.1.2 the yielding of the adhesive is described by a hydrostatic dependent criterion. The stress and strain state within the adhesive bondline is represented by the effective equivalents represented by respectively equations 7.2 and 7.7. For four load steps of the geometrical and physical non-linear calculation presented above, the effective stress and strain distributions along the adhesive bondline are given in figure 7.17. It is observed that with an increasing load the stresses along the bondline become almost uniform and stabilize, while the strains are still increasing. The proposed failure criterion assumes that the ultimate load is reached as soon as somewhere along the bondline the strain exceeds a given value.

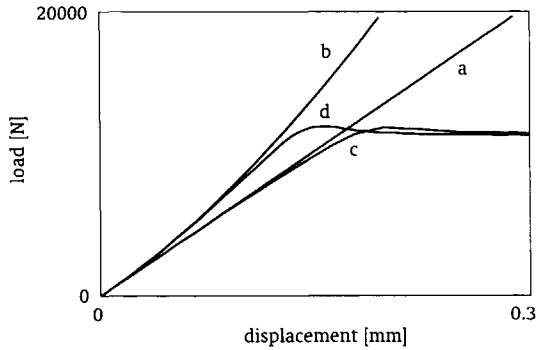


Figure 7.16 Load-displacement curves according to:
 a) linear elastic calculation, b) geometrical non-linear calculation,
 c) physical non-linear calculation, and
 d) geometrical and physical non-linear calculation

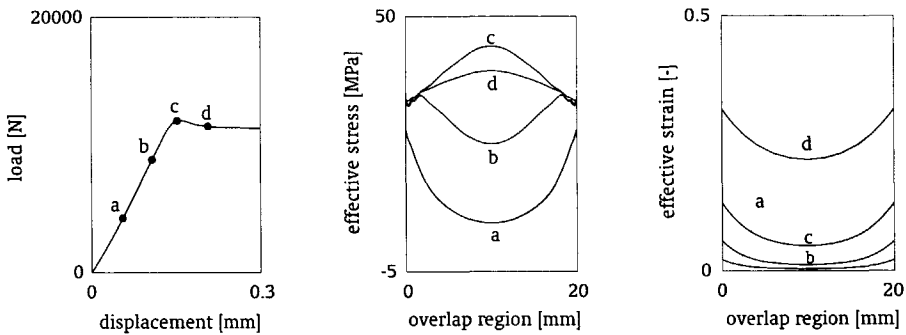


Figure 7.17 Distribution of the effective stresses and strains along the adhesive bondline for four load steps

The contradiction that for load step c and d given in figure 7.17 the effective stresses reach the highest values in the middle of the overlap region, while the matching strains reach the lowest values, is caused by the reduction of the Young's and shear moduli. Figure 7.18 shows for step c the distributions of the transverse normal strain $\epsilon_{zz;a}$, the shear angle γ_a and the matching effective strain calculated with the concept of Gali, et.al. (1981) given by equations 7.7 to 7.9. Based on the effective strain the reduction of the Young's modulus and the shear modulus is calculated according to the method given in figure 7.13. From figure 7.18 it can be seen that the value of the reduction factor in the middle of the overlap region is much higher than the value at the ends. This affects the distribution of the transverse normal stress $\sigma_{zz;a}$ and the shear stress τ_a significantly and causes the observed contradiction in the effective stress calculated with the concept of Gali, et.al. (1981) given by equation 7.2 to 7.6.

A parameter which influences the calculation results is the bondline thickness. To study these effects calculations are made for the same single lap joint as studied above. Bondline thicknesses of $t_a = 0.09, 0.18$ and 0.36 mm are considered. The load-displacement curves

Design Rules for Overlap Joints

according to geometrical and physical non-linear calculations are given in figure 7.19. The maximum loads are equal to 11651, 11886 and 12052 N respectively. The main observation is that the bondline thickness has some effect on the displacements, while the influence on the strength is not significant.

A direct comparison between the prediction model and the test results is made by considering the load-displacement curves. A double strap joint and a single overlap joint with

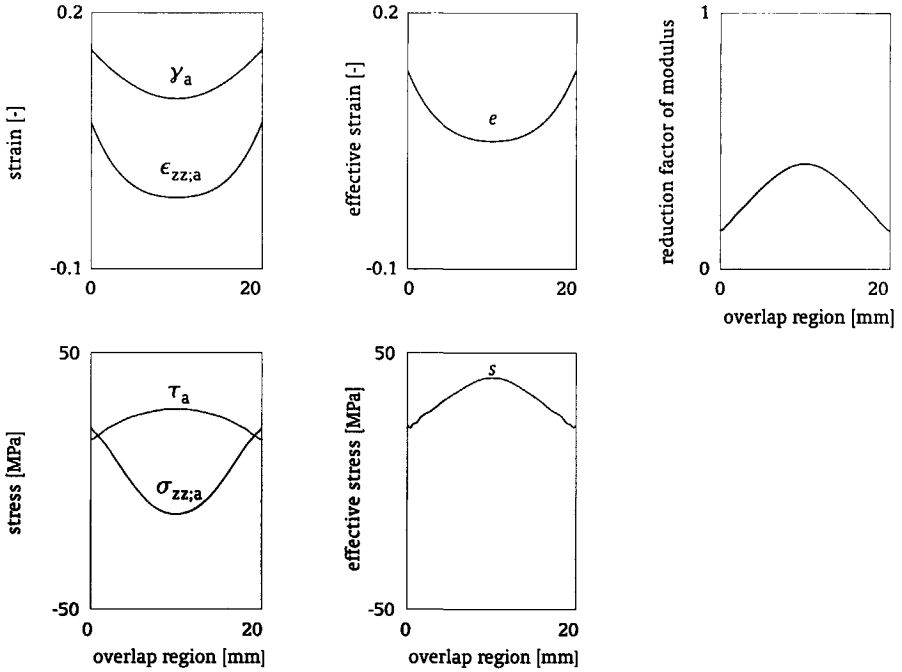


Figure 7.18 Stresses and strains calculated for load step c given in figure 7.17

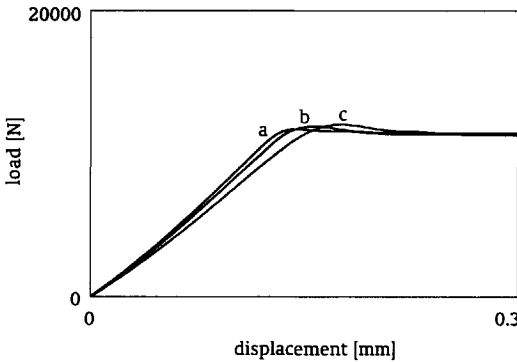


Figure 7.19 Load displacement curve for three adhesive bondline thicknesses: a) 0.09 mm, b) 0.18 mm, and c) 0.36 mm

4 mm thick steel adherends and 20 mm overlap length are considered. Tests were done under ambient laboratory conditions within the temperature range 21-25 °C. The calculations are based on the mean value of the measured bondline thickness, overlap length and width of the tested specimens. Nominal values for the adherend properties and the average adhesive properties are used. It is noted that in the tests of the single overlap joints the specimen endings were not only clamped, but were also displaced in transverse direction. This is because the two clamps of the tensile test machine were placed in line. The performed calculations take this additional boundary condition into account, by adding a transverse displacement equal to the sum of the adherend thickness and the adhesive bondline thickness.

For the adhesive DP 490 the load-displacement curves of both joints are given in figure 7.20 together with the calculated maximum effective strain within the bondline. From these curves it is concluded that the strength is predicted rather well. For the single overlap joint the calculated displacements are slightly overestimated. This is caused by the fact that the test specimens were slightly curved. In figure 7.21 the effect of an additional transverse displacement of the specimen endings is illustrated. From this comparison it is concluded that this does not affect the calculated strength. Before the calculated maximum load is reached, the matching effective strain already exceeds the value of the ultimate tensile strain $\epsilon_{u;t;ult} = 0.031$ according to the tensile bulk test as given in table 7.1. It is believed that this value is not representative as the actual value of the failure criterion, because the measured values are influenced by a local necking of the tensile bulk specimen if the failure load is reached. Since the maximum strength is predicted rather well it is concluded that the extrapolated stress-strain curve might be used for the adhesive DP 490.

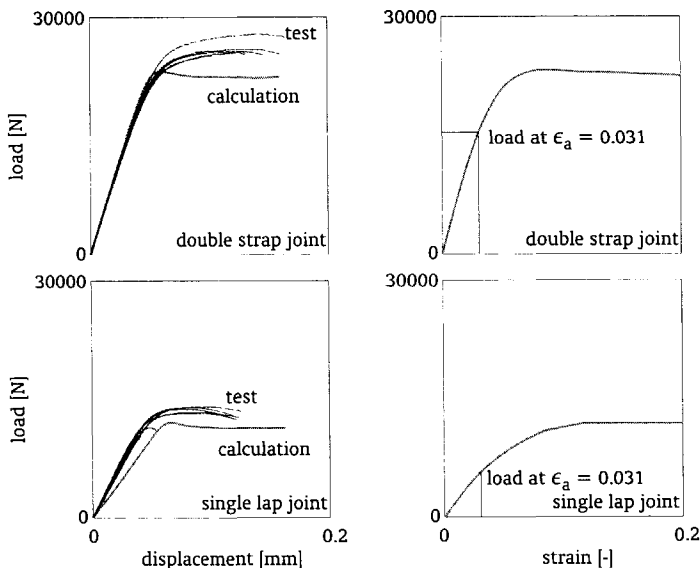


Figure 7.20 Comparison between the calculated load-displacement curves and the curves based on the tested joints for the adhesive DP 490, together with the calculated load-maximum effective strain curves

Design Rules for Overlap Joints

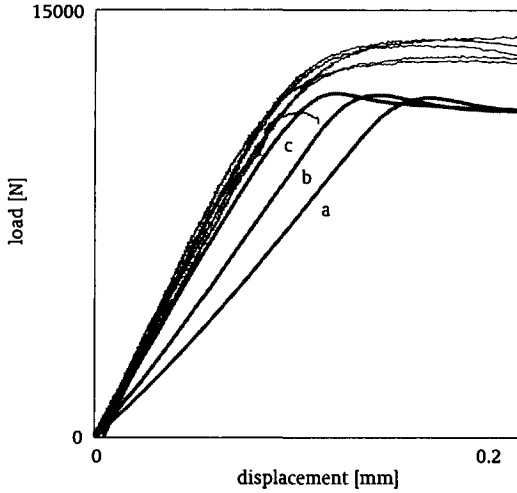


Figure 7.21 Effect of the transverse displacement of the specimen endings on the load-displacement curve, compared with the curves based on the tested joints for the adhesive DP 490; total transverse displacement equal to: a) 0 mm, b) 4.21 mm and c) 8.42 mm

For the adhesive UK 8202 the load-displacement curves of both joints are given in figure 7.22 together with the calculated maximum effective strain within the bondline. Not only the calculation based on the average stress-strain relation is presented, but also calculations based on the highest and lowest stress-strain relations of the tensile bulk tests presented in section 7.1.3 are given. The used values of the coefficients of equation 7.1 are presented in table 7.5. From these load-displacement curves it is concluded that the match between the prediction and the test results is less significant than for the calculations performed for the DP 490 adhesive. It seems that the determined stress-strain curves are not fully representative for the actual behaviour of the adhesive, but it is believed that the calculations can still be used to predict the strength. Before the calculated maximum strength is reached, the matching effective strain already exceeds the value of the ultimate tensile strain $\epsilon_{u;t;ult} = 0.181$ according to the tensile bulk test as given in table 7.2. It is assumed that this value is not representative as the actual value of the failure criterion, because the measured values are influenced by a local necking of the tensile bulk specimen if the failure load is reached. Based on a comparison between the predictions and the test results it is assumed that the extrapolated stress-strain curve with a maximum strain of 0.75 might be used for the adhesive UK 8202.

The general conclusion of the comparison is that with use of the unified spring model approach in combination with a pressure dependent yielding criterion, the strength of overlap joints can be predicted rather well.

7.1.7 Calibration of the partial factor

The essence of the procedure to calibrate the partial factor is the comparison of a set of data with matching strengths calculated by the proposed prediction model. For the studied overlap joints the procedure described in section 4.3.2 is used. It is assumed that the prediction model

is deterministic, which means that equation 4.18 is used. The calculations of the matching predicted strengths are based on the measured mean values for the dimensions, nominal values for the adherend properties and the average stress-strain curve of the adhesive. The results of these calculations give also the characteristic strengths, which are used to calibrate the actual value of the partial factor. Referring to the considerations made about the tests and the calculations in the previous section, overviews for the adhesives DP 490 and UK 8202 of the measured data and calculated strengths are given in respectively tables 7.6 and 7.7. To illustrate the potential of the used prediction model, the predictions are compared with the measured load-displacement curves in figures 7.23 to 7.26.

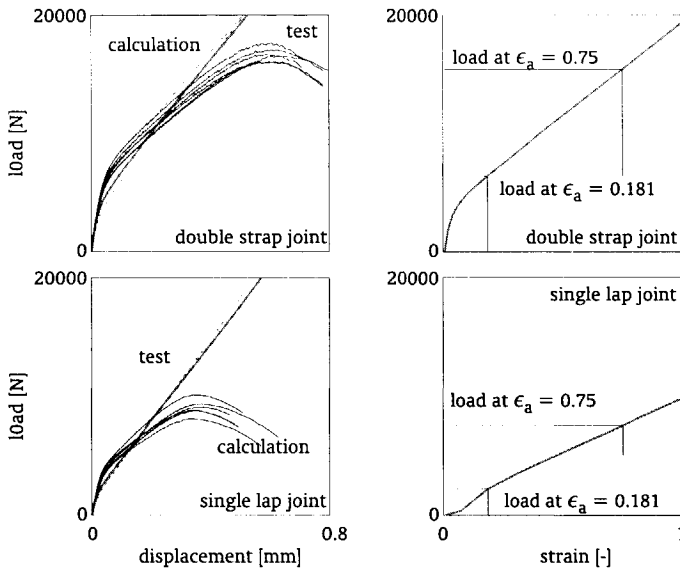


Figure 7.22 - Comparison between the calculated load-displacement curves for the average (straight lines), maximum and minimum (dotted lines) stress-strain relation and the curves based on the tested joints for the adhesive UK 8202, together with the calculated load-maximum effective strain curves

Table 7.5 Overview of the determined values of the coefficients of equation 7.1 and the ratio λ_a between the compression and tensile stresses, for the adhesive UK 8202

adhesive	curve	E_a [MPa]	c_1 [-]	p_1 [-]	σ_0 [MPa]	F_a [MPa]	c_2 [-]	p_2 [-]	λ_a [-]
UK 8202	average	726	791.0	1.64	7.03	36.10	102.0	1.12	1.2
	highest	918	688.0	1.69	9.46	33.44	109.8	1.29	1.2
	lowest	525	1934	2.20	5.98	39.49	83.47	0.91	1.2

Table 7.6 Overview of measured data and calculated strength for adhesive DP 490

joint type	adherend thickness [mm]	bondline thickness [mm]		plate thickness [mm]		overlap length [mm]		width overlap [mm]		test results		ultimate strength		predictions [N]					
		m	s	m	s	m	s	m	s	m	s	m	s						
double strap steel	2 mm	10	0.18	0.03	2.03	0.01	9.61	0.19	24.89	0.20	13037	10498	12158	12769	13599	12695	13062	11345	
		20	0.18	0.04	2.04	0.00	19.53	0.16	25.00	0.00	23690	23413	23535	23730	23120	23413	23560	23157	
		40	0.20	0.01	2.03	0.01	39.32	0.18	25.00	0.00	26650	27500	27000	27000	27500	27600			45925
4 mm	10	10	0.15	0.03	4.03	0.02	9.44	0.08	25.00	0.00	13306	13647	13110	13354	13257	13599			11213
		20	0.16	0.04	4.04	0.02	19.58	0.28	25.03	0.05	25537	27954	26001	25830	25806	25732			23150
		40	0.20	0.01	4.03	0.01	39.30	0.19	25.00	0.00	52734	53125	53662	52148	50000	52686			46275
6 mm	10	10	0.12	0.02	6.16	0.01	9.49	0.11	25.01	0.04	13721	13525	12744	14282	13110	13306	13330		11290
		20	0.12	0.02	6.17	0.02	19.51	0.16	25.00	0.00	26855	26831	26758	26880	26904	27490	27173		22988
		40	0.17	0.04	6.15	0.02	39.43	0.07	25.00	0.00	52002	53223	52783	53369	51807	53027	52832		46450
single overlap steel	2 mm	10	0.17	0.03	2.03	0.01	9.98	0.04	25.00	0.00	7178	7207	7529	7051	7090	7148			5942
		20	0.19	0.03	2.02	0.01	19.80	0.18	24.97	0.05	12148	13164	13564	13193	14014	14072			11823
		40	0.22	0.03	2.03	0.01	39.88	0.12	24.99	0.04	20535	21805	22876	19336	21704	19116			23686
4 mm	10	10	0.16	0.01	4.01	0.01	9.95	0.29	25.05	0.05	7354	7480	7588	7080	7422	7744			6185
		20	0.18	0.02	4.03	0.01	19.75	0.15	25.05	0.05	14063	13989	13403	13770	11426	13232			11876
		40	0.18	0.01	4.04	0.01	39.82	0.13	25.02	0.04	25903	23877	25684	25293	26416			23489	
6 mm	10	10	0.10	0.04	6.16	0.01	9.70	0.35	24.98	0.04	7275	7754	8066	6807	7490	7314			6078
		20	0.14	0.05	6.15	0.02	19.85	0.10	25.00	0.00	14136	13965	13770	13745	12988	13379			12025
		40	0.19	0.03	6.14	0.01	39.98	0.04	24.98	0.04	25977	26025	25293	25830	25464	25708			23529
single overlap alum.	2 mm	20	0.20	0.00	2.00	0.00	20.45	0.16	25.00	0.00	10234	10381	10518	10518	10303	10332			12058
	4 mm	20	0.18	0.02	4.09	0.01	20.02	0.04	25.02	0.04	11943	11504	11182	11299	11455	11377			11782
	6 mm	20	0.19	0.01	5.99	0.02	21.80	2.75	25.07	0.05	12705	12725	13398	12842	13184	12646			12916

Table 7.7 Overview of measured data and calculated strength for adhesive UK 8202

joint type	adherend	overlap		bondline		plate thickness		overlap length		width overlap		test results		ultimate strength		predictions [N]		
		m	s	m	s	m	s	m	s	m	s	m	s	m	s			
double strap steel	2 mm	10 mm	0.17	0.03	2.04	0.02	0.02	9.51	0.06	25.00	0.00	8936	9302	9351	8130	8716	9595	8233
		20 mm	0.19	0.02	2.04	0.01	19.50	0.08	25.00	0.00	18506	17749	18408	18408	18408	18213	18188	15288
		40 mm	0.22	0.03	2.03	0.01	39.40	0.13	25.00	0.00	21631	23020	22046	22412	22046	22192	21826	30156
4 mm	10 mm	0.12	0.05	4.04	0.03	9.52	0.08	25.00	0.00	9253	9229	8887	9619	8887	9619	8984	9033	8154
	20 mm	0.17	0.03	4.03	0.02	19.54	0.08	25.00	0.00	16040	16699	17065	17651	17065	16577	16089	15393	
	40 mm	0.19	0.03	4.03	0.02	39.47	0.18	25.00	0.00	28345	29175	30200	30200	30200	28613	29321	29714	
6 mm	10 mm	0.10	0.02	6.15	0.01	9.55	0.09	25.00	0.00	9277	9473	10059	9448	10059	9448	10034	9790	9630
	20 mm	0.16	0.02	6.15	0.01	19.47	0.14	25.00	0.00	15356	14966	14673	14893	14673	14673	14502	14868	16689
	40 mm	0.17	0.02	6.15	0.01	39.57	0.07	25.00	0.00	30029	29785	30542	31055	30542	30054	29736	31030	28810
single overlap steel	2 mm	10 mm	0.20	0.06	2.02	0.01	9.95	0.05	25.00	0.00	5088	4541	5156	4678	4883	4688	4569	4569
		20 mm	0.17	0.04	2.02	0.01	16.03	0.08	25.00	0.00	7109	6699	6250	6533	6250	7197	6650	5891
		40 mm	0.20	0.02	2.02	0.01	39.90	0.13	24.95	0.05	16289	15391	16416	14521	16416	14912	16133	12131
4 mm	10 mm	0.15	0.02	4.03	0.01	9.97	0.05	25.00	0.00	5264	4990	5156	5479	5156	5322	5020	5111	5111
	20 mm	0.15	0.04	4.03	0.01	20.97	1.92	25.03	0.05	8867	8828	8145	9102	8145	9385	10146	8439	
	40 mm	0.19	0.02	4.03	0.01	40.00	0.19	24.98	0.10	16846	16426	16299	16904	16299	16465	15186	12197	
6 mm	10 mm	0.12	0.06	6.15	0.01	9.90	0.17	25.02	0.04	5059	5332	5137	5342	5137	4912	5254	5341	
	20 mm	0.12	0.07	6.16	0.02	19.97	0.08	25.00	0.00	8701	7705	8906	8828	8906	8857	8604	9139	
	40 mm	0.16	0.02	6.15	0.01	40.13	0.29	25.00	0.00	16089	14814	16504	17383	16504	16953	16758	12667	
single overlap alum.	2 mm	20 mm	0.24	0.04	2.00	0.01	19.98	0.04	24.90	0.20	7354	7217	7305	7129	7305	7568	7148	5958
	4 mm	20 mm	0.20	0.04	4.09	0.02	19.80	0.17	25.02	0.04	7373	7666	7793	7402	7793	7383	7949	6847
	6 mm	20 mm	0.21	0.01	6.00	0.01	19.95	0.08	25.05	0.08	8047	7861	7930	7842	7930	7520	7793	8523

Design Rules for Overlap Joints

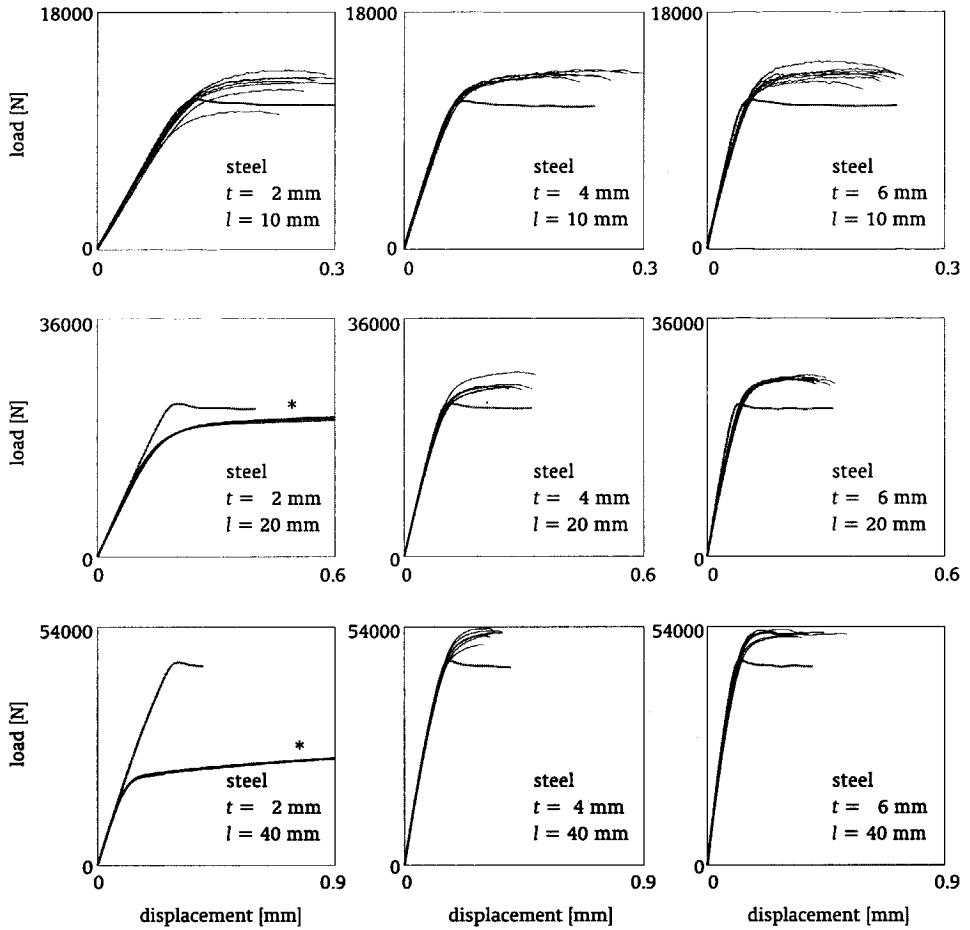


Figure 7.23 Comparison between the calculated load-displacement curves and the curves based on tested double strap joints for the adhesive DP 490; for the graphs indicated by an *, plastic yielding of the adherends was observed

According to the calibration procedure described in section 4.3.2, there are various methods to quantify the differences between the set of data and matching calculated values predicted by the model. The proposal for adding a factor $K_{a,i}$ to the prediction model, see equation 4.20, is not preferred here for two reasons. First of all the analyses will end up with a design value of the factor $K_{a,d}$, which has to be added to the prediction model. As a consequence the value of the partial factor is not a constant value, but it is a function of the strength level. Secondly a Weibull distribution which is preferred for adhesive bonded joints as explained in sections 4.2.3 and 4.2.4, can not be used to determine the design value of the factor $K_{a,d}$. This is, because the Weibull distribution will not give negative values of the factor $K_{a,d}$, which are necessary for a realistic description. The proposal for multiplying the prediction model with a factor $K_{m,i}$ according to equation 4.21 is preferred here. The value of the determined partial factor is a constant and a Weibull distribution can be used to describe the stochastic nature of the strength realistic.

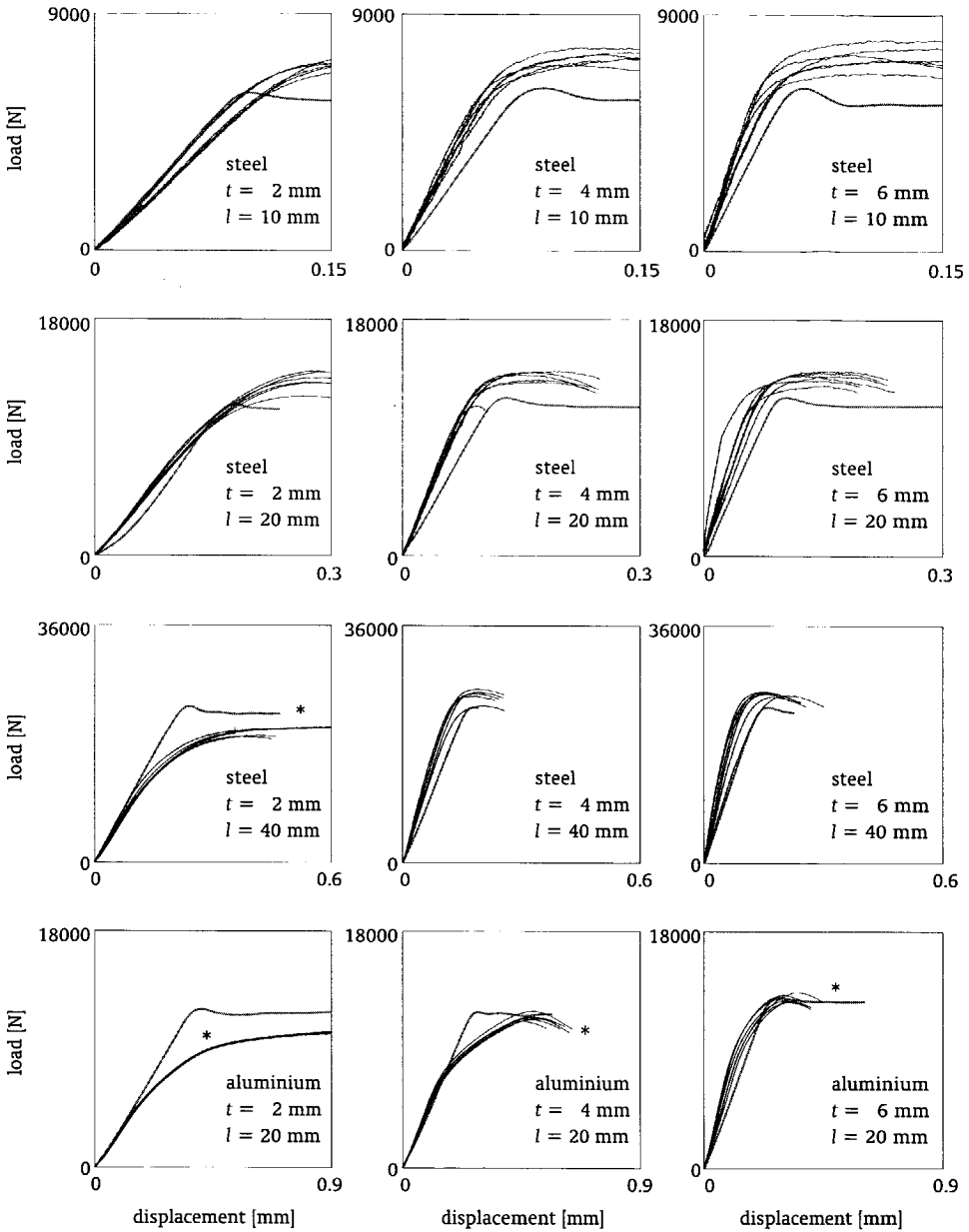


Figure 7.24 Comparison between the calculated load-displacement curves and the curves based on tested single overlap joints for the adhesive DP 490; for the graphs indicated by an *, plastic yielding of the adherends was observed

Design Rules for Overlap Joints

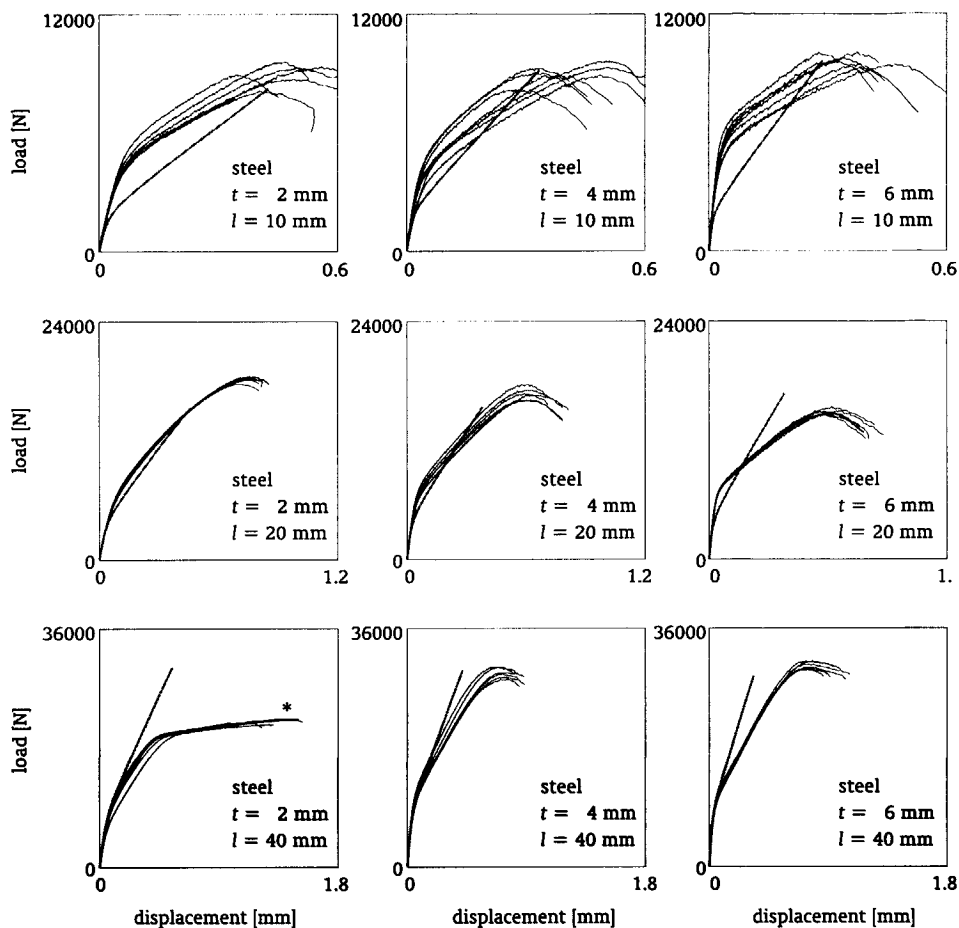


Figure 7.25 - Comparison between the calculated load-displacement curves and the curves based on tested double strap joints for the adhesive UK 8202; for the graphs indicated by an *, plastic yielding of the adherends was observed

To explain the calibration procedure the followed steps are described for the double strap joints with the adhesive DP 490. The graphs shown in figure 7.23 indicate that the test results for the 2 mm thick adherend with an overlap length of 20 and 40 mm are influenced by plastic yielding of the adherends. These results are excluded. The experimentally determined failure loads $R_{\text{test},i}$ (46 in total) are compared with the predicted strength $R_{\text{pm},i}$. The graph shown in figure 7.27, with the set of test data points i on the vertical axis and the corresponding predicted values on the horizontal axis, indicates that the prediction model slightly underestimate the test data. The differences between both provide quantitative information that is used to perform a probabilistic analysis. As mentioned above, here the procedure to multiply for all data points i the prediction model with a factor $K_{\text{m},i}$ is followed. The determined values of this multiplication factor are also indicated in figure 7.27. The estimated mean and standard deviations of the sample of these correction factors are equal to respectively $m_{K,m} = 1.15$ and $s_{K,m} = 0.051$. For a Weibull distribution with the estimated

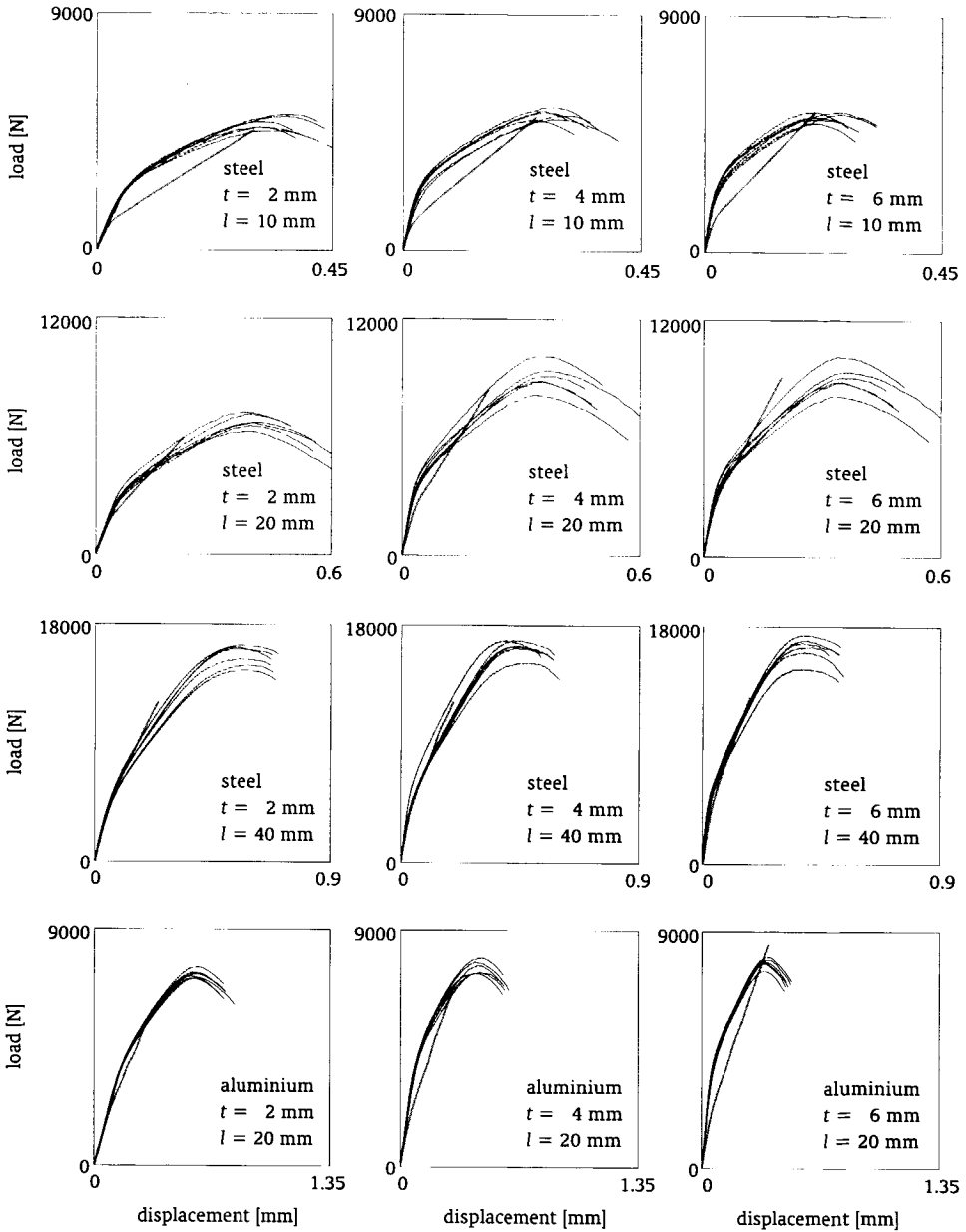


Figure 7.26 Comparison between the calculated load-displacement curves and the curves based on tested single overlap joints for the adhesive UK 8202

Design Rules for Overlap Joints

shape parameter equal to $\beta'_{K,m} = 28.1$ and the estimated scale parameter equal to $\alpha'_{K,m} = 1.17$, the design value of the factor $K_{m;d}$ is determined according to the principles of equation 4.11:

$$K_{m;d} = \alpha'_{K,m} [-\ln(1 - \Phi(\alpha_R \beta))]^{1/(k_{\alpha_R \beta}(n) \beta'_{K,m})} \quad (7.21)$$

where n is the number of correction factors. The value the parameter $k_{\alpha_R \beta}(n)$ depends on the value of the product of the weighting factor and the reliability index $\alpha_R \beta = 0.8 \cdot 3.8$ discussed in section 3.2.2. In this example with $n = 46$ the value is calculated in addition to table 4.2 and its value is equal to $k_{\alpha_R \beta}(46) = 0.92$, which means that the design value of the multiplication factor is $K_{m;d} = 0.90$. Now the design values referring to all data points i can be calculated with equation 4.23. It is assumed here that the characteristic values of the strength according to the prediction model are equal to the already calculated values. Now the partial factor is calculated with use these two values of the strength according to equation 4.24. For this example a value of the calibrated partial factor equal to $\gamma_R = 1.11$ is determined.

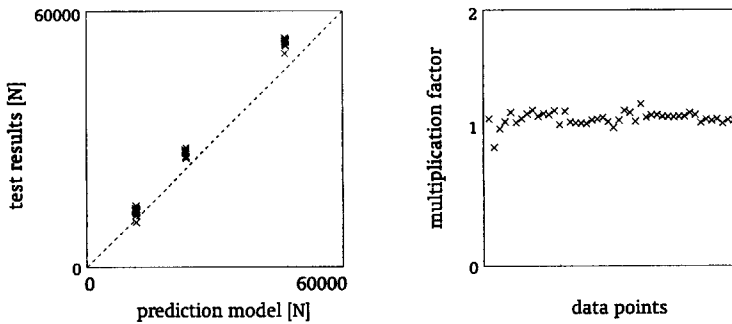


Figure 7.27 Determination of multiplication factors for double strap joints with the DP 490 adhesive: a) comparison of test data with corresponding predicted values, and b) corresponding values of the factor $K_{m;i}$

For the studied joints with the adhesives DP 490 and UK 8202 the results of the calibrations are given in table 7.8. The results have been excluded within the calibration procedure as indicated in this table. The graphs shown in figures 7.23 to 7.26 indicate that these test are influenced by plastic yielding of the adherends. It is noted here that the determined values of the partial factors only match with the defined characteristic values of the strength. This means that the values have to be based on nominal values of the measured bondline thickness, overlap length and width of specimens, nominal values of the adherends properties and the average adhesive properties. The results of the calibrations indicate that the value of the partial factor for the single overlap joint is slightly higher than for the double strap joint. Based on these results it is proposed to use in general for overlap joints with the adhesive DP 490 a partial factor of $\gamma_R = 1.2$ and for the adhesive UK 8202 a partial factor of $\gamma_R = 1.9$.

Table 7.8 Overview of results of calibrations

adhesive	joint type curve	n [-]	m_K [-]	s_K [-]	β' [-]	α' [-]	$k_{\alpha R \beta^{(n)}}$ [-]	K_d [-]	γ_R [-]
DP 490	double strap ¹⁾	46	1.15	0.051	28.1	1.17	0.92	0.90	1.11
	single overlap ²⁾	47	1.15	0.070	20.4	1.18	0.92	0.83	1.21
UK 8202	double strap ³⁾	52	1.03	0.092	13.7	1.07	0.92	0.63	1.59
	single overlap	72	1.12	0.147	9.06	1.18	0.94	0.53	1.87

1) Results for the 2 mm thick adherend with an overlap length of 20 and 40 mm are excluded

2) Results for the 2 mm thick adherend with an overlap length of 40 mm and the results for the aluminium adherends are excluded

3) Results for the 2 mm thick adherend with an overlap length of 40 mm are excluded

7.2 Ageing behaviour

7.2.1 Studied overlap joints

This study focuses on the degradation behaviour of the strength of overlap joints under short-term static load conditions. The geometry of a 25 mm wide single overlap joint with 12 mm overlap length as indicated in figure 7.28, is selected. The adherends are 1 mm thick polyester coated steel sheetings of Corus and the bondline thickness is approximately 0.2 mm. A cross section of the coating is given in figure 7.28. The two adhesives studied in detail are the cold cured two-component polyurethane adhesives UD 400 of Scholten Lijmen and 1897 of Casco Products.

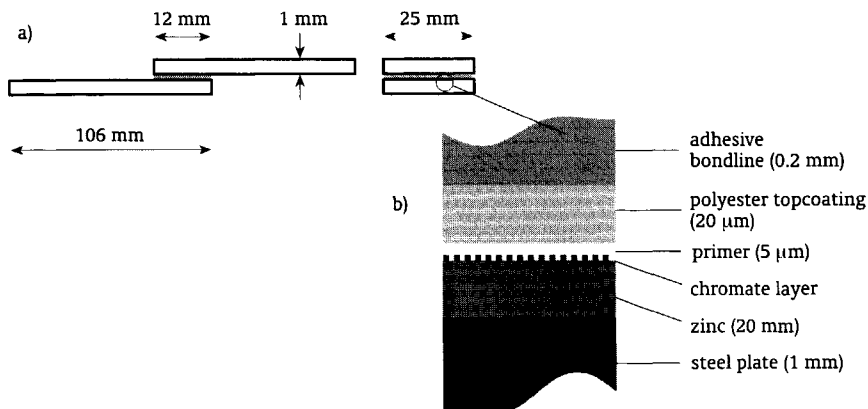


Figure 7.28 Studied overlap joints: a) geometry, b) cross-section coating

To be able to provide quantitative information about the degradation of the strength of the studied overlap joints, the CIB/RILEM procedure is applied. In addition to what is described in section 6.2.2, the following remarks are made:

- 1) **Definition.** The users' need is specified as the quantification of the degradation of the strength during lifetime. Short-term static load conditions and normal Dutch weathering conditions are identified as the considered building context. The performance requirement of adhesive bonded joints is represented by the target reliability level as defined in section 3.2.1. The strength of the joint after a period of ageing is the performance criterion to be used in the analyses.
- 2) **Preparation.** This phase deals with the definition of ageing tests and methods of interpretation. Water is considered to be the most relevant environmental action. As discussed in section 6.2.3 the degradation mechanism is described by an empirical function that gives an exponential relation between the strength and time. Degradation characteristics of in-use performances are induced by ageing tests, assuming constant environmental conditions and severe humidity conditions. Based on meteorological data it is concluded by Botter (1997) that the average relative humidity of the Dutch climate is rather high. To accelerate the ageing process higher temperatures have to be used. Results available for various levels of temperature provide information essential to extrapolate the results for in-use environmental conditions. It is assumed that the average year temperature of 10 °C (Botter, 1997) is representative for the Dutch weathering conditions.
- 3) **Pre-testing.** Preliminary short-term ageing tests demonstrate which failure mode is dominant and indicate degradation mechanisms. To limit the ageing period the specimens have to be aged at a high temperature and under severe humidity conditions.
- 4) **Testing.** This phase deals with the actual testing of specimens aged under short-term laboratory based environments and the in-use environment. Short-term laboratory based environments with a high relative humidity have to be defined for at least two temperatures. The selection of ageing periods, after which the strength has to be determined by testing, has to be based on the results of the pre-testing phase. The in-use environment is represented by outside exposure for a period of many years. For the short-term ageing tests the rate of the degradation of the strength has to be determined. The short-term test results have to be extrapolated to the in-use environmental conditions by using time transformation functions. It is noted here that if the prediction based on the short-term tests is not representative for in-use environmental conditions, the analysis has to be continued from phase 1 on.
- 5) **Discussion and interpretation.** If a relationship between short-term and long-term tests is found, the degradation of the strength during lifetime has to be formulated on basis of the results of the preceding phases.

Based on this procedure an experimental research programme was worked out. This programme contained two phases. In the first phase a preliminary study with short-term ageing tests was done to support the definition of the main part of the test programme. In the second phase the main tests were done. The results are analysed and a prediction of the degradation of the considered overlap joints is made.

7.2.2 Preliminary study

Within the preliminary study accelerated ageing tests were performed on various types of adhesives (Van Straalen, 1997E). The aged specimens were immersed in demineralized water with a constant temperature of 40 or 60 °C to accelerate the ageing process. Ultimate strengths of both aged and not-aged specimens were determined.

The results for the two studied cold cured two-component polyurethane adhesives are given

in table 7.9. In figure 7.29 the mean values are plotted. Based on these results the following findings were drawn:

- Compared with the results without ageing, the strengths increase after ageing at 40 °C for 43 days. For the UD 400 adhesive this effect was moderate and for the 1897 adhesive significant. This is probably caused by post-curing of the two-component polyurethane adhesives.
- Due to ageing the strength of the UD 400 adhesive decreased significantly for the longer ageing periods. For the 1897 adhesive on the other hand no significant change was observed.
- None of the cracked surfaces showed a completely cohesive failure mode. For the UD 400 adhesive it is concluded that the drop of strength is related to the change of failure mode.
- During ageing the specimens corroded easily in demineralized water. This effect probably influenced the degradation behaviour.

Table 7.9 Results of preliminary short-term tests

adhesive	water immersion		ultimate strength								failure mode ¹⁾ indication ²⁾					
	<i>T</i>	<i>t</i>	test results								<i>m</i>	<i>s</i>	A	B	C	D
	[°C]	[days]	[N]								[N]	[N]				
UD 400	-	0	5069	4623	4700	4147	4088	4805	4572	383			x	(x)		
	40	43	4892	5361	5468				5240	306			x	x		
	60	43	4580	3965	3909				4151	372				x		
	60	106	2837	2397	1676				2303	586					x	
1897	-	0	3008	2524	2898	2977	2860	2962	2872	179			x	(x)		
	40	43	5555	5443	4913				5304	343	x			x		
	60	43	4747	5422	5299				5156	360	x			x		
	60	106	5509	5535	5345				5463	103	x				x	

1) A is cohesive failure of the adhesive, B is failure within the interface between adhesive and primer, C is failure within the interface between primer and zinc, and D is failure between zinc and steel

2) A qualitative indication is given which failure mode was dominant; a less significant failure mode is indicated by a marking between parentheses

Based on these findings the following recommendations for the main test programme were made:

- Ageing the specimens by soaking them in demineralized water might cause additional effects due to corrosion of the used materials. To avoid such effects the specimens will be aged in air with a relative humidity of 95%.
- Accelerating the ageing process by using constant temperatures of 40 and 60 °C seems to be reasonable. It is expected that at 40 °C the strength will degrade significantly within a period of one year. To be convinced that the degradation mechanisms will not be affected at a temperature of 60 °C, an additional series specimens will be aged at 50 °C.
- An ageing period of maximum 12 weeks for ageing at 60 °C seems to be reasonable. For

Design Rules for Overlap Joints

ageing at 50 and 40 °C maximum periods of respectively 24 and 48 weeks will be proposed. Since less is known about the actual degradation behaviour of the considered adhesive bonded joints under the selected conditions, it was decided not to use an optimized test plan as suggested in section 6.2.5. A traditional test plan is preferred, because more information will become available about the degradation process if the specimens are equally distributed over various ageing conditions.

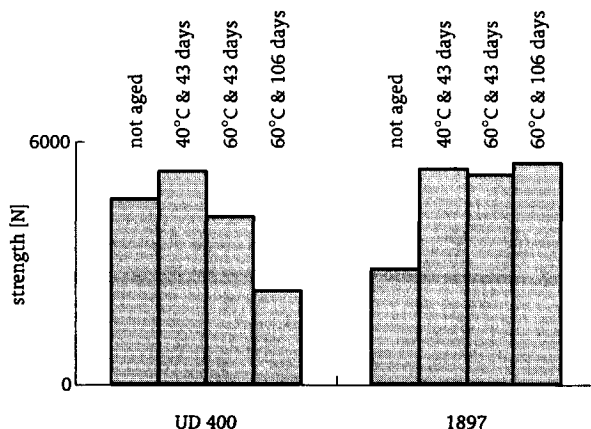


Figure 7.29 Mean values of strength based on the results of preliminary short-term ageing tests

7.2.3 Prediction of the degradation

To quantify the degradation of the two studied cold cured two-component polyurethane adhesives UD 400 of Scholten Lijmen and 1897 of Casco Products, accelerated ageing tests were performed according to the test plan given in table 7.10 (Van Straalen, 1999G & 2000C). For each situation 6 or 7 specimens were tested. Also the situation without ageing was considered. Additional specimens have been exposed outside on the roof of the Structures and Materials Laboratory of Delft University of Technology in The Netherlands. All specimens were cured under normal laboratory conditions for approximately 7 weeks, before they were placed in the climate chamber. To maintain the constant humidity conditions during the ageing period, the specimens were placed in a closed container inside an oven with the required temperature. The relative humidity of 95% was guaranteed by placing an open tank with water and calcium sulphate (250 gram per litre) into the container. Tests were done under ambient laboratory conditions within the temperature range 21-25 °C. This plan was based on the recommendations of the preliminary study.

The results of the ageing tests are given in table 7.11. In figure 7.30 the mean values of the strength as a function of time are plotted. Based on the results presented in table 7.11 and figure 7.30 the following conclusions are drawn:

- Compared with the results without ageing, the strengths for the adhesive UD 400 decreased after the first period of ageing, while the strengths for the adhesive 1897 increased. This phenomenon was probably caused by post-curing of the two-component polyurethane adhesive. The not-aged specimens were tested approximately 7 weeks after manufacturing.

Table 7.10 Test plan accelerated ageing tests

ageing conditions	ageing period [weeks]					
	0	3	6	12	24	48
no ageing	test					
95% RH at 60 °C	start	test	test	test		
95% RH at 50 °C	start		test	test		
95% RH at 40 °C	start			test	test	test
outside exposure	start					test

Table 7.11 Results of ageing tests of the main test programme

adhesive	95% RH	ultimate strength										failure mode ¹⁾²⁾					
		T	t	test results								m	s	[%]			
		[°C]	[days]	[N]								[N]	[N]	A	B	C	D
UD 400	-	0	5693	5342	5459	5410	5518	5615	5264	5472	150	51	30	19			
	60	21	5049	5342	4990	5498	5420	5254		5259	203	72		28			
		46	4619	4502	4766	4590	4443	4707	4697	4618	116	85	4	11			
		84	4355	4600	4688	4688	4561	3926	4883	4528	310	89	1	10			
	50	46	4492	4111	4072	4531	4238	4336	4170	4279	181	87	7	6			
		84	4434	4658	4473	4512	4512	5000	4541	4590	194	93		7			
		166	4531	4326	4746	4795	4512	4482	4473	4552	164	87		13			
	40	84	5303	4990	4990	4805	4600	4668	5254	4944	272	96		4			
		166	4639	4678	4395	4717	4512	4365	4375	4526	152	83	11	6			
		362	4453	4551	4199	4121	4092	4453	4102	4282	197	95	1	4			
	outside	327	4922	5254	4844	5234	5361	5117		5122	202	65	12	23			
	1897	-	0	4746	4531	4375	4219	4414	4580	4370	4462	172	79	19	2		
60		21	4814	5049	5371	5117	5166	4990	5303	5116	189	96		4			
		46	5010	5029	4902	4951	4814	4883		4932	81	92		8			
		84	4600	4980	5029	4941	4883	4922	4814	4881	142	93		7			
50		46	5156	4932	5156	4961	4893-5010	5088	5028	5028	107	97		3			
		84	4844	4854	4834	5020	5107	4941	5088	4955	117	91		9			
		166	5117	5098	4727	4727	5049	4551		4878	240	92		8			
40		84	5020	5029	5225	5146	5029	5293	5313	5151	128	84		16			
		166	4893	4932	5000	4746	4932	4990	4902	4914	84	93		7			
		362	4668	4551	4668	4238	4141	4502	4668	4491	218	90		10			
outside		327	5127	5098	5088	5264	5283	5342		5200	109	95		5			

1) A is cohesive failure of the adhesive, B is failure within the interface between adhesive and primer, C is failure within the interface between primer and zinc, and D is failure between zinc and steel

2) For each failure mode the percentages of the fracture surface is given in the columns by taking the average observed value for the considered specimens

Design Rules for Overlap Joints

The results indicate that for the adhesive UD 400 the post-curing effect was stabilized, while for the adhesive 1897 this effect was still going on.

- The strength of both adhesives decreased significantly after longer periods of ageing.
 - The cracked surfaces for the adhesive UD 400 were dominated by cohesive failure of the bondline, but the not-aged specimens also showed a significant contribution of failure in the interface. The cracked surfaces for the adhesive 1897 were mainly dominated by cohesive failure of the bondline.
 - For the adhesive UD 400 aged at 50 °C a sudden drop of the strength was observed after 6 weeks. For overlap joints this is a known phenomenon. Within the British MTS Adhesive Project (Beevers, 1995) this behaviour was replicated by different laboratories and with different treatments. It is suggested that this is due to changes in modulus of elasticity and stress relaxation with absorbed water in the adhesive.
 - For none of the specimens corrosion of the coated steel plate was observed.
- In general these findings are confirmed by the results of the preliminary study.

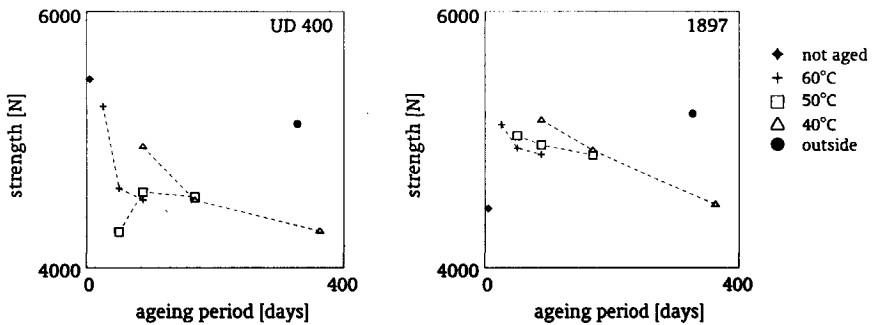


Figure 7.30 Mean values of the strength based on test results of the main programme

A relationship is defined that gives a proper description of the degradation process and the effect of accelerated ageing. As mentioned in section 7.2.1 it is decided in step 2 of the CIB/RILEM procedure to describe for the studied adhesive bonded joints the degradation of the strength with an empirical relation. The following assumptions are made:

- The relation between the strength R and time t is exponential.
- The strength at time $t = 0$ is equal to a value R_0 .
- After a long period of time the strength stabilizes and becomes equal to a value R_{inf} .

Based on these assumptions, the time dependent strength $R(t)$ can be described as:

$$R(t) = (R_0 - R_{inf}) \exp(C_1 t) + R_{inf} \quad (7.22)$$

where C_1 is an unknown constant. To extrapolate the accelerated ageing test results determined at 60, 50 and 40 °C to an in-use environmental condition, it is decided in step 4 of the CIB/RILEM procedure as mentioned in section 7.2.1, to use a time-transformation function. If the acceleration is only controlled by temperature, the well-known Arrhenius relation (Martin, 1982) might be used. This time transformation function $\rho(t, T)$ is formulated as follows:

$$\rho(t,T) = \exp\left[C_2 - \frac{C_3}{T}\right]t \quad (7.23)$$

where T is the absolute temperature in Kelvin, while C_2 and C_3 are unknown constants to be determined on basis of test results. Combining equations 7.22 and 7.23 gives the following general relation of the degradation of the strength as a function of time t and temperature T :

$$R(t,T) = (R_0 - R_{\text{inf}}) \exp\left[C_1 \exp\left[C_2 - \frac{C_3}{T}\right]t\right] + R_{\text{inf}} \quad (7.24)$$

To determine the values of the unknown constants of equation 7.24 on basis of the data set $R_{\text{test};i}(t,T)$ as presented in table 7.11, a least squares method is mostly used (Mood et.al., 1974). The values of R_0 , R_{inf} , C_1 , C_2 and C_3 that minimize the following sum of squares of the total number of test results n_{tot} :

$$\sum_{i=1}^{n_{\text{tot}}} (R_{\text{test};i}(t,T) - R(t,T))^2 \quad (7.25)$$

are defined to be the least-square estimators. Since there is no tendency that the values of the standard deviations given in table 7.11 decrease or increase as a function of time, it is assumed that the error of equation 7.24 can be described by a constant value of the standard deviation. But the used least squares method does not give an estimator for the standard deviation. An alternative estimator s is proposed, which is based on equation 7.24 and the least-squares estimators determined with equation 7.25:

$$s = \sqrt{\frac{1}{n_{\text{tot}} - 5} \sum_{i=1}^{n_{\text{tot}}} (R_{\text{test};i}(t,T) - R(t,T))^2} \quad (7.26)$$

It is noted here that this estimator s only partly represents the stochastic nature of the relation given by equation 7.24. The determined values of the unknown constants are mean values; within a full statistical description also estimated values for the standard deviations of and correlations between the constants are included. To avoid complicated statistical analyses in this study the engineering approach to consider only the estimator s is adopted.

For the adhesive UD 400 all 69 test results are taken into account to determine the values of the unknown coefficients of equation 7.24. To minimize the sum of squares according to equation 7.25, built-in functions of modern spreadsheet programs can be used. But attention has to be paid to the fact that these functions can find more than one optimum solution. In table 7.12 the results of two attempts are presented. It is found that other attempts stabilize around these two. The two determined relations are compared in figure 7.31 with the test results for the temperatures 60, 50 and 40 °C. These graphs show that the two determined relations fit well with the test data. Based on the fact that the sum of squares for the first attempt is smaller than for the second one, it is concluded that the results of the first attempt is considered to be the most representative.

For the adhesive 1897 only the 61 test results of the aged specimens are taken into account to determine the values of the unknown coefficients of equation 7.24. As explained earlier this is, because the not-aged specimens were not fully cured. From various attempts to calculate the values of the unknown coefficients it is observed that in spite of the fact that the sum of squares are close together, the results as presented in table 7.12, differ significantly. For attempts 1 and 3 this effect is illustrated in figure 7.32. From a statistical point of view it is concluded that there is not enough data available to determine a proper relation. Valid test

Design Rules for Overlap Joints

results of not-aged specimens might improve the least squares method, but for a better description of the relation test results for longer ageing periods have to be determined. Since the results of the preliminary study as shown in figure 7.29, indicates that the magnitude of degradation is low, it is expected that the first attempt is representative.

Table 7.12 Overview of values determined for the coefficients of equation 7.24 and values for the estimator s of the standard deviation

adhesive attempt	sum of squares	R_0 [N]	R_{inf} [N]	C_1 [s ⁻¹]	C_2 [-]	C_3 [K]	s [N]	
UD 400	1	$5.47 \cdot 10^6$	5491	4416	$-11.13 \cdot 10^{-3}$	10.01	2995	292
	2	$7.43 \cdot 10^6$	5075	1946	$-2.937 \cdot 10^{-3}$	10.06	3482	341
1897	1	$1.58 \cdot 10^6$	5243	4181	$-5.350 \cdot 10^{-3}$	9.427	3171	168
	2	$1.52 \cdot 10^6$	5203	2771	$-9.510 \cdot 10^{-3}$	9.749	3082	164
	3	$1.57 \cdot 10^6$	5157	-19	$-2.760 \cdot 10^{-3}$	5.027	1493	167

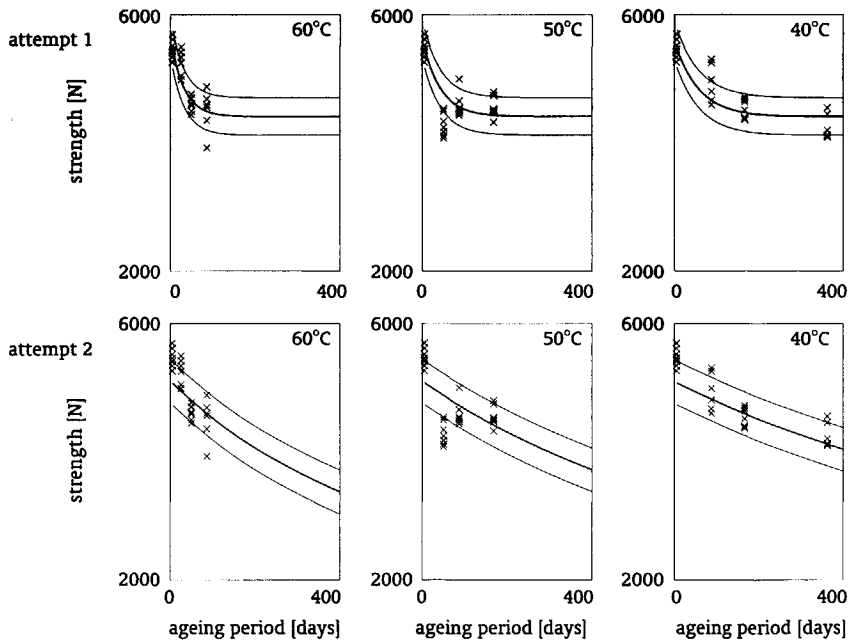


Figure 7.31 Comparison of determined relations with the matching test results of the adhesive UD 400; the middle line represents the best fit, while the outside lines indicate plus and minus the estimated value of s

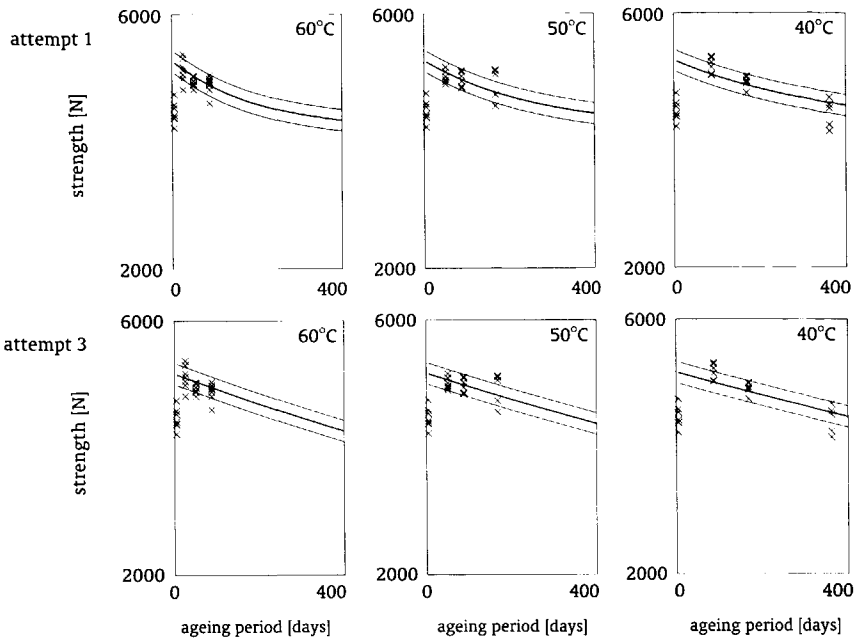


Figure 7.32 Comparison of determined relations with the matching test results of the adhesive 1897; the middle line represents the best fit, while the outside lines indicate plus and minus the estimated value of s

To predict the degradation of the strength under normal Dutch weathering conditions, the determined relations for both adhesives are extrapolated. A constant temperature $T = 10\text{ }^{\circ}\text{C}$ is assumed, as is decided in step 2 of the CIB/RILEM procedure mentioned in section 7.2.1. In figure 7.33 the predicted degradation of the strength during the first 10 years is compared with the test results of the specimens exposed outside for one year. The comparison between the predicted curves and the test results of specimens exposed outside indicates that the predicted curves are conservative. To draw a final conclusion, additional specimens have been exposed outside for longer periods of time. The results of tests of these specimens will become available during the coming years. Together with the observations that mainly cohesive failure occurred and that the failure mode did not change during ageing, it is concluded that the relation according to equation 7.24 might be used to predict the degradation behaviour of the considered overlap joints.

7.2.4 Calibration of the conversion factor for time dependent effects

Based on the results of the preceding section, conversion factors are calibrated with use of the procedure proposed in section 4.3.3. This simplified procedure can be used if the action is stationary and the strength decreases continuously during time. The essence is that a design value of the strength $R_{\text{ref;d}}$ representative for the whole reference period has to be determined for the target reliability $\alpha_R\beta$. Here a product of the weighting factor and the reliability index of $\alpha_R\beta = 0.8\cdot 3.8$ and a reference period of 50 years are considered. Together with the design value of the strength for time $t = 0$, $R_d(t_0)$, the value of the conversion factor η_t can be calculated.

Design Rules for Overlap Joints

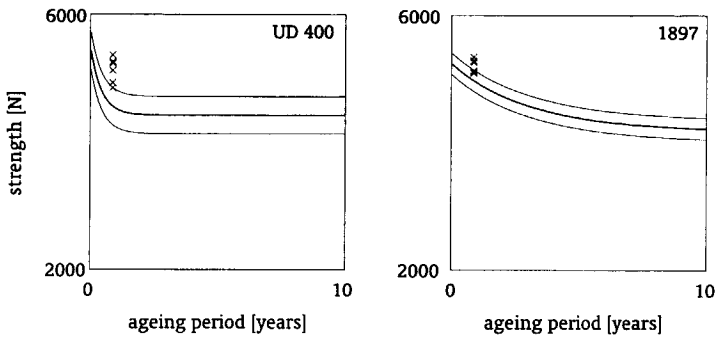


Figure 7.33 Comparison of the determined relation with the test results of the specimens exposed outside; the middle line represents the best fit, while the outside lines indicate plus and minus the estimated value of s

It is a conservative approximation to take for the design value of the strength $R_{ref;d}$ the design value at the end of the reference period. For the design value of the strength $R_d(t_0)$ two results are available. One is based on the test results for the not-aged specimens and the other is based on the relation according to equation 7.24. Both are considered here. The calculation of the design values is based on a Weibull distribution as explained in sections 4.2.3 and 4.2.4. An overview of the results of the calculations is given in table 7.13. The values of the shape parameters β' and scale parameters α' of the Weibull distribution are estimated with the procedure described in section 4.2.1. The design value of the strength is calculated with equation 4.11. It is noted here that the values of the parameter $k_{\alpha_R\beta}(n)$ are calculated additional to those given in table 4.2 (Van Straalen and Vrouwenvelder, 2000). For the adhesive UD 400 69 test results are used to determine the five unknown coefficients of equation 7.24; this number of test results is reduced by the number of coefficients minus 1 to get the value of n used in table 4.2, which means that $n = 69 - (5 - 1) = 65$. For the adhesive 1897 with 61 test results $n = 57$. Using equation 4.35 the values of the conversion factors for both adhesives are calibrated. For the adhesive UD 400 the conversion factor is equal to $\eta_t = 0.75$ if the design value of the strength $R_d(t_0)$ is based on the predicted relation, while it is equal to $\eta_t = 0.71$ if the design value of the strength $R_d(t_0)$ is based on the results of the not-aged specimens. For the adhesive 1897 these conversion factors are equal to respectively $\eta_t = 0.76$ and $\eta_t = 1.04$. The difference between the values of the two conversion factors shows that for the development of design rules it is essential to define the value of the strength for time $t = 0$ properly.

A more advanced alternative to calibrate the conversion factor divides the reference period into a number of periods. As explained in section 4.3.3 the unknown design value of the strength representative for the whole reference period can be found by solving a set of relations given by equations 4.33 and 4.34. It is expected that the use of this procedure will not affect the value of the calibrated conversion factor for the adhesive UD 400. This is, because the degradation of the strength stabilizes within one year as can be seen in figure 7.33. For the adhesive 1897 this process will take approximately 10 years, which might increase the value of the calibrated conversion factor. An overview of the results of the calculations is given in table 7.14. For each period of time the probability is giving, which match with the whole reference period. From this table it can be seen that for the adhesive

Table 7.13 Overview of the results of a conservative procedure to calibrate conversion factor adhesive ageing

adhesive	ageing	m [N]	s [N]	β' [-]	α' [N]	n [-]	$k_{\alpha_R\beta}(n)$ [-]	R_d [N]
UD 400	not-aged	5472	150	45.969	5539	7	0.61	4355
	0 years	5491	292	23.419	5620	65	0.938	4135
	50 years	4416	292	18.705	4544	65	0.938	3095
1897	not-aged	4462	172	32.638	4538	7	0.61	3235
	0 years	5243	168	39.314	5318	57	0.931	4423
	50 years	4181	168	31.212	4256	57	0.931	3375

UD 400 the design value of the strength does not differ from the value determined with the conservative approximation. For the adhesive 1897 on the other hand there is a minor effect. The matching probabilities calculated for each period of time are indeed very low for the first periods and stabilize during the later periods where the degradation of the strength no longer varies. For the followed calculation procedure this means that the value of the parameter $k_p(n)$ as used in equation 4.33, is a function of the probability p and has to be calculated additional to the values given in table 4.2 (Van Straalen and Vrouwenvelder, 2000). It is noted that for n the same values are used as for the conservative approximation. Another aspect of the followed calculation procedure is that for the considered Weibull distribution the values of the shape and scale parameters β' and α' respectively are also time dependent. For the adhesive UD 400 the conversion factors are equal to those according to the conservative approximation. For the adhesive 1897 the conversion factor is equal to $\eta_t = 0.77$ if the design value of the strength $R_d(t_0)$ is based on the predicted relation, while it is equal to $\eta_t = 1.05$ if the design value of the strength $R_d(t_0)$ is based on the results of the not-aged specimens. There is only a minor difference between these values and the conversion factors according to the conservative approximation. It is concluded that the more advanced alternative is only useful if it takes a long period of time before the degradation of the strength stabilizes.

Design Rules for Overlap Joints

Table 7.14 Overview of the results of the advanced procedure to calibrate the conversion factor

adhesive	considered period of time		matching probability	$R_{ref,d}$ [N]
	from year	to year		
UD 400	0	1	$6.737 \cdot 10^{-4}$	3096
	1	2	$1.126 \cdot 10^{-3}$	
	2	3	$1.185 \cdot 10^{-3}$	
	3	4	$1.191 \cdot 10^{-3}$	
	4	5	$1.192 \cdot 10^{-3}$	
	5	7	$1.192 \cdot 10^{-3}$	
	7	10	$1.192 \cdot 10^{-3}$	
	10	15	$1.192 \cdot 10^{-3}$	
	15	20	$1.192 \cdot 10^{-3}$	
	20	50	$1.192 \cdot 10^{-3}$	
1897	0	1	$2.311 \cdot 10^{-6}$	3393
	1	2	$1.439 \cdot 10^{-5}$	
	2	3	$5.287 \cdot 10^{-5}$	
	3	4	$1.336 \cdot 10^{-4}$	
	4	5	$2.589 \cdot 10^{-4}$	
	5	7	$5.827 \cdot 10^{-4}$	
	7	10	$1.001 \cdot 10^{-3}$	
	10	15	$1.294 \cdot 10^{-3}$	
	15	20	$1.359 \cdot 10^{-3}$	
	20	50	$1.375 \cdot 10^{-3}$	

Design Rules for Sandwich Panels

A sandwich panel is a layered composition of various materials bonded together. Designers use sandwich panels for a wide variety of structural applications, because of their lightness and ability to combine and optimise various performances as strength, stiffness, sound insulation and thermal insulation. To guarantee the required reliability level designers need proper design rules. These have to deal with the prediction of the mechanical behaviour and the degradation of the performances. In this chapter design rules based on the partial factor approach are developed on basis of a number of case studies. Attention is given towards useful mechanical prediction models and the calibration of the partial factor.

8.1 Mechanical behaviour of the support region

8.1.1 Description of the case study

The case study focuses on the detailing of the ends of sandwich panels. The local geometry, dimensions and properties of the core and faces influence the mechanical behaviour near these ends. To investigate these influences, a research programme is worked out. The core materials studied in detail are the mineral wool core material Conrock 700 of Rockwool and the polystyrene core material EPS 30 of Isobouw.

The research programme contains a theoretical and an experimental part. Within the theoretical part a prediction model for sandwich panels loaded in bending with flexible core materials and thin metal faces is developed. Shear failure of the core material and delamination of the interface between the core and the sandwich face are assumed. The prediction model as proposed in section 5.3.5, is based on linear elastic material behaviour and ultimate values for the shear and tensile stresses of the core material. The core material properties were determined with use of standard tensile, compression and shear tests. The stress states within

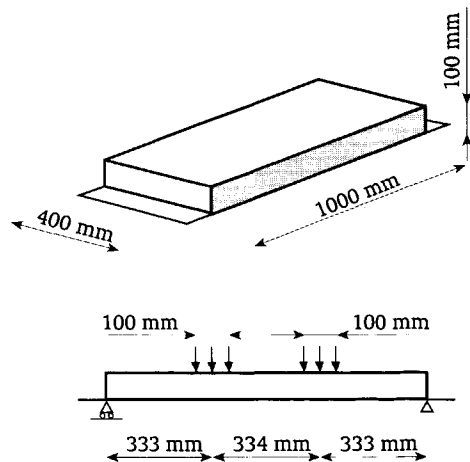
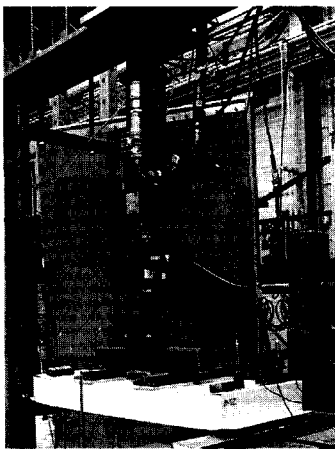


Figure 8.1 Four-point bending tests on sandwich panels

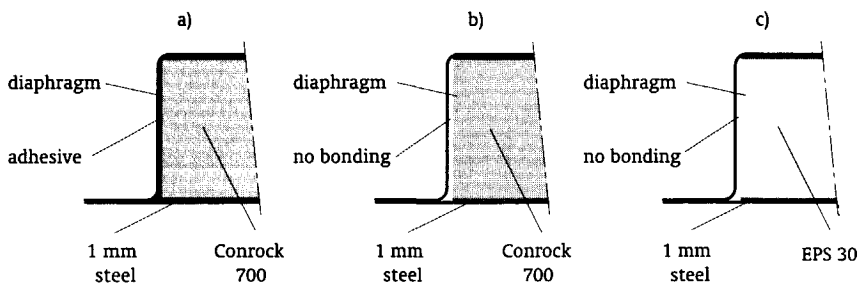


Figure 8.2 Three considered sandwich panel endings:
 a) outside diaphragm bonded to the mineral wool core material,
 b) outside diaphragm not bonded to the mineral wool core material, and
 c) outside diaphragm not bonded to the polystyrene core material

the core material and the interface are calculated with a higher-order theory. Beside tests on core materials, the experimental part of the case study contained four-point bending tests on sandwich panels. These panels with a span of 1000 mm and a width of 400 mm, were made of a 100 mm thick flexible core material with 1 mm thick steel faces bonded on both sides with an one-component polyurethane adhesive. The core materials Conrock 700 as well as EPS 30 were used. The dimensions of the specimens and the test set up are given in figure 8.1. The end of the sandwich panel was strengthened by bending the upperface in such a way that an outside diaphragm was formed. The three situations indicated in figure 8.2 are considered. The main objectives of these tests are to verify the proposed prediction model and to calibrate the partial factor.

8.1.2 Background of considered failure criteria

For the considered case study two possible failure modes are assumed. It is expected that for the sandwich panels with the outside diaphragm bonded to the core material, shear failure of the core will occur due to shear stresses. For the sandwich panels with the outside diaphragm not bonded to the core material on the other hand, it is expected that delamination of the adhesive bonded interface between the core material and the upperface near the support region will occur due to transverse tensile stresses. The used criteria for both failure modes are defined by ultimate stresses.

The design rules given by ECCS and CIB (1995) use the ultimate shear stress of the core material as the criterion for the shear failure mode. For mineral wool core material the value of the ultimate shear stress is influenced by the orientation of the fibres. For the tested sandwich panels with the core material Conrock 700 the fibres are oriented approximately normal to the faces. In the proposed prediction model it is assumed that the core behaviour of Conrock 700 can be described with an isotropic model, as long as the shear properties are determined on basis of a sandwich beam test. For the core material EPS 30 the value of the ultimate shear stress is assumed to be direction independent. The proposed shear failure criterion is used within the selected prediction model.

The recommendations given by ECCS and CIB (1995) do not give guidelines how to verify delamination of the adhesive bonded interface between the core material and the face due to transverse tensile stresses. But it is generally expected that the actual failure occurs within

the core material and not the adhesive bondline. For this reason the ultimate tensile stress of the core material is proposed as an additional failure criterion within the selected prediction model.

8.1.3 Background of tensile, compression and shear tests on the core material

To determine the ultimate stress and modulus properties of the core materials used for the case study, tensile, compression and shear tests according to ECCS and CIB (1995) were performed. The results and interpretations of the tensile and compression tests are reported by Van Straalen (2000F) and (2000G) for respectively the core materials Conrock 700 and EPS 30. The results and interpretations of the shear tests of both core materials are reported by Van Straalen (2000E) and (2000H). An overview is given in this section.

Tensile test specimens with a square cross-section were prepared and axially loaded. The specimens were made of the same 100 mm thick core material as used for the beam test of the case study. For the core material Conrock the used cross-section was 200·200 mm, while for EPS 30 the used cross-section was 150·150 mm. To ensure an equally distributed stress distribution over the cross-section, 15 mm thick steel plates were bonded on both sides of the core. Care was taken to ensure that the specimens were symmetrically located and axially aligned before applying the load. Tests were done under ambient laboratory conditions within the temperature range 21-25 °C. The load was applied at a testing rate of the connecting devices of 2 mm/minute until the specimen failed. The load cell and the average displacement over the joint's height were registered. On basis of these measurements the stresses are calculated by dividing the force by the cross-section area and the strains are calculated by dividing the lengthening by the initial height of the specimen. The stress-strain curves for both core materials according to all tests are given in figure 8.3. It is observed that some of

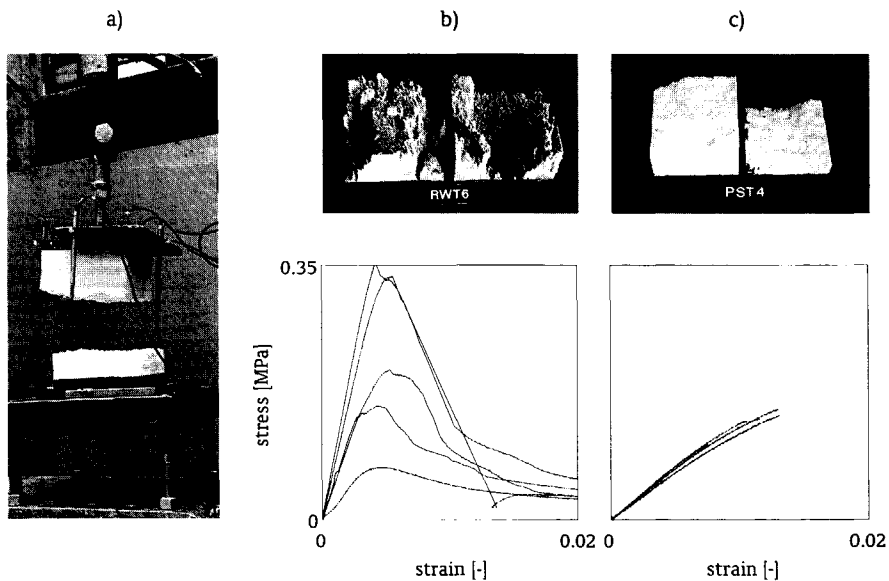


Figure 8.3 Tensile tests: a) test rig, b) stress-strain curves for the core material Conrock 700, c) stress-strain curves for the core material EPS 30

the specimens failed partly in the interface between the core and the adhesive bonded steel plate. But it is still assumed that for those cases the measured failure load and the calculated ultimate tensile stress are representative for the core material. On basis of these stress-strain curves the values of the Young's modulus are calculated by taking the secant modulus at a strain of 0.2 %.

Compression test specimens with a square cross-section were prepared and axially loaded. The same type of specimen and testing procedure were used, and an identical method to determine the stress-strain curves is applied. The stress-strain curves for both core materials according to all tests are given in figure 8.4. On basis of these stress-strain curves the values of the Young's modulus are calculated by taking the secant modulus at a strain of 0.2 %.

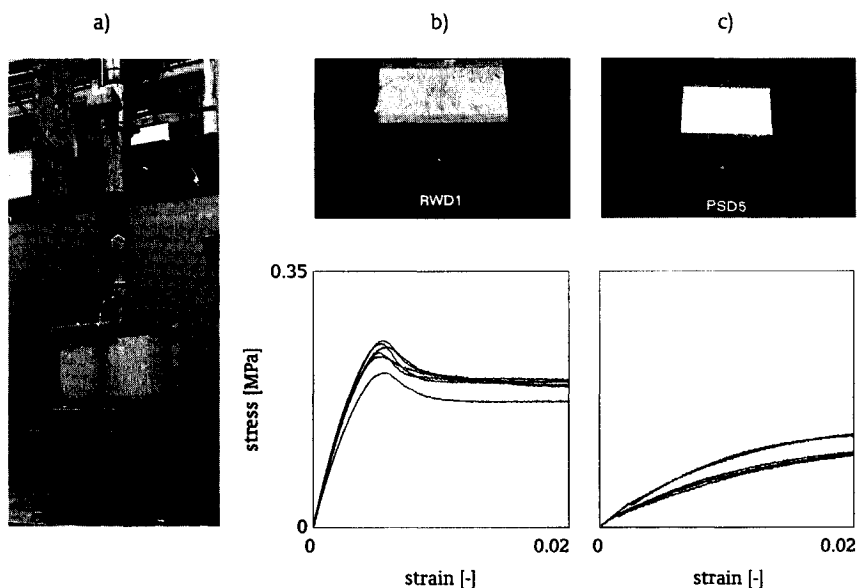


Figure 8.4 Compression tests: a) test rig, b) stress-strain curves for the core material Conrock 700, c) stress-strain curves for the core material EPS 30

To determine the shear properties of the core material the recommendations given by ECCS and CIB (1995) propose to base these on a four-point bending test. Since the used specimens of the case study fulfil the requirements of this standardised test, the measured loads and matching deflection of the middle span are used to determine the shear modulus. A description of the performed tests is given in section 8.1.6. On basis of the determined load-deflection curves the values of the shear modulus are calculated by the procedure given by ECCS and CIB (1995) at a relative value of the deflection divided by the span equal to 0.2 %. The results of the case study do not provide information about the failure load for shear failure. For this reason additional four-point bending tests on 1000 mm long and 200 mm wide sandwich beams were performed to determine these failure loads (Van Straalen, 2000H). The ultimate shear stress is calculated by dividing the maximum shear force by the core height times the sandwich beam width.

Overviews of the properties based on the test results of the core materials Conrock 700 and

Table 8.1 Overview of properties based on test results for the core material Conrock

	tensile properties		compression properties		shear properties		
	$\sigma_{c;t;ult}$ [MPa]	$E_{c;t}$ [MPa]	$\sigma_{c;c;ult}$ [MPa]	$E_{c;c}$ [MPa]	$\tau_{c;ult}$ [MPa]	G_c [MPa]	
test results	0.21	50.1	0.23	64.6	0.079	8.6 ¹⁾	7.4 ²⁾
	0.35	91.0	0.21	56.2	0.096	8.7 ¹⁾	7.7 ²⁾
	0.16	53.8	0.24	65.4	0.091	7.0 ¹⁾	8.1 ²⁾
	0.07	20.9	0.25	68.6	0.11	9.9 ¹⁾	9.4 ²⁾
	0.34	76.2	0.25	64.3	0.11	8.8 ¹⁾	7.6 ²⁾
		0.26	66.8	0.10	7.0 ¹⁾	7.7 ²⁾	
<i>m</i>	0.22	58.4	0.24	64.3	0.098	8.2	
<i>s</i>	0.12	26.8	0.016	4.3	0.012	0.95	

1) Based on the sandwich panel with the outside diaphragm bonded to the core

2) Based on the sandwich panel with the outside diaphragm not bonded to the core

Table 8.2 Overview of properties based on test results for the core material EPS 30

	tensile properties		compression properties		shear properties	
	$\sigma_{c;t;ult}$ [MPa]	$E_{c;t}$ [MPa]	$\sigma_{c;c;ult}$ [MPa]	$E_{c;c}$ [MPa]	$\tau_{c;ult}$ [MPa]	G_c [MPa]
test results	0.14	12.6	0.13	9.6	0.11	5.5
	0.10	14.7	0.13	8.7	0.11	5.0
	0.14	13.9	0.15	11.3	0.11	5.3
	0.15	13.9	0.16	13.8	0.11	4.9
	0.14	14.4	0.14	11.0	0.12	5.5
	0.14	13.0	0.13	9.0		
<i>m</i>	0.14	13.8	0.14	10.6	0.11	5.2
<i>s</i>	0.016	0.81	0.013	1.9	0.004	0.29

EPS 30 are given in respectively tables 8.1 and 8.2. These tables include the mean and standard deviation of the considered test sample. A significant observation is that the tensile properties of the core material Conrock 700 show a large scatterband. It is believed that this is caused by the used test setup and the non-homogeneity of the material. If a weaker part of the core material near one of the outer parts of the specimen fails, the specimen will be loaded asymmetrically and high peel stresses will occur near the failed region. Further research is

Design Rules for Sandwich Panels

needed to confirm the cause of the high scatterband found for the tensile properties of the core material Conrock 700.

The characteristic values of the core properties are determined with use of statistical techniques. The calculation of the characteristic values of the ultimate tensile and shear stresses is based on a Weibull distribution. Based on the same considerations as discussed in section 4.2 for adhesive bonded joints, it is assumed that this distribution function can be adopted for mineral wool and polystyrene core materials. An overview of the results of the calculations is given in table 8.3. The values of the shape parameter β' and scale parameter α' of the Weibull distribution are estimated with the procedure described in section 4.2.1. The characteristic values of the tensile and shear stresses are calculated with equation 4.12 for a target probability of 0.05. The characteristic values of the Young's and shear moduli are equal to the mean values. The mean and characteristic values of the core properties as presented in table 8.3 are used to validate the proposed prediction model and to calibrate the partial factor of a design rule.

Table 8.3 Overview of the calculation of the characteristic values of the properties of the core materials Conrock 700 and EPS 30

core material	property	m [MPa]	s [MPa]	β' [-]	α' [MPa]	n [-]	$k_{0.05}(n)$ [-]	characteristic value [-]
Conrock 700	$E_{c;k}^{1)}$	61.6	-	-	-	-	-	61.6
	$G_{c;k}$	8.2	-	-	-	-	-	8.2
	$\sigma_{c;t;k}$	0.23	0.020 ²⁾	8.669	0.238	5	0.69	0.15
	$\tau_{c;k}$	0.098	0.012	9.727	0.103	6	0.73	0.068
EPS 30	$E_{c;k}^{1)}$	12.2	-	-	-	-	-	12.2
	$G_{c;k}$	5.2	-	-	-	-	-	5.2
	$\sigma_{c;t;k}$	0.14	0.016	10.12	0.142	6	0.73	0.095
	$\tau_{c;k}$	0.11	0.004	32.44	0.112	5	0.69	0.098

1) For this property the mean value of the tensile and compression tests is used.

2) Instead of using the value of 0.12 MPa as mentioned in table 8.1, a probably more realistic value of 0.020 MPa is used, which is slightly larger than the value according to the compression tests.

8.1.4 Background of stress analyses

Since the period after the Second World War a large variety of analytical solutions for sandwich panels loaded in bending has been proposed. Most of the theories are based on a three-layer concept. A distinction is made between classical theories, superposition approaches and higher-order theories. Each derivation makes assumptions in modelling the behaviour of the core, the faces and their interaction. This will result into a set of differential equations, which have to be solved analytically or with a numerical calculation procedure. To calculate the stress state near the support region, the higher-order theory seems to be the most promising of the three distinguished categories of analytical solutions.

Compared with classical theories, higher-order theories apply a more realistic modelling.

Higher-order theories take into account the fact that the normal stresses deviate over the core thickness, while classical theories assume one value. Higher-order theories also model a zero-shear stress condition at a free sandwich end, while classical theories do not. This means that according to higher-order theories the deflections of the upper- and lowerface are no longer equal and that the section planes are no longer linear for local circumstances. See figure 8.5. As a result a more realistic stress state can be determined for sandwich panels with a flexible core material. Superposition approaches are not adequate alternatives for higher-order theories, because the local effects are only combined with classical theories without taking interaction effects into account. Another advantage of the higher-order theories is that the boundary conditions are described properly. Classical theories assume that the boundary conditions are the same for the entire height of the section, which is not very realistic for practical applications. Solutions of higher-order theories for various applications have been developed by Frostig from the end of the 1980's on.

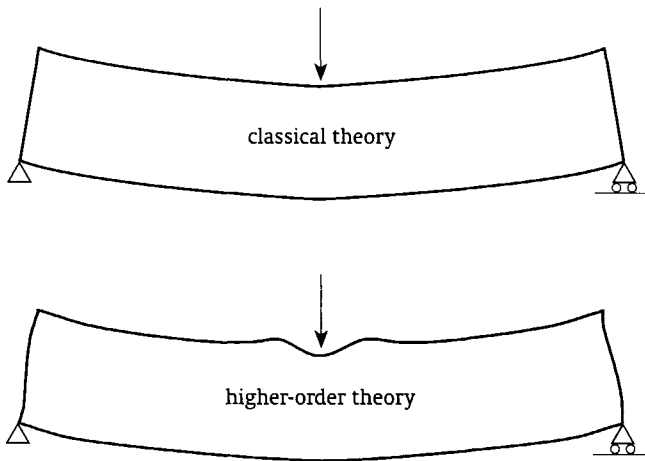


Figure 8.5 Schematic presentation of the deformations of a sandwich beam loaded in three-point bending

A number of publications of Frostig about higher-order theories are related to the considered case study of a sandwich panel under four-points bending. The derivations presented and discussed by Frostig et.al. (1992A), and Frostig (1992B, 1993A and 1993B) focus on sandwich beams. The faces are considered as ordinary beams, which are interconnected through equilibrium and compatibility at the interface layer with the core. The core is considered to be a two-dimensional elastic medium. Different boundary conditions and continuity requirements for the two faces and the core are allowed and different continuous and local loads may be applied on the faces. With these derivations it is possible to analyse sandwich beams with, see also figure 8.6:

- point loads and support regions (Frostig et.al., 1992A);
- edge and inner delamination regions (Frostig, 1992B);
- edge and inner transverse diaphragms (Frostig, 1993A);
- edge supports (Frostig, 1993B).

Design Rules for Sandwich Panels

A summary of these derivations is given by Frostig (1993B), while Thomsen and Frostig (1997) give an experimental verification for a sandwich beam under three-point bending. A further development is made by Frostig and Baruch (1996) for a sandwich panel, which can bend in two directions.

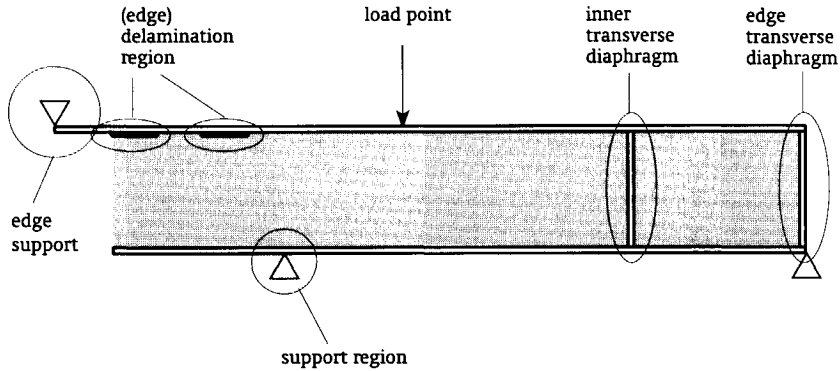


Figure 8.6 Overview of a sandwich beam with local geometry for which higher-order theories are available

Instead of using the higher-order theory for sandwich beams as originally derived by Frostig, for the case study a higher-order theory for sandwich panels is used. The main difference is that the faces are not modelled as beams, but as plates. The thin plate theory is adapted, assuming a two-dimensional modelling with cylindrical bending of the faces. Another difference is that a numerical procedure is used to solve the derived boundary value problem, instead of solving it with rather difficult analytical methods as Frostig has done.

8.1.5 Higher-order theory

The principle of a higher-order theory for modelling a beam, a plate, a shell or a sandwich is that the displacement fields as described by a classical theory, are extended by higher-order terms. The essential contribution of Frostig to the derivation of higher-order theories for sandwich panels is that this derivation is based on the actual physical behaviour of the flexible core material, instead of simply adding higher-order terms.

The higher-order theory derived by Frostig can be seen as an extension of the unified spring model approach for adhesive bonded lap joints presented in section 7.1.5. To model the mechanical behaviour of a sandwich panel the same general procedure of derivation can be followed. The kinematic relations of the faces and core, the compatibility conditions of the interface layer, the equilibrium equations of the interface layer and the constitutive relations of the faces and core have to be described. A summary of this procedure is given in figure 8.7.

The main differences in derivation are the formulation of the kinematic relations of the core material and the possibility to meet the zero-shear stress condition at the free core ends. The kinematic relations of the core are formulated such that the transverse normal stress $\sigma_{zz;c}$ varies linear over the core height. Instead of linear (first-order) displacement fields derived according to the simple spring approach for the adhesive bondline, a quadratic (second-order) transverse displacement field w_c and a third-order longitudinal displacement field u_c over the

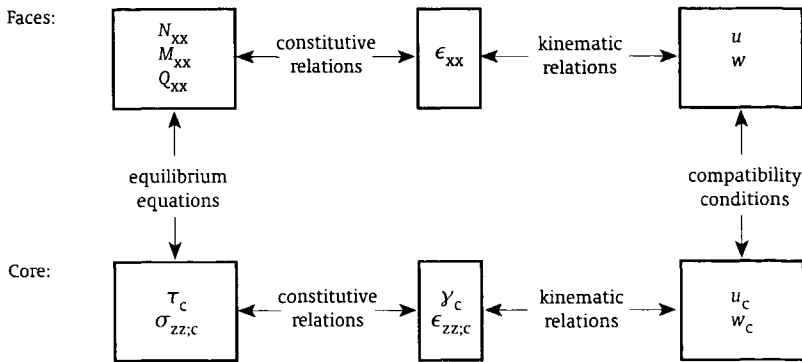


Figure 8.7 General procedure of derivation

core height is derived. The derivation of the higher-order theory also differs on some other aspects from the simple spring approach. The following assumptions are made:

- Cylindrical bending of the faces. Both the beam theory as described by Frostig, as well as the plate theory might be used.
- Elastic isotropic material behaviour of faces and core.
- The effect of shear deformation of the faces is not taken into account, because it is assumed that these effects are negligible.
- Zero shear stress condition at the free core's ends.
- Constant shear stress over the core height.
- No longitudinal normal stress in the core.

The derivation is originally presented by Frostig et.al. (1992A), and Frostig (1992B), (1993A) and (1993B).

The result of this derivation is a set of second and fourth order differential equations and matching continuity and boundary conditions. An overview is given in appendix B. The derived boundary value problem is of the 14th order. The set of differential equations contains the unknown functions of the displacements of the faces (longitudinal displacement in the centre line u_0 , its first derivative, the transverse displacement w and its first, second and third derivatives) and the shear stress in the core (τ_c and its first derivative). The matching continuity and boundary conditions are also formulated within these displacements and stresses. The section forces in the faces (normal force N_{xx} , shear force Q_{xx} and bending moment M_{xx}), transverse normal stress within the core ($\sigma_{zz;c}$) and displacement fields of the core (transverse displacement w_c and longitudinal displacement u_c) are formulated in terms of the unknown functions.

The boundary value problem according to the higher-order theory can be solved with the same numerical algorithm as used for the unified spring model approach for adhesive bonded overlap joints. The derived set of second and fourth order differential equations has to be rewritten as a set of first order differential equations. Together with the boundary and continuity conditions this set can be solved with the multi-segment method of integration developed by Kalnins (1964).

To validate the proposed higher-order theory for sandwich panels, a comparison is made with detailed finite element calculations. During the Euromech 360 Colloquium 'Mechanics of

Design Rules for Sandwich Panels

Sandwich Structures' (Vautrin, 1998), a round robin calculation of a sandwich beam under four-point bending was initiated. The dimensions and properties of the considered sandwich beam are given in figure 8.8. Within the round robin it was asked to calculate for 24 points the displacements, shear stresses and transverse normal stresses. Various calculations were made within the framework of the Brite/Euram BET2-530 Thematic Network project DOGMA (Design Optimisation and Guidelines for Multimaterial Applications). The results of the calculation of the displacements, shear stresses and transverse normal stresses according to the higher-order theory are presented in figure 8.9. Comparing these results with the finite element calculations made by Ferreira (1999) shows that the agreement between both approaches is within a few percent.

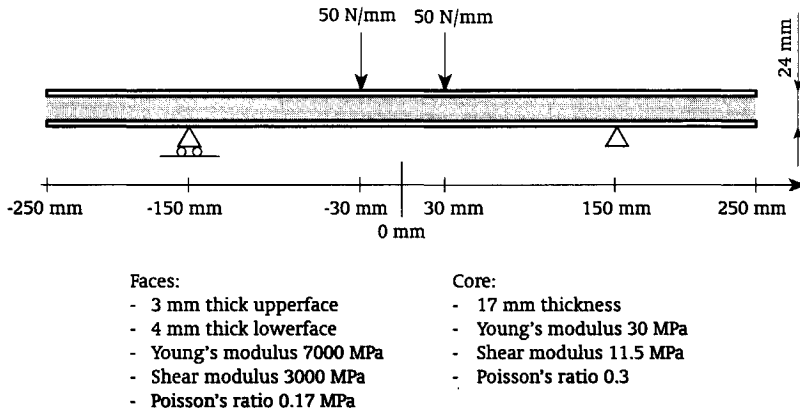


Figure 8.8 Dimensions and properties of the round robin sandwich beam

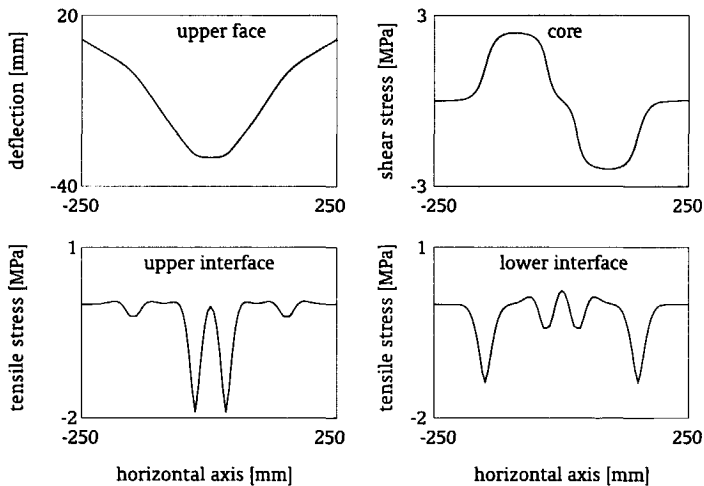


Figure 8.9 Results of calculations according to the higher-order theory

8.1.6 Comparison between tests and predictions

To validate the proposed prediction model, calculations are compared with the test results of the case study dealing with various sandwich panel endings (Van Straalen, 2000B). The dimensions of the sandwich panel under a four-point bending load are given in figure 8.1, while the considered endings are illustrated in figure 8.2. The loading of the specimens was displacement controlled. The applied load, the deflection of the midspan and the initiation of the delamination of the interface between the upperface and the core were continuously recorded. The delamination was measured by four displacement receivers, which were placed in small holes drilled in the upperface near both sandwich panel endings. If delamination initiated, a significant displacement was recorded. For each situation 5 or 6 specimens were tested. Tests were done under ambient laboratory conditions within the temperature range 21-25 °C. A complete description of the tests and the results is given by Van Straalen (2000E). The ultimate loads, the loads at which delamination initiated and the load-deflection curves are compared.

The used prediction model is based on the higher-order theory discussed in the previous section. For the properties of the 100 mm thick core materials Conrock 700 and EPS 30 the mean values given in table 8.3 are used. For the properties of the 1 mm thick steel faces a Young's modulus of $E_f = 210000$ MPa and a Poisson's ratio of $\nu_f = 0.3$ are applied. Since the geometry is symmetrical, only the right hand side is modelled. Figure 8.10 gives an overview of the division of the right hand side of the sandwich panel into three elements. The mechanical behaviour of each element is described by a set of differential equations. These elements are connected with proper boundary and continuity conditions. Boundary conditions are formulated for the line of symmetry and for the support region, while continuity conditions are formulated at both sides of the loaded region. An essential aspect is the modelling of the support region. The lowerface is simply supported just underneath the vertical outside diaphragm. The point of the upperface just above this diaphragm is related to the displacements and rotation of the supported point of the lowerface as indicated in figure 8.10-b. The difference between the situations of an outside diaphragm bonded or not bonded to the core material is modelled by assuming respectively a vertical displacement of the core equal to zero or a shear stress equal to zero. Detailed information about the used differential equations, boundary conditions and continuity conditions is given in appendix B.

The situations of the outside diaphragm bonded and not bonded to the core are studied for the core material Conrock 700. With the prediction model the shear stress distribution within the core and the transverse normal stress distribution in the interface between the upperface and the core are calculated. A total load of 6000 N is applied to the specimen. The results of these calculations are plotted in figure 8.11. The distributions of the shear stresses are almost equal for both situations. The only difference is that close to the outside diaphragm the shear stress lowers only slightly for the situation of the bonded diaphragm, while the shear stress becomes zero for the situation of the not bonded diaphragm. The difference of the distributions of the transverse normal stresses becomes more significant. The value for the situation of the not bonded diaphragm is approximately three times higher than for the situation of the bonded diaphragm. This conclusion is confirmed by the test results. It was observed that for the situation of the bonded diaphragm mainly shear failure of the core occurred, while for the situation of the not bonded diaphragm delamination of the interface occurred. This example shows that with use of the higher-order theory detailed calculations can be made.

Design Rules for Sandwich Panels

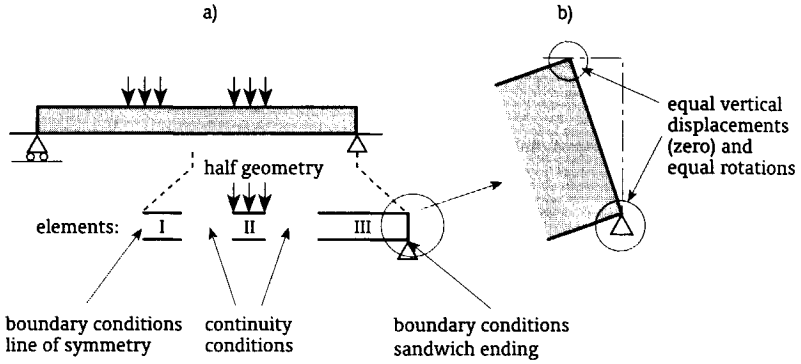


Figure 8.10 Modelling of the geometry: a) division of half the geometry into three elements, and b) support region

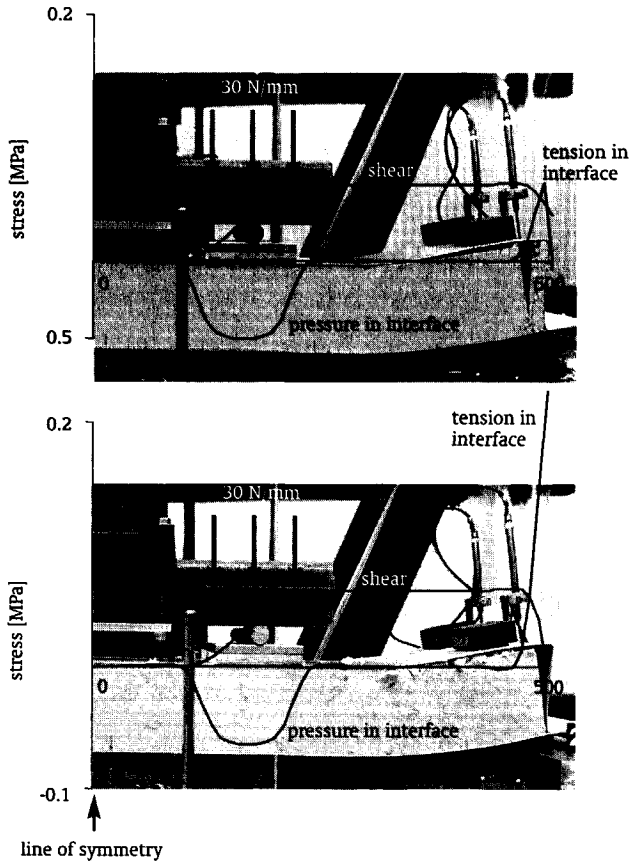


Figure 8.11 Distribution of shear stresses in the core and transverse normal stresses in the interface between the upperface and the core, for: a) the outside diaphragm bonded to the core material Conrock 700, and b) the outside diaphragm not bonded to the core material Conrock 700

A direct comparison between the prediction model and the test results is made by considering the load-deflection curves. Using the prediction model the linear elastic deflection of the midspan is calculated. Additionally the load levels at which failure occurs, are calculated. It is assumed that shear failure of the core occurs as soon as somewhere in the core the mean value of the ultimate shear stress of the core material is reached. Delamination of the interface occurs as soon as somewhere between the upperface and the core the mean value of the ultimate tensile stress of the core material is reached. The mean values of the ultimate shear and tensile stresses for the core materials Conrock 700 and EPS 30 are taken from table 8.3. For the three tested situations the load-deflection curves are given in figure 8.12. From these curves it is concluded that the stiffness is predicted rather well. But this is not a surprise, because the shear moduli of the core materials are based on the same test results. For the situation of the diaphragm bonded to the core material Conrock 700 the predicted strength is higher than the measured ones. This is caused by the fact that for most specimens the diaphragm and the core were not completely bonded. It was also observed during the tests that in some cases delamination of the interface occurred. For the situations of the not bonded diaphragm the predicted values are in agreement with the measured values. The load-displacement curves show that after initiation of delamination the load carrying capacity increased slightly until final failure occurred. The general conclusion of the comparison is that with use of the higher-order theory in combination with ultimate stress criteria, the actual mechanical behaviour of sandwich panels loaded in bending can be predicted rather well.

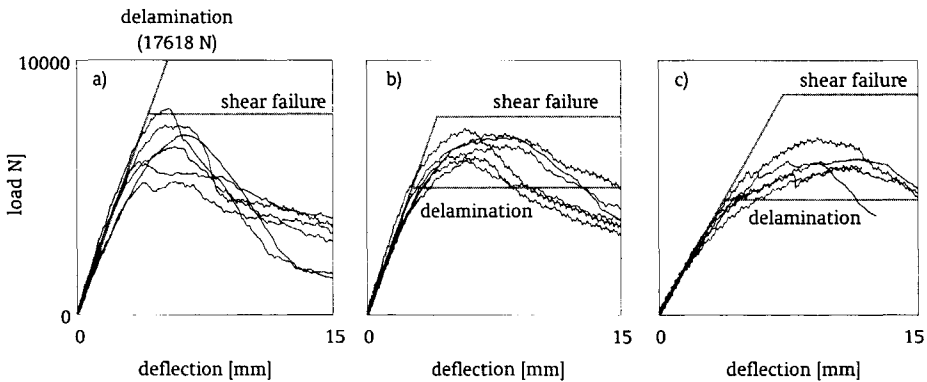


Figure 8.12 Comparison between the calculated load-deflection curves (straight lines) and the curves based on the tested sandwich panels, for: a) the outside diaphragm bonded to the core material Conrock 700, b) the outside diaphragm not bonded to the core material Conrock 700, and c) the outside diaphragm not bonded to the core material EPS 30

8.1.7 Calibration of the partial factor

The essence of the procedure to calibrate the partial factor is the comparison of a set of data with matching strengths calculated by the proposed prediction model. For the case study the procedure described in section 4.3.2 is used. It is assumed that the prediction model is deterministic. The calculations of the matching predicted strengths are based on nominal values for the dimensions, nominal values for the face properties and mean values for the core properties. Additional calculations are performed to determine the characteristic strengths,

Design Rules for Sandwich Panels

which are also used to calibrate the actual value of the partial factor. These calculations are based on nominal values for the dimensions and face properties, and characteristic values for the core properties as given in table 8.3. Referring to the considerations made about the tests and calculations in the previous section, an overview of the measured loads and calculated strengths is given in table 8.4.

Table 8.4 Overview of measured failure loads and calculated strengths

	test results				max. failure load	remark	predictions			
	initiation of delamination ^{a)}						delamination		shear failure core	
	left side of specimen	right side of specimen					R_m	R_k	R_m	R_k
	[N]	[N]	[N]	[N]	[N]	[N]	[N]	[N]		
mineral wool bonded	-	-	6018	5908	6042	b), c)	17618	12012	7879	5467
	7312	7251	-	4016	7458	b), c)				
	-	-	5237	5188	5249	b), d)				
	-	8093	-	-	8105	b), c)				
	-	-	6140	5640	6604	b), c)				
	-	-	6946	4492	7068	b), c)				
mineral wool not bonded	-	-	5981	5835	6238	d), e)	5007	3414	7781	5399
	6506	6213	6201	6189	6702	d)				
	6055	6018	5359	6201	7129	d)				
	-	-	6604	6104	7336	d)				
	4175	2844	6189	3162	7031	d), e)				
	4993	4260	1978	3442	6079	d), e)				
polystyrene not bonded	3760	4102	-	-	6067	d), e)	4536	3078	8653	7709
	3552	2930	3589	4260	5908	d), e)				
	4858	4688	-	4126	6140	d)				
	5054	5542	4590	4651	5884	d)				
	-	-	5579	5505	6995	d)				

a) no value is given if no initiation of delamination was registered

b) the diaphragm is only partial bonded to the core

c) dominated by shear failure of the core

d) dominated by delamination of the interface

e) the interface between the upperface and the core near the support is not fully bonded

To explain the calibration procedure the followed steps are described for one situation. For the core material Conrock 700 with the outside diaphragm bonded to the core the experimentally determined six failure loads $R_{test,i}$ are compared with the predicted strength $R_{pm,i}$ assuming shear failure of the core material. The graph shown in figure 8.13, with the set of test data

points i on the vertical axis and the corresponding predicted values on the horizontal axis, indicates that the prediction model slightly overestimate the test data. The differences between both provide quantitative information that is used to perform a probabilistic analysis. Here the procedure is followed to multiply for all data points i the prediction model with a factor $K_{m,i}$ according to equation 4.21. The results are given in figure 8.13. The estimated mean and standard deviations of the sample of these correction factors are equal to respectively $m_{K;m} = 0.86$ and $s_{K;m} = 0.13$. Assuming a Weibull distribution with the estimated shape parameter equal to $\beta'_{K;m} = 7.84$ and the estimated scale parameter equal to $\alpha'_{K;m} = 0.911$ the design value of the factor $K_{m;d}$ is determined according to the principles of equation 4.11:

$$R_{m;d} = \alpha'_{K;d} [-\ln(1 - \Phi(\alpha_R \beta))]^{1/(k_{\alpha_R \beta}(n) \beta'_{K;m})} \quad (8.1)$$

where n is the number of correction factors. The value of the parameter $k_{\alpha_R \beta}(n)$ depends on the value of the product of the weight factor and the reliability index $\alpha_R \beta = 0.8 \cdot 3.8$ discussed in section 3.2.2. In this example with $n = 6$ the value according to table 4.2 is equal to $k_{\alpha_R \beta}(6) = 0.55$, which means that the design value of the correction factor is $K_{m;d} = 0.191$. Now the design values referring to all data points i can be calculated with equation 4.23, which give for all data points i the same value $R_{d;i} = 1504$ N. The characteristic value of the strength $R_k = 5467$ N according to the prediction model, is already given in table 8.4. Now the partial factor is calculated with use these two values of the strength according to equation 4.24. For this example a relative high value of the calibrated partial factor equal to $\gamma_R = 3.6$ is determined.

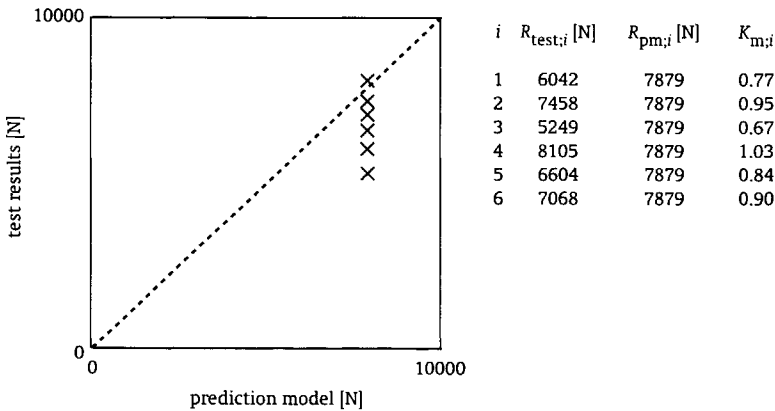


Figure 8.13 Example of comparison of test data with corresponding predicted values

An essential step within the calibration procedure is the selection of a valid and useful data set. The above given example of the core material Conrock 700 with the diaphragm bonded to the core shows that without reviewing the validity of the actual data set, a rather high and probably unrealistic value for partial factor is found. If the test result dominated by delamination of the interface between the upperface and the core is excluded, the calibrated value of the partial factor will be lower. Table 8.5, which gives an overview of the results of

the calibration on basis of various data sets, indicates that for this situation the calibrated value of the partial factor is reduced to $\gamma_R = 2.8$. This value is still rather high, mainly because the number of test results is limited. To increase this number it is decided to take also the failure loads of the tests with the diaphragm not bonded to the core into account. This will be a conservative approximation, since these values are influenced by delamination of the interface. The result of this estimation is promising; an acceptable value of the calibrated partial factor of $\gamma_R = 1.8$ is determined for the core material Conrock 700 with the outside diaphragm bonded to the core.

For the core material Conrock 700 with the outside diaphragm not bonded to the core a comparable analysis is made. If all results are taken into account a relative high value of the calibrated partial factor of $\gamma_R = 4.4$ is determined. See also table 8.5. This value is much lower if the lowest two or four test results are simply excluded. Values of the calibrated partial factors of respectively $\gamma_R = 2.3$ and 1.4 are determined. The drawback of this arbitrary assumption is that a physical background is missing. After inspection of the tested specimens it was found that for some of the specimens the interface of the upperface near the supports was not fully bonded. If the results for these specimens are excluded, a value of the calibrated partial factor of $\gamma_R = 0.8$ is found. This value is low, because the found standard deviation is rather small. Based on the engineering judgement that a higher standard deviation is probably more realistic, a value for the partial factor of $\gamma_R = 1.4$ is proposed.

Also for the core material EPS 30 with the outside diaphragm not bonded to the core an analysis is made. If all results are taken into account a value of the calibrated partial factor of $\gamma_R = 2.4$ is determined. See also table 8.5. After inspection of the tested specimens it was found that for some of the specimens the interface of the upperface near the supports was not fully bonded. If the results for these specimens are excluded, a value of the calibrated partial factor of $\gamma_R = 1.4$ is found. This value seems to be realistic, because the value of the standard deviation is reasonable.

8.2 Mechanical behaviour of a sandwich panel with an adhesively bonded plate

Within the preceding section a design rule is proposed for sandwich panels loaded in bending. With this design rule it is possible to validate shear failure of the core material and delamination of the interface. In addition to the research programme to develop a suitable prediction model and to calibrate the partial factor for this application, another case study is performed. This case study focuses on a sandwich panel in combination with a loaded plate adhesively bonded on one of the sandwich faces.

The research programme contains a theoretical part and an experimental part. Within the theoretical part a prediction model is used, based on the model developed in section 8.1 for sandwich panels in combination with the model developed in section 7.1 for adhesive bonded overlap joints. The experimental part of the case study contained tests on sandwich panels with an angle section adhesively bonded on one of the faces. The panels with a length of 1000 mm and a width of 400 mm, were made of a 100 mm thick flexible core material with 1 mm thick steel faces bonded on both sides with a one-component polyurethane adhesive. The core materials Conrock 700 as well as EPS 30 were used. The plate adhesively bonded on one of the faces in width direction was a steel angle section 80-80-8 mm. The cold cured two-component polyurethane adhesive UK 8202 of Henkel was used. The dimensions of the specimens and the

Table 8.5 - Overview of results of various calibrations

used data set	n [-]	m_K [-]	s_K [-]	β' [-]	α' [-]	$k_{\text{CRG}}(m)$ [-]	K_d [-]	R_d [N]	γ_R [-]
mineral wool bonded									
all failure loads	6	0.86	0.13	7.84	0.911	0.55	0.19	1504	3.6
all failure loads excluding one value dominated by delamination of interface	5	0.90	0.10	10.8	0.938	0.47	0.25	1958	2.8
all failure loads of bonded and not bonded situation (conservative estimation)	12	0.86	0.10	10.6	0.904	0.74	0.38	3026	1.8
								2988	
mineral wool not bonded									
all loads of initiation	20	1.04	0.28	4.21	1.15	0.80	0.16	775	4.4
all loads of initiation excluding two lowest values	18	1.10	0.21	6.04	1.19	0.80	0.30	1478	2.3
all loads of initiation excluding four lowest values	16	1.16	0.15	9.51	1.22	0.79	0.50	2494	1.4
loads for which interface of upperface near support are fully bonded	10	1.23	0.07	23.0	1.26	0.71	0.83	4167	0.8
polystyrene not bonded									
all loads of initiation	15	0.98	0.18	6.57	1.05	0.79	0.29	1302	2.4
loads for which interface of upperface near support are fully bonded	9	1.09	0.11	11.9	1.14	0.68	0.50	2251	1.4

Design Rules for Sandwich Panels

test set up are given in figure 8.14. The angle section was oriented in two positions and the load on the angle section was applied at two distances Δ , as indicated in figure 8.15. The main objective of these tests is to verify the design rules proposed in sections 7.1 and 8.1 for the combination of a sandwich panel and an adhesive bonded joint.

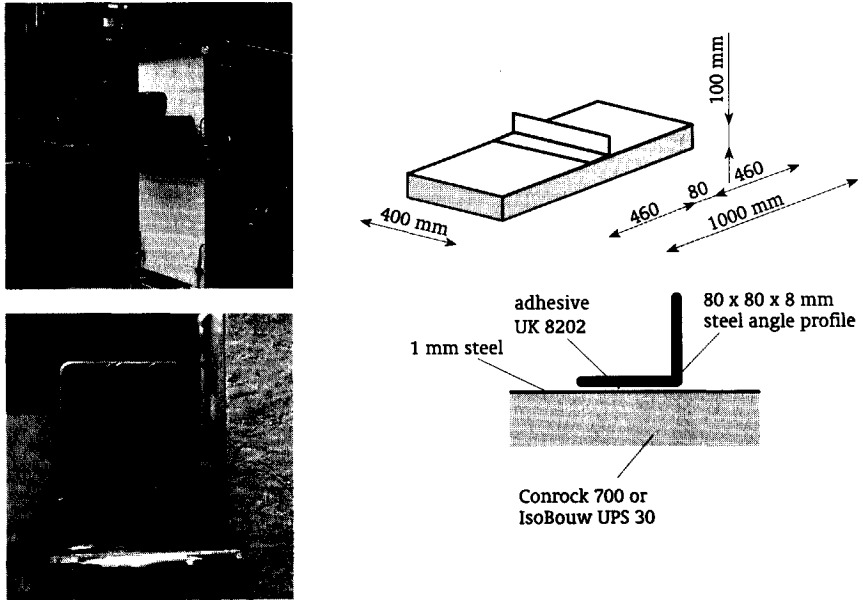


Figure 8.14 Tests on sandwich panel with an adhesively bonded plate

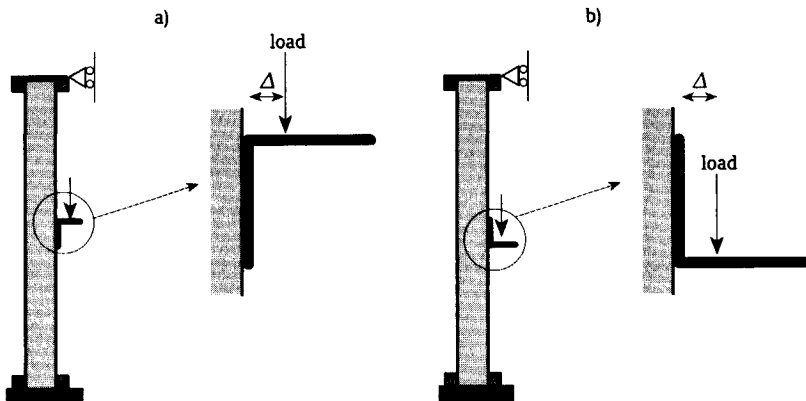


Figure 8.15 Considered situations: a) angle section in position "Γ" and line load placed at distance Δ (10 or 25 mm), and b) angle section in position "L" and line load placed at distance Δ (10 or 25 mm)

The developed prediction model is a combination of the models discussed in sections 7.1 and 8.1. Shear failure of the core material, delamination of the interface and cohesive failure of the bondline are assumed. The combined prediction model is based on linear elastic material behaviour of the faces, plate and core material, while for the adhesive non-linear material behaviour is assumed. The same failure criteria and material properties are used as determined in sections 7.1 and 8.1. In addition to the prediction models proposed in these sections, a new theory is derived to calculate mechanical action effects.

The theory to calculate mechanical action effects combines the higher-order theory and the spring model approach. The higher-order theory is applied for the sandwich panel and provides detailed information about the stress and strain states. The spring model approach on the other hand is applied for the adhesive bonded joint and provides information about the stress and strain states within the bondline, including non-linear behaviour of the adhesive. To combine the two theories, it is necessary that the assumptions as discussed in sections 7.1.5 and 8.1.5 match with each other. A comparison of these assumptions shows that there is only one mismatch. The higher-order theory does not take the effect of shear deformation of the faces into account, while the spring model approach does. To solve this problem, the derivation of the higher-order theory as presented in appendix B is reformulated by Van Straalen (1999D). The result of this derivation is a set of second order differential equations and matching continuity and boundary conditions. An overview is given in appendix C. The derived boundary value problem is also of the 14th order. The difference between this set of differential equations and the original set given in appendix B, is that instead of the unknown functions of the second and third derivative of the transverse displacement w , the rotation ψ and its first derivative are used. For a five-layer concept of a sandwich panel with an adhesively bonded plate, these derivations are extended by Van Straalen (1999D). The result is a set of second order differential equations and matching continuity and boundary conditions. An overview is given in appendix C. The derived boundary value problem is of the 20th order. The set of differential equations contains the same unknown functions of the displacements of the faces and the shear stress in the core as for the sandwich panel. The matching continuity and boundary conditions are also formulated within these displacements and stresses. The section forces in the faces, transverse normal stresses within the core, displacement fields of the core and stress and strain states within the bondline are formulated in terms of the unknown functions. The set of differential equations together with the boundary and continuity conditions can be solved with the multi-segment method of integration developed by Kalnins (1964).

To verify the proposed prediction model, calculations are compared with the test results of the case study. The loading of the specimens was displacement controlled. The applied load, the vertical displacement of the angle section and the rotation of the angle section were continuously recorded. Tests were done under ambient laboratory conditions within a temperature range 21-25 °C. A complete description of the tests and the results is given by Van Straalen (2000D). The ultimate loads and the load-displacement curves are compared.

The calculations are performed with the proposed prediction model. For the properties of the 100 mm thick core materials Conrock 700 and EPS 30 the mean values given in table 8.3 are used. For the stress-strain relation of the adhesive UK 8202 the average tensile curve given in table 7.3 is used. For the properties of the 1 mm thick steel faces and the 8 mm thick steel angle section a Young's modulus of $E = 210000$ MPa and a Poisson's ratio of $\nu = 0.3$ are applied. The geometry of the sandwich panel is completely modelled and the loaded angle

Design Rules for Sandwich Panels

section 80-80-8 mm is modelled as an 8 mm thick plate, which is loaded by an axial force and an additional bending moment. For the adhesive bondline a thickness of 0.2 mm is assumed. Figure 8.16 gives an overview of the division of the complete geometry into three elements. These elements are connected with proper boundary and continuity conditions. Detailed information about the used differential equations, boundary conditions and continuity conditions is given in appendix C.

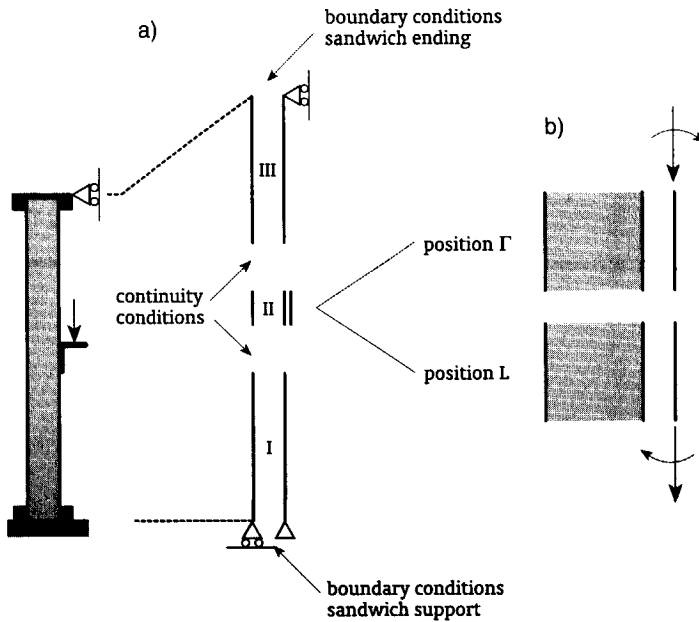


Figure 8.16 Modelling of the geometry: a) division of the geometry into three elements, and b) applied load on adhesively bonded plate

For both core materials linear elastic calculations are performed to determine the shear stress distribution within the core, the transverse normal stress distribution in the interface near the adhesively bonded plate and the vertical displacement of the angle section. In figure 8.17 the shear stress and the transverse normal stress distributions are presented for one of the considered situations. Based on this type of calculations the elastic deformations and the load levels at which shear failure or delamination occurs, are calculated. Additional physical non-linear calculations are performed to determine the strength of the adhesive bonded joint according to the iterative procedure described in section 7.1.5.

A direct comparison between the prediction model and the test results is made by considering the load-displacement curves. For the considered situations these curves are given in figure 8.18. The values of the measured failure loads and predicted strengths are also given in table 8.6. It is difficult to compare the predicted strengths with the test results for various reasons. It was difficult to identify the actual failure mode of each test and it was possible that shear failure became visible while delamination already occurred at a lower load level. Another problem was that for some tests an adhesive failure of the bondline occurred, due to

the coating put on the angle section. Unless these problem it is concluded that the prediction of failure load for delamination is lower than the test results, while most of the test results are close to the predicted failure loads for shear failure of the core material. Based on these findings it is concluded that with the proposed model a reliable prediction of the strength can be made.

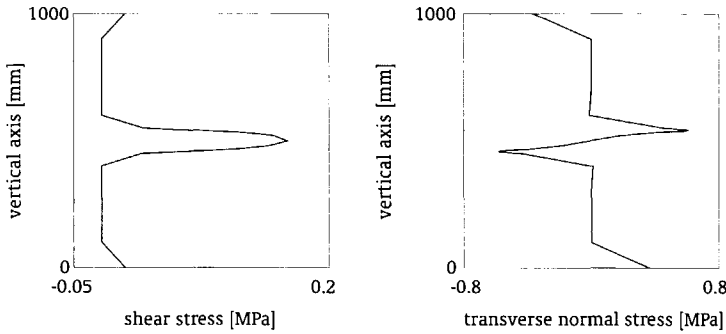


Figure 8.17 Calculation results for a sandwich panel with the core material Conrock 700, angle section in position "Γ" and line load of 40000 N placed at a distance $\Delta = 10$ mm: a) shear stress in the core, and b) transverse normal stress in the interface near the adhesively bonded plate

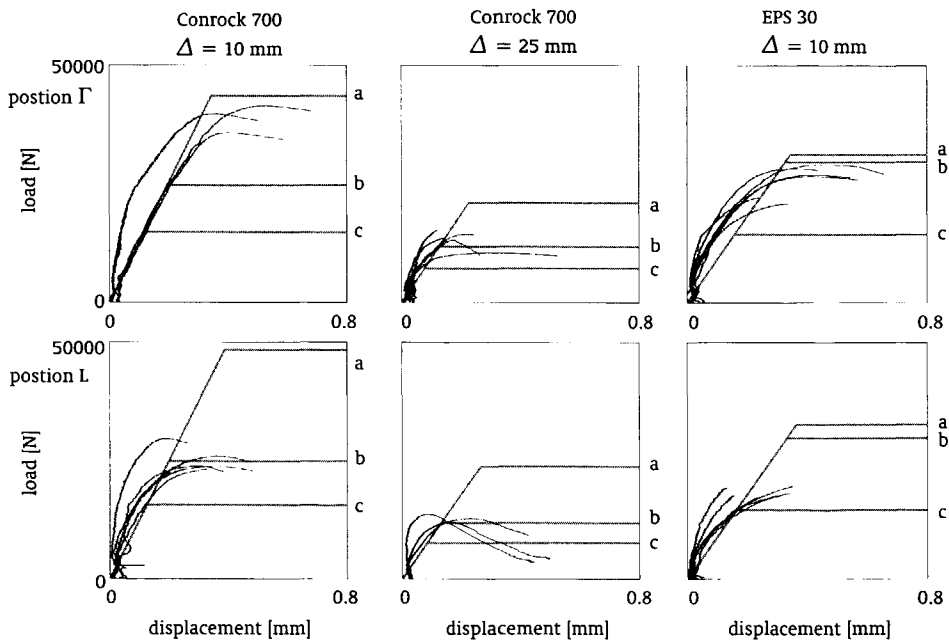


Figure 8.18 Comparison between the calculated load-displacement curves (straight lines) and the curves based on the tested sandwich panels: a) failure of the adhesive bonded joint, b) shear failure of the core, and c) delamination of the interface

Design Rules for Sandwich Panels

Table 8.6 Overview of measured failure loads and calculated strengths

core material	position		test results						predictions				
	Δ	Γ	maximum failure load [N]						m	s	a)	b)	c)
		or L							[N]	[N]	[N]	[N]	[N]
Con-rock 700	10	Γ	41455	35889	39819	20776	28931		31354	8366	24772	14807	43587
	mm	L	18896	23730	29565	23096	23853	25879	25225	2642	24838	15616	48396
	25	Γ	12354	13208	15186	10498	14429	13647	13394	1786	11809	7206	21082
	mm	L	14404	12793	13721	11987	12793		12823	709	11850	7681	23755
EPS 30	10	Γ	20972	22266	28320	29175	26733	27051	26709	2671	29741	14414	31241
	mm	L	19653	17798	18115	17896	19263	17285	18071	732	29794	14636	32684

a) shear failure core

b) delamination

c) cohesive failure

Conclusions

In the preceding chapters a systematic approach to develop reliable design rules for structural adhesive bonded joints is presented. The principles how to apply structural reliability methods and how to draft prediction models are discussed. Various examples of design rules for overlap joints and sandwich panels are worked out to illustrate the potential of the approach. Straightforward models to predict the mechanical behaviour and durability of adhesive bonded joints are given. Calibration techniques that compare prediction models with test results are applied. Based on the findings, the following conclusions are made:

- To formulate reliable design rules for daily design practice the partial factor approach is the most convenient structural reliability method. The introduction of the conversion factor additional to the partial factor is a practical method to incorporate the effect of the degradation of the resistance within a design rule.
- Besides engineering judgement, probabilistic techniques provide useful information to calibrate the values of the partial factor and conversion factor. It is found that the stochastic nature of the resistance of adhesive bonded joints can be represented by a Weibull distribution.
- For adhesive bonded overlap joints there is a good agreement between the proposed prediction model based on the spring model approach and results of tests done for a cold cured two-component epoxy adhesive and a cold cured two-component polyurethane adhesive. To achieve this agreement, it is important to model the physical non-linear behaviour of the adhesive and the geometrical non-linear behaviour of the joint.
- To perform calculations with the proposed prediction model for adhesive bonded overlap joints, it is necessary to extrapolate the stress-strain curve based on tensile bulk tests. A reason why this has to be done is that due to local necking of the specimen at higher load levels the local strain can not be measured. The extrapolation has to be done on engineering judgement.
- The values of the partial factor calibrated for the design rule developed for adhesive bonded overlap joints, are consistent. For the studied polyurethane adhesives the partial factor is higher than for the studied epoxy adhesive. It is concluded that the determined stress-strain relation of the polyurethane adhesive is not fully representative for the actual behaviour of the adhesive bondline.
- The five-step CIB-RILEM procedure is a helpful tool to structure the analysis of the degradation behaviour. It pays attention toward the identification of degradation mechanisms and the use of accelerated ageing tests.
- The two examples of single overlap joints made of polyester coated steel sheeting and bonded with cold cured two-component polyurethane adhesives of two suppliers, indicate that the conversion factor can be calibrated on the basis of accelerated ageing tests.
- For sandwich panels there is a good agreement between the proposed prediction model based on the higher-order theory and results of tests on sandwich panels loaded in bending done for a mineral wool and a polystyrene core material. To achieve this agreement, it is important to model the effects of local detailing. It is also shown that for a sandwich panel with a loaded plate adhesively bonded on one of the sandwich faces the strength can be predicted with a model based on a combination of the spring model approach and the higher-order theory.

Conclusions

- The results of the performed tests on sandwich panels show that various failure modes might occur at the same load level. To calibrate the partial factor for the design rule it is important to make a distinction between the results valid for the actual failure modes. The presented methodology to develop design rules is straightforward and systematic. Various aspects of reliable design rules, models to predict the resistance, methods to quantify the degradation of the resistance during time and probabilistic techniques to calibrate partial and conversion factors are studied and discussed in detail. The systematic approach is a novel method to develop reliable design rules for structural adhesive bonded joints.

Future Research Activities

Future research activities within the field of structural adhesive bonded joints have to follow new developments in industry. Within the marine sector adhesive bonding is a promising technique to join materials such as aluminium and fibre reinforced plastics. The fatigue properties and fire resistance of adhesive bonded joints are important topics, while for navy applications also the effects of an impact load are of concern. The interest of the transport sector focuses on the development of adhesively bonded monocoque structures for buses and trains. But present knowledge about the impact resistance and the effect of an adhesive bonded joint on the dynamic behaviour of the structure is limited. Within the building and civil engineering sector adhesive bonded joints can be used to join dissimilar materials and to reinforce existing structures. One of the most important issues is the durability of adhesive bonded joints under long-term loads and environmental actions. For the automotive sector the use of adhesive bonded joints within the car body opens new possibilities of weight reduction and performance optimization. For a successful application a better understanding of durability and impact resistance is essential. The aerospace industry has a long tradition in the application of adhesive bonded joints and is nowadays interested in optimising designs of adhesive bonded joints. These examples of developments and needs of knowledge indicate that a wide variety of research activities is necessary to stimulate the application of adhesive bonded joints.

Various questions about prediction models are directly related to the relevant mechanical action. In the present study only the short-term load condition is considered. To validate designs for impact loads, long-term static loads, low cycle fatigue loads or high cycle fatigue loads, other prediction models have to be used. Methods of modelling based on continuum mechanics or fracture mechanics are discussed in section 5.1. A prediction model for impact loads might consider the absorbed energy within the bondline. The creep behaviour of adhesives under long term static load conditions can be described by various visco-elastic models developed for polymers, which take time dependent effects into account. If failure of the bondline is a progressive process as might be the case for low cycle fatigue loads, a prediction model based on the theory of damage modelling seems to be fruitful. For high cycle fatigue loads on the other hand the classical SN-curve approach or a crack growth model based on fracture mechanics might be used to predict the resistance of adhesive bonded joints.

Most of the proposed prediction models assume cohesive failure of the adhesive, while in many practical situations adhesive failure or a mixture of both failures is dominant. The phenomenon of adhesive failure is ignored for many years, because for various applications the occurrence of this failure mode is not allowed. But there are no arguments why adhesive failure is refused, as long as the target reliability level is guaranteed. A better understanding of the complex behaviour of the interlayer between the adhesive bondline and the adherend is essential. To propose improved prediction models it is advised to perform physico-chemical studies together with the development of mechanical models.

The examples of developing design rules for adhesive bonded overlap joints and sandwich panels show that the use of tests is essential within the proposed systematic approach. Various aspects of doing tests are still under discussion. It is important to know what type of small-scale tests is preferred to determine material properties and how the specimens have to

be produced. To calibrate partial and conversion factors it is necessary to have a better understanding of selecting specimens representative for practical applications and of designing an optimum test plan. For accelerated ageing tests it will be helpful to have a better understanding of the selection of the intensified conditions in relation with the extrapolation of the test results for in-use conditions. Full-scale tests and in-use exposure of specimens might extend the knowledge about structural and durability behaviour.

The studies performed for adhesive bonded overlap joints and sandwich panels indicate that the adhesive material has to be modelled non-linearly, while the core material can still be modelled linear elastically. But still questions remain about the application of theories to calculate mechanical action effects. Are fracture mechanics a good alternative for continuum mechanics and what are the potentials of theories based on damage modelling? Another controversy is the use of analytical solutions or finite element methods. As long as the basic assumptions are similar there is only a difference in application; it is mostly easier to work with an analytical solution while the finite element method is more flexible. Since the proposed unified spring model approach and the higher-order theory are applied successfully, the formulation of finite elements based on these theories is suggested.

To calibrate the conversion factor to quantify the degradation of the resistance, a degradation mechanism and a time transformation function to extrapolate accelerated ageing tests for in-use conditions have to be formulated. Instead of using empirical relationships, it is probably better to develop a theory based on mechanistic studies and validated by tests. Not only the effects of water uptake have to be considered, but also changes in the polymer structure due to chemical ageing of the adhesive have to be studied. The ageing of the adhesion properties of the interlayer between the adhesive and the adherend also have to be modelled. If more knowledge is available it might be easier to make a prediction for in-use conditions on basis of accelerated ageing tests.

An important aspect within the development of reliable design rules is the effect of the manufacturing process. In the presented examples it is assumed that the test series are representative for practical applications. But less is known about the actual influences of the manufacturing process on the reliability of the resistance. Researching the manufacturing process in view of structural reliability methods might provide knowledge about followed procedures, sensitivity of the selected adhesive bonding system and the necessity to qualify personal. Based on this a qualification system can be developed for adhesive bonded joints, for example similar to those used for welded joints.

In chapter 4 probabilistic methods are introduced for the calibration of design rules. Simple techniques are used for the examples of adhesive bonded overlap joints and sandwich panels. The results of these examples illustrate that these techniques provide valuable quantitative information about the reliability. If more advanced techniques based on level III or II probabilistic methods have to be used, a better understanding of the stochastic nature of various properties is required. Also more sophisticated software programmes have to be applied or developed. Instead of using test results to calibrate design rules, it is also possible to perform simulations with validated models, which predict the mechanical and the degradation behaviour. Probabilistic methods are not only useful within the calibration process, but will also provide additional information about the influence of various parameters on the reliability. In spite of the fact that most of the probabilistic methods are available, it is important to gather more experience with these techniques.

Future research activities on failure modes, test methods, theories to calculate mechanical

action effects, degradation mechanisms, influences of manufacturing and probabilistic methods will support further developments of design rules for adhesive bonded joints. Using the presented systematic approach this process can be structured. A drawback of this process might be that the proposed prediction models would be more complicated. This is, because the suggested research activities are focused on getting a better description of the mechanical behaviour or the durability. For daily design practice on the other hand it is essential to develop easy to use design rules. For this reason researchers also have to look after simplified prediction models with matching partial factor and limited test plans to determine the value of the conversion factor.



References

- Adams, R.D., Wake, W.C. (1984), *Structural adhesive joints in engineering*, Elsevier Applied Science Publishers, United Kingdom.
- Adams, R.D. (1989), *Strength Prediction for Lap Joints, Especially with Composite Adherends - A Review*, J. Adhesion, Vol. 30, pp. 219-242.
- Allman, D.J. (1977), *A theory for elastic stresses in adhesive bonded lap joints*, Quart. J. Mech. Appl. Math., Vol. 30, pp. 377-386.
- ASTM E 632-81 (1981), *Standard practice for developing accelerated tests to aid prediction of the service life of building components and materials*, American Society for Testing and Materials, United States of America.
- ASTM D 638-96 (1996), *Standard test method for tensile properties of plastics*, American Society for Testing and Materials, United States of America.
- ASTM D 695-96 (1996), *Standard test method for compressive properties of rigid plastics*, American Society for Testing and Materials, United States of America.
- Bauwens, J.C. (1970), *Yield condition and propagation of Lüders' lines in tension - torsion experiments on poly(vinyl chloride)*, Journal of Polymer Science: Part A-2, Vol. 8, pp.893-901.
- Beeby, A.W. (1994), *γ -factors: A second look*, The Structural Engineer, Volume 72, No. 2.
- Beevers, A. Editor (1995), *MTS Adhesive Project 3: Environmental durability of adhesive bonds - Report no. 8: Experimental assessment of durability test methods*, AEA-ESD-0319, AEA Technology, United Kingdom.
- Beevers, A. (1997), Test results available by private communications with JTRC, Oxford Brookes University, United Kingdom.
- Benjamin, J.R., Cornell, C.A. (1969), *Probability, statistics and decision for civil engineers*, Mc. Graw Hill Book Company, United States of America.
- Berg, A. van den (2000), *On the stresses near the interface in adhesively bonded joints on aluminium and failure criteria suitable to predict the failure of the interface*, submitted to the International Journal of Adhesion & Adhesives, Delft University of Technology, Structures and Materials Laboratory, The Netherlands.
- Bigwood, D.A., Crocombe, A.D. (1990), *Non-linear adhesive bonded joint design analyses*, International Journal of Adhesion and Adhesives, Vol.10, No.1.
- Botter, H. (1997), *Overzicht omgevingscondities in Nederland en hun relatie met het lijmen en lijmverbindingen*, TNO-Report 97MI-00923, TNO Industry, The Netherlands.
- Box, G.E.P., Tiao, G.C. (1992), *Bayesian inference in statistical analysis*, Addison-Wiley Classics library, United States of America.
- Brandon, D., Kaplan, W.D. (1997), *Joining processes - An introduction*, John Wiley & Sons, United Kingdom.
- Brinson, H.F., Technical chairman (1990), *Engineering materials handbook. Volume 3: Adhesives and sealants*, ASM International, United States of America.
- Broek, J.A. van den (1940), *Theory of limit design*, Transactions, ASCE, Vol. 105, pp. 638-730.
- Carpenter, W.C. (1991), *A Comparison of Numerous Lap Joint Theories for Adhesively Bonded Joints*, J. Adhesion, Vol. 35, pp. 55-73.
- CEN (1994), *Eurocode 3 - Design of steel structures: Draft Annex Z - Determination of design resistance from tests*, Document CEN/TC250/SC 3 N422E.
- Chakrabarty, J. (1987), *Theory of plasticity*, McGraw-Hill Book Company, United States of America.
- Chen, D., Cheng, S. (1983), *An analysis of adhesive-bonded single-lap joints*, Journal of Applied

References

- Mechanics, Vol. 50, pp 109-115.
- Clarke, J.L., Editor (1996), *EUROCOMP Design Code and Handbook, Structural design of polymer composites*, E & FN Spon, United Kingdom.
- Comité Européen du Béton (1964), *Recommendations for an international code of practice for reinforced concrete*, Fédération International de la Précontrainte.
- Comité Européen du Béton (1970), *International recommendations for the design and construction of concrete structures - Principles and recommendations*, Fédération International de la Précontrainte.
- Crocombe, A.D. (1989), *Global yielding as a failure criterion for bonded joints*, International Journal of Adhesion & Adhesives, Vol.9, No.3.
- Crocombe, A.D., Kinloch, A.J. (1994), *Task 1: Detailed study of joint failure - MTS Adhesive Project 2: Failure modes and criteria - Report no. 1: Review of adhesive bond failure criteria*, AEA-ESD-0107, AEA Technology, United Kingdom.
- Crocombe, A., Hancox, N., McCarthy, J.C. (1995), *Task 1: Detailed study of joint failure - MTS Adhesive Project 2: Failure modes and criteria - Report no. 3: Summary*, AEA-ESD-0320, AEA Technology, United Kingdom.
- Cross, N. (1994), *Engineering design methods: strategies for product design*, 2nd edition, John Wiley & Sons, United Kingdom.
- Delale, F., Erdogan, F., Aydinoglu, M.N. (1981), *Stresses in adhesively bonded joints: a closed-form solution*, J. Composite Materials, Vol. 15, pp. 249- 271.
- ECCS, CIB (1995), *Preliminary European recommendations for sandwich panels with additional recommendations for panels with mineral wool core material - part 1: Design*, European Convention for Constructural Steelwork TWG 7.4 and International Council for Building Research, Studies and Documentation W56, CIB Report Publication 148, reprint.
- Elias, H.-G. (1997), *An introduction to polymer science*, VCH Verlagsgesellschaft, Germany.
- EN 1991 (1995/1997/1998), *Eurocode 1 - Basis of design and actions on structures*, 5 Parts published as Pre-standards by CEN Technical Committee CEN/TC 250.
- EN 1992 (1994/1996/1997), *Eurocode 2 - Design of concrete structures*, 2 Parts published as Pre-standards by CEN Technical Committee CEN/TC 250.
- EN 1993 (1995/1996/1997/1998), *Eurocode 3 - Design of steel structures*, 1 Part published as Pre-standards by CEN Technical Committee CEN/TC 250.
- EN 1994 (1994/1995/1997), *Eurocode 4 - Design of composite steel and concrete structures*, 1 Part published as Pre-standards by CEN Technical Committee CEN/TC 250.
- EN 1995 (1994/1995/1997), *Eurocode 5 - Design of timber structures*, 2 Parts published as Pre-standards by CEN Technical Committee CEN/TC 250.
- EN 1996 (1995/1998/1999), *Eurocode 6 - Design of masonry structures*, 3 Parts published as Pre-standards by CEN Technical Committee CEN/TC 250.
- EN 1997 (1995), *Eurocode 7 - Geotechnical design*, 1 Part published as Pre-standards by CEN Technical Committee CEN/TC 250.
- EN 1998 (1995/1996/1997/1998), *Eurocode 8 - Design provisions for earthquake resistance of structures*, 5 Parts published as Pre-standards by CEN Technical Committee CEN/TC 250.
- EN 1999 (1998), *Eurocode 9 - Design of aluminium structures*, 2 Parts published as Pre-standards by CEN Technical Committee CEN/TC 250.
- Ewalts, H.L., Wanhil, R.J.H. (1984), *Fracture mechanics*, Delftse Uitgevers Maatschappij, The Netherlands.
- Eureka EU716 (1995), *Quality assurance in adhesive technology*, Abington Publishing, United

- Kingdom.
- Ferreira, A.J.M. (1999), Calculation results available by private communications with University of Porto, IDMEC, Portugal.
- Freudenthal, A.M. (1945), *The safety of structures*, Transactions, ASCE, Paper 2296, pp. 125-159.
- Frostig, Y., Baruch, M., Vilnay, O., Sheinman, I. (1992A), *High-Order Theory for Sandwich-Beam Behaviour with Transversely Flexible Core*, Journal of Engineering Mechanics, Vol. 118, No. 5, pp. 1026-1043.
- Frostig, Y. (1992B), *Behaviour of Delaminated Sandwich Beams with Transversely Flexible Core High-Order Theory*, Composite structures, 20, pp. 1-16.
- Frostig, Y. (1993A), *High-Order Behaviour of Sandwich Beams with Flexible Core and Transverse Diaphragms*, Journal of Engineering Mechanics, Vol. 119, No. 5, pp. 955-972.
- Frostig Y. (1993B), *On Stress Concentration in the Bending of Sandwich Beams with Transversely Flexible Core*, Composite Structures 24, pp. 161-169.
- Frostig, Y., Baruch, M. (1996), *Localized Load Effects in High-Order Bending of Sandwich Panels with Transversely Flexible Core*, J. ASCE, EM Div, 122 (11), pp. 1069-1076.
- Frostig, Y., Thomsen, O.T., Mortensen, F. (1999), *Analysis of adhesive-bonded joints, square-end, and spew-fillet - Higher-order theory approach*, Journal of Engineering Mechanics, November 1999, pp. 1298-1307.
- Gali, S., Dolev, G., Ishai, O. (1981), *An effective stress/strain concept in the mechanical characterisation of structural adhesive bonding*, International Journal of Adhesion & Adhesives, January 1981, pp. 135-140.
- Goland, M., Reissner, E. (1944), *The stress in cemented joints*, Journal of Applied Mechanics, pp. A17-A27.
- Gualtherum, D., Rivium, H. (1548), *Vitruvius Teutsch. Nämlichen des ... Marci Vitruvii Pollionis zehen Bücher von der Architectur und künstlichem Bawen. Ein Schlüssel und Einleitung aller mathematischen und mechanischen Künst u.s.w. verteutsch und in Truck verordnet durch D. Gualtherum H. Rivium, Nürnberg.*
- Habenicht, G. (1990), *Kleben - Grundlagen, Technologie, Anwendungen*, second print, Springer-Verlag, Germany.
- Hart-Smith, L.J. (1973), *Adhesive-bonded single-lap joints*, NASA CR 112236.
- Hasofer, A.M., Lind, N.C. (1974), *Exact and invariant second moment code format*, Journal of the Engineering Mechanics Division, SCE, Vol. 100, No. EM1.
- Hertzberg, R.W. (1976), *Deformation and fracture mechanics of engineering materials*, John Wiley & Sons, United States of America.
- Hertzberg, R.W., Manson, J.A. (1980), *Fatigue of engineering plastics*, Academic Press, United States of America.
- Hussey, B., Wilson, J. (1996), *Structural Adhesives: Directory and Databook*, Chapman & Hall, United Kingdom.
- Ingen, J.W. van, Vlot, A. (1993), *Stress Analysis of Adhesively Bonded Single Lap Joints - Survey and Evaluation of Analyses*, Report LR-740, Delft University of Technology.
- ISO/DIS 2394 (1996), *General principles on reliability for structures*, draft version, International Organization of Standardization.
- Jeandrau, J.P. (1987), *Analysis and design of adhesive-bonded structural joints: new tools for engineers*, Mechanical Behaviour of Adhesive Joints, Pluralis, pp. 493-507.
- Kaasschieter, C.C.J., Sluis, H.H. van der (1991), *Lijmen van metalen*, VM 87, Vereniging FME, The Netherlands.

References

- Kalnins, A. (1964), *Analysis of Shells of Revolution Subjected to Symmetrical and Nonsymmetrical Loads*, Transactions of the ASME, Journal of Applied Mechanics 31, pp. 467-476.
- Kinloch, A.J., Editor (1983), *Durability of structural adhesives*, Applied Science Research, United Kingdom.
- Kinloch, A.J. (1990), *Adhesion and adhesives - Science and Technology*, Chapman and Hall, United Kingdom.
- Lankreijer, R.M., Logtenberg, E.H.P., Editors, (1991), *Lijmen algemeen - Algemene inleiding in de kenmerken van de lijimtechniek en in de kenmerken van lijmsystemen*, VM 86, Vereniging FME, The Netherlands.
- Lawless, J.F. (1982), *Statistical models and methods for lifetime data*, John Wiley & Sons, United States of America.
- Martin, J.W. (1982), *Time transformation functions commonly used in life testing analysis - Durability of building materials 1*, Elsevier Scientific Publishing Company, The Netherlands, pp. 175-194.
- Martin, J.W., Saunders, S.C., Floyd, F.L., Wineburg, J.P. (1994), *Methodologies for predicting the service lives of coating systems*, NIST Building Science Series 172, National Institute of Standards and Technology, USA.
- Masters, L.W., Editor (1985), *Problems in service life prediction of building and construction materials*, NATO ASI Series, Series E: Applied Science - No. 95, Martinus Nijhoff Publishers, The Netherlands.
- Masters, L.W., Brandt, E. (1987), *Prediction of service life of building materials and components*, CIB W80/RILEM 71-PSL.Final Report.
- Mays, G.C., Hutchinson, A.R. (1992), *Adhesives in civil engineering*, Cambridge University Press, United Kingdom.
- McCarthy, J.C. (1996), *Task 1: Detailed study of joint failure - MTS Adhesive Project 2: Failure modes and criteria - Report no. 6: Failure criteria for adhesive joints - Summary report*, AEAT-0126, AEA Technology, United Kingdom.
- Mood, A.M., Graybill, F.A., Boes, D.C. (1974), *Introduction to the theory of statistics - Third edition*, McGraw-Hill, Singapore.
- Mortensen (1998), *Development of tools for engineering analysis and design of high-performance FRP-composite structural elements*, Ph.D. Thesis, Institute of Mechanical Engineering Aalborg University, Special Report No. 37.
- Navier (1833), *Résumés des leçons données à l'École des Ponts et Chaussées sur l'application de la mécanique à l'établissement des constructions et des machines. 2e Edition. Part. I-III*, Paris.
- Nelson, W. (1990), *Accelerated testing - Statistical model, test plans, and data analysis*, John Wiley & Sons, USA.
- Noor, A.K., Burton, W.S., Bert, C.W. (1996), *Computational Models for Sandwich Panels and Shells*, Appl. Mech. Rev. 49 (3), pp. 155-199.
- Oplinger, D.W. (1994), *Effects of adherend deflections in single lap joints*, Int. J. Solids Structures, Vol. 31, No. 18, pp.2565-2587.
- Pugsley, A.G. (1951), *Concepts of safety in structural engineering*, Journal of the Institution of Civil Engineers, Volume 36, No. 5.
- Raghava, R., Caddell, R.M. (1973), *The macroscopic yield behaviour of polymers*, Journal of Material Science, 8, pp. 225-232.
- Raiffa, H., Schlaifer, R. (1961), *Applied statistical decision theory*, M.I.T. Press, United States of America.

- Regt, P.A. de (1998), Test results available by private communications with the Adhesion Institute, Delft University of Technology, The Netherlands.
- Reismann, H. (1988), *Elastic plates - Theory and applications*, John Wiley & Sons, United States of America.
- Renton, W.J., Vinson, J.R. (1977), *Analysis of adhesively bonded joints between panels of composite materials*, Journal of Applied Mechanics, March, pp. 101-106.
- Schindel-Bidinelli, E.H., Guthertz, W. (1988), *Konstruktives Kleben*, VCH-Verlagsgesellschaft mbH, Germany.
- Schliekelmann, R.J (1970), *Gelijmde metalen constructies*, Agon Elsevier, The Netherlands.
- Schmitz, B.H. (1989), *Auswirkungen der Feuchtigkeit auf das Alterungs- und Langzeitverhalten von Metallklebverbindungen*, D 82 Dissertation RWTH Aachen, DVS-Verlag GmbH, Germany.
- Shields, J. (1985), *Adhesives handbook - Third edition*, Butterworths, United Kingdom.
- Skeist, I., Editor (1990), *Handbook of adhesives - Third edition*, Van Nostrand Reinhold, United States of America.
- Straalen, I.J.J. van, Wardenier, J., Voegesang, L.B., Soetens, F. (1997A), *Structural adhesive bonded joints in building engineering - Principles and requirements of design*, 5th Conference on Advanced Materials and Processes and Applications, Euromat 97, Maastricht, 21-23 April 1997, The Netherlands.
- Straalen, I.J.J. van, Wardenier, J., Voegesang, L.B., Soetens, F. (1997B), *Durable design of structural adhesive bonded joints in engineering*, Mechanical Behaviour of Adhesive Joints - Analysis, Testing and Design, Euromech Colloquium 358, Nevers, 4-6 September 1997, France.
- Straalen, I.J.J. van (1997C), *Analysis of durability aspects of adhesive bonded joints*, TNO-Report 97-CON-R0904, TNO Building and Construction Research, The Netherlands.
- Straalen, I.J.J. van (1997D), *Calibration of design rules from tests on basis of probabilistic techniques - First step to reformulate Annex Z of Eurocode 3 for normal distributions - final report*, TNO-report 97-CON-R0905/2, TNO Building and Construction Research, The Netherlands.
- Straalen, I.J.J. van (1997E), *Adhesive bonded joints in thin gauge steel sheeting: Pilot test series on single lap joints*, TNO-Reports 97-CON-R1516/1 and 97-CON-R1517/1, TNO Building and Construction Research, The Netherlands.
- Straalen, I.J.J. van, Wardenier, J., Voegesang, L.B., Soetens, F. (1998A), *Structural adhesive bonded joints in engineering - drafting design rules*, International Journal of Adhesion & Adhesives, Vol. 18, pp. 41-49.
- Straalen, I.J.J. van, Wardenier, J., Voegesang, L.B., Soetens, F. (1998B), *Structural adhesively bonded joints in engineering - Structural design*, Structural Adhesives in Engineering V, 5th International Conference, Bristol, 1-3 April 1998, United Kingdom.
- Straalen, I.J.J. van, Wardenier, J., Voegesang, L.B., Soetens, F. (1998C), *Structural adhesive bonded joints in engineering - Process of drafting design rules for aluminium applications*, 7th International Conference Joints in Aluminium, INALCO '98, Cambridge, 15-17 April 1998, United Kingdom.
- Straalen, I.J.J. van, Wardenier, J., Voegesang, L.B., Soetens, F. (1998D), *Drafting design rules for adhesive joints in thin-gauge steel sheeting*, 12th International Symposium Swiss Bonding 98, Rapperswil, 12-14 May 1998, Switzerland.
- Straalen, I.J.J. van (1998E), *Comprehensive overview of theories for sandwich panels*, Workshop Modelling of Sandwich Structures and Adhesive Joints, DOGMA Thematic Network Project BET2-530 Design Optimisation and Guidelines for Multimaterial Applications, Porto, 17-18 September 1998, Portugal.

References

- Straalen, I.J. van (1998F), *Statistical data analysis of tests on adhesive bonded joints*, TNO-report 98-CON-R1453/2, TNO Building and Construction Research, The Netherlands.
- Straalen, I.J. van, Soetens, F., Kaasschieter, C.C.J. (1999A), *Gelijmde verbindingen in dunne staalplaat voor de bouw*, IOP-Metalen Kennisoverdracht nr. 6.7 & Vereniging FME-CWM Tech-Info-blad TI.99.09, The Netherlands.
- Straalen, I.J. van (1999B), *Multi-segment method to solve boundary value problems*, TNO-Report 98-CON-R1556/2, TNO Building and Construction Research, The Netherlands.
- Straalen, I.J. van (1999C), *Analysis of adhesive bonded lap joint theories*, TNO-Report 1999-CON-BIS-R5029, TNO Building and Construction Research, The Netherlands.
- Straalen, I.J. van (1999D), *Theory to analyse a sandwich panel with an adhesively bonded section*, TNO-Report 1999-CON-BIS-R5044, TNO Building and Construction Research, The Netherlands.
- Straalen, I.J. van (1999E), *Test on overlap joints - Henkel UK 8202*, TNO-Report 1999-CON-BIS-R5048, TNO Building and Construction Research, The Netherlands.
- Straalen, I.J. van (1999F), *Test on overlap joints - 3M DP 490*, TNO-Report 1999-CON-BIS-R5049, TNO Building and Construction Research, The Netherlands.
- Straalen, I.J. van (1999G), *Test on aged overlap joints - Scholten Lijmen UD 400*, TNO-Report 1999-CON-BIS-R5051, TNO Building and Construction Research, The Netherlands.
- Straalen, I.J. van (1999H), *Test on adhesive bulk specimens - Henkel UK 8202*, TNO-Report 1999-CON-BIS-R5052, TNO Building and Construction Research, The Netherlands.
- Straalen, I.J. van (1999I), *Test on adhesive bulk specimens - 3M DP 490*, TNO-Report 1999-CON-BIS-R5053, TNO Building and Construction Research, The Netherlands.
- Straalen, I.J. van (2000A), *Development of design rules for adhesive bonded joints*, 14th International Symposium Swiss Bonding 2000, Rapperswil, 16-18 May 2000, Switzerland.
- Straalen, I.J. van (2000B), *Experimental validation of the higher-order theory approach for sandwich panels with flexible core materials*, 5th International Conference on Sandwich Constructions, Zurich, 5-7 September 2000, Switzerland.
- Straalen, I.J. van (2000C), *Test on aged overlap joints - Casco Products 1897*, TNO-Report 2000-CON-BIS-R4001, TNO Building and Construction Research, The Netherlands.
- Straalen, I.J. van (2000D), *Test on a sandwich panel with an adhesive bonded joint*, TNO-Report 2000-CON-BIS-R4002, TNO Building and Construction Research, The Netherlands.
- Straalen, I.J. van (2000E), *Test on sandwich beams*, TNO-Report 2000-CON-BIS-R4003, TNO Building and Construction Research, The Netherlands.
- Straalen, I.J. van (2000F), *Test on core specimens - IsoBouw EPS 30*, TNO-Report 2000-CON-BIS-R4007, TNO Building and Construction Research, The Netherlands.
- Straalen, I.J. van (2000G), *Test on core specimens - Rockwool Conrock 700*, TNO-Report 2000-CON-BIS-R4008, TNO Building and Construction Research, The Netherlands.
- Straalen, I.J. van (2000H), *Additional tests on sandwich beams*, TNO-Report 2000-CON-BIS-R4014, TNO Building and Construction Research, The Netherlands.
- Straalen, I.J. van, Vrouwenfelder, A.C.W.M. (2000I), *Estimation of design and characteristic values from a limited number of observations for a Weibull distribution*, TNO-report 2000-CON-BIS-R4021, TNO Building and Construction Research, The Netherlands.
- The Institute of Structural Engineers (1999), *Guide to: The structural use of adhesives*, SETO, United Kingdom.
- Thomsen, O.T. (1992A), *Analysis of local bending effects in sandwich panels subjected to concentrated loads*, Sandwich construction 2 (Eds.: K.-A. Olssen and D. Weissman-Berman),

- Second International Conference on Sandwich Construction, University of Florida, Gainesville, U.S.A., 9-12 March.
- Thomsen, O.T. (1992B), *Elasto-static and elasto-plastic stress analysis of adhesive bonded tubular joints*, *Composite Structures*, 21, pp. 249-259.
- Thomsen, O.T., Frostig, Y. (1997), *Localized Bending Effects in Sandwich Panels: Photoelastic Investigation versus High-Order Sandwich Theory Results*, *Composite Structures* 37, pp. 97-108.
- Tiainen, T., Hiekkanen, I. (1995), *Life-time prediction of adhesively bonded joints and sandwich structures on the basis of short-term laboratory test*, 4th International Conference on New Century Partnership for Material Systems, Virginia Polytechnic Institute & State University, United States of America.
- Tippett, L.H.C. (1925), *On the extreme individuals and the range of samples taken from a normal population*, *Biometrika* 17, pp. 364-387.
- Trividi, K.S. (1982), *Probability and statistics with reliability, queuing, and computer science applications*, Prentice-Hall, United States of America.
- Tsai, M.Y., Morton, J. (1994), *An evaluation of analytical and numerical solutions to the single-lap joint*, *Int. J. Solids Structures*, Vol. 31, No. 18, pp. 2537-2563.
- Vautrin, A. Editor (1998), *Mechanics of sandwich structures*, Proceedings of the EUROMECH 360 Colloquium, Saint-Étienne, France, 13-15 May 1997, Kluwer Academic Publisher.
- Vitruvius, Morgan, M.H., Warren, H.L. (1960), *Vitruvius; the ten books on architecture*, Dover Publications, United States of America.
- Volkersen, O. (1938), *Die Nietkraft verteilung in zugbeanspruchten Nietverbindungen mit konstanten laschen querschnitten*, *Luftfahrtforschung band* 15, pp. 41-47.
- Vrouwenvelder, A.C.W.M., Siemes, A.J.M. (1987), *Probabilistic calibration procedure for the derivation of partial safety factors for the Netherlands building codes*, *HERON*, Volume 32, No. 4, pp.9-30.
- Vrouwenvelder, A.C.W.M., Editor (1996), *Basis of design and actions on structures - Background and application of Eurocode 1: Plenary Session 4 Integration with other Eurocodes*, IABSE Colloquium Delft 1996, IABSE Report Volume 74.
- Weibull, W. (1949), *A statistical representation of fatigue failures in solids*, *Transaction of the Royal Institute of Technology Stockholm, Sweden*, No. 27.
- Young, R.J., Lovell, P.A. (1991), *Introduction to polymers*, Second Edition, Chapman & Hall, United Kingdom.
- Yuceoglu, U., Updike, D. (1980), *Stress analysis of bonded plates and joints*, *ASCE Journal of the Engineering Mechanics Division*, Vol. 106, pp.37-56.
- Yuceoglu, U., Updike, D. (1981), *Bending and shear deformation effects in lap joints*, *ASCE Journal of the Engineering Mechanics Division*, Vol. 107.
- Zenkert, D. (1995), *An Introduction to Sandwich Construction*, EMAS Publishing.



Unified Spring Model Approach

In this appendix all relevant equations of the unified spring model approach are presented. Information is provided about:

- material properties and stiffness parameters used in the equations;
- differential equations for the three-layer overlap region, the five-layer overlap region and the outer adherends, including equations to calculate the stress and strain state within the adhesive bondline;
- boundary and continuity conditions;
- extension of the governing differential equations for geometrical non-linear effects.

A.1 Material properties and stiffness parameters

The used material properties for the adherends are:

- Young's modulus E_i of adherend i ;
- shear modulus G_i of adherend i ;
- Poisson's ratio ν_i of adherend i .

The used material properties for the adhesive are:

- Young's modulus $E_{a,j}$ of adhesive j ;
- shear modulus $G_{a,j}$ of adhesive j ;
- Poisson's ratio $\nu_{a,j}$ of adhesive j ;

The following stiffness parameters are used in the governing differential equations:

- Axial rigidity per unit width of adherend i with plate thickness t_i :

$$A_i = \frac{E_i t_i}{1 - \nu_i} \quad (\text{A1})$$

- Shear coefficient per unit width (Reissman, 1988) of adherend i with plate thickness t_i :

$$B_i = \kappa_i^2 G_i t_i$$

with:

$$\kappa_i = 0.874 + 0.162 \nu_i, \text{ valid for } 0 < \nu_i < 0.5 \quad (\text{A2})$$

- Flexural rigidity per unit width of adherend i with plate thickness t_i :

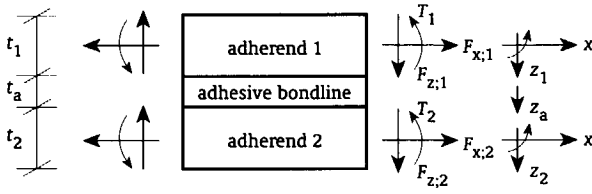
$$D_i = \frac{E_i t_i^3}{12 (1 - \nu_i^2)} \quad (\text{A3})$$

A.2 Governing differential equations, stress and strain state in bondline

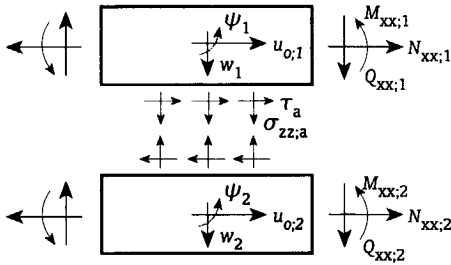
A.2.1 Three-layer overlap region

The following geometry, applied loads and coordinate system are considered:

Unified Spring Model Approach



The following section forces, stresses and deformations are considered:



The derived set of first-order differential equations is:

$$\frac{d}{dx} u_{o;1} = \frac{1}{A_1} N_{xx;1} \quad (A4)$$

$$\frac{d}{dx} w_1 = \frac{1}{B_1} Q_{xx;1} - \psi_1 \quad (A5)$$

$$\frac{d}{dx} \psi_1 = \frac{1}{D_1} M_{xx;1} \quad (A6)$$

$$\frac{d}{dx} N_{xx;1} = \frac{G_a}{t_a} u_{o;1} + \frac{G_a t_1}{2 t_a} \psi_1 - \frac{G_a}{t_a} u_{o;2} + \frac{G_a t_2}{2 t_a} \psi_2 \quad (A7)$$

$$\frac{d}{dx} M_{xx;1} = Q_{xx;1} + \frac{G_a(t_1 + t_a)}{2 t_a} u_{o;1} + \frac{G_a t_1(t_1 + t_a)}{4 t_a} \psi_1 - \frac{G_a(t_1 + t_a)}{2 t_a} u_{o;2} + \frac{G_a t_2(t_1 + t_a)}{4 t_a} \psi_2 \quad (A8)$$

$$\frac{d}{dx} Q_{xx;1} = \frac{E_a}{t_a} w_1 - \frac{E_a}{t_a} w_2 \quad (A9)$$

$$\frac{d}{dx} u_{o;2} = \frac{1}{A_2} N_{xx;2} \quad (A10)$$

$$\frac{d}{dx} w_2 = \frac{1}{B_2} Q_{xx;2} - \psi_2 \quad (A11)$$

$$\frac{d}{dx} \psi_2 = \frac{1}{D_2} M_{xx;2} \quad (A12)$$

$$\frac{d}{dx} N_{xx;2} = -\frac{G_a}{t_a} u_{o;1} - \frac{G_a t_2}{2 t_a} \psi_1 + \frac{G_a}{t_a} u_{o;2} - \frac{G_a t_2}{2 t_a} \psi_2 \quad (A13)$$

$$\begin{aligned} \frac{d}{dx} M_{xx;2} = & Q_{xx;2} + \frac{G_a(t_2 + t_a)}{2 t_a} u_{o;1} + \frac{G_a t_1(t_2 + t_a)}{4 t_a} \psi_1 - \\ & \frac{G_a(t_2 + t_a)}{2 t_a} u_{o;2} + \frac{G_a t_2(t_2 + t_a)}{4 t_a} \psi_2 \end{aligned} \quad (A14)$$

$$\frac{d}{dx} Q_{xx;2} = -\frac{E_a}{t_a} w_1 + \frac{E_a}{t_a} w_2 \quad (A15)$$

The shear stress state in the adhesive layer is equal to:

$$\tau_a = \frac{G_a}{t_a} \left[u_{o;2} - u_{o;1} - \frac{t_2}{2} \psi_2 - \frac{t_1}{2} \psi_1 \right] \quad (A16)$$

The shear strain state in the adhesive layer is equal to:

$$\gamma_a = \frac{1}{t_a} \left[u_{o;2} - u_{o;1} - \frac{t_2}{2} \psi_2 - \frac{t_1}{2} \psi_1 \right] \quad (A17)$$

The transverse normal stress state in the adhesive layer is equal to:

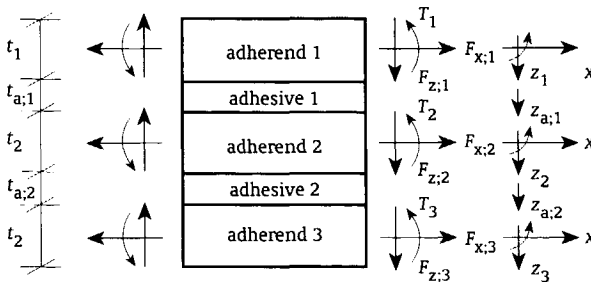
$$\sigma_{zz;a} = \frac{E_a}{t_a} (w_2 - w_1) \quad (A18)$$

The transverse normal strain state in the adhesive layer is equal to:

$$\epsilon_{zz;a} = \frac{1}{t_a} (w_2 - w_1) \quad (A19)$$

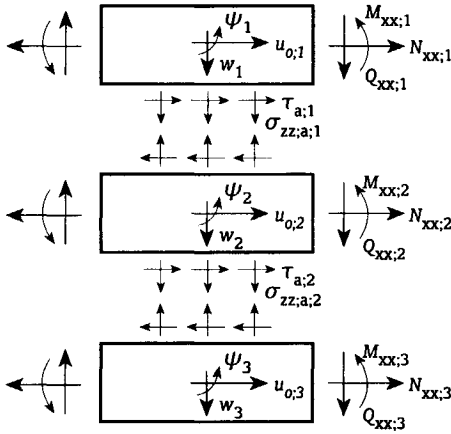
A.2.2 Five-layer overlap region

The following geometry, applied loads and coordinate system are considered:



Unified Spring Model Approach

The following section forces, stresses and deformations are considered:



The derived set of first-order differential equations is:

$$\frac{d}{dx} u_{o;1} = \frac{1}{A_1} N_{xx;1} \quad (\text{A20})$$

$$\frac{d}{dx} w_1 = \frac{1}{B_1} Q_{xx;1} - \psi_1 \quad (\text{A21})$$

$$\frac{d}{dx} \psi_1 = \frac{1}{D_1} M_{xx;1} \quad (\text{A22})$$

$$\frac{d}{dx} N_{xx;1} = \frac{G_{a;1}}{t_{a;1}} u_{o;1} + \frac{G_{a;1} t_1}{2 t_{a;1}} \psi_1 - \frac{G_{a;1}}{t_{a;1}} u_{o;2} + \frac{G_{a;1} t_2}{2 t_{a;1}} \psi_2 \quad (\text{A23})$$

$$\begin{aligned} \frac{d}{dx} M_{xx;1} = & Q_{xx;1} + \frac{G_{a;1}(t_1 + t_{a;1})}{2 t_{a;1}} u_{o;1} + \frac{G_{a;1} t_1 (t_1 + t_{a;1})}{4 t_{a;1}} \psi_1 - \\ & \frac{G_{a;1}(t_1 + t_{a;1})}{2 t_{a;1}} u_{o;2} + \frac{G_{a;1} t_2 (t_1 + t_{a;1})}{4 t_{a;1}} \psi_2 \end{aligned} \quad (\text{A24})$$

$$\frac{d}{dx} Q_{xx;1} = \frac{E_{a;1}}{t_{a;1}} w_1 - \frac{E_{a;1}}{t_{a;1}} w_2 \quad (\text{A25})$$

$$\frac{d}{dx} u_{o;2} = \frac{1}{A_2} N_{xx;2} \quad (\text{A26})$$

$$\frac{d}{dx} w_2 = \frac{1}{B_2} Q_{xx;2} - \psi_2 \quad (\text{A27})$$

$$\frac{d}{dx} \psi_2 = \frac{1}{D_2} M_{xx;2} \quad (\text{A28})$$

$$\begin{aligned} \frac{d}{dx} N_{xx;2} = & -\frac{G_{a;1}}{t_{a;1}} u_{0;1} - \frac{G_{a;1} t_2}{2 t_{a;2}} \psi_1 + \left[\frac{G_{a;1}}{t_{a;1}} + \frac{G_{a;2}}{t_{a;2}} \right] u_{0;2} + \\ & \left[-\frac{G_{a;1} t_2}{2 t_{a;1}} + \frac{G_{a;2} t_2}{2 t_{a;2}} \right] \psi_2 - \frac{G_{a;2}}{t_{a;2}} u_{0;3} + \frac{G_{a;2} t_3}{2 t_{a;2}} \psi_3 \end{aligned} \quad (\text{A29})$$

$$\begin{aligned} \frac{d}{dx} M_{xx;2} = & Q_{xx;2} + \frac{G_{a;1}(t_2 + t_{a;1})}{2 t_{a;1}} u_{0;1} + \frac{G_{a;1} t_1 (t_2 + t_{a;1})}{4 t_{a;1}} \psi_1 + \\ & \left[-\frac{G_{a;1} (t_2 + t_{a;1})}{2 t_{a;1}} + \frac{G_{a;2} (t_2 + t_{a;2})}{2 t_{a;2}} \right] u_{0;2} + \\ & \left[\frac{G_{a;1} t_2 (t_2 + t_{a;1})}{4 t_{a;1}} + \frac{G_{a;2} t_2 (t_2 + t_{a;2})}{4 t_{a;2}} \right] \psi_2 - \\ & \frac{G_{a;2} (t_2 + t_{a;2})}{2 t_{a;2}} u_{0;3} + \frac{G_{a;2} t_3 (t_2 + t_{a;2})}{4 t_{a;2}} \psi_3 \end{aligned} \quad (\text{A30})$$

$$\frac{d}{dx} Q_{xx;2} = -\frac{E_{a;1}}{t_{a;1}} w_1 + \left[\frac{E_{a;1}}{t_{a;1}} + \frac{E_{a;2}}{t_{a;2}} \right] w_2 - \frac{E_{a;2}}{t_{a;2}} w_3 \quad (\text{A31})$$

$$\frac{d}{dx} u_{0;3} = \frac{1}{A_3} N_{xx;3} \quad (\text{A32})$$

$$\frac{d}{dx} w_3 = \frac{1}{B_3} Q_{xx;3} - \psi_3 \quad (\text{A33})$$

$$\frac{d}{dx} \psi_3 = \frac{1}{D_3} M_{xx;3} \quad (\text{A34})$$

$$\frac{d}{dx} N_{xx;3} = -\frac{G_{a;2}}{t_{a;2}} u_{0;2} - \frac{G_{a;2} t_2}{2 t_{a;2}} \psi_2 + \frac{G_{a;2}}{t_{a;2}} u_{0;3} - \frac{G_{a;2} t_3}{2 t_{a;2}} \psi_3 \quad (\text{A35})$$

$$\begin{aligned} \frac{d}{dx} M_{xx;3} = & Q_{xx;3} + \frac{G_{a;2} (t_3 + t_{a;2})}{2 t_{a;2}} u_{0;2} + \frac{G_{a;2} t_2 (t_3 + t_{a;2})}{4 t_{a;2}} \psi_2 - \\ & \frac{G_{a;2} (t_3 + t_{a;2})}{2 t_{a;2}} u_{0;3} + \frac{G_{a;2} t_3 (t_3 + t_{a;2})}{4 t_{a;2}} \psi_3 \end{aligned} \quad (\text{A36})$$

$$\frac{d}{dx} Q_{xx;3} = -\frac{E_{a;2}}{t_{a;2}} w_2 + \frac{E_{a;2}}{t_{a;2}} w_3 \quad (\text{A37})$$

Unified Spring Model Approach

The shear stress states in adhesive layers $j = 1$ and 2 are equal to:

$$\tau_{a;1} = \frac{G_{a;1}}{t_{a;1}} \left[u_{o;2} - u_{o;1} - \frac{t_2}{2} \psi_2 - \frac{t_1}{2} \psi_1 \right] \quad (\text{A38})$$

$$\tau_{a;2} = \frac{G_{a;2}}{t_{a;2}} \left[u_{o;3} - u_{o;2} - \frac{t_3}{2} \psi_3 - \frac{t_2}{2} \psi_2 \right] \quad (\text{A39})$$

The shear strain states in adhesive layers $j = 1$ and 2 are equal to:

$$\gamma_{a;1} = \frac{1}{t_{a;1}} \left[u_{o;2} - u_{o;1} - \frac{t_2}{2} \psi_2 - \frac{t_1}{2} \psi_1 \right] \quad (\text{A40})$$

$$\gamma_{a;2} = \frac{1}{t_{a;2}} \left[u_{o;3} - u_{o;2} - \frac{t_3}{2} \psi_3 - \frac{t_2}{2} \psi_2 \right] \quad (\text{A41})$$

The transverse normal stress states in adhesive layers $j = 1$ and 2 are equal to:

$$\sigma_{zz;a;1} = \frac{E_{a;1}}{t_{a;1}} (w_2 - w_1) \quad (\text{A42})$$

$$\sigma_{zz;a;2} = \frac{E_{a;2}}{t_{a;2}} (w_3 - w_2) \quad (\text{A43})$$

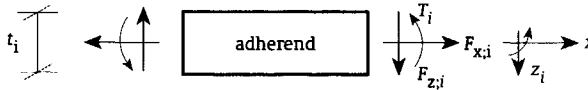
The transverse normal strain states in adhesive layers $j = 1$ and 2 are equal to:

$$\epsilon_{zz;a;1} = \frac{1}{t_{a;1}} (w_2 - w_1) \quad (\text{A44})$$

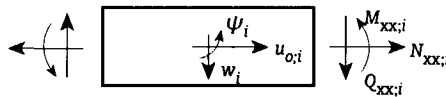
$$\epsilon_{zz;a;2} = \frac{1}{t_{a;2}} (w_3 - w_2) \quad (\text{A45})$$

A.2.3 Outer adherends

The following geometry, applied loads and coordinate system are considered:



The following section forces, stresses and deformations are considered:



The derived set of first-order differential equations is:

$$\frac{d}{dx} u_{o,i} = \frac{1}{A_i} N_{xx,i} \quad (\text{A46})$$

$$\frac{d}{dx} w_i = \frac{1}{B_i} Q_{xx,i} - \psi_i \quad (\text{A47})$$

$$\frac{d}{dx} \psi_i = \frac{1}{D_i} M_{xx,i} \quad (\text{A48})$$

$$\frac{d}{dx} N_{xx,i} = 0 \quad (\text{A49})$$

$$\frac{d}{dx} M_{xx,i} = Q_{xx,i} \quad (\text{A50})$$

$$\frac{d}{dx} Q_{xx,i} = 0 \quad (\text{A51})$$

A.3 Boundary and continuity conditions

Three boundary conditions at one end of a considered adherend i , have to be expressed as follows:

- normal force per unit width $N_{xx,i} = F_{x,i}$ or longitudinal displacement $u_{o,i} = 0$;
- bending moment per unit width $M_{xx,i} = T_i$ or rotation;
- shear force per unit width $Q_{xx,i} = F_{z,i}$ or transverse displacement $w_i = 0$.

Six continuity conditions at an intermediate point between two adherends indicated by "min" and "plus", have to be expressed as follows:

- longitudinal displacement $u_{o,i}^{\text{min}} - u_{o,i}^{\text{plus}} = 0$;
- transverse displacement $w_i^{\text{min}} - w_i^{\text{plus}} = 0$;
- rotation $\psi_i^{\text{min}} - \psi_i^{\text{plus}} = 0$;
- axial force per unit width $N_{xx,i}^{\text{min}} - N_{xx,i}^{\text{plus}} = 0$;
- bending moment per unit width $M_{xx,i}^{\text{min}} - M_{xx,i}^{\text{plus}} = 0$;
- shear force unit per width $Q_{xx,i}^{\text{min}} - Q_{xx,i}^{\text{plus}} = 0$.

A.4 Extension of governing differential equations for geometrical non-linear effects

A.4.1 Three-layer overlap region

Of the set of first-order differential equations presented in A.2.1, equations A4, A8, A10 and A14 are modified as follows:

$$\frac{d}{dx} u_{o,1} = \frac{1}{A_1} N_{xx,1} - \frac{1}{2} \left[\frac{d}{dx} w_1 \right]^2 \quad (\text{A52})$$

Unified Spring Model Approach

$$\begin{aligned} \frac{d}{dx} M_{xx;1} = Q_{xx;1} + \frac{G_a (t_1 + t_a)}{2 t_a} u_{o;1} + \frac{G_a t_1 (t_1 + t_a)}{4 t_a} \psi_1 - \\ \frac{G_a (t_1 + t_a)}{2 t_a} u_{o;2} + \frac{G_a t_2 (t_1 + t_a)}{4 t_a} \psi_2 - \left[\frac{d}{dx} w_1 \right] N_{xx;1} \end{aligned} \quad (A53)$$

$$\frac{d}{dx} u_{o;2} = \frac{1}{A_2} N_{xx;2} - \frac{1}{2} \left[\frac{d}{dx} w_2 \right]^2 \quad (A54)$$

$$\begin{aligned} \frac{d}{dx} M_{xx;2} = Q_{xx;2} + \frac{G_a (t_2 + t_a)}{2 t_a} u_{o;1} + \frac{G_a t_1 (t_2 + t_a)}{4 t_a} \psi_1 - \\ \frac{G_a (t_2 + t_a)}{2 t_a} u_{o;2} + \frac{G_a t_2 (t_2 + t_a)}{4 t_a} \psi_2 - \left[\frac{d}{dx} w_2 \right] N_{xx;2} \end{aligned} \quad (A55)$$

The values of $\frac{d}{dx} w_1$ and $\frac{d}{dx} w_2$ can be determined with respectively equations A5 and A11.

A.4.2 Five-layer overlap region

Of the set of first-order differential equations presented in A.2.2, equations A20, A24, A26, A30, A32 and A36 are modified as follows:

$$\frac{d}{dx} u_{o;1} = \frac{1}{A_1} N_{xx;1} - \frac{1}{2} \left[\frac{d}{dx} w_1 \right]^2 \quad (A56)$$

$$\begin{aligned} \frac{d}{dx} M_{xx;1} = Q_{xx;1} + \frac{G_{a;1} (t_1 + t_{a;1})}{2 t_{a;1}} u_{o;1} + \frac{G_{a;1} t_1 (t_1 + t_{a;1})}{4 t_{a;1}} \psi_1 - \\ \frac{G_{a;1} (t_1 + t_{a;1})}{2 t_{a;1}} u_{o;2} + \frac{G_{a;1} t_2 (t_1 + t_{a;1})}{4 t_{a;1}} \psi_2 - \\ \left[\frac{d}{dx} w_1 \right] \cdot N_{xx;1} \end{aligned} \quad (A57)$$

$$\frac{d}{dx} u_{o;2} = \frac{1}{A_2} N_{xx;2} - \frac{1}{2} \left[\frac{d}{dx} w_2 \right]^2 \quad (A58)$$

$$\begin{aligned}
\frac{d}{dx} M_{xx;2} &= Q_{xx;2} + \frac{G_{a;1} (t_2 + t_{a;1})}{2 t_{a;1}} u_{0;1} + \frac{G_{a;1} t_1 (t_2 + t_{a;1})}{4 t_{a;1}} \psi_1 + \\
&\left[-\frac{G_{a;1} (t_2 + t_{a;1})}{2 t_{a;1}} + \frac{G_{a;2} (t_2 + t_{a;2})}{2 t_{a;2}} \right] u_{0;2} + \\
&\left[\frac{G_{a;1} t_2 (t_2 + t_{a;1})}{4 t_{a;1}} + \frac{G_{a;2} t_2 (t_2 + t_{a;2})}{4 t_{a;2}} \right] \psi_2 - \\
&\frac{G_{a;2} (t_2 + t_{a;2})}{2 t_{a;2}} u_{0;3} + \frac{G_{a;2} t_3 (t_2 + t_{a;2})}{4 t_{a;2}} \psi_3 - \\
&\left[\frac{d}{dx} w_2 \right] N_{xx;2}
\end{aligned} \tag{A59}$$

$$\frac{d}{dx} u_{0;3} = \frac{1}{A_3} N_{xx;3} - \frac{1}{2} \left[\frac{d}{dx} w_3 \right]^2 \tag{A60}$$

$$\begin{aligned}
\frac{d}{dx} M_{xx;3} &= Q_{xx;3} + \frac{G_{a;2} (t_3 + t_{a;2})}{2 t_{a;2}} u_{0;2} + \frac{G_{a;2} t_2 (t_3 + t_{a;2})}{4 t_{a;2}} \psi_2 - \\
&\frac{G_{a;2} (t_3 + t_{a;2})}{2 t_{a;2}} u_{0;3} + \frac{G_{a;2} t_3 (t_3 + t_{a;2})}{4 t_{a;2}} \psi_3 - \\
&\left[\frac{d}{dx} w_3 \right] N_{xx;3}
\end{aligned} \tag{A61}$$

The values of $\frac{d}{dx} w_1$, $\frac{d}{dx} w_2$ and $\frac{d}{dx} w_3$ can be determined with respectively equations A21, A27 and A33.

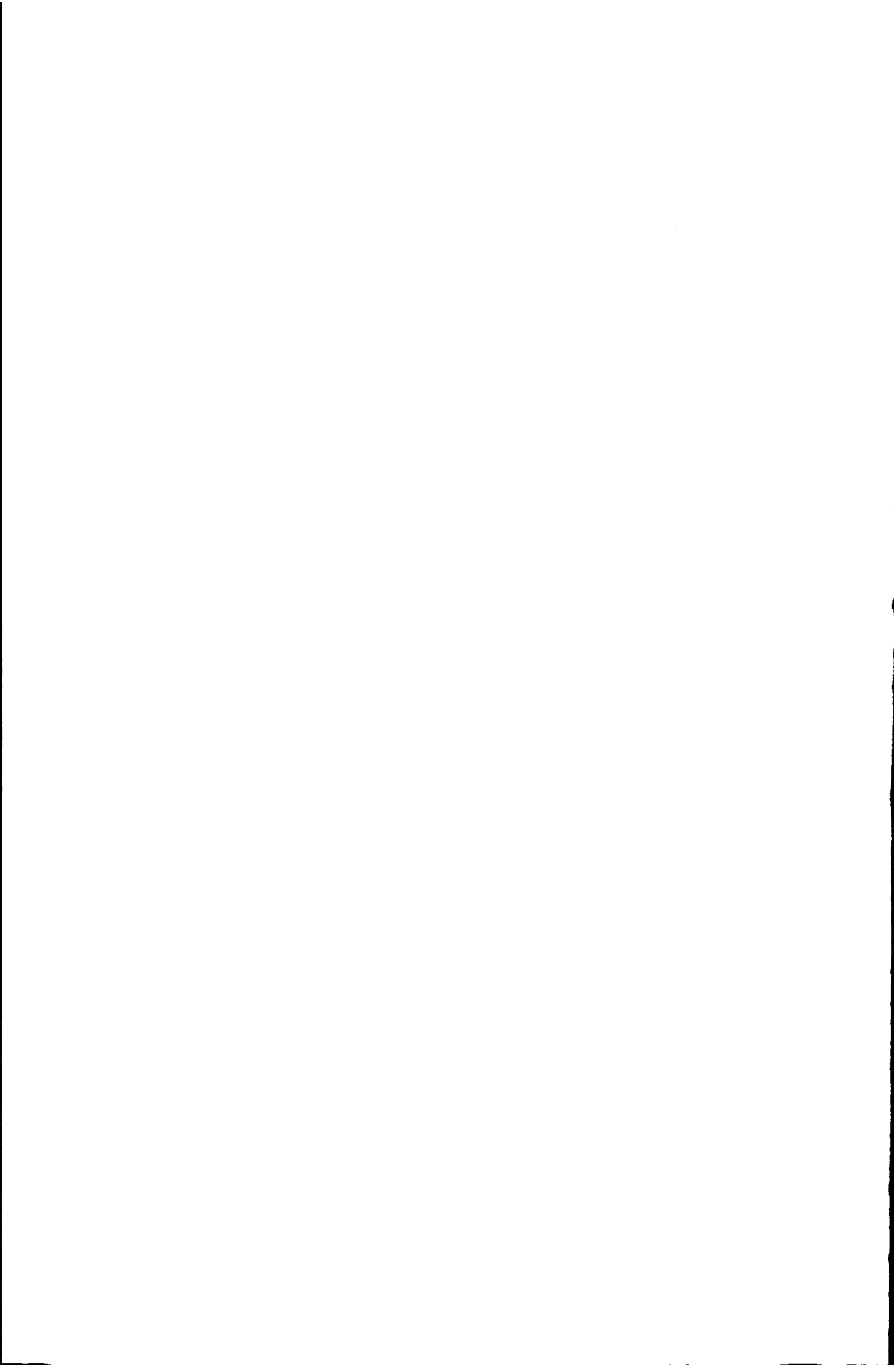
A.4.3 Outer adherends

Of the set of first-order differential equations presented in A.2.3, equations A46 and A50 are modified as follows:

$$\frac{d}{dx} u_{0;i} = \frac{1}{A_i} N_{xx;i} - \frac{1}{2} \left[\frac{d}{dx} w_i \right]^2 \tag{A62}$$

$$\frac{d}{dx} M_{xx;i} = \frac{1}{A_i} Q_{xx;i} - \left[\frac{d}{dx} w_i \right] N_{xx;i} \tag{A63}$$

The values of $\frac{d}{dx} w_i$ can be determined with equation A47.



Higher-Order Theory for Sandwich Beams and Panels Loaded in Bending

In this appendix all relevant equations of the higher-order theory according to the derivations of Frostig are presented. Information is provided about:

- material properties and stiffness parameters used in the equations;
- differential equations for the three-layer sandwich, including equations to calculate the stress and strain state in the sandwich;
- boundary and continuity conditions.

B.1 Material properties and stiffness parameters

The used material properties for the faces are:

- Young's modulus E_i of adherend i ;
- Poisson's ratio ν_i of adherend i .

The used material properties for the core are:

- Young's modulus E_C of the core;
- shear modulus G_C of the core;
- Poisson's ratio ν_C of the core.

The following stiffness parameters are used in the governing differential equations:

- Axial rigidity of face i with plate thickness t_i :

$$\text{for a sandwich beam: } A_i = E_i t_i \quad (\text{B1a})$$

$$\text{for a sandwich panel: } A_i = \frac{E_i t_i}{1 - \nu_i} \quad (\text{B1a})$$

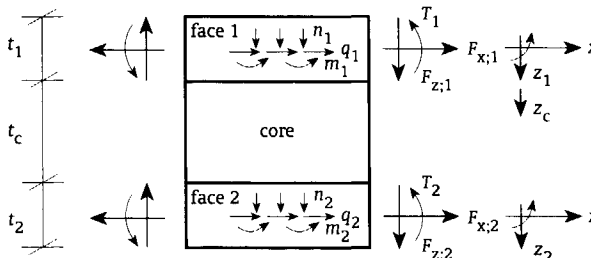
- Flexural rigidity of face i with plate thickness t_i :

$$\text{for a sandwich beam: } D_i = \frac{E_i t_i^3}{12} \quad (\text{B2a})$$

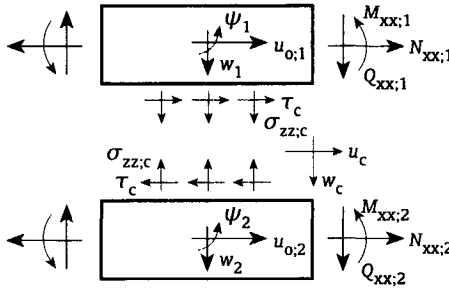
$$\text{for a sandwich panel: } D_i = \frac{E_i t_i^3}{12 (1 - \nu_i^2)} \quad (\text{B2b})$$

B.2 Governing differential equations, stress and strain state in sandwich

The following geometry, applied loads and coordinate system are considered:



The following section forces, stresses and deformations are considered:



The following set of five coupled differential equations is derived:

$$A_1 \frac{d^2}{dx^2} u_{o;1} + \tau_c = -n_1 \tag{B3}$$

$$A_2 \frac{d^2}{dx^2} u_{o;2} - \tau_c = -n_2 \tag{B4}$$

$$D_1 \frac{d^4}{dx^4} w_1 + \frac{E_c}{t_c} w_1 - \frac{E_c}{t_c} w_2 - \frac{t_c + t_1}{2} \frac{d}{dx} \tau_c = q_1 - \frac{d}{dx} m_1 \tag{B5}$$

$$-\frac{E_c}{t_c} w_1 + D_2 \frac{d^4}{dx^4} w_2 + \frac{E_c}{t_c} w_2 - \frac{t_c + t_2}{2} \frac{d}{dx} \tau_c = q_2 - \frac{d}{dx} m_2 \tag{B6}$$

$$u_{o;1} - u_{o;2} - \frac{t_c + t_1}{2} \frac{d}{dx} w_1 - \frac{t_c + t_2}{2} \frac{d}{dx} w_2 - \frac{t_c^3}{12E_c} \frac{d^2}{dx^2} \tau_c + \frac{t_c}{G_c} \tau_c = 0 \tag{B7}$$

These differential functions contain the unknown functions of the displacements of the faces $u_{o;1}(x)$, $u_{o;2}(x)$, $w_1(x)$ and $w_2(x)$, and the shear stress within the core $\tau_c(x)$. The normal force, bending moment and shear force in face i are respectively:

$$N_{xx;i}(x) = A_i \frac{d}{dx} u_{o;i} \tag{B8}$$

$$M_{xx;i}(x) = -D_i \frac{d^2}{dx^2} w_i \tag{B9}$$

$$Q_{xx;i}(x) = -D_i \frac{d^3}{dx^3} w_i \tag{B10}$$

The transverse normal stress in the core is described by:

$$\sigma_{zz;c}(x, z_c) = -\frac{E_c}{t_c} w_1 + \frac{E_c}{t_c} w_2 + \left(-z_c + \frac{t_c}{2}\right) \frac{d}{dx} \tau_c \quad (\text{B11})$$

and the matching normal strain is:

$$\epsilon_{zz;c}(x, z_c) = \frac{1}{E_c} \sigma_{zz;c}(x, z_c) \quad (\text{B12})$$

The shear stress in the core is one of the unknown functions described by the differential equations. The matching shear angle is:

$$\gamma_c(x) = \frac{1}{G_c} \tau_c(x) \quad (\text{B13})$$

The transverse and longitudinal displacements of the core are described by respectively:

$$w_c(x, z_c) = \left(-\frac{z_c}{t_c} + 1\right) w_1 + \frac{z_c}{t_c} w_2 - \frac{1}{2E_c} (z_c^2 - z_c t_c) \frac{d}{dx} \tau_c \quad (\text{B14})$$

$$u_c(x, z_c) = u_{o;1} + \left(\frac{z_c^2}{2t_c} - z_c - \frac{t_1}{2}\right) \frac{d}{dx} w_1 - \frac{z_c^2}{2t_c} \frac{d}{dx} w_2 - \frac{1}{2E_c} \left(\frac{z_c^2 t_c}{2} - \frac{z_c^3}{3}\right) \frac{d^2}{dx^2} \tau_c + \frac{z_c}{G_c} \tau_c \quad (\text{B15})$$

B.3 Boundary and continuity conditions

Three boundary conditions at one end of a considered face i , have to be expressed as follows:

- normal force $N_{xx;i} = F_{x;i}$ or longitudinal displacement $u_{o;i} = 0$;
- bending moment $M_{xx;i} = T_i$ or rotation $\psi_i = -\frac{dw_i}{dx} = 0$;
- shear force $\frac{d}{dx} M_{xx;i} + \frac{t_i}{2} \tau_c - m_i = F_{z;i}$ or transverse displacement $w_i = 0$.

And at any point through the height of the core an additional boundary condition has to be expressed as follows:

- transverse displacement $w_c = 0$ or shear stress $\tau_c = 0$.

Six continuity conditions at an intermediate point between two faces indicated by "min" and "plus", have to be expressed as follows:

- longitudinal displacement $u_{o;i}^{\min} - u_{o;i}^{\text{plus}} = 0$;
- transverse displacement $w_{o;i}^{\min} - w_{o;i}^{\text{plus}} = 0$;
- rotation $\psi_i^{\min} - \psi_i^{\text{plus}} = -\frac{d}{dx} w_i^{\min} + \frac{d}{dx} w_i^{\text{plus}} = 0$;
- axial force $N_{xx;i}^{\min} - N_{xx;i}^{\text{plus}} = F_{x;i}$;

Higher-Order Theory for Sandwich Beams and Panels Loaded in Bending

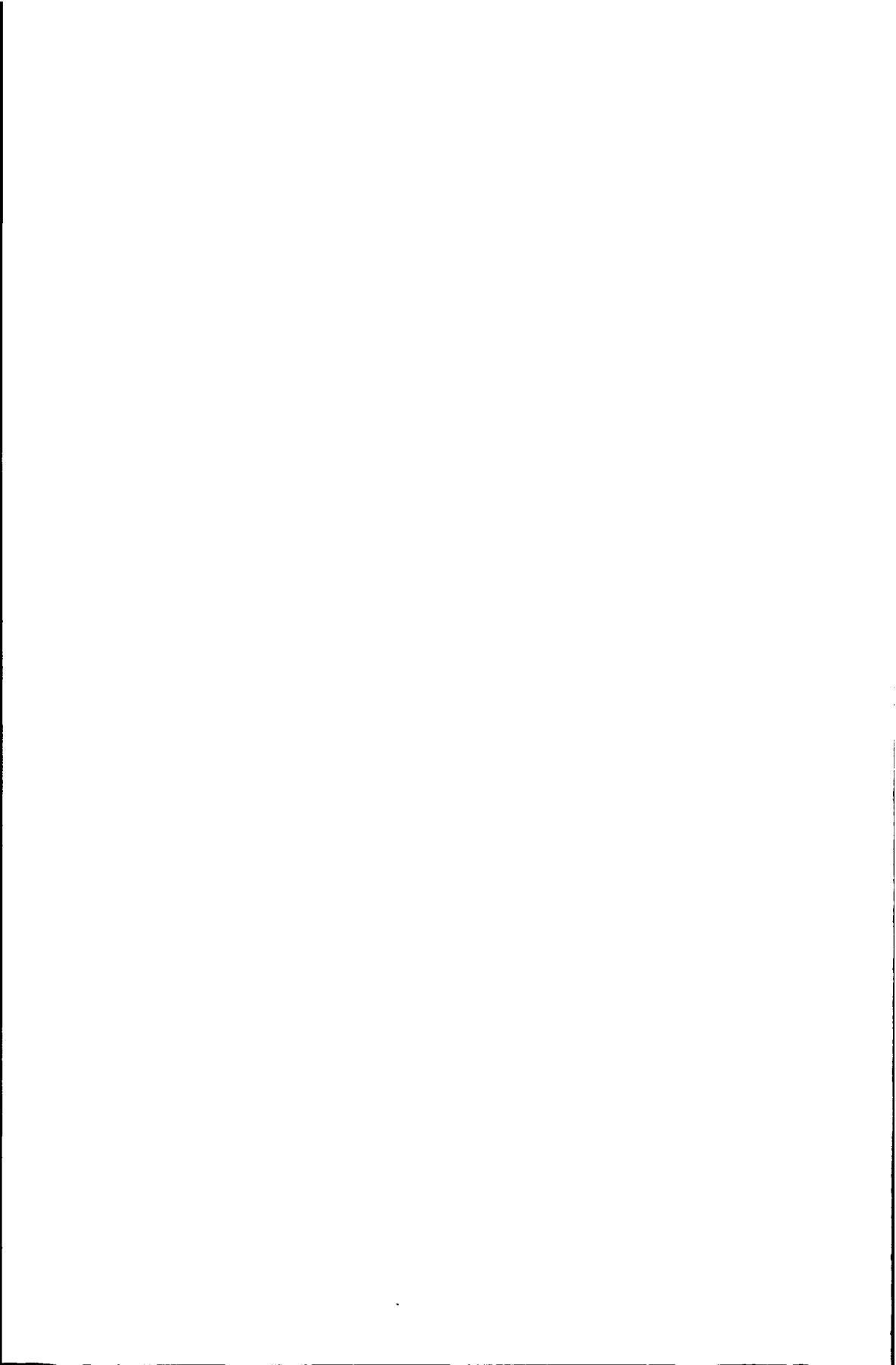
- bending moment $-M_{xx,i}^{\min} + M_{xx,i}^{\text{plus}} = T_i$;

- shear force $\frac{d}{dx} M_{xx,i}^{\min} + \frac{t_i^{\min}}{2} \tau_c^{\min} - m_i^{\min} - \frac{d}{dx} M_{xx,i}^{\text{plus}} - \frac{t_i^{\text{plus}}}{2} \tau_c^{\text{plus}} + m_i^{\text{plus}} = F_{z,i}$.

And at any point of the height of the core additional boundary conditions has to be expressed as follows:

- transverse displacement $w_c^{\min} - w_c^{\text{plus}} = 0$;

- shear stress $\tau_c^- - \tau_c^+ = 0$.



Combination of Higher-Order Theory and Spring Model Approach for a Sandwich Panel with an Adhesively Bonded Plate

In this appendix all relevant equations of the combined higher-order theory and spring model approach for a sandwich panel with an adhesively bonded plate are presented. Information is provided about:

- material properties and stiffness parameters used in the equations;
- revised version of the higher-order theory for the three-layer sandwich presented in appendix B, which includes shear deformation of the faces and plate;
- differential equations for the five-layer concept of a sandwich panel described by the higher-order theory and an adhesively bonded plate described by the spring model approach, including equations to calculate the stress and strain state in the sandwich and within the adhesive bondline;
- boundary and continuity conditions.

C.1 Material properties and stiffness parameters

The used material properties for the faces and the adhesively bonded plate are:

- Young's modulus E_i of adherend i ;
- Poisson's ratio ν_i of adherend i .

The used material properties for the core are:

- Young's modulus E_c of the core;
- shear modulus G_c of the core;
- Poisson's ratio ν_c of the core;

The used material properties for the adhesive are:

- Young's modulus E_a of the adhesive;
- shear modulus G_a of the adhesive;
- Poisson's ratio ν_a of the adhesive;

The following stiffness parameters are used in the governing differential equations:

- Axial rigidity of face or plate i with plate thickness t_i :

$$\text{for a sandwich beam: } A_i = E_i t_i \quad (\text{C1a})$$

$$\text{for a sandwich panel: } A_i = \frac{E_i t_i}{1 - \nu_i} \quad (\text{C1b})$$

- Shear coefficient per unit width (Reissman, 1988) of face or plate i with plate thickness t_i :

$$B_i = \kappa_i^2 t_i$$

$$\text{with:} \quad (\text{C2})$$

$$\kappa_i = 0.874 + 0.162 \nu_i, \text{ valid for } 0 < \nu_i < 0.5$$

Combination of Higher-Order Theory and Spring Model Approach for a Sandwich Panel with an Adhesively Bonded Plate

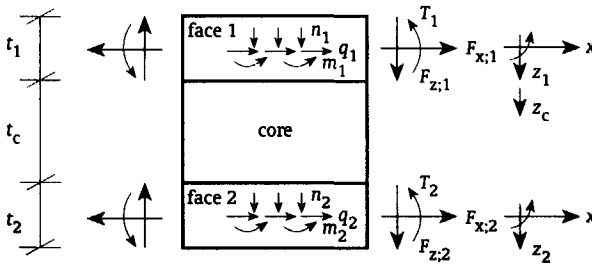
Flexural rigidity of face or plate i with plate thickness t_i :

$$\text{for a sandwich beam: } D_i = \frac{E_i t_i^3}{12} \tag{C3a}$$

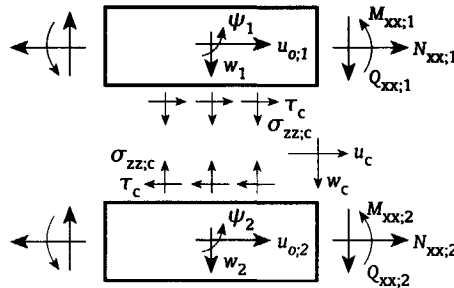
$$\text{for a sandwich panel: } D_i = \frac{E_i t_i^3}{12 (1 - \nu_i^2)} \tag{C3b}$$

C.2 Revised version of the higher-order theory for the three-layer concept including shear deformation of the faces and plate

The following geometry, applied loads and coordinate system are considered:



The following section forces, stresses and deformations are considered:



The following set of seven coupled differential equations is derived:

$$A_1 \frac{d^2}{dx^2} u_{o;1} + \tau_c = -n_1 \tag{C4}$$

$$A_2 \frac{d^2}{dx^2} u_{o;2} - \tau_c = -n_2 \tag{C5}$$

$$D_1 \frac{d^2}{dx^2} \psi_1 - B_1 \psi_1 - B_1 \frac{d}{dx} w_1 + \frac{t_1}{2} \tau_c = -m_1 \quad (C6)$$

$$D_2 \frac{d^2}{dx^2} \psi_2 - B_2 \psi_2 - B_2 \frac{d}{dx} w_2 + \frac{t_2}{2} \tau_c = -m_2 \quad (C7)$$

$$B_1 \frac{d}{dx} \psi_1 + B_1 \frac{d^2}{dx^2} w_1 - \frac{E_c}{t_c} w_1 + \frac{E_c}{t_c} w_2 + \frac{t_c}{2} \frac{d}{dx} \tau_c = -q_1 \quad (C8)$$

$$B_2 \frac{d}{dx} \psi_2 + B_2 \frac{d^2}{dx^2} w_2 + \frac{E_c}{t_c} w_1 - \frac{E_c}{t_c} w_2 + \frac{t_c}{2} \frac{d}{dx} \tau_c = -q_2 \quad (C9)$$

$$u_{o;1} - u_{o;2} + \frac{t_1}{2} \psi_1 + \frac{t_2}{2} \psi_2 - \frac{t_c}{2} \frac{d}{dx} w_1 - \frac{t_c}{2} \frac{d}{dx} w_2 - \frac{t_c^3}{12E_c} \frac{d^2}{dx^2} \tau_c + \frac{t_c}{G_c} \tau_c = 0 \quad (C10)$$

These differential functions contain the unknown functions of the displacements and rotations of the faces and plate $u_{o;1}(x)$, $u_{o;2}(x)$, $\psi_1(x)$, $\psi_2(x)$, $w_1(x)$ and $w_2(x)$, and the shear stress within the core $\tau_c(x)$. The normal force, bending moment and shear force in face or plate i are respectively:

$$N_{xx;i}(x) = A_i \frac{d}{dx} u_{o;i} \quad (C11)$$

$$M_{xx;i}(x) = D_i \frac{d}{dx} \psi_i \quad (C12)$$

$$Q_{xx;i}(x) = B_i \psi_i + B_i \frac{d}{dx} w_i \quad (C13)$$

The transverse normal stress in the core is described by:

$$\sigma_{zz;c}(x, z_c) = -\frac{E_c}{t_c} w_1 + \frac{E_c}{t_c} w_2 + \left(-z_c + \frac{t_c}{2}\right) \frac{d}{dx} \tau_c \quad (C14)$$

and the matching normal strain is:

$$\epsilon_{zz;c}(x, z_c) = \frac{1}{E_c} \sigma_{zz;c}(x, z_c) \quad (C15)$$

The shear stress in the core is one of the unknown functions described by the differential equations. The matching shear angle is:

$$\gamma_c(x) = \frac{1}{G_c} \tau_c(x) \quad (C16)$$

The transverse and longitudinal displacement of the core are described by respectively:

$$w_c(x, z_c) = \left(-\frac{z_c}{t_c} + 1\right) w_1 + \frac{z_c}{t_c} w_2 - \frac{1}{2E_c} (z_c^2 - z_c t_c) \frac{d}{dx} \tau_c \quad (C17)$$

Combination of Higher-Order Theory and Spring Model Approach for a Sandwich Panel with an Adhesively Bonded Plate

$$u_c(x, z_c) = u_{o,1} + \frac{t_1}{2} \psi_1 + \left(\frac{z_c^2}{2t_c} - z_c \right) \frac{d}{dx} w_1 - \frac{z_c^2}{2t_c} \frac{d}{dx} w_2 - \frac{1}{2E_c} \left(\frac{z_c^2 t_c}{2} - \frac{z_c^3}{3} \right) \frac{d^2}{dx^2} \tau_c + \frac{z_c}{G_c} \tau_c \quad (C18)$$

C.3 Boundary and continuity conditions

Three boundary conditions at one end of a considered face i , have to be expressed as follows:

- normal force $N_{xx;i} = F_{x;i}$ or longitudinal displacement $u_{o,i} = 0$;
- bending moment $M_{xx;i} = T_i$ or rotation $\psi_i = 0$;
- shear force $B_i \psi_i + B_i \frac{d}{dx} w_i = F_{z,i}$ or transverse displacement $w_i = 0$.

And at any point through the height of the core an additional boundary condition has to be expressed as follows:

- transverse displacement $w_c = 0$ or shear stress $\tau_c = 0$.

Six continuity conditions at an intermediate point between two faces indicated by "min" and "plus", have to be expressed as follows:

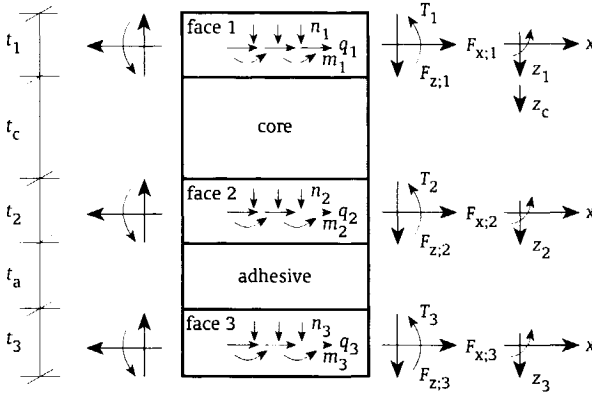
- longitudinal displacement $u_{o,i}^{\min} - u_{o,i}^{\text{plus}} = 0$;
- transverse displacement $w_{o,i}^{\min} - w_{o,i}^{\text{plus}} = 0$;
- rotation $\psi_i^{\min} - \psi_i^{\text{plus}} = 0$;
- axial force $N_{xx;i}^{\min} - N_{xx;i}^{\text{plus}} = F_{x,i}$;
- bending moment $-M_{xx;i}^{\min} + M_{xx;i}^{\text{plus}} = T_i$;
- shear force $Q_{xx;i}^{\min} - Q_{xx;i}^{\text{plus}} = F_{z,i}$.

And at any point of the height of the core additional boundary conditions has to be expressed as follows:

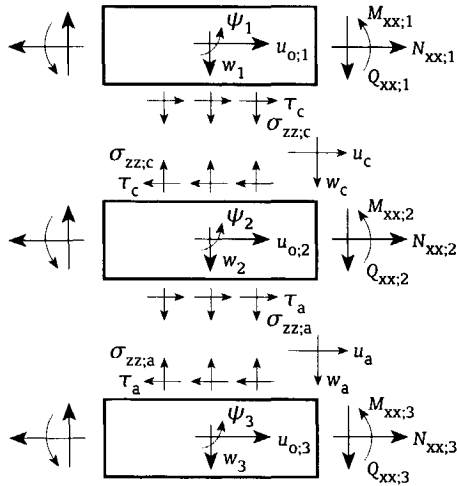
- transverse displacement $w_c^{\min} - w_c^{\text{plus}} = 0$;
- shear stress $\tau_c^- - \tau_c^+ = 0$.

C.4 Combined higher-order theory and spring model approach for the five-layer concept

The following geometry, applied loads and coordinate system are considered:



The following section forces, stresses and deformations are considered:



The following set of ten coupled differential equations is derived:

$$A_1 \frac{d^2}{dx^2} u_{o;1} + \tau_c = -n_1 \quad (C19)$$

$$A_2 \frac{d^2}{dx^2} u_{o;2} - \frac{G_a}{t_a} u_{o;2} + \frac{G_a}{t_a} u_{o;3} - \frac{t_2 G_a}{2t_a} \psi_2 - \frac{t_3 G_a}{2t_a} \psi_3 - \tau_c = 0 \quad (C20)$$

Combination of Higher-Order Theory and Spring Model Approach for a Sandwich Panel with an Adhesively Bonded Plate

$$A_3 \frac{d^2}{dx^2} u_{0;3} + \frac{G_a}{t_a} u_{0;3} - \frac{G_a}{t_a} u_{0;3} + \frac{t_2 G_a}{2t_a} \psi_2 - \frac{t_3 G_a}{2t_a} \psi_3 = -n_3 \quad (C21)$$

$$D_1 \frac{d^2}{dx^2} \psi_1 - B_1 \psi_1 - B_1 \frac{d}{dx} w_1 + \frac{t_1}{2} \tau_c = -m_1 \quad (C22)$$

$$-\frac{t_2 G_a}{2t_a} u_{0;2} + \frac{t_2 G_a}{2t_a} u_{0;3} + D_2 \frac{d^2}{dx^2} \psi_2 - (B_2 + \frac{t_2^2 G_a}{4t_a}) \psi_2 - \frac{t_2 t_3 G_a}{4t_a} \psi_3 - B_2 \frac{d}{dx} w_2 + \frac{t_2}{2} \tau_c = 0 \quad (C23)$$

$$-\frac{t_3 G_a}{2t_a} u_{0;2} + \frac{t_3 G_a}{2t_a} u_{0;3} - \frac{t_2 t_3 G_a}{4t_a} \psi_2 + D_3 \frac{d^2}{dx^2} \psi_3 - (B_3 + \frac{t_3^2 G_a}{4t_a}) \psi_3 - B_3 \frac{d}{dx} w_3 = -m_3 \quad (C24)$$

$$B_1 \frac{d}{dx} \psi_1 + B_1 \frac{d^2}{dx^2} w_1 - \frac{E_c}{t_c} w_1 + \frac{E_c}{t_c} w_2 + \frac{t_c}{2} \frac{d}{dx} \tau_c = -q_1 \quad (C25)$$

$$B_2 \frac{d}{dx} \psi_2 + \frac{E_c}{t_c} w_1 + B_2 \frac{d^2}{dx^2} w_2 - (\frac{E_c}{t_c} + \frac{E_a}{t_a}) w_2 + \frac{E_a}{t_a} w_3 + \frac{t_c}{2} \frac{d}{dx} \tau_c = 0 \quad (C26)$$

$$B_3 \frac{d}{dx} \psi_3 + \frac{E_a}{t_a} w_2 + B_3 \frac{d^2}{dx^2} w_3 - \frac{E_a}{t_a} w_3 = -q_3 \quad (C27)$$

$$u_{0;1} - u_{0;2} + \frac{t_1}{2} \psi_1 + \frac{t_2}{2} \psi_2 - \frac{t_c}{2} \frac{d}{dx} w_1 - \frac{t_c}{2} \frac{d}{dx} w_2 - \frac{t_c^3}{12E_c} \frac{d^2}{dx^2} \tau_c + \frac{t_c}{G_c} \tau_c = 0 \quad (C28)$$

These differential functions contain the unknown functions of the displacements and rotations of the faces and plate $u_{0;1}(x)$, $u_{0;2}(x)$, $u_{0;3}(x)$, $\psi_1(x)$, $\psi_2(x)$, $\psi_3(x)$, $w_1(x)$, $w_2(x)$ and $w_3(x)$, and the shear stress within the core $\tau_c(x)$. The normal force, bending moment and shear force in face or plate i are respectively:

$$N_{xx;i}(x) = A_i \frac{d}{dx} u_{0;i} \quad (C29)$$

$$M_{xx;i}(x) = D_i \frac{d}{dx} \psi_i \quad (C30)$$

$$Q_{xx;i}(x) = B_i \psi_i + B_i \frac{d}{dx} w_i \quad (C31)$$

The transverse normal stress in the core is described by:

$$\sigma_{zz,c}(x, z_c) = -\frac{E_c}{t_c} w_1 + \frac{E_c}{t_c} w_2 + (-z_c + \frac{t_c}{2}) \frac{d}{dx} \tau_c \quad (C32)$$

and the matching normal strain is:

$$\epsilon_{zz,c}(x, z_c) = \frac{1}{E_c} \sigma_{zz,c}(x, z_c) \quad (C33)$$

The shear stress in the core is one of the unknown functions described by the differential equations. The matching shear angle is:

$$\gamma_c(x) = \frac{1}{G_c} \tau_c(x) \quad (C34)$$

The transverse normal stress in the adhesive is described by:

$$\sigma_{zz,a}(x) = -\frac{E_a}{t_a} w_2 + \frac{E_a}{t_a} w_3 \quad (C35)$$

and the matching normal strain is:

$$\epsilon_{zz,a}(x) = \frac{1}{E_a} \sigma_{zz,a}(x) \quad (C36)$$

The shear stress in the adhesive is described by:

$$\tau_a(x) = -\frac{G_a}{t_a} u_{0,2} + \frac{G_a}{t_a} u_{0,3} - \frac{t_2}{2} \psi_2 - \frac{t_3}{2} \psi_3 \quad (C37)$$

The matching shear angle is:

$$\gamma_a(x) = \frac{1}{G_a} \tau_a(x) \quad (C38)$$

The transverse and longitudinal displacements of the core are described by respectively:

$$w_c(x, z_c) = (-\frac{z_c}{t_c} + 1)w_1 + \frac{z_c}{t_c} w_2 - \frac{1}{2E_c} (z_c^2 - z_c t_c) \frac{d}{dx} \tau_c \quad (C39)$$

$$u_c(x, z_c) = u_{0,1} + \frac{t_1}{2} \psi_1 + (\frac{z_c^2}{2t_c} - z_c) \frac{d}{dx} w_1 - \frac{z_c^2}{2t_c} \frac{d}{dx} w_2 - \quad (C40)$$

$$\frac{1}{2E_c} (\frac{z_c^2 t_c}{2} - \frac{z_c^3}{3}) \frac{d^2}{dx^2} \tau_c + \frac{z_c}{G_c} \tau_c$$

C.5 Additional boundary and continuity conditions

For the faces of the sandwich and for the core the boundary and continuity conditions as discussed in section C.3 have to be used. For the adhesively bonded plate the same boundary and continuity conditions as give in section C.3 have to be applied, while for the adhesive bondline no additional conditions are formulated.



Curriculum Vitae

Ijsbrand Jan van Straalen was born on June 4th 1963 in 's-Gravenzande. He completed Atheneum-B in 1982 and afterwards studied civil engineering at the Delft University of Technology where he graduated in 1988. His MSc study on the subject of fatigue and fracture mechanics of steel structures was carried out at TNO Building and Construction Research during the period 1986-1988. After military service he is employed at TNO Building and Construction Research. From 1989 on he is involved in a variety of projects dealing with normalisation of building standards, formulation of guidelines for storage racking structures, development of design methods for greenhouses, research into the fatigue behaviour of steel and aluminium structures, review of design proposals, analysis of the reliability of structures, application of multimaterials and research into adhesive bonded joints. From 1995 until 2000 he worked part-time on his PhD study at TNO Building and Construction Research.



